Network Scale Sediment Transport Modelling with the Perspective of Improved Sediment Connectivity and Delivery: A case of small dam removal.

SHOBHIT PIPIL

Network Scale Sediment Transport Modelling with the Perspective of Improved Sediment Connectivity and Delivery: A case of small dam removal.

(Eamont River Catchment, Lake District, U.K.)

Shobhit Pipil

Department of Geography

Durham University

A thesis submitted in partial fulfilment of the requirements for the degree of Doctor of Philosophy

August 2021

Declaration of Authorship

I confirm that I have not submitted the current thesis and its part for a degree in the current and foreign university. The thesis written part and material used from the other works have been acknowledged.

The present thesis work should not be published without the author's prior written permission, and information extracted from the thesis should be acknowledged.

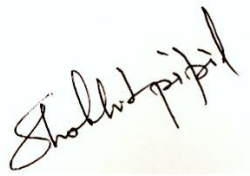

Shobhit Pipil

Department of Geography

Durham University

August 2021

Abstract

Sediment movement from the headwater region (source) to the catchment outlet (sink) constantly transforms the river geomorphology and produces various geomorphic features. The geomorphic diversity in the river supports hydro-morphic sediment conditions that formulate suitable physical habitat for the riverine ecosystem. Water, sediment, and organic matter must flow uninterrupted for a healthy ecosystem. However, humans have raised civil engineering structures on many rivers. River fragmentation (dam/weirs) in the European river has crossed the 630,000 marks, and the projected number is 1 million. Fragmentation restricts the free movement of discharge, sediment, organic matter, and riverine species. The impacts of dams on river geomorphology, discharge and sediments are well documented. At the same time, the declining riverine species trend is a significant cause of concern.

Recent studies revealed a 95% decline since 1970 (in the living planet index). Though, dam removal is gaining momentum to reverse the negative impacts on the riverine ecosystem. Dam removal studies have shown positive outcomes on river geomorphology and ecology. However, it would not be admissible to remove all the obstacles present on the river course; for example, there is a considerable cost involved and the economic benefits offered during the lifespan of a dam. Political will is another obstacle in river restoration projects beyond the cost and benefits analysis of the dams and weirs.

The previous dam removal studies addressed site-specific geomorphological and ecological recovery, though case studies often lack long term monitoring. Thus, a few cases reported no significant differences in the river. Still, the presence of a dam or weirs footprint impacts the upstream and downstream river course, which turns a river's lotic environment into a lentic. In addition, the existence of multiple dams or weirs further deteriorates the river's condition by restricting water and matter movement. Thus, dam or weir removal impact assessment must be studied for the catchment and river network scale.

The current study is applied to the Eamont river catchment (396.2 km^2), located in the lake district region, which receives maximum rainfall in the U.K. region. Hard rocks dictate the regional geology, and rivers are confined. Thus, no significant changes in river form have occurred in the Eamont catchment rivers. However, rivers of the

Eamont catchment have high stream power and sediment continuity. 2 major and 20 small weirs interrupt the natural sediment transport. Additionally, enormous Ullswater and other lakes provide local sinks in the catchment. The catchment area and the number of obstacles present in the Eamont river catchment offers a suitable catchment setting to address the European river fragmentation case.

Two models and other tools are employed to quantify the impacts of multiple obstacles (dam and wires) on a river network. In hierarchical processes and quantification bases, the tools can be briefly summarised; *First*, a semi-distributed hydrological model SWAT that has quantified the distributed discharge for 166 reaches, at daily frequency, over 55 years (1960 – 2015). *Second*, SWAT model calibration and validation in SWAT-CUP, using the SUFI algorithm. *Third*, the DJI-4 drone's images were captured for gravel bars at low altitudes for higher ground resolution. *Forth*, the Metashape application processed orthophotos of gravel bars, which are further processed in BASEGRAIN, to perform optical-granulometry and develop grain size distribution at the river network scale. *Fifth*, integration of hydrologic and grain size distribution information in the CASCADE framework for sediment connectivity, dam and weir removal impact analysis on sediment flux, at the network scale.

The CASCADE framework provided sediment entrainment, transport, and deposition pattern on the Eamont network. The study's key findings have highlighted that the Lowther River contributes more sediment than the Eamont river, despite the high entrainment in the headwater regions. The entrained sediment gets deposited in the Brothers water and Ullswater lake on the Eamont river course. Whilst the Lowther river's significant deposition takes place in Haweswater reservoir. The main reason why Lowther River provide high sediment flux is that it has a high gradient and transport power than Eamont.

Moreover, based on the geomorphological difference between the Eamont river and its tributary Lowther, the presence of multiple weirs with approximately similar sediment trap efficiency, the CASCADE simulation showed higher sediment flux would be released when weir removal activity performed on the Lowther River.

The current study had presented an opportunity to analyse the multiple river obstacle (dam/ weirs) impacts on sediment flux and sediment connectivity at a network scale. Such an experiment can be applied to formulate the dam removal planning for a

complex river catchment. However, future integration of the CASCADE framework with ecological modelling would improve analysis for riverine ecosystem benefits.

Acknowledgements

I am immensely grateful to my supervisors – Dr Patrice Carbonneau and Dr Martin Lucus (Bio-science department), for their guidance and support throughout the PhD research work. I want to thank them for sharing their knowledge experience and motivating me during the odd phase. When I look back in 2017, I find myself getting anxious about everything, but research has undoubtedly evolved me to deal with academic problems and life in general. However, this would not be possible without their valuable guidance and support. Though, I still need to learn so much.

This research work was supported by EC Horizon 2020 Research & Innovation Programme (AMBER Project, grant agreement no. 689682). I am grateful to the European Commission for providing me research grant. Without their support, I cannot imagine that I could/would have dreamt of pursuing higher studies in one of the world's premier universities. Interestingly, in my professional career, I had been engaged with two EU funded projects.

I want to extend my thanks to UHI, Inverness, Dr Eric Verspoor and Dr Lucio Marcello for their collaboration and support for fieldwork. The field and aerial survey have helped me understand river science, hydrological modelling concepts, and practical problems such as field data limitations. I also want to thank Dr Sun Jinrui and Mr Amit Bhadula for their support for drone data collection.

This research work has allowed me to work with Bio-scientists. Through collaboration and support, I learned about the ecological importance of the riverine environment. I volunteered support for their electro-fishing survey that involves identifying and measuring the fish species. I met Dr Jeroen Tummers, Dr Shams Galib, Dr Sun Jinrui, Miss Holly Appleby, and they have enlightened me so much about the subject.

I joined this project with the perspective eyes of a geomorphological consequence analysis of a fragmented river, but I understood how important this project is with regards to ecological implications; whenever I felt dejected by the details of modelling work, then the declining rate of biodiversity in European river compelled me to stay motivated and do my best. This project has impacted me a lot, and sometimes I think about joining conservation-related jobs in future endeavours. But how can I forget to thank the Durham department community, especially Dr Richard J. Hardy and Dr Sim

Reaney, for their positive feedback during the progression interview. They had raised my confidence at that moment because when I arrived in the UK. I could not understand the accent and communicate well with other natives, not just that, but they had appreciated my approach towards the project.

Thanks to Ms Kathy Wood, other departmental staff members, CIS support engineers, and PhD cohorts. I do not want to name just a few individuals, as everyone has contributed to or helped me in this journey.

I want to share my experience with people outside the university who have provided crucial insights regarding modelling work. I want to extend thanks to Dr Srinivasan (Texas A&M), people from the US Agriculture Department, Dr Darren L. Ficklin (Indiana University), Dr Martin Detert (ETH Zurich), Dr Simone Bizzi (University of Padova), Marco Tangi (PhD student at Politecnico di Milano), people on SWAT and SWAT-CUP Google community group. Dr Surya Gupta (ETH Zurich), who was with me at IIT Kanpur, kept on motivating me since our IELTS course preparation to the day I submitted this work. How can I forget to mention Dr Deep Sengupta, a Post-doc researcher at the University of California, Berkeley, who had encouraged and motivated me to join research since he joined PhD at the DRI, Nevada, in 2015.

I also want to thank all my teachers who shaped my life from my school days to university. I want to thank Dr Rajiv Sinha, Dr V Hari Prasad, Dr A. K. Gosain, Sandhya Rao. My teachers at IIRS, Dehradun, and Jiwaji University. A junior friend Dr Vikram Ranga and many others whom I cannot recall now.

I want to thank Miss Kathrine Jelpke; she helped me to deal with matters outside the academic work in the UK because this was my first international visit, and I had no friends. She is a great girl with a clear vision of her life—finally, my Ustinov college friends and special ones Mr Kelly Dueck, Dr Ajaz Ahmed. I met a few multinational friends in college and learned about their culture.

Now I know that why it is vital to stay grounded and to learn from people around us. Thank you, everyone; if I forgot to mention your name, please count yourself. My final thanks goes to you.

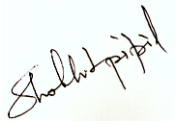

Contents

List of Figures

List of Tables

Chapter 1: Introduction

1.1 Rationale

Small dams or weir structures are omnipresent on the European rivers, thus turning the European rivers among the most fragmented river systems. A small weir and dams' collective impacts on river morphology and ecology are underreported because of site-specific impact evaluation studies (Walker, 2001; Sindelar et al., 2017; Wang et al., 2018; Patriadi, 2021). Thus, at the river network scale, multiple weirs impact assessment is required to support the evaluation of the geomorphological, physical habitat, and ecological state of a highly fragmented river system (Stanley and Doyle, 2003).

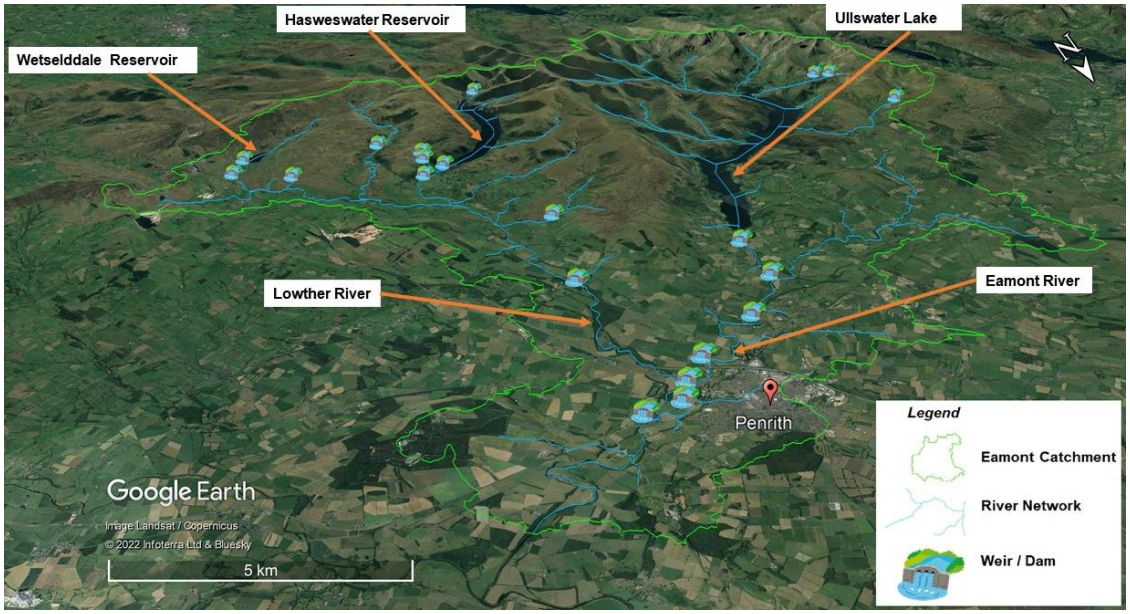

Figure 1.1 shows the physiographic setup of the Eamont river catchment and multiple weirs and dams showing river fragmentation.

Such studies can provide insight for scenario development based on the adversity brought to the river system by multiple weir or dam structures (Schmitt et al., 2018a; Van Looy et al., 2014). It is crucial since the ecological state of river systems are degrading (Dias et al., 2017; Grizzetti et al., 2017; Helfman, 2007, pp. 130–157), and dam or weir removal activities provided evidence regarding the recreation of physical habitat; resulting in species diversity (Fjeldstad et al., 2012). However, the unavailability of small dam characteristics

and structural information often hinders their impact evaluation (Habets et al., 2018). Despite that, studies have reported impacts of small dams on sediment (Galia et al., 2021; Tonitto and Riha, 2016; Yang et al., 2011), river channels (Tullos et al., 2014), biodiversity (Tang et al., 2021). Small weirs and their removal to reconnect the river course and physical habitat is still limited in the European and UK catchment (Foster et al., 2021).

1.2 Global and European river fragmentation

Nearly 80% of the world's population resides in regions affected by threats to water security or biodiversity (Vorosmarty et al., 2010). The biodiversity threat in recent times has shown exponential growth. Across the world, biodiversity is declining, and observed trends are distressing. Human anthropogenic actions and unsustainable approaches to exploit natural resources contribute to the declining trends of biodiversity. It is not an exaggerated view that water is one of the most exploited natural resources (Ruz, 2011). Water exploitation has been recorded in human history, with dams constructed as early as 5000 years ago, and construction is ongoing (Biswas and Tortajada, 2001; Ansar et al., 2014). Dam planning and removal activity are important because freshwater biodiversity has shown the highest declining rate in a global scale study (WWF., 2016).

A revised assessment of biodiversity, measured as 'living planet index', has declined from 81% to 84% in 2016 and 2020, respectively, Figure 1.2, (Almond et al., 2020). The living planet index declining rate shows a 0.60 per cent average biodiversity decline in the freshwater living planet index per year. At this rate, within the next 27 years, the freshwater ecosystem will be in a severe state. The declining rate is a grave concern because physical and ecological disturbances impact human lives (Alcamo, 2003; Duffy, 2009; Cardinale et al., 2012; Hough, 2014; UNEP, 2017).

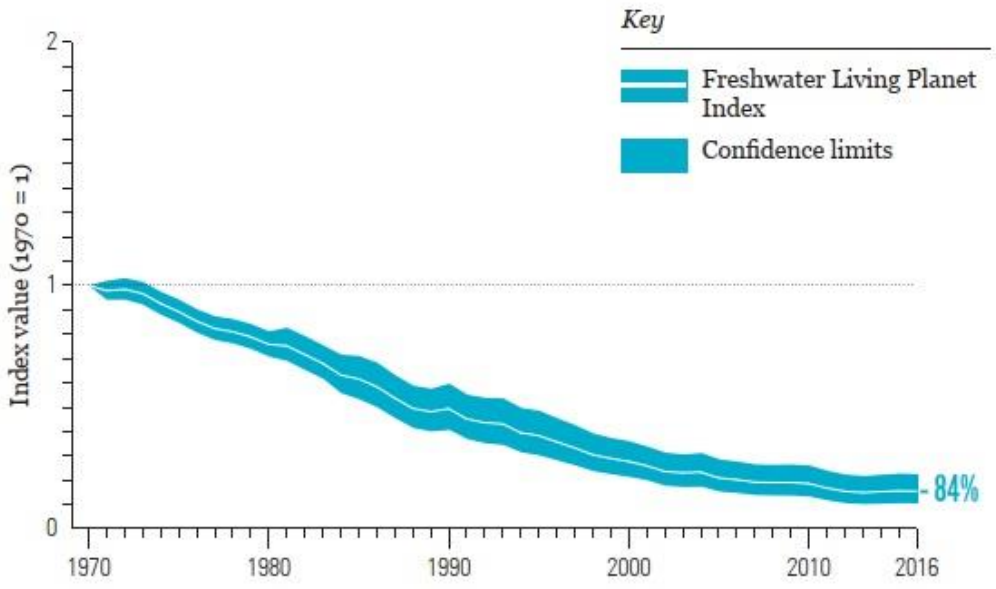

Figure 1.2 The Freshwater Living Planet Index: 1970 to 2016 (source: - http://stats.livingplanetindex.org/).

River fragmentation is equally responsible for the declining biodiversity trend in freshwater ecosystems (Schiermeier, 2018; McKie, 2019). Freshwater is a renewable resource; however, given its limited availability, it should be dealt with judicious and sustainable manner. A global-scale study revealed that 37% of rivers longer than 1000 Km remained free-flowing over their entire length, and out of which, only 23% remained uninterrupted before merging with the sea (Grill et al., 2019). Free-flowing rivers obstructed and diverted to meet specific human demands such as agricultural, industrial, power generation or inter-basin transfers to satisfy the water demand in water-scarce regions. Free-flowing River water flows are stored or diverted through raising dam structures and other water resource engineering structures.

The global number of large and small dams is high but not recorded in a single database (Zarfl et al., 2015). The objective of developing such a kind of dam database is to facilitate hydrological and environmental effects-related studies. Therefore, barrier impact studies persisted on regional or catchment specific. Some studies were also performed beyond cross country catchment boundary and even at continental scale (Yang and Musiake, 2003; Norman et al., 2012; Abbaspour et al., 2015). One reason for the limited assessment of dam and barrier's impact at global scales is the lack of spatial data availability (Sood and

Smakhtin, 2015). However, a global assessment of the impacts of barriers on freshwater ecosystems is urgently needed (Rosenberg et al., 2000; Richter et al., 2010; Vorosmarty et al., 2010).

Precise geographical mapping of dams on a continental and global scale has been largely insufficient (Lehner et al., 2011). Progressively, there are efforts to expand the dam database, and a few comprehensive databases now exist, such as GranD and ICOLD. The GranD (Global Reservoir and Dam Database, version 1.3) and ICOLD (International Commission on Large Dams) consist of 7,320 and 58,000 large dam records, respectively (Lehner et al., 2011; Mulligan et al., 2020). In a recent attempt, a comprehensive dam database named GOODD (GlObal geOreferenced Database of Dams) has also included medium-sized dams and represents 38,000 dam records. This development of dam databases has improved dam information and can be helpful for global environmental impact assessment (Mulligan et al., 2020).

However, the mentioned dam databases do not consider dams with a height < 15 meters. Therefore, there remains a need for a reliable database of dams of all dimensions. Nevertheless, much of the dam information comes from multiple sources, projected globally in a single portal like Global Dam Watch (Beames, 2021).

Small dams and small water management structures such as weirs outnumber the big dams' numbers (Couto and Olden, 2018; Zarfl and Lehner, 2020), and at least 85 per cent of barriers on European rivers are smaller structures (Lovgren, 2020). Recently, there has been growing interest in river barrier mapping on European rivers, as seen in the AMBER atlas (Figure 1.3). It has been estimated that 1.2 million obstacles fragment European rivers, and most of them are small dams and weirs (Belletti et al., 2020). This level of river water exploitation and abuse has resulted in the degradation of freshwater habitat and continuous biodiversity decline. Thus, an aggregated extent of small dams must not be underrated (McCully, 1996).

A healthy ecosystem provides numerous benefits to humankind, and any regional and global biodiversity transformation would cause irreparable damage to the global ecosystem (Dudgeon et al., 2006; Albert et al., 2020). The

existing and future large dams will adversely impact river connectivity and freshwater fish populations (Barbarossa et al., 2020). Thus, river management should prioritise freshwater management to prevent further deterioration (Zarfl et al., 2019; European Environment Agency, 2021).

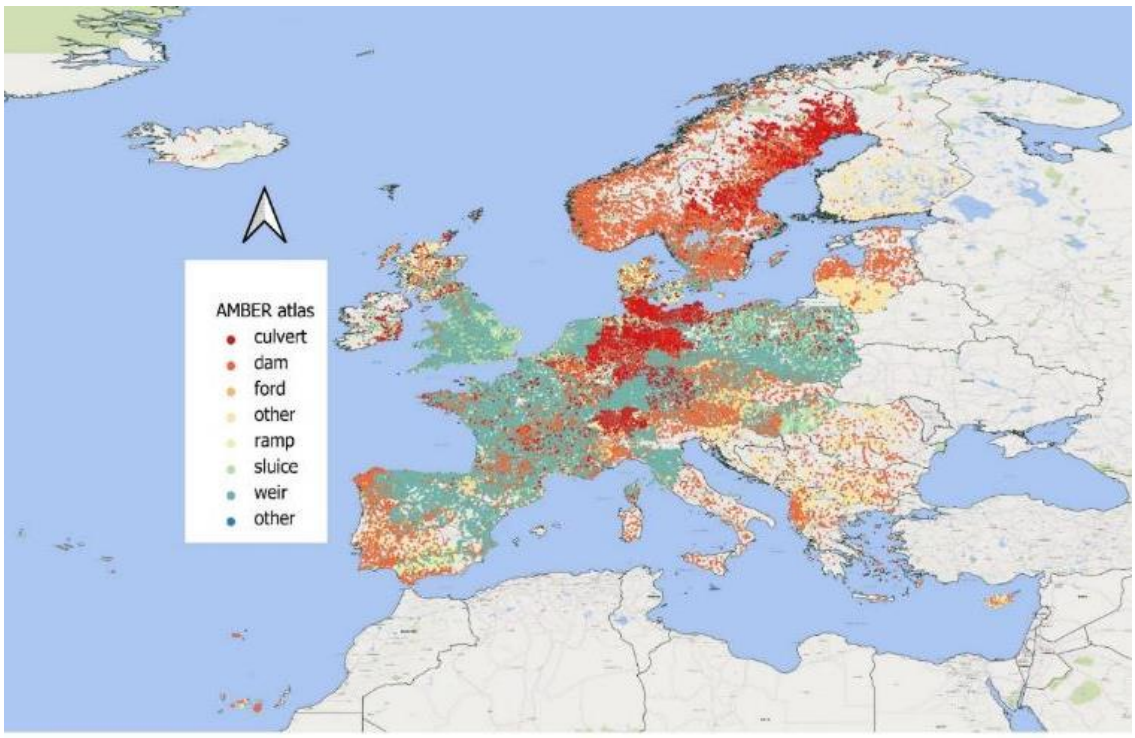

Figure 1.3 AMBER atlas showing 630,000 barriers across Europe (source - https://amber.international/).

The extreme fragmentation of European rivers and their adverse impact on river geomorphology and ecology have yet to be analysed (de Leaniz, 2020). The fragmentation of rivers that brings multiple stressors (flow reduction, biological oxygen demand, fine sediments entry, temperature variation) and multiple stressors turned the European river ecosystem into one of the vulnerable parts of the world (European Environment Agency, 2011; Freyhof and Brooks, 2011; Markovic et al., 2017; European Environment Agency., 2018; Birk et al., 2020).

The recent development for mapping river obstruction on European rivers turns them into the most fragmented river systems on the planet (AMBER Consortium, 2020; Schwarz, 2021), and freshwater habitat in the EU classified as 46% and 38% for endangered and vulnerable categories, respectively (Janssen et al., 2016). Therefore, it is imperative to find a solution to reduce

river fragmentation and reconnect the river system considering sediment dynamics and spatial-temporal dimension (Hauer et al., 2018). In addition, Europe's Biodiversity strategy for 2030 has proposed to free up to 25000Km of river length till 2030 in fragmented rivers of European nations (de Leaniz, 2020). Accordingly, it becomes crucial to develop scientific aptitude in conjunction with modelling tools; to defragment the rivers by adopting weir and dam removal based on scientific justification (Hermoso et al., 2021).

Climate change and consequent hydro-climatic conditions also accelerate adverse implications on the freshwater system (Heino et al., 2009). A global-scale study has revealed human influence on global freshwater fluctuation, and surface water storage trends are worrying (Cooley et al., 2021).

1.2.1 Adverse impacts of river fragmentation

The geomorphology of river systems reflects the balance between sediment supply and transport capacity distribution in the river network (Montgomery et al., 1996; Montgomery and Buffington, 1997). The balance between the two generates suitable habitats according to process domain concepts based on spatial and temporal variation of geomorphic processes (Montgomery, 1999). Distinctive river morphologies in the river network provide valuable information regarding sediment source, erosion of bank and riverbed, flow resistance, flow characteristics (velocity, shear stress), and become valuable for river engineering, habitat and river restoration applications (Brierley and Fryirs, 2005).

Functional geomorphological changes deviate when climate and human activity disrupts the normal sediment transport process along the river continuum (Allan and Castillo, 2007). Low order rivers tributaries are sources that provide sediment, discharge and unique habitat in a river catchment (Meyer and Wallace, 2001). Alteration of low order reaches can produce biophysical changes apart from sediment, nutrient, and discharge fluctuation. The ecological consequences of low reach alteration could induce genetic variation due to an isolated patch of the reaches.

The movement of species for upstream spawning area availability is subjected to the provisions implemented on the alteration structures (fish passage), which

may cause reduction of native population and invasion of alien species to the region (Pringle, 1997; Kerr et al., 2021). Therefore, headwater to downstream connectivity becomes crucial for river restoration and river ecosystem management.

In a free-flowing river system, mid-reaches are associated with a gentler gradient than headwater and supports more diversity in geomorphic conditions; a broad river section with warm water and groundwater supply provides highly diverse biodiversity (invertebrates and fish species). In lower reaches, the slope is gentler than mid-reach, and wide channels with deep water flow through the vast floodplain, fine sediment substrate. Lower reaches support fish species adapted to flooding. However, alteration to the rivers by dams leads to sediment-starved river flow (hungry water). Thus discharge, which is sediment deficit erodes the riverbed and bank, aggravates the riverbed downcutting and river bedrock exposure. Therefore, the eroded part of the river gets deficit in limited or no gravel availability, while gravel provides suitable spawning habitat for the fish community (Kondolf, 1997).

The excessive erosion leads to armoured riverbeds that have exposed bedrock at the bottom of the river. Such river condition restricts the vertical connectivity, where hyporheic zone does not exist; therefore, benthic (river- bottom) invertebrates such as molluscs, crustaceans, and insects will no longer be part of the ecosystem or food chain. The benthic fauna becomes food for fish species. Contrary to such conditions, sand or silt aggradation smooths the river bottom by clogging interstitial space between gravel riverbeds (McCully, 1996; Jones et al., 2012; Buendia et al., 2013; Itsukushima, 2021). Thus, excessive riverbed degradation and aggradation lead to the destruction of the aquatic habitat (Lisle, 1989).

Thus, headwater and downstream connectivity must be viewed and managed from the perspective of sediment dynamics problem to restore near-real pristine geomorphic condition in conjunction with an ecologist viewpoint, preferably because deviation in river connectivity hampers adaptability of the aquatic biota to the adverse river environment (Pringle et al., 2000).

The following section discusses river connectivity, hydrological connectivity and modelling tools to establish spatial-temporal variation for the catchment hydrology. The section also highlights the physical habitat and small dam or weir impacts. Lastly, sediment management approach addresses sediment dynamics at the river network scale by utilising tools that provide insights regarding strategies and prioritising dam removal as an option for sediment management. Sediment routing model deals with multiple dam situations and their ability to trap sediment (sediment trap efficiency), and it explains how multiple dams and weirs impact sediment flux under various discharge scenarios?

1.3 River connectivity

A river's ability to redistribute sediment, organic matter, water, and organisms depends on connected pathways and the inherent nature of free-flowing rivers. A river's connected pathways exhibit four different connectivity dimensions; longitudinally, laterally, vertical, and temporal (Ward and Stanford, 1993, 1995a; Grill et al., 2019). *First*, the flux (water, sediment, solute, organic matter) in the longitudinal direction leading from headwater zone to mouth defines the river's longitudinal connectivity (Wohl et al., 2017). The longitudinal connectivity often gets disrupted by a dam or barrier structure, and it impacts discharge, sediment, nutrient, and organisms in the upstream to downstream direction of the river channel.

Second, lateral connectivity is between the river channel and its floodplain, which can be temporary or permanent, and lateral connectivity varies on flow regime in parts of the river reach. Lateral connectivity provides space for peak discharge conditions to maintain the water level downstream by flooding the river floodplain. The lateral connectivity flourishes healthy floodplain habitat by exchanging sediment, nutrients and organism movement (Bolland et al., 2012). Thus, lateral connectivity plays a vital role in floodplain and wetland habitat sustenance Figure 1.4, (Ickes et al., 2005; Burgess et al., 2013; Cienciala et al., 2020). The dis-connectivity between the active river and floodplain results in the loss of marginal transitional habitat, which serves as a refuge to juvenile fishes during peak flow conditions. Hence, in river restoration plans, emphasis

must be given to re-establishing lateral connectivity that gets influenced due to flow regulation (Ward and Stanford, 1995b).

Third, vertical connectivity signifies the connection between hyporheic water and river water. The hyporheic zone with suitable sediment becomes an essential habitat for invertebrates, providing food for other aquatic fauna. The symbiotic relation between hyporheic riverbed and fauna gets disturbed under varying conditions such as extraction of sediments from the riverbed, hydrological regime change, quality of river and groundwater degradation and temperature variations. Vertical connectivity faces local interference because a dam and other water resource structures form reservoirs for storage purposes. The stored water changes local groundwater level by the fluctuations in river water level. However, increased water level improves soil pore water pressure and facilitates bank and valley erosion (Fujita, 1977; Zhan et al., 2006). The released sediment pulse into the river system is challenging to trace, and the volume of released sediment is equally difficult to measure. However, aggradation of fine sediment on the riverbed or excessive bed erosion can indicate past transport conditions. Thus, maintaining vertical connectivity in a river environment supports a healthy riverine ecosystem (Boulton, 2007).

Fourth, temporal connectivity superimposes time dimension on longitudinal, lateral and vertical connectivity (Ward, 1989; Grill et al., 2019). All river connectivity pathways are dynamic and subject to alterations in spatial and temporal river flow.

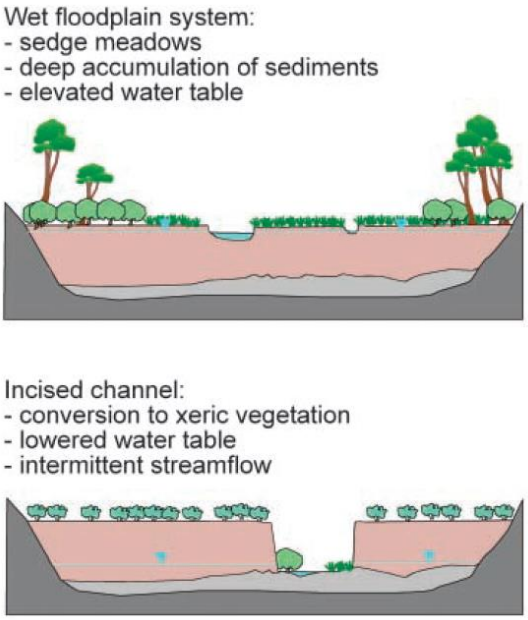

Figure 1.4 Channel incision had transformed the river ecosystem from wet meadow and forest ecosystem with stable river condition to intermittent river with xeric floodplain upland vegetation (Beechie et al., 2010).

Why is river connectivity of prime importance? The natural river response to pristine vs highly obstructed river system, and river's role in landscape modification because a river acts as a conveyer belt and redistributes matter from degrading landscape or source to sink areas. The nutrient, sediment, water, and organic matter are delivered from distributed catchment parts to the sink area. A highly connected river system provides life to the biotic component (flora and fauna) movement in a back-and-forth direction that depends on the life stages of the organism and their adaptability to the specific geomorphic condition of the river system.

Apart from mentioned reasoning, river connectivity can be helpful in many ways. First, the river system's spatial and temporal connectivity can proxy sediment flux measurement and landscape degradation. Second, river connectivity defines natural or human-induced impacts and the river's resistance and resilience to those changes. Human activity impacts a river's morphology and ecosystem (Sabater et al., 2018; Vercruysse and Grabowski, 2021). In other words, river connectivity is defined or transformed by natural and human-induced geomorphological adjustments. The river's ability to adapt with geomorphological adjustments can transform the landscape and fluvial forms, ecology and resilience over time (McCluney et al., 2014). River connectivity alterations can induce new hydro-sedimentary conditions and reduce the river's resilience property (Calle et al., 2017). Third, connectivity

conceptualises the river's connected processes as a framework to monitor processes in a spatial context. Forth, river connectivity facilitates the recognition of river network parts and the causative factor that can emerge as an obstacle to the natural process. Fifth, the connectivity framework explains the non-linear behaviour of the river system or to what extent rivers exhibit disconnectivity at the network scale. Finally, connectivity contributes to identifying factors for river restoration or management purposes (Wohl, 2017). Since river's obstructed or disconnected reach sections offer the best sites for restoration and management works, irrespective of natural or artificial disconnectivity.

The river connectivity framework is crucial to deal with the complexities of the fragmented river system and its restoration (Poeppl et al., 2017). However, the primary energy source responsible for the movement of sediment, organisms, and nutrients is hydrological drag generated through flowing water. It is a prerequisite to address the issues of hydrological connectivity and its influence on sediment connectivity and physical habitat.

1.3.1 Concept of Hydrological connectivity

The hydrological connectivity in its purest sense is the transfer of matter, energy and organism through flowing water within different components of riverine landscape (Hooke, 2003; Freeman et al., 2007; Bracken and Croke, 2007; Bracken et al., 2013). The flow response of a river catchment varies on multiple characteristics such as the shape of the catchment, land use, geology, soil, and rainfall pattern for the region. However, a catchment under the same characteristics could vary its hydrological response if the catchment is subjected to artificial barriers of different sizes and storage capacity. Stored water is channelised for irrigation, hydroelectric or inter-basin transfer. Thus, it can heavily fluctuate longitudinal river connectivity because the water volume released downstream is not adequate to maintain a natural connection between all components of the riverine landscape and in downstream region of the catchment. Therefore, dams with significant storage can severely impact the hydrological connectivity (Ibàñez et al., 1996).

Consequently, low discharge in the downstream river creates hydrological conditions that prevent lateral connectivity between the river and floodplain.

From the ecosystem perspective, river flow and longitudinal connectivity have a functional effect on river biota since flow alters oxygen demand of water, sediment transport and deposition, which result in habitat modification, and such cumulative conditions become hostile for fish like salmonid (Bunn and Arthington, 2002; Warren et al., 2015). The flow variability (peak flow) increases the risk of dislodgment of the lotic organism (Giller et al., 1998; Statzner et al., 2003). Peak flow can wash out juvenile fish. However, fish get stranded in disconnected river reach at low discharge conditions (longitudinal dis-connectivity under low discharge). Thus, river hydrological connectivity is essential for a healthy and thriving river ecosystem.

At present, river restoration-related efforts have concentrated on the ecological integrity of the river system, and restoration of the natural flow regime is becoming a prime objective since the flow regime directly influences inorganic and organic matter transported to the physical habitat of the river. Alteration to the natural flow regime can threaten the river and wetland ecosystem (Petts, 2009; Yarnell et al., 2015) by disrupting longitudinal and lateral connectivity. Thus, It is imperative to address the flow regime influence on riverine ecology, river structure and physical processes.

The flow regime stages impact river connectivity and habitat, illustrated in Figure 1.5, expressed in four basic principles (Bunn and Arthington, 2002). Principle 1 explains the interrelationship between a river’s physical nature and associated biodiversity under varying hydraulic conditions that influence channel form and shape, controlling aquatic organisms' distribution and abundance. Principle 2 explains flow regime events that have influenced aquatic organisms' life history, according to the adaptability to suitable habitat availability with flow seasonality or flow pattern (in space and time). Principle 3 explains the natural flow regime's maintenance, facilitating organism movement and accessibility to aquatic habitat in the longitudinal and lateral direction (floodplain & wetland access). Principle 4 explains the changes in the river's past decade's flow regime due to catchment management and land use alteration.

Consequently, native biodiversity declines because aquatic biota adapts to the catchment's natural flow regime. Abrupt changes in flow regime cause a decline in native biodiversity fauna and favour invasive species invasion. Therefore, studying and establishing hydrological connectivity for a longer time scale which is highlighting spatial and temporal variation in the system and leads to insightful information for restoration of the natural regime from a river engineer and conservationist perspective (Tharme, 2003; Arthington et al., 2006; Beechie et al., 2010).

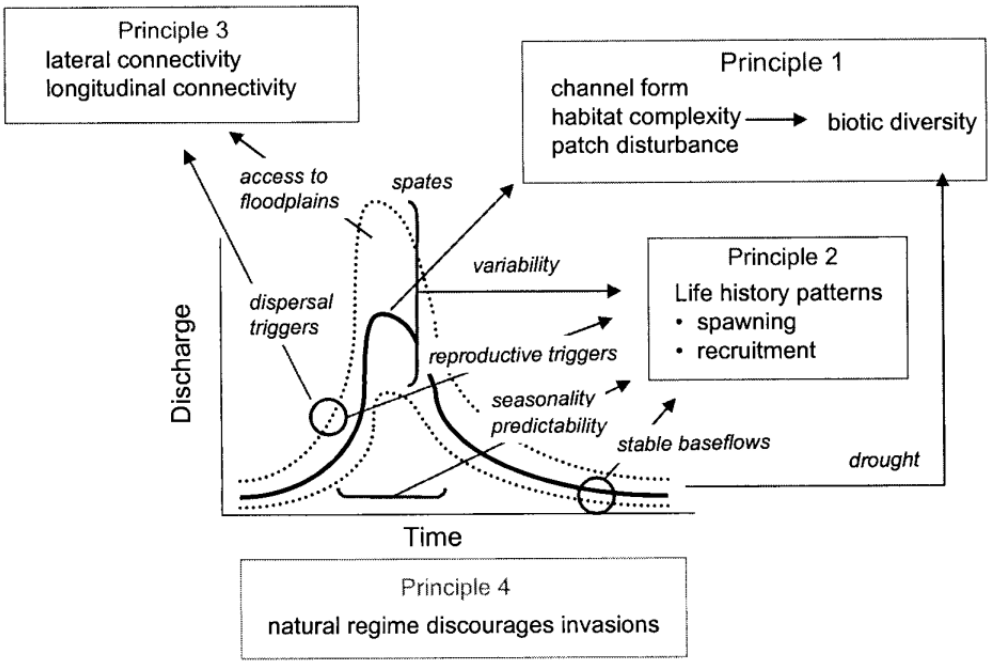

Figure 1.5 Different stages of flow regime influence aquatic habitat (Bunn and Arthington, 2002).

In managed river catchments, the flow regime varies under different spatial-temporal conditions. Thus, the longitudinal, lateral, vertical connectivity of rivers (base flow contribution when river faces low flow conditions) fluctuates under different seasons (temporal connectivity), and thus four river connectivity dimensions can be a conceptual tool for the assessment of human impact (Tockner et al., 1999; Amoros and Bornette, 2002; Freeman et al., 2007).

The river connectivity and ecological adaptation are based on river gradient available energy. The river continuum concept (RCC) interprets a river system as an uninterrupted system, and in principle, RCC provides a framework for the

predictable existence of biological features under varying physical-geomorphological environments (Vannote et al., 1980). However, river fragmentation gives rise to the serial discontinuity concept (SDC) in lotic systems (Stanford, 1983; Ward and Stanford, 1995a).

Moreover, serial discontinuity can leave a river system in many lotic and lentic sub-systems, resulting from longitudinal (hydrology, sediment transport) and biotic disconnection at the reach scale. Hence, longitudinal connectivity in a fragmented river system must be understood based on hydrology, sediment transport and collective repercussion on fluvial ecology (Jungwirth et al., 2000).

Therefore, assessing hydrological connectivity in a river catchment for a more extended period requires hydrological modelling that provides distributed hydrograph for sub-catchments based on mentioned physical, climatic, and human influence conditions for overland, river routing estimation. It is crucial to assess catchment hydrological behaviour for an extended period because selecting a short duration hydrological assessment can result in a completely different picture of a river catchment. The river catchment's hydrological response changes yearly, and observation made only on drought years or flood years can be misleading. Therefore hydrological assessment and hydrological connectivity should be assessed for a long duration, together with spatial-temporal diversification in hydrology provides an evaluation of sediment transport, consequently evolution in morphology & physical habitat (Sedell et al., 1990; Richter et al., 1998; Covino, 2017; Mellado-Díaz et al., 2019).

1.3.2 Establishing hydrological connectivity with modelling

The hydrological response defines the pace of the geomorphological adjustment based on multiple natural factors such as hydroclimatic, land use, soil and human interventions. However, the River’s reach processes and their connected links at the river network scale should be observed at various space and time dimensions to estimate distributed discharge and sediment flux (diffused and concentrated) of different intensities (Passalacqua, 2017; Wohl et al., 2018). However, hydrological connectivity between landscapes and in-stream environments is complicated, non-linear, and scale-dependent (Lesschen et al., 2009).

In addition to the real-world river connectivity gets virtually interrupted in the digital environment; for example, a local sink in a DEM can act as a dis-connectivity for water and sediment movement in a high-resolution modelling environment. The digital imperfections of elevation data can be prevented with processing algorithms – fill sink. However, a high-resolution environment severely limits processing time but offers better spatial diversity in the modelling environment, and thus it improves distributed hydrological assessment (Di Luzio et al., 2005).

A rainfall-runoff model can simulate good quality distributed hydrograph at the river reach scale; for example, MIKE SHE, MIKE HYDRO Basin, HEC-RAS, HEC-HMS, HBV, SWAT, WEPP models (Devi et al., 2015; Yuan et al., 2019; Horton et al., 2021). Studies show that basin and catchment scale hydrological diversity is well represented by the SWAT model and can model hydrology, nutrients, sediment, bacterial pollution, and impact of management practices (Dilks et al., 2003; Jayakrishnan et al., 2005; Ullrich and Volk, 2009; Vu et al., 2012; Baker and Miller, 2013; Thavhana et al., 2018). SWAT model also utilised for climate change studies (Bouraoui et al., 2002; Boorman, 2003; Gassman et al., 2007; Ficklin and Barnhart, 2014a), and it is capable of simulating hydrology and sediment concentration at daily time-step (Glavan et al., 2011; Glavan and Pintar, 2012). In the European water framework directive that suggests integrative river catchment management, and has the fundamental goal of the better ecological and chemical state of water bodies, in such cases, SWAT can address EU water framework objectives (Arnold and Fohrer, 2005; Van Griensven et al., 2006; Volk et al., 2009; Grusson et al., 2017b).

However, physical model like WEPP (Water Erosion Prediction Project) has performed slightly well compared to conceptual semi-distributed SWAT model (Shen et al., 2009). Nevertheless, the SWAT model can simulate large river catchment with higher spatial variability than the WEPP model, designed for small watersheds. Though, nutrient pollution modelling at higher temporal frequency is not recommended with the SWAT model (Glavan et al., 2011; Hollaway et al., 2018). Contrary to that, some studies have stated that the SWAT model can perform realistic simulation of nutrients load (Jayakrishnan et al., 2005; Radcliffe et al., 2015; Nguyen et al., 2019).

A deterministic physically based distributed model, MIKE-SHE, had simulated better results than the SWAT model (El-Nasr et al., 2005). However, MIKE-SHE requires input data sporadically, whilst SWAT can simulate hydrology in a data-poor region. In addition to that SWAT, parameters can be estimated with calibration if boundary condition related information is accessible to the modeller. A comparative review of a hydrological model such as VIC (variable infiltration capacity), MIKE-SHE, HBV (Hydrologiska Byråns Vattenbalansavdelning), and TOPMODEL; only SWAT model with little direct calibration found to be capable of simulating better hydrological results than mentioned models (Borah and Bera, 2004; Devi et al., 2015; Hamman et al., 2018).

The groundwater component of the SWAT model is of lumped nature, and therefore it is not suitable for hydraulic conductivity, aquifer storativity and distributed pumping influence on catchment-scale hydrology (Singh and Frevert, 2010). Thus, a catchment unaffected by extreme groundwater exploitation, SWAT can still be used for hydrological analysis.

Despite mentioned advantages and disadvantages, the SWAT model has algorithm and sub-models that are capable of simulating land use, soil, management practice and climate change variability on hydrology, sediment and water quality (Romanowicz et al., 2005; Bärlund et al., 2007; Easton et al., 2008; Vigiak et al., 2017; Yu et al., 2018; Holder et al., 2019; Jodar-Abellan et al., 2019; Bauwe et al., 2019). The model can also simulate sub-daily hydrology and sediment erosion pattern for an extended period (Jeong et al., 2011; Jodar-Abellan et al., 2019). SWAT model's potential is used to address ecosystem services presented in studies conducted across the world (Post et al., 2008; Swallow et al., 2009; Cools et al., 2011; Vigerstol and Aukema, 2011; Mwangi et al., 2015; Francesconi et al., 2016), and it is recommended as a decision making ecological model for evaluation of freshwater resources and planning purposes (Ranganathan et al., 2008; Arias et al., 2011; Norman et al., 2012; Logsdon and Chaubey, 2013). In conclusion, the SWAT model can address a range of hydrologic and environmental problems, which is why it has been utilised worldwide (Horton et al., 2021).

The distributed hydrograph provides valuable insight into sediment flux moment at river network scale since variations in hydrograph are simulated at different times and spaces. However, many hydrological models can overwhelm a modeller for the suitable tool selection to simulate a specific catchment's physiographic and climatic conditions and their consequence on hydrology. The selection of hydrological model can be based on its ability to address the catchment specific requirements such as data input, ability to simulate secondary data (input parameter), ease of parametrisation, and quantification of uncertainty in the model's result (Beven, 1990; Beven and Binley, 1992; Beven, 1993; Bloschl and Sivapalan, 1995; Beven, 2006, 2012).

Moreover, in the present case, a hydrological simulation was performed to achieve distributed hydrograph of varying intensity in the last 55 years (for 166 reach) to infer the resulting changes in sediment flux at the Eamont river network.

1.4 Physical Habitat

Before addressing the physical habitat and its importance for the river ecosystem, one of the broader questions arises, *what is river health, and why it is of prime importance?* Physical habitat conditions monitored and appreciated for riverine ecology, geomorphic and river conservation studies (Frissell et al., 1986; Fitzpatrick, 1998; Palmer et al., 2005; Thomson et al., 2001; Fisher et al., 2012), and state of river habitat direct reflection of river health condition, in terms of geomorphic, variation in flow within river reach, diversity and abundance of aquatic flora and fauna. Traditionally, river health is measured based on river water's physical, chemical, and biological character. It is subject to change at short time scales and represents the conditions at the river reach scale. However, each sample characterising physical, chemical, and biological nature varies with space and time.

Freshwater biotic measurements for the physical habitat or ecological quality have gained acceptance (Norris and Thoms, 1999). The main reason for biotic measurements based on aquatic biota adaptation to river's specific physical habitat state: flow regime, sediment transport, which defines the availability of

suitable physical habitat, water quality, and biological interaction with abiotic factors define the overall health of the river system.

Abiotic factors like fine sediment are the biggest threat to physical habitat quality and biological mortality under high turbidity conditions (Jones et al., 2012; Buendia et al., 2013). Hence, spatial-temporal change in flow, sediment transport, grain size distribution, substrate type and aquatic vegetation provide suitable physical habitat or state of the river (Maddock, 1999; Brooks et al., 2005; McCabe, 2010).

The continuum concept addresses biological factors' adaptability to river geomorphic forms at different scales of physical habitat macro, meso, and microhabitats. The physical habitat information measured and recorded at the field investigation unit is defined for different scales under physical habitat survey guidelines (*e.g.,* the *River Habitat Survey* framework used in the UK).

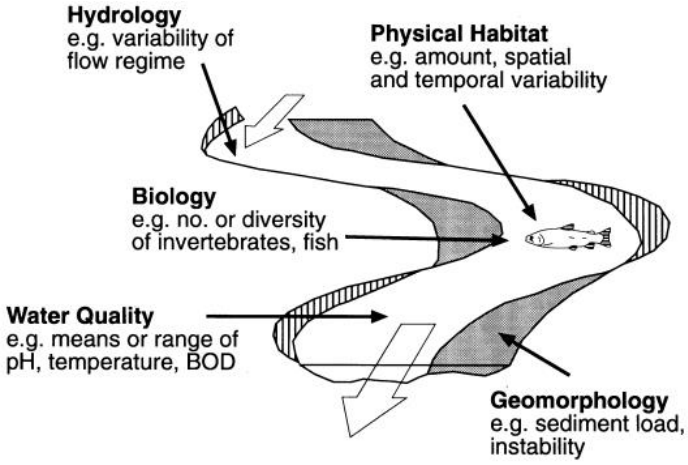

Figure 1.6 Tools for assessing the health of the River (Maddock, 1999).

Physical habitat units are easy to identify from the riverbank and recorded in the physical habitat survey questionnaire. Habitat survey information is very detailed and subjective and performed at a few meters' intervals for river habitat classification purposes. Because field assessment and verification are limited to 100s of meters, completing a physical habitat survey of a river network becomes subject to the experience and interpretation of the surveyor. Physical habitat survey is a tedious and time taking process. However, habitat unit

identification is possible from the riverbank, yet biological diversity and their function are difficult to ascertain (Maddock, 1999; Hill et al., 2008).

A geomorphic unit survey was proposed for the spatial hydro-morphological features identification at the river to reach scale for European rivers (Rinaldi et al., 2015; Gurnell et al., 2016). The geomorphic units survey (GUS) constitutes the physical structure that underpins the habitat units. The geomorphic units (Macro unit, unit and sub-unit) are organised into spatial domains, bankfull channel, and floodplain (Belletti et al., 2017). The repeated assessment of geomorphic units for physical habitat can reveal their dynamics by integrating remote sensing and field survey methods. For that reason, high-resolution data suggested and in the case of unavailability of DEM or LiDAR data will require intensive field survey. This method is faster than conventional field based physical habitat survey. GUS method supports integration with hydro-morphological assessment at reach scale (i.e., Morphological quality index (Rinaldi et al., 2013)), thus providing a better understanding of hydro-morphological conditions of the geomorphic unit and related biological conditions assessment. However, assessing physical habitat conditions for a river network scale still requires a high amount of remote sensing data and field surveys.

Although river fragmentation interferes with environmental flows, it also impacts the sediment transport process at the river scale. Thus, it is essential to maintain the natural flow condition and preserve the in-stream physical habitat state. The river flow conditions often deviate from the natural flow regime for most rivers. Contrary to that, the dam's prime objective is to exploit the water and energy in a regulated river system. Semi-arid and sometimes temperate regions experience drought conditions; in such a scenario, environmental flow set limits are seldom achieved. In a highly regulated river environment, the sediment transport processes are heavily impeded by the sediment trap efficiency of the dam structures and several dams situated in the upstream and downstream region of a river catchment. Thus, employing physical habitat survey or GUS hydro-morphologic feature assessment at a higher frequency would not add much value to the last survey unless the flow and sediment transport process managed to near pristine condition.

The following section highlights the sediment trap and physical habitat conditions that emerged because of a small dam or weir situated at the river network. The drone images describe the weirs impact taken from the ‘Europe dam removal movement’, and the case represent pre-and post-dam removal conditions of "Mollo dam" on the River Ritort (Catalonia, Spain).

1.4.1 Small dam or weir's impact on physical habitat

Understanding the fundamental geomorphic changes, a weir or small dam can bring into the river system is crucial. Regardless of their size, the weir acts as a sediment barrier and creates a backwater effect that promotes gravel accumulation in upstream river reach, which changes the local base level (Gardner, 2017) (Figure 1.8 & Figure 1.9).

Figure 1.7 Weir removal (also known as Mollo Dam) at the Ritort River (Spain) shows upstream gravel accumulation and local base-level changes while the weir was functional.

In downstream reaches, flow over a weir, or small dam structures perform churning effect of water (downward & upward cyclic movement of water) that intensify riverbed erosion, this churning action forms a deep pool immediate to weir location. The churning effect of water and weir height adds a double whammy to fish's ability to migrate in the upstream direction, searching for spawning habitat. Water flowing on the weir structure is devoid of sediment at

normal flow conditions except peak flow state. The water devoid of sediments (hungry water) affects bank stability, bed-erosion, and it transforms riffle-pool morphology that acts as a spawning zone for many species into pool morphology. Thus, river hydraulic conditions deteriorate due to such obstructions and result in loss of natural flow variation, leading to adverse effects such as incised and upstream backwater effects (Csiki and Rhoads, 2010) (Figure 1.9).

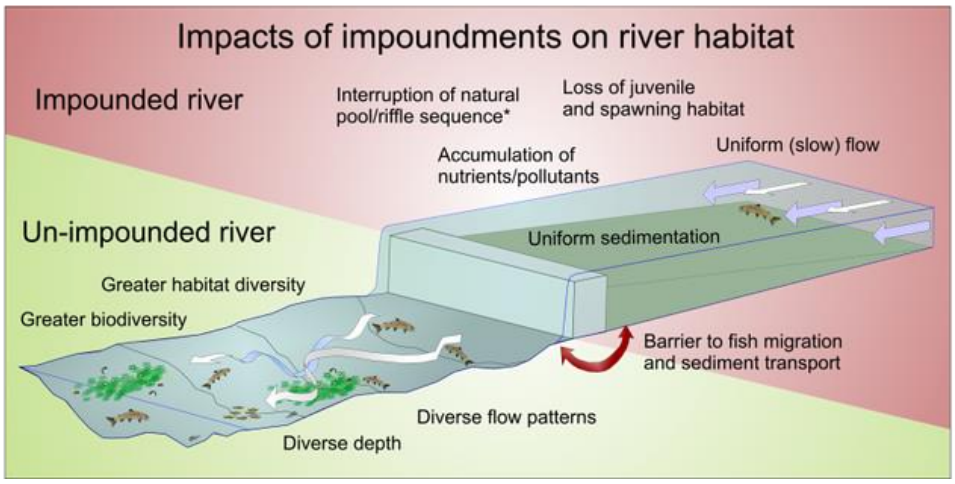

Figure 1.8 Weir's impact on river flow, sediment, and habitat (Gaskell, 2021).

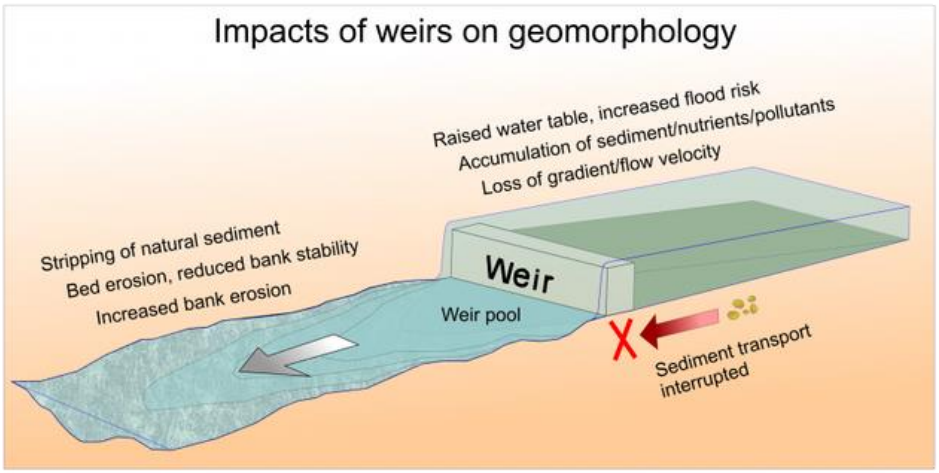

Figure 1.9 Weir's impact on river geomorphology & Sediment transport (Gaskell, 2021).

Even small weir structures can have marked control on river ecology and in-stream flora and fauna (Morita and Yamamoto, 2002; Shafroth et al., 2002; Sethi et al., 2004; Mueller et al., 2011; Yan et al., 2013). The degraded habitat

can impact along river stretch both upstream and downstream. The siltation of weirs upstream reach and coarsening of downstream riverbed degrades the physical habitat condition. The installation of a fish pass cannot restore the spawning site, which is vanished due to sediment trapped in the backwater region of the river. Therefore, weir removal will lead to the healing of the river stream through the recovery of natural sediment transport patterns. Consequently, weir removal or partial removal is preferred over cosmetic treatment like fish pass installation (Leaniz, 2008; Fjeldstad et al., 2012; King and O'Hanley, 2016).

On the other hand, weirs or small dams' impacts on sediment transport and geomorphology can be site-specific (Csiki and Rhoads, 2014). The response to geomorphic adjustment on physical habitat may vary with the temporal history of the river regime, habitat heterogeneity, and spatial scale (Poff and Ward, 1990). Habitat heterogeneity varies throughout the river space, and thus, physical habitat diversity is emphasised at the river network scale (Wiens, 2002). On a river network scale, river morphology and physical habitat contrasts based on river network's basin size, drainage density & pattern, confluence density, geology, substrate and many other factors, thus employing an approach to address the hydro-geomorphology and physical habitat heterogeneity at river network scale would contribute to strategies river habitat or health restoration efforts (Benda et al., 2004). However, physical habitat mapping to ascertain the river health condition or planning for river restoration is recommended at the meso-habitat scale (Newson and Newson, 2000). Though, mesoscale habitat information establishment is time-consuming and tedious because a river habitat survey questionnaire performed at 10m spot-checks for a section of a river reach (Raven, 1998).

The current study is performed at the Eamont river catchment on a reach scale. The study executed on the focal point of sediment transport from source to sink approach and its impact on geomorphology and physical habitat based on grain specific sediment flux entrainment, transport, and deposition pattern at river network scale under different discharge scenarios. Thus, it tries to solve spatial and temporal dimensions for sediment flux delivery for the Eamont river.

1.5 Sediment transport and geomorphic impact

Rivers carry an enormous amount of sediment from continents to oceans (Milliman and Meade, 1983), although the amount carried by European rivers is smaller than other continental rivers. Evans (2006) had suggested that with the change of land use pattern, sediment yield had increased in British rivers. Still, sediment yield remains low in UK rivers compared to the rest of the world. However, river fragmentation in the UK and Europe could be one factor for low yield. The adverse impact of dams is evident since sediment starved water promote the downstream bed and bank erosion; consequently, geomorphological change occurs in the river system (Baxter, 1977; Petts, 1979, 1980, 1984; Kondolf, 1997; Nilsson, 2005; Graf, 2006). On the other hand, an inter-dam setting brings a morphological change in the river, in which erosion is immediately downstream of an upper valley dam and depositional geomorphic condition in the downstream valley dam. The concept of inter-dam river morphology shows geomorphological features development from the upper valley dam to downstream valley dam, Figure 1.10 (Skalak et al., 2013).

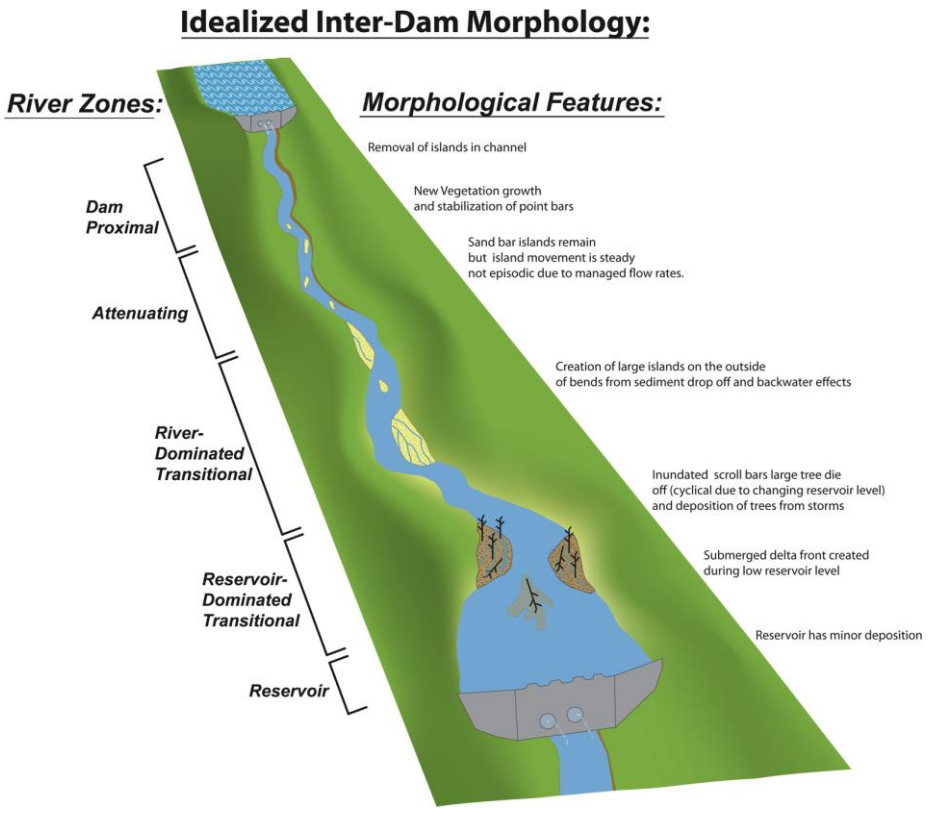

Figure 1.10 Conceptual model of river morphology resulting from Dam interaction (Skalak et al., 2013).

Small dams and weir structures impact river geomorphology to a lesser and more subtle extent compared to big dams. In recent time awareness related to small dams removal impact studies has increased (Juracek, 1999; Doyle et al., 2003, 2005; Santucci et al., 2005; Ahearn and Dahlgren, 2005; Thomson et al., 2005; Ashley et al., 2006; Orr et al., 2006; Roberts et al., 2007; Leaniz, 2008; Skalak et al., 2009; Walter and Tullos, 2010; Skorulis, 2014; Csiki and Rhoads, 2014; Dufour et al., 2017; Casserly et al., 2020). The early studies stressed finding solutions and developing science to tackle dam removal prioritisation problems in a multiple dam river site scenario (Charlton, 2010). Studies have also indicated changes in the depth and width of the downstream river and grain size distribution. The primary change followed by constructing a small dam was in the grain size distribution, and it favoured coarsening of the river bed and reduced fine grain size (Skalak et al., 2009). However, the geomorphic impact of weir studies have contradictory findings; few studies recommend that weir has no measurable impact on the river (Abbasi and Abbasi, 2011; Skorulis, 2014). Though dam impacts can vary based on the location of the dam related to rivers functional morphology (Montgomery and Buffington, 1997), because the rate of flow and sediment erosion and transport alters with hydro-geomorphic conditions in the different river reach sections (Mueller, 2005; Schmidt and Wilcock, 2008; Grant et al., 2013). The river transformation could be due to the alteration in the river's local base level and length. Any alteration in base level or river length can stimulate riverbed degradation (Galay, 1983), and local bed degradation can shift sediment erosion, transport, and deposition patterns in a managed river. In addition to that, a considerable amount of sediment gets trapped by dams and weirs. A sediment trap is a function of the dam's ability to capture incoming sediment flux and represents sediment trap efficiency.

A significant alteration in bed material load can occur at the tributary river confluence. It depends on tributary river catchment characteristics such as catchment's size & shape, soil, geology, slope, rainfall-runoff processes and resulting competent discharge in the tributary river valley. In contrast, bedload sediment size difference can occur due to the main river course obstructed by

dam and weirs, while the tributary river flows through pristine river valley settings. Thus, it is imperative to quantify small dams' sediment transport and geomorphic impacts and their coexistence with big dams at the river network. Multiple dams can heavily impact natural geomorphic processes and degrade habitat (Anderson et al., 2015). Consequently, habitat damage causes threats to aquatic flora and fauna adaptability to degraded habitat and ultimately decreases biodiversity (Shafroth et al., 2002; Lucas et al., 2009).

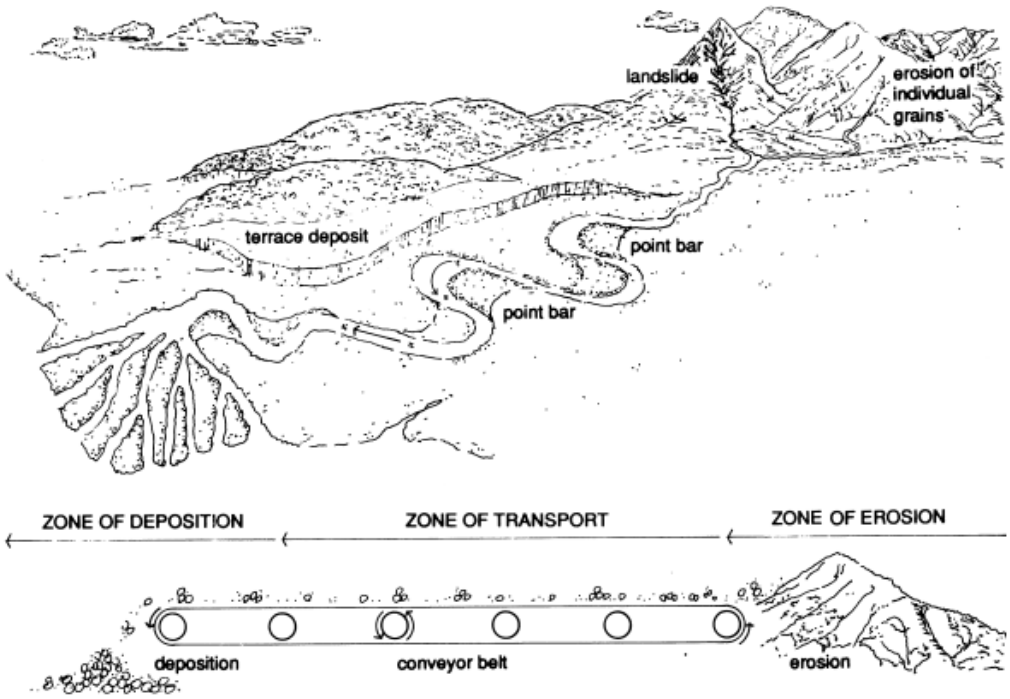

Figure 1.11 The interconnected river system, in which the sediment transport process plays a functional role in transforming fluvial geomorphology and ecology (Kondolf, 1997).

Ideally, sediment transport should be analysed at a river network scale with the perspective concept of a source to sink (Fryirs et al., 2007; Semrau and Hurck, 2012; Bracken et al., 2015; Li et al., 2016). The concept views sediment entrainment and transport through various geomorphic connected zones. It is imperative to address the sediment transport at the network scale because spatial and temporal variability occurs for suspended and bedload sediments (Ashmore and Day, 1988; Church et al., 1999; Ashmore and Rennie, 2013). In addition, sediment size diminution is observed in the longitudinal direction, which is affected by incoming sediment flux from headwater reach and the river

mouth (Rice, 1999). Distinctly, sediment size diminution occurs under available transport capacity, and shear stress variation from source reach to sink (terminus) reach. The spatial and temporal variation in sediment distribution reveals historical sediment transport patterns for a river system. Therefore, having hydro-geomorphic and sediment size distribution evidence at a river catchment provides crucial knowledge & evidence for river management and restoration planning. In gravel-bed rivers, disparate sediment sorting is caused by size-selective transport, which is most prevalent in the headwater region of the catchment (Lisle, 1995). The size-selective sediment transport is the consequence of the threshold difference (shear stress and transport capacity) for fine and coarse sediment entrainment and sediment supply (Lisle and Hilton, 1992). Sediment entrainment and transfer processes occur at the grain scale (Cooper et al., 2012).

A better connection between the hillslope erosion process and the in-stream network can enhance sediment transfer assessment (Cavalli et al., 2013). The connectivity can establish hydrological and sediment connectivity under various hydro-geomorphic conditions responsible for sediment flux and water transfer through different parts of river catchment (Cavalli et al., 2019). Thus, connectivity provides insight for landscape and instream degradation and aggradation information at different spatial & temporal scales, which fluctuate with the intensity of overland flow and river discharge. However, overland flow connectivity (hydrological connectivity) is hard to establish and yet to be implemented in models to quantify it spatially. (Bracken and Croke, 2007; Bracken et al., 2013).

On the other hand, sediment connectivity framework, which addresses sediment detachment, transfer, and deposition processes from a source to sink through the landscape and in-stream of a river catchment, analyse key sediment connectivity elements: 1) frequency and magnitude distribution of sediment transport process; 2) spatial-temporal quantification of sediment entrainment and transport processes; 3) mechanism of sediment detachment and transport. However, the hydrological drag intensity controls sediment entrainment, transport, and deposition processes, in the connected pathways (Bracken et al., 2015). The connectivity defines the connected pathways for

transferring water and sediment (Czuba and Foufoula-Georgiou, 2015; Fryirs et al., 2016). Thus, hydrological and sediment connectivity is implemented to analyse and predict how sediment flux moves across the catchment through connected and disconnected pathways. The established connectivity will explain landscape dynamics and enhance catchment environmental management practices by improving the river's natural connectivity (Kondolf et al., 2006; Csiki and Rhoads, 2010; Anderson et al., 2015; Dufour et al., 2017). Sediment connectivity can provide evolutionary trends and sensitivity to perturbation for a river with coarse sediments (Hooke, 2003), subject to linked sediment source, sediment supply and transport capacity variability at different space and time dimensions.

The river observation-based studies have supported size-selective sediment transport under steady flow conditions (Mao and Lenzi, 2007; Madej et al., 2009; Mao and Surian, 2010). Studying a river's morphology is complex, with varying hydro and sediment dynamic conditions, especially at the river confluence (Best and Rhoads, 2008). In such a complex environment, the implementation of numerical models favoured assessing sediment transport for the connected river sections responsible for sediment flux transfer (Jain and Tandon, 2010; Kleinhans et al., 2013; Heckmann et al., 2015).

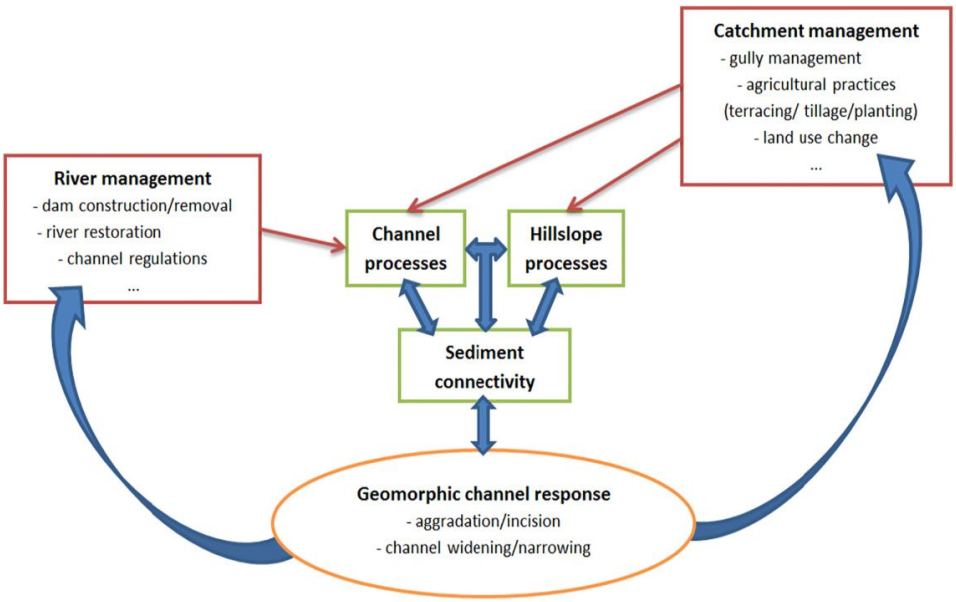

Figure 1.12 Schematic diagram explaining the role of sediment connectivity concept in the river and catchment processes and its importance in river management (Poeppl et al., 2017; Keesstra et al., 2018).

The graph theory models were applied at the field scale (Fressard and Cossart, 2019), coastal area (Pearson et al., 2020), at river network (Connor-Streich et al., 2018; Khan et al., 2021), within the catchment (Cossart and Fressard, 2017) for the assessment of sediment transport. Implementing and adopting a size-selective grain size model that processes sediment entrainment transport and deposition at a network scale can be a better option. To establish the connected source and their respective sink, in conjunction with dis-connected parts of the river network, which is based on transport capacity (hydro-geomorphic conditions), and dam or weir's sediment trap efficiency that affects the incoming flux from upstream reach to downstream reach.

Since sediment connectivity concept offers means to understand the complexity among river hydrology, geomorphology and ecology, which also provide an additional dimension for understanding human impacts on the river system and its feedback mechanism, Figure 1.12 (Poeppl et al., 2017). Thus, sediment connectivity helps evaluate the system dynamics, and it is recommended for the scientific application to aid policy-making (Keesstra et al., 2018).

For the mentioned statement, a sediment connectivity tool named "*CAtchment Sediment Connectivity And DElivery* (CASCADE) "framework uses graph theory to process the connected sediment pathways implemented in the current project. Sediment connectivity with graph theory finds possible connected sediment pathway that is implemented a numerical model (Wenger et al., 1999; Heckmann and Schwanghart, 2013; Schmitt et al., 2018b; Wohl et al., 2019). Such numerical models find connected sediment pathways and establish sediment connectivity. However, at the same time, it results in natural or artificial sediment disconnectivity, which helps in predicting dam removal scenarios development. Thus model will guide us in the management of better dam operation or in planning dam removal analysis (Pizzuto, 2002; Schick and Lindley, 2007; McKay et al., 2013; Branco et al., 2014; King and O'Hanley, 2016; McKay et al., 2017; Schmitt et al., 2018a; Ishiyama et al., 2018; de Leaniz and O'Hanley, 2021).

The project implementation and goals defined in the following section explains why it is crucial to develop insight into river fragmentation's impact on the

geomorphic state of the river and consequent degradation of physical habitat and ecology of the river system. However, the project was executed and processed at the resolution of the river reach scale.

1.6 Dam Removal as an option of river restoration

As mentioned earlier, the level of fragmentation in the world and the European continent is becoming a significant problem; fragmentation and the resulting decline of biodiversity is a fundamental cause of concern. River fragmentation is a functional dis-connectivity, which restricts an organism's movement to complete crucial life stages. The physical dam removal that reconnects the river and its removal authority often fall with political will and bureaucratic administration. Hence, scientific reasoning and planning would be appropriate to convince all to achieve harmonious river restoration objectives.

Adaptive management of barrier removal is a way forward to find a balance between environmental protection and the ever-increasing human population (Lee and Lawrence, 1985; Stanford et al., 1996; Ormerod, 2009; Wilby et al., 2010). Human reliance on water resources and their exploitation has to find a solution without conflicting environmental protection and water requirement for human consumption or use (Falkenmark, 1986; Poff et al., 2003; Palmer et al., 2008; Newson, 2008). During the industrialisation era, water resources were exploited as a free resource, and river space was fragmented by barriers, resulting in rivers clogged with trapped sediments. The declining trends of freshwater biodiversity have compelled river managers and policymakers to accelerate river restoration efforts. River restoration is more inclined towards biological community restoration than just geomorphic conditions. However, river restoration efforts must focus on the catchment scale rather than site-specific restoration attempts (Stanford et al., 1996; Bohn and Kershner, 2002).

In other words, restoration work restricted to limited river stretch may fail to produce a fruitful outcome because of its piecemeal restoration nature. Additionally, site-specific measures are against the river continuum concept, and it keeps geomorphic conditions and biodiversity declining threats unsolved unless entire river network scale fragmentation is considered to improve overall river and habitat connectivity (Bond and Lake, 2003; Bernhardt et al., 2005).

Removal of barriers that are impassable for the biotic community, especially fish and other communities because they move in back & forth direction in the river, and towards sea based on their life stages. They search for suitable spawning physical habitat required for offspring.

Climate simulation models predicted elevated flood risk in the winter months due to winter rainfall patterns (Richardson, 2002; Wilby et al., 2008; Coulthard et al., 2012). While in the northern part of the globe, winter months will be wetter than the southern region in the projected runoff change trend for Europe (Stahl et al., 2010; Kiesel et al., 2019). Earlier, climate model projections at the river catchment scale were complicated due to the climate data downscaling problem (Prudhomme et al., 2002, 2003). Recently, high-resolution climate data (1km resolution) availability provides an opportunity to access hydrological alteration in space & time at the river catchment scale (Prudhomme et al., 2012). Therefore, adaptation strategies to minimise climate ramifications in managed river catchments are highly recommended and termed "adaptive management". The typical management recommendations for a regulated river catchment are stormwater and sediment management, dam removal or retrofitting, riparian vegetation, channel reconfiguration, riverbank and floodplain management, water quality and flow management, fish pass installation, and addressing conjunctive ground/ surface water uses (Palmer et al., 2008). These management actions in regulated rivers would improve the longitudinal and lateral connectivity, and it is going to impact available free-flowing river space in regulated river catchment than other site-specific management action. Therefore, dam removal is a widely accepted river restoration activity (Magilligan et al., 2016; Foley et al., 2017). However, uncertainty associated with dam removal action is higher because dam removal impacts projects typically involve less than five years of monitoring, and lack of catchment condition assessment (alteration in river catchment pre & post dam removal period) can be the reason for the paucity of knowledge (Darby and Sear, 2008; Foley et al., 2017). The recommended time scale for studying fluvial restoration work is defined as at least a decade or more, and this is because the geomorphological process takes longer space and time scale than civil engineering works (Sear et al., 1995). Management actions to restore

fluvial systems have uncertainty, yet these actions and monitoring provide valuable feedback, which is essential for understanding adaptive management actions (Newson and Clark, 2008). Because sustainability itself is an evolutionary approach and restoration efforts may not recover the system in its original state, river restoration can bring the system in a better environmental condition even if it is not identical to past conditions (Large et al., 2012; Schmutz et al., 2018).

The problem with restoration at the river catchment scale is that water physio-chemical properties change at a higher frequency, and biological diversity requires a history of the species and may require reintroducing the species to the physical habitat. However, the availability of pristine habitat is subjected to human influence regarding the land-use change (Sutherland et al., 2002), river management related issues such as pollution point sources, flood control, sediment trap efficiency. These issues fall between the process-based and evidence-based approaches, and both vary in space and time. However, process-based approaches often employ empirical models to guide management approaches, and with the advancement in computing power and sediment transport modelling, this has opened a new avenue for river restoration (Nelson et al., 2003).

Physical habitat suitability and geomorphic conditions are linked with coarse sediment supply, transport, and deposition. Fine-grain sediment transport is supply-limited and coarse sediment both supply-limited and transport-limited and controlled by flow conditions variation in the riverscape (Milhous, 1973; Cui and Parker, 2005), and this variation facilitates the formation of different morphological and physical habitat conditions. Disparities in morphology and habitat occur with size-selective transport and the advancements in fractional sediment transport equations, now it is possible to implement fractional sediment transport equation in the numerical model (Tangi et al., 2019a) and predict the sediment transport and depositional pattern, which consider the presence of sand and gravel, and mutual impact of sediment movement (Wilcock and Crowe, 2003). There is a surge in the development of numerical models to simulate dam removal impacts (Cantelli et al., 2007; Grant et al., 2008; Downs et al., 2009; Greimann, 2013; Podolak and Wilcock, 2013; Gartner

et al., 2015), and revealed the importance of grain size distribution information in numerical modelling (Ferrer-Boix et al., 2014).

Sediment movement from the prospective sediment source to sink can be achieved in conjunction with graph theory and sediment transport modelling, preferably fractional sediment transport modelling, and it has been realised in the CASCADE framework (Tangi et al., 2019a). CASCADE is adopted in the present case to develop fractional sediment flux analysis for the Eamont river catchment by simulating impacts for barriers on the Eamont river network. The simulation was performed with different flow conditions and a combination of dam removal scenario impacts at the reach scale. In the current study, the Eamont river catchment's sediment routing was performed with the consideration of 18-grain size classes mentioned in 'Krumbein phi scale (Φ)' that ranges between Boulder (-9.5 Φ) and silt (7.5 Φ). Therefore, the CASCADE model has simulated sediment routing for the entire grain size range used for the parametrization. However, the Eamont river flows through a hard rock train and predominantly a gravel-bed river. Hence, routing for sediment phase is performed for the gravel & sand particles because weir structures allow the movement of fine and suspended sediment contrary to that traps gravel and sand particles. The analysis is based on sediment class range between -5.5 Φ and -1.5 Φ for weir removal scenario development, and annual sediment flux is estimated for the whole sediment class used for the parametrization.

Dam removal has gained popularity among river engineers, environmentalists and fish biologists, and it is recommended to focus on hydrology, geomorphology and ecological integrity for any river restoration programme (Hart et al., 2002; Clarke et al., 2003). Europe is adopting dam removal to improve rivers' ecological state, which has gained momentum following the Europe water framework directive in 2000 (Schiermeier, 2018). Dam removal is the quickest way to improve the hydrological, sediment and ecological connectivity because any limitation to RCC would result in fragmented habitat conditions and its causative impact on the migratory fish community (Neraas and Spruell, 2001; Santucci et al., 2005). The negative response of small dam removal can be transit nature and local, while their ecological benefits may require long term monitoring (Bushaw-Newton et al., 2002).

However, dam removal may not be an appropriate option for ecological balance as fine sediments can suffocate downstream reaches in a post-dam removal scenario (Sethi et al., 2004). Though sediment flux leaving post dam removal activity may vary, which is subject to the dam's size (height) and trap efficiency. Predominantly, big dams trap a more significant fraction of sediments than small dams that trap a modest amount of sediments. As mentioned earlier, the ecological benefit cannot be expected in a short span post dam removal; therefore, considering and assessing the geomorphic impact of dam removal requires longer timescales of monitoring. Dam removal activity can bring a few notable geomorphic changes in the downstream river, such as reservoir erosion, downstream deposition, river gradient & river width change, river bed texture, bedforms and channel pattern change (Major et al., 2017). Crucially, grain size distribution plays a vital role because it determines the sediment movement and extent of sediment transport under different discharge scenarios, thereby likely changes in the geomorphic state of the river. Fine sediments have less impact than coarse sediments on the downstream river because fine sediments fill interstitial space and become part of the suspended load, which causes turbidity current under high discharge conditions (Doyle et al., 2002, 2003; Granata et al., 2008; Major et al., 2012; Magirl et al., 2015). In a gravel-bed river, grain size distribution becomes a required parameter to ascertain the geomorphic impact of dam removal and sediment transport as gravels are predominant compared to fine-grain sediment. However, geological setting, land use and agricultural practices can significantly modify fine-grain sediment in the river system and species friendly habitat.

1.6.1 Questions concerning river fragmentation and weir removal

The prevalent presence of small dams on our river network system is comparatively higher than big dams. It is unbiased to say that small dams do fragment river systems at a higher frequency than large dams, and scientific research of small dam removal and their impact on river geomorphic state is supported in the past (Poff and Hart, 2002; Stewart and Grant, 2005). This has ignited the focused research related to dam removal while considering other dams' influence, which is present on a river network scale. Sediment management approaches recommend minimising the environmental impacts of

the dams on river physical habitat conditions (Kondolf et al., 2014a; Null et al., 2014). The myth that small dams or hydro projects are environmentally friendly has no rational basis and must be evaluated for severe impacts (Abbasi and Abbasi, 2011). Small dam or weir removal has shown positive results because, despite their small size, weir acts as an impediment for fish movement, and thereby the existence of weir causes a decline in species diversity (Santucci et al., 2005; Leaniz, 2008). Removal of small dams or weirs is strongly supported based on positive changes in the biotic community supported by the past 30 years of data (Birnie-Gauvin et al., 2017).

On the other hand, small dam removal and its influence on geomorphology and sediment transport are gaining recognition (Doyle et al., 2005; Csiki and Rhoads, 2014). Moreover, quantifying the geomorphic response of small dam removal with numerical modelling was recommended (Csiki and Rhoads, 2010). However, the emphasis is given to an integrated approach that considers neighbouring dam influences on small dam removal (Fencl et al., 2015; Poeppl et al., 2015).

This work examines the dam removal scenario for the river Eamont catchments via a modelling approach. We encountered a few bottlenecks that have been resolved with multiple models and a network scale river survey, in hierarchical order and following the thesis structure, a few crucial modelling and surveying approaches were adopted. *First*, the SWAT (Soil and Water Assessment Tool) model was performed to establish distributed hydrological conditions for the Eamont river network. *Second*, the Eamont river catchment and many other UK river catchment lacks sediment records, severely restricting sediment transport modelling simulation. Hence, a drone-based low altitude, high-resolution database created for the Eamont river catchment represents non-cohesive gravel beds. Gravel bed images were pre-processed for transforming them into scaled images, which serves as input for image-based optical granulometric analysis. The developed gran size distribution information was collected for the river source area and river confluence point because the grain size distribution difference reflects the river's hydro-geomorphic state. *Finally*, a sediment transport model CASCADE was selected to analyse dams' mutual impact on sediment transport and geomorphic conditions; the model uses size-selective

transport equations and considers the hiding function responsible for sand and gravel presence and their mutual impact on sediment transport.

It is crucial to mention that the main reason for implementing the CASCADE performs grain-specific sediment routing compared to SWAT, which can process the sediment routing for grain size between 2mm to 10mm as a bulk sediment load. The justification for the CASCADE model is elaborated in section 4.2.

This leads us to address the following research questions:

- What is the temporal and spatial response scale of impounded channels to barrier removal in small channels?
- At the network scale, how can we prioritise which barriers to remove when a network is affected by multiple impoundments?
- Which removal scenarios can lead to predictable improvements in in-stream physical habitats?

1.7 Thesis structure

The content of this thesis is organised into five main chapters, a summary, an appendix and concluding remarks.

Chapter 2. Study area and Hydro-morphological parameters. This chapter explains the physiography and geomorphology of the Eamont river catchment. In addition, the chapter consists of data used in the hydrological model parametrization and provides information on data synthesis in the weather generator of the hydrological model. The chapter explains the data used for water released from dam structures and the catchment outlet gauge station. Furthermore, it explains the method suitable for sediment trap efficiency calculation in a poor data region. Sediment trap efficiency is a crucial input for sediment transport model that can quantify the weir or dam's geomorphic footprint based on sediment trapped by a dam structure.

Chapter 3. Fluvial Morphotypes and Grain Sizes: assessment and modelling implications. This chapter explains the methodology adopted for grain size distribution (GSD) data is extracted based on hyper-spatial drone images. However, drones provide a faster data collection approach for the

various part of the river gravel bed and their photographic analysis (optical granulometric). It is impractical to get the image sample for each reach considered in the hydrological and sediment transport model. Therefore, river morphotype's are identified based on the morphological and grain size samples, which provide insight for probable grain distribution in the unsampled river reaches. The model also explains the utility of the sample grain size in the modelling environment.

Chapter 4. SWAT model simulation and its calibration analysis for long-term hydrological assessment in the Eamont catchment. This chapter introduces the modelling principles of SWAT (Soil & Water Assessment Tool) and distributed hydrological modelling. The chapter explains model calibration, validation, and uncertainty analysis for hydrological modelling daily between 1960 and 2015. The Eamont river catchment is highly managed and consists of 22 dams and weirs. One of the dams is a major dam and impacts the hydrology of the catchment, located on a major tributary (Lowther River) of the catchment. Eamont River flow through an open lake (Ullswater Lake), and big lakes can attenuate the hydrological fluctuation. Therefore, the SWAT model was implemented and explained to assess the distributed hydrology of the Eamont and establish variations within the catchment.

Chapter 5. CASCADE Model: an introduction & its utility in weir removal analysis in a data-poor river catchment. This chapter discusses the CASCADE model structure and its application in the Eamont River Catchment presented. CASCADE model performs sediment transport modelling with graph theory, and model simulates sediment transport information from the 'source to sink' approach at a river network scale. This chapter also highlights the integration of the SWAT and CASCADE model, in which SWAT provides river network and distributed long term hydrological information, and CASCADE process sediment transport with the hydro-geomorphological parameter of the different river reach section.

Chapter 6. The adaptive management approach for prioritising barrier removal with CASCADE Model Simulation: (Eamont river catchment: a weir removal case). This chapter discusses an integrated approach of the

SWAT and CASCADE model to develop adaptive management scenarios based on different discharge conditions and by switching dams on & off (virtually), which would provide sediment entrainment, transport, and deposition pattern on the Eamont river network. This base decision has based on the catchment outlet sediment yield and dam removal scenario. The adaptive management is based on a dam or weir's sediment trap efficiency and in conjunction with hydro-geomorphic settings experienced in the CASCADE simulation.

Chapter 7. Thesis summary and future perspectives. The research approach's implications and justification, and limitations are presented. This chapter would also provide an insight into the thesis. It will also discuss the pros and cons that will set future opportunities to enhance confidence and resolution beyond the reach scale.

Chapter 2: Study area and Hydro-morphological parameters

2.1 Study Area

The Eamont River catchment covers 396.2 km^2 (Figure 2.1) (National River Flow Archive, 2021). The geographic extent of the catchment is between 54.70^{0}N, -3.07^{0}E and 54.45^{0}N, -2.61^{0}E. The catchment area is a part of the mountainous Lake District region, the largest National Park of England. This part of the country has England's highest mountain peaks. One of the highest peaks, Hellvelyn (950m), divides Ullswater and Windermere lakes catchments.

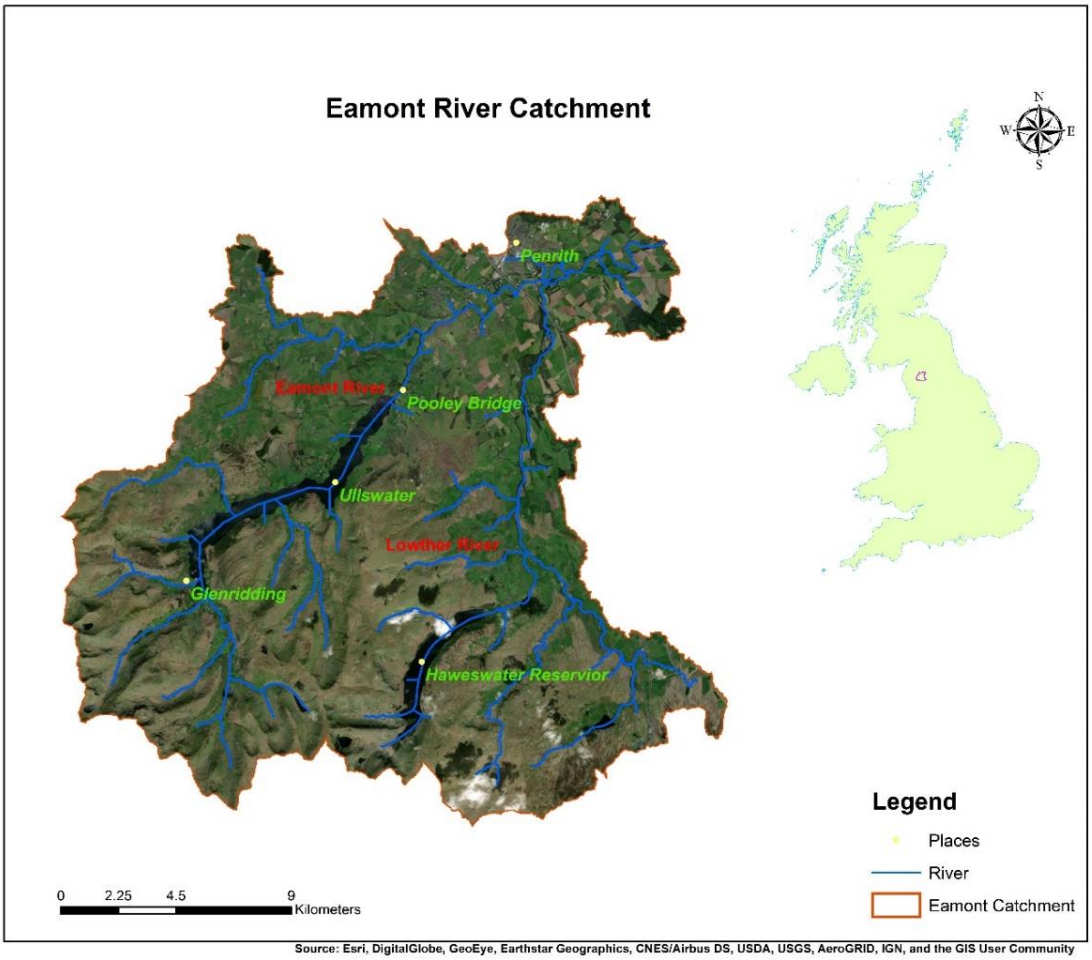

Figure 2.1 The Eamont river catchment area in Lake District (North-West U.K.).

Moreover, Ullswater Lake feeds the Eamont River and is the second-largest natural Lake in England. It has a surface area of 8.68 Km^2 and 25.3 meters of

mean depth (UKCEH, 2021). Ullswater Lake is a ribbon lake, and its formation is favoured by the alternate bend of hard and soft rock resistance to erosion. The hard rocks remained intact, leaving an open Lake after the erosion of soft rock. The open Lake attenuates the hydrological response of the catchment by reducing the fluctuation and intensity of the river discharge. The hard rock geology predominates the area, mainly igneous and metamorphic rocks, Figure 2.2. River catchment's grassland land-use class outweighs the other classes, Figure 2.5, and the region receives maximum rainfall compared to other parts of the U.K., and for the catchment, it is reflected in Figure 2.9.

The Lowther River, a major tributary of the Eamont River, has two dams: Haweswater and Wet Sleddale. Both dams form reservoirs for water storage and inter-basin water transfer schemes (Rigby et al., 2016). Haweswater is one of the most significant reservoirs (88 million m^3) in the U.K., while the Wet Sleddale reservoir stores a modest volume of water (two million m^3). Haweswater, Wet Sleddale and Ullswater (since 1971) collectively transfer water (477000 m^3/ day) to Manchester via an underground aqueduct, which originates from Haweswater reservoir. Thus, the Lowther River tributary significantly influences catchment discharge and sediment transport processes.

2.2 Regional Geology and Physiography

The lake district region originated from volcanic activity between the Ordovician and Devonian period (Moseley, 1986), and the oldest rocks date back to the 500 million years of the Skiddaw group. The youngest rocks of the region belong to the Permian & Triassic periods. The Skiddaw group rocks are siltstone, mudstone, shales, and sandstone. These sedimentary rocks form an inlier (older rocks surrounded by younger rocks) at the headwater region of Ullswater lake. The igneous rock found in the catchment is Basalt, Andesite, Porphyritic andesite and Rhyolite (Smith, 2019). Superficial geology broadly consists of peat, clay, sand, silt, gravel, and angular rock fragments. The most prominent superficial geological forms are Diamiction (poorly sorted unconsolidated sediments) and scree deposits on hillslopes of high relief areas of the Eamont river catchment.

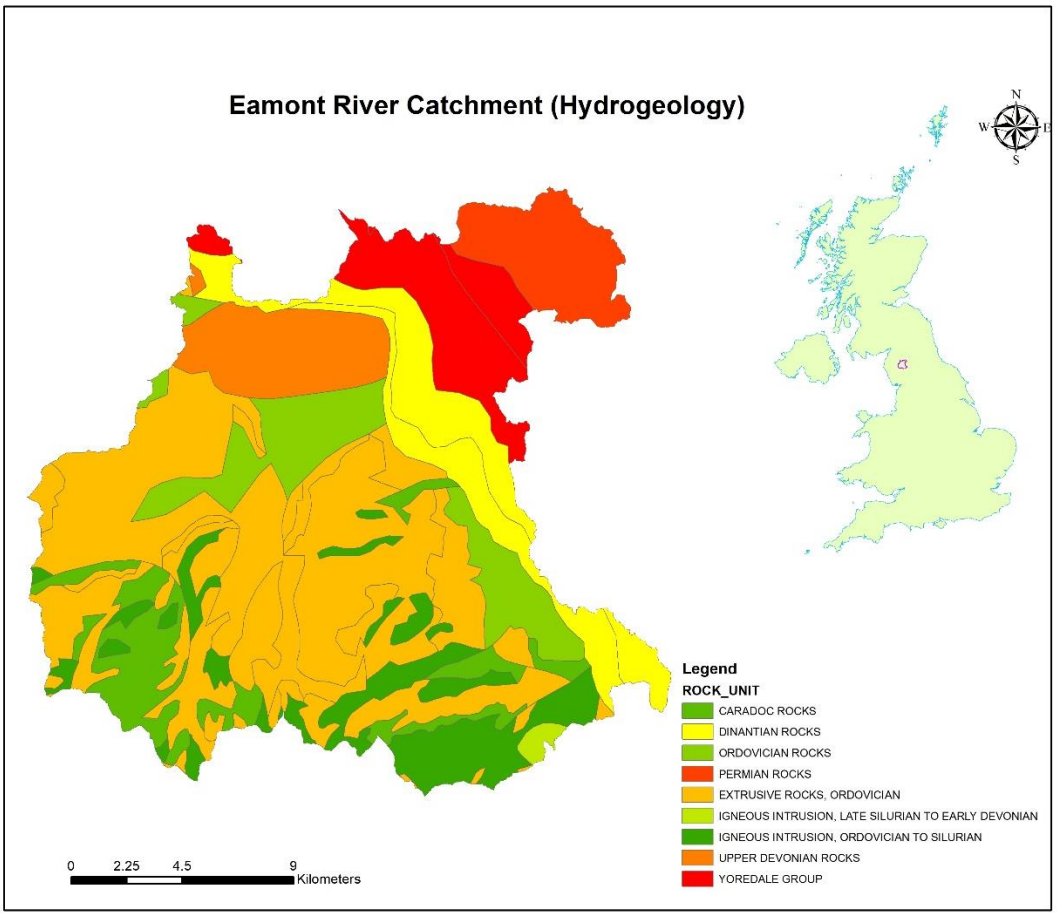

Figure 2.2 Hydrogeology of the Eamont River Catchment (Source: British Geological Survey materials © UKRI [2019]).

The landscape and geomorphology of the Lake district are primarily dictated by the region's glaciation history (Evans, 2020). Cirque, hanging valley and glacial till deposits were carved out by glacial activity in the past. The drainage pattern in the region is radial, which acknowledges the presence of hard rock in the region.

The hydrogeology of the catchment rock formation and geological succession is illustrated in Figure 2.2. The rock formations for the Eamont region show characteristics of poor aquifer conditions. The Yoredale group, Permian rocks and Dinantian rocks form moderate productivity aquifers, while the remaining other rock formations have low productivity aquifer characteristics. The water table in the catchment lies between 50m below ground surface and 100m below high ground (Allen et al., 2010). The hydraulic gradient is gentle in the Eamont river catchment at Penrith and directed towards the catchment

rivers (Ingram, 1978). The Penrith area has an underlying sandstone aquifer suitable for water transmission. Baseflow contributes significantly to the catchment outlet in the summer months.

However, in the case of Eamont, the catchment hydrological response deviates from the natural conditions because of multiple factors. *First*, the presence of Ullswater in the Eamont river catchment and Haweswater reservoir in the Lowther, along with Haweswater aqueduct (an inter-basin transfer scheme), has collectively impacted the hydrology of the Eamont river catchment. *Second*, the volume transferred to Manchester via aqueduct is approximately 477 million litres of water per day (Lewis and Atkinson, 2020). The cumulative impact of natural lake and management structures on the course of Eamont river network natural processes plays a secondary role, and thus it influences hydrology of the catchment (Abbaspour, 2008; Pattison et al., 2014).

A river catchment's hydrograph or hydrological response is a cumulative response of catchment's environmental, surface and sub-surface conditions. The catchment's response is subdivided into many physical processes that strongly affect rainfall and resulting runoff. Runoff varies at spatial and temporal scales of soil variability, land use, topography and weather parameters (Wood et al., 1988). Multiple tributaries have respective sub-catchments; however, catchment properties show spatial variation in soil, land use and topography in distinct categories and spatial rainfall variability. Thus, the hydrology of sub-catchment can have their unique response to the same intensity rainfall event over various parts of the river catchment.

Hydrological modelling at a catchment scale tries to achieve the primary objective of reporting water balance equation components and their quantification (infiltration, evaporation, groundwater recharge, baseflow, runoff, in-stream discharge). A simple water balance mathematical representation of catchment processes is provided in equation 2.1,

$$R = P - ET - IG - \Delta S \qquad 2.1$$

In equation 2.1, where R is runoff, P precipitation, ET Evapotranspiration, IG infiltration **/** groundwater, and ΔS change in soil storage.

Hydrological models solve the water balance equation components at the spatial unit of discretisation. Moreover, the models were discretised at the thematic layer's resolution unit (topographic data resolution). The spatial diversity in the catchment and its hydrological response modelled for a spatial discretised unit, Figure 2.3. In addition, physical, geographic, and human-induced impacts and inclusion of human impacts may define characteristics of a river catchment hydrology, which is different from the natural hydrological response of a catchment.

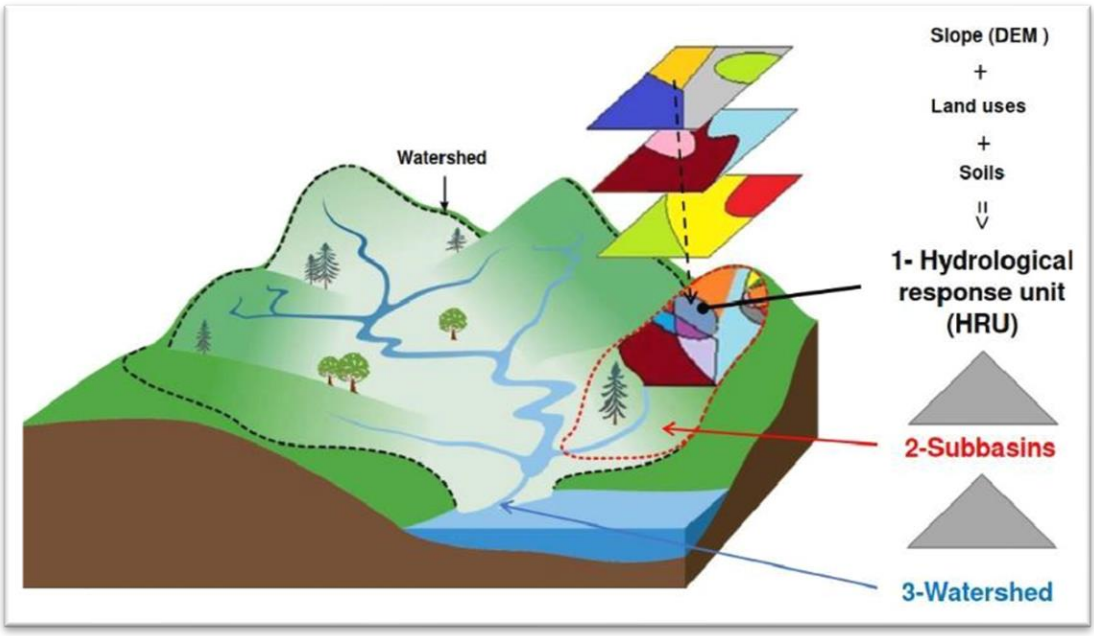

Figure 2.3 Hydrological model's spatial processes discretisation at catchment and sub-catchment of thematic information (source: https://bit.ly/3t1hhv1).

2.3 Hydrological model input data

As mentioned earlier, the Eamont catchment's physiography and human anthropogenic actions impact the hydrological response. For example, the ponds and lakes attenuate a catchment's hydrological response along with the sub-catchment scale (Nicholson et al., 2012; Yasarer et al., 2018). In the case of the Eamont catchment, various glacial lakes are present at the high-altitude headwater region and at the low altitude downstream region, which affects the headwater region and river outlet sub-catchments. In other words, the presence of lakes and ponds at different elevations in the catchment area does not only affect the flow in the main river, but also it can affect the sediment erosion and

deposition pattern from the source area, in the transport region, and consequently, flow and delivery of water & sediment to the outlet. Thus, lake and ponds presence in different river tributaries sub-catchments can have a pronounced impact on catchment hydrology (Pattison et al., 2014). In addition to that, river sub-catchments are influenced by anthropogenic water resources management structures and schemes (Petts, 1988; Smithers and Walker, 1997; Robinson et al., 1998; Fowler et al., 2007; Nicholson, 2015; Rigby et al., 2016).

A physics-based hydrological requires a diversity of input data regarding climatic variables, hydrological parameters, and river catchment's geomorphic, physiographic states. The physical information of the catchment is provided in the form of spatial and non-spatial data, which abstract the physical nature of the catchment, including surface and sub-surface boundary conditions.

2.3.1 Digital Elevation Model (DEM)

The catchment topography and its representation in the DEM have a pronounced impact on the hydrological response of the catchment. An acceptable resolution digital elevation model provides the estimation of relief difference, catchment delineation and river gradients. Appropriate resolution is a crucial factor because a poor resolution DEM influences the hydrological assessment (Chaubey et al., 2005; Tan et al., 2015; Nazari-Sharabian et al., 2020). Thus, the accuracy and resolution of a DEM play a crucial role in hydrological parameters derivation are essential in a hydrological model (Tarboton et al., 1991; Zhang and Montgomery, 1994; Vaze et al., 2010).

The SRTM product is highly recommended for hydrological applications because it is a hydrologically corrected dataset (Jarihani et al., 2015). However, considering the relatively small Eamont river catchment size (396.2 km^2), a higher resolution DEM is required to represent and capture the high spatial diversity in catchment topography. For this reason, a 5m DTM produced with low altitude aerial photogrammetry (Bluesky, 2014) is tested with the ASTER (30m) and the SRTM (90m) digital elevation models. The 5m DEM performed better in catchment delineation and river reach extraction compared with other available DEM raster datasets (ASTER and SRTM). Since 5m DEM is a product

of aerial photogrammetry, the DTM dataset is impacted by a few spatial surface features that create salt and pepper. The salt and pepper noise explains the sudden change in pixel values in a digital image. However, in the digital elevation model, pixel value represents elevation, and therefore salt and pepper noise in the context of DEM refers to an abnormal change in relief. To avoid elevation inconsistency in the DTM dataset, it undergoes a pre-processing step required to form a DEM model. It requires sink filling pre-processing before deriving subsequent flow direction and flow accumulation terrain properties (free from the artificial sink and surface object errors) (Djokic and Ye, 2000).

The processed DEM has shown a minimal error (surface objects) and hydrological sinks. Therefore, it is utilised as the hydrological model's DEM (Figure 2.4) input raster. This DEM is used for catchment delineation based on hydrological and geomorphological divides, for instance, location of barriers and change in river width.

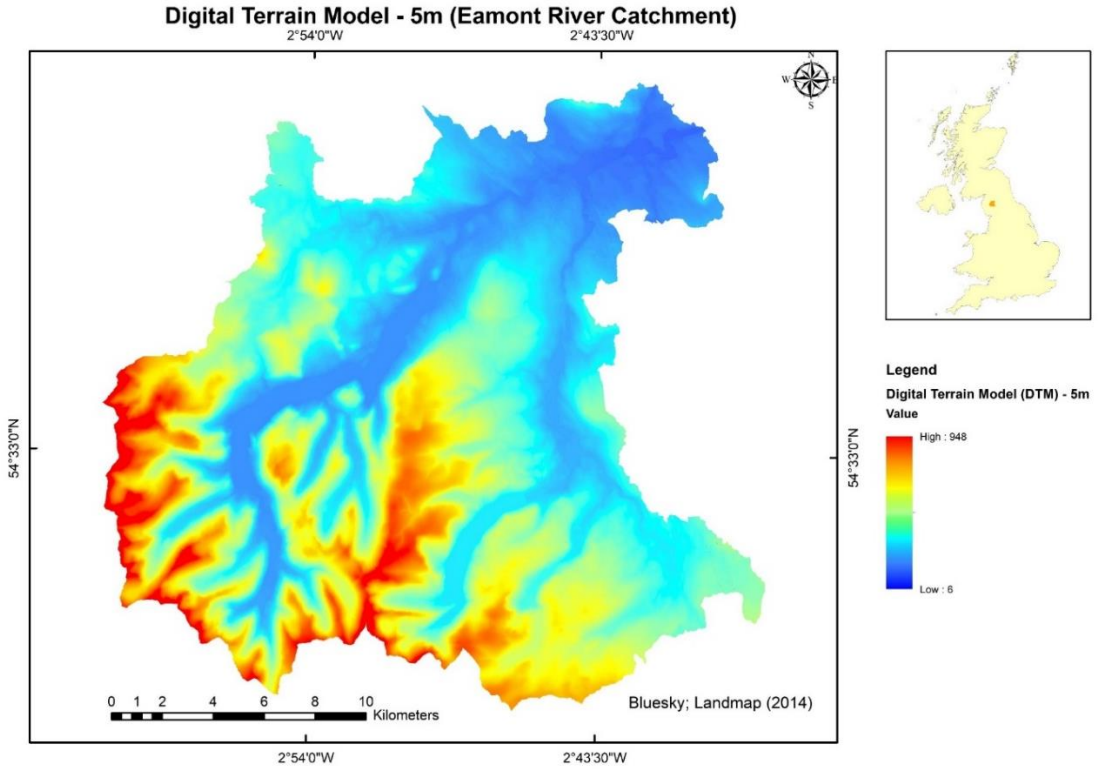

Figure 2.4 A 5m digital terrain model.

2.3.2 Land use

The land use of a river catchment determines the hydrological response of the river catchment because the primary water interaction of any given rainfall event occurs at the land use unit. The runoff volume generated from a well-vegetated area or forest land vs bare land will not be the same. Therefore, the time of concentration will vary among the various land use units. In the hydrological model, the runoff response of a rainfall event is generated through a land-use unit, and it is assessed with the curve number (CN), defined in the SCS method for abstractions (Chow et al., 1988, p. 147–150).

In the current study, the land cover of 2015 is classified into 21 land use classes.

Figure 2.5 indicates the distribution of different Land use classes within the Eamont River catchment. Despite the 21 classes, only 15 land use classes cover the Eamont river catchment boundary. The Eamont river catchment area falls mainly under the Grassland category 77.97%, further divided into acidic and neutral categories. The remainder is Woodland (7.68%), Bogs (5.56%), Horticultural land (3.22%) and Urban land (2.07%) and water bodies (3.5%) ("Land Cover Map-2015," 2018).

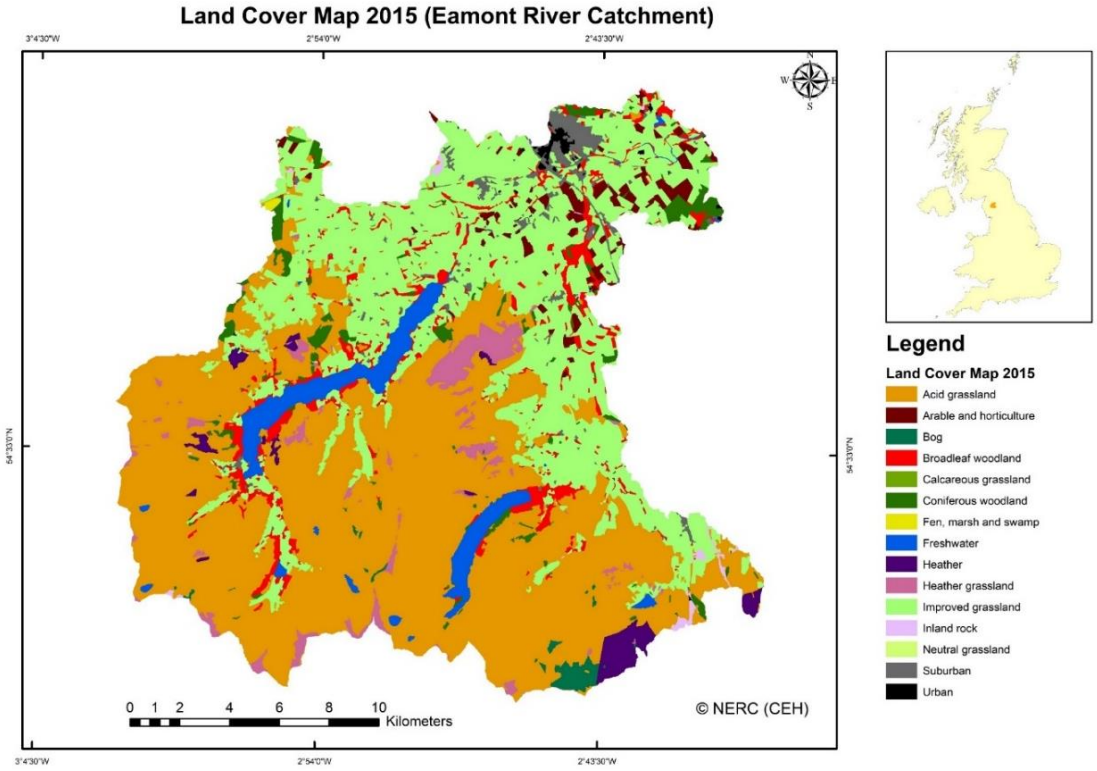

Figure 2.5 The land use of Eamont River Catchment (2015).

For input into the hydrological model, land use classes need to be converted to scientific attributes such as Leaf area index (LAI), Curve Number (C.N.), plant growth, nutrient uptake, and many others. Therefore, the land cover dataset is reclassified according to predefined hydrological models recognisable Land Use codes. Table 2.1 shows the reclassification of 2015 land-use into defined hydrological models land-use classes reduced to ten classes.

Land use 2015	***SWAT Code***	***SWAT Numeric Code***
Arable and Horticulture	ORCD	4
Acid Grassland	RNGE	15
Bog	WETL	9
Broadleaf woodland	FRST	6
Calcareous Grassland	RNGE	15
Coniferous Woodland	FRSE	8
Freshwater	WATR	18
Heather	RNGB	16
Heather Grassland	RNGB	16
Improved Grassland	RNGB	15
Inland Rock	BARR	118
Natural Grassland	RNGE	15
Suburban	URHD	2
Urban	URBN	1

Table 2.1 The land use translation table explains the reclassification of land use 2015 to SWAT database code.

In Table 2.1, the hydrological model's land-use code converts the 2015 land-use data into urban (URBN), urban high density (URHD), grassland (RNGE), range shrubland (RNGB), mixed forest (FRST), evergreen forest (FRSE), orchards (ORCD), bare rocks (BARR), and water/lake (WATR). Finally, the spatial land use entity gets its non-spatial characteristics described in the SWAT relational database, and these are used for hydrological cycle processes related to model and equation calculation.

2.3.3 Soil

A rainfall event recharges surface and sub-surface water, and the soil category controls the allocation of water to each soil profile region. Soil moisture depends

on soil type, soil matrix and determines water content retained in the soil profile. Simultaneously, soil moisture depletion occurs in the plant uptake (transpiration) or evapotranspiration process, along with excess soil moisture, which seeps through the soil profile and recharges the subsurface aquifer. Antecedent soil moisture in the soil profile can significantly influence the fraction of rainfall converted into runoff. Similarly, a saturated soil profile reacts faster than an unsaturated soil profile at the time of the rainfall-runoff process. Conversely, unsaturated soil profile increases soil saturation time and thereby, the time of concentration would be higher. Therefore, knowledge and access to soil characteristics data can improve the hydrological assessment via a modelling procedure.

The Eamont river catchment data concerning soil water condition, soil characteristics & soil profile provide insight for calculating antecedent moisture condition in the related mathematical equations of the hydrological cycle. We use the Harmonized World Soil Database (FAO/IIASA/ISRIC/ISSCAS/JRC, 2012), a global soil dataset with 16,000 soil mapping units that has a resolution of three arc-second (Batjes, 2009). The HWSD soil database contains soil mapping unit information related to soil phases (solid, liquid, gaseous and living phase). The HWSD data provides chemical and physical characteristics of topsoil (0-30cm) and subsoil (30-100cm). The soil database comprises soil characteristics such as pH, water storage capacity, organic carbon, soil depth, cation exchange capacity, clay fraction, total exchangeable nutrients, lime and gypsum contents, salinity, sodium exchange percentage, soil texture and granulometry (Figure 2.6).

HWSD Soil Mapping Unit Details

Coverage ESDB
Soil Mapping Unit 10787
Dominant Soil Group LV - Luvisols

Selected SMU 10787

	Dominant Soil	Associated Soils and Inclusions		
TOPSOIL (0-30 cm)				
Topsoil Sand Fraction (%)	37	41	78	19
Topsoil Silt Fraction (%)	44	37	13	32
Topsoil Clay Fraction (%)	19	22	9	49
Topsoil USDA Texture Classification	loam	loam	sandy loam	clay (light)
Topsoil Reference Bulk Density (kg/dm3)	1.41	1.4	1.6	1.24
Topsoil Bulk Density (kg/dm3)	1.4	1.43	1.36	1.27
Topsoil Gravel Content (%)	4	4	10	4
Topsoil Organic Carbon (% weight)	0.99	0.74	0.57	1.19
Topsoil pH (H2O)	5.8	6.5	6.3	6.2
Topsoil CEC (clay) (cmol/kg)	48	47	48	38
Topsoil CEC (soil) (cmol/kg)	12	13	6	24
Topsoil Base Saturation (%)	62	91	74	91
Topsoil TEB (cmol/kg)	8.4	11	4.7	22.7
Topsoil Calcium Carbonate (% weight)	0	0	0	0
Topsoil Gypsum (% weight)	0	0	0	0
Topsoil Sodicity (ESP) (%)	1	1	2	1
Topsoil Salinity (ECe) (dS/m)	0.1	0.1	0.1	0.1
SUBSOIL (30-100 cm)				
Subsoil Sand Fraction (%)	31	37	64	21
Subsoil Silt Fraction (%)	38	34	13	32
Subsoil Clay Fraction (%)	31	29	23	47
Subsoil USDA Texture Classification	clay loam	clay loam	sandy clay loam	clay (light)
Subsoil Reference Bulk Density (kg/dm3)	1.33	1.35	1.43	1.24
Subsoil Bulk Density (kg/dm3)	1.6	1.51	1.55	1.39
Subsoil Gravel Content (%)	4	3	20	3
Subsoil Organic Carbon (% weight)	0.29	0.36	0.3	0.55
Subsoil pH (H2O)	5.9	6.7	6.4	6.8

Figure 2.6 HWSD database (top & sub-soil physical, chemical properties).

The HWSD database is visualised and accessed in a prescribed application software named *Harmonized World Soil Database Viewer* (version 1.21, Figure 2.7). The catchment specific spatial soil unit information is extracted and connected to the soil attribute database (Microsoft Access database for soil properties) (FAO, 2021). This information plays a crucial role in land phase hydrological processing because it determines soil water availability for the plant. The excess water in the soil layer is modelled through evapotranspiration and groundwater recharge.

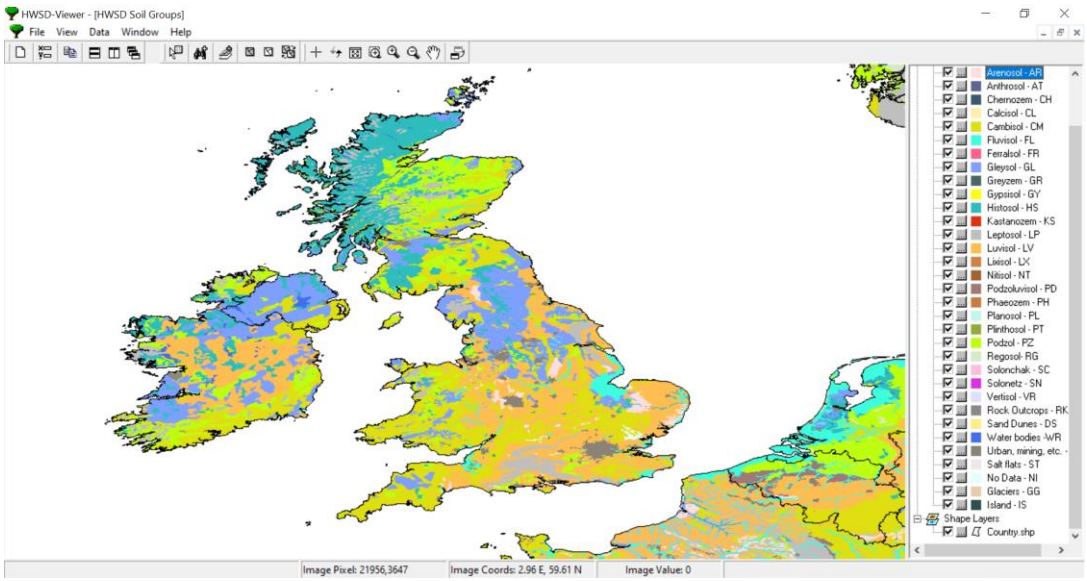

Figure 2.7 The Harmonised World Soil Database (HWSD) accessed in HWSD-Viewer application (Version 1.21).

Furthermore, the soil thematic information is enhanced with the integration of a waterbody layer. This is essential since water bodies in the Eamont catchment have a cumulative area of 3.5% of the total catchment area. Rain falling over any water body is directly converted into water volume, and therefore processes such as infiltration in soil and sub-soil layer can be avoided for Lake, pond, and reservoir areas if we add a water body layer.

The HWSD soil raster database is updated with the waterbodies layer. Then the updated soil data is utilised as soil input. In the model, the HRU (hydrological response unit) is created based on unique combinations of Land use, soil and elevation conditions, and this HRU provides crucial information for quantifying rainfall-runoff related simulation processes (Figure 2.8).

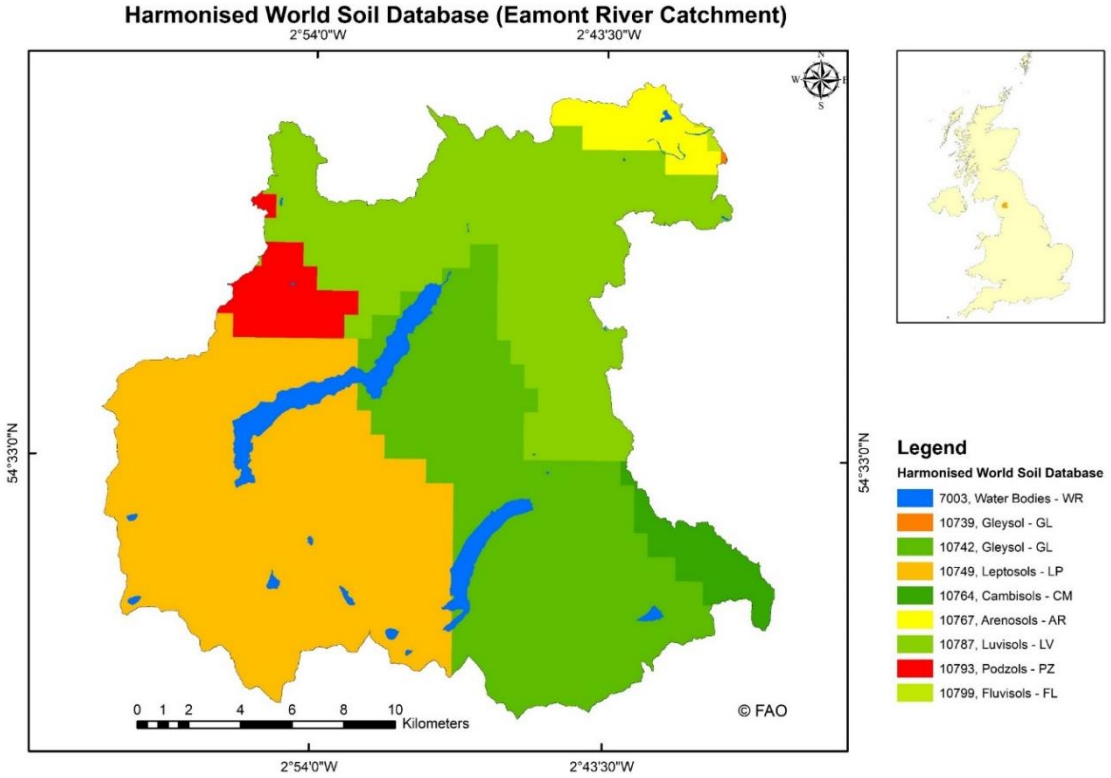

Figure 2.8 Showing the HWSD database soil unit distribution in the Eamont river catchment.

2.3.4 Precipitation

The Eamont river flows through the wettest part of the U.K. (Barker et al., 2004; Whyte, 2009). The Atlantic Ocean's air circulation pattern creates westerly wind force, which drives moistures and raises it at an elevation to get condensed and forms rainfall and strongly influences the study area's climate (Hurrell, 1995; Hurrell and Van Loon, 1997). The high mountains of the Lake District then favour orographic rainfall (Dore et al., 1992; Malby et al., 2007). Furthermore, a high amount of rainfall is reported for the northwest U.K. region. Figure 2.9 shows a high annual average rainfall in the mountainous southwest part of the Eamont catchment. As a result, the headwater zone of Eamont and the tributary river Lowther are receiving the highest rainfall.

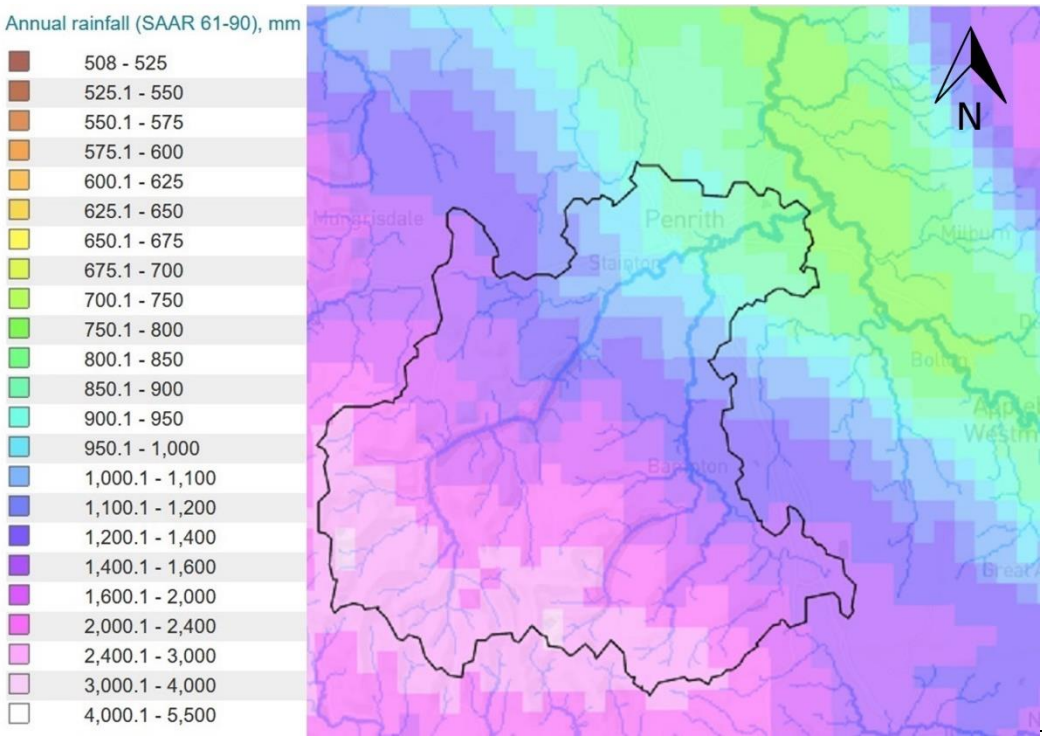

Figure 2.9 Spatial distribution of annual average rainfall in the Eamont river catchment at the 1km grid resolution - 1961 -1990 (UKCEH, 2019).

Precipitation events have significant control over the water balance and catchment hydrology. Therefore, it is recommended that the precipitation data of high spatial-temporal accuracy should be adopted. Previous studies have demonstrated that the gridded data produces better hydrological simulation results when compared with conventional ground-based weather gauge station datasets in a hydrological model (Fuka et al., 2014; Grusson et al., 2017a). The selection of gridded data becomes crucial because the selected hydrological model assigns rainfall station data point for each sub-catchment at the time of hydrological simulation (Dile and Srinivasan, 2014). Hence, the 'Centre of Ecology and Hydrology's Gridded Estimates' of areal rainfall (Tanguy et al., 2016), which have a temporal resolution of daily precipitation and spatial resolution of *1km x 1km,* is preferred (data availability at the time of model simulation was 1890-2015, which is now updated for beyond 2015) (Keller et al., 2015; Tanguy et al., 2016). This precipitation dataset is a natural neighbour interpolation output of in-situ observation to a regular grid. These synthesised gridded rainfall estimates are derived from the Met Office national database. The gridded rainfall is extracted in MATLAB (NetCDF to text files) (Ficklin and

Barnhart, 2014b). The original code is modified and updated for other weather parameters extraction, including precipitation (Ficklin, 2018; Pipil, 2018).

In the current study, hydrological simulation is performed for 50 years daily frequency between 1966 and 2015. However, the precipitation data before the 1960s is discarded since the Haweswater aqueduct and a major inter-basin transfer scheme became operational in the mid-60s. In addition to that, the Eamont river catchment's outlet at Udford gauging station only started collecting daily flow data in January 1960. Therefore, hydrological simulation for the Eamont river catchment cannot be calibrated before 1960.

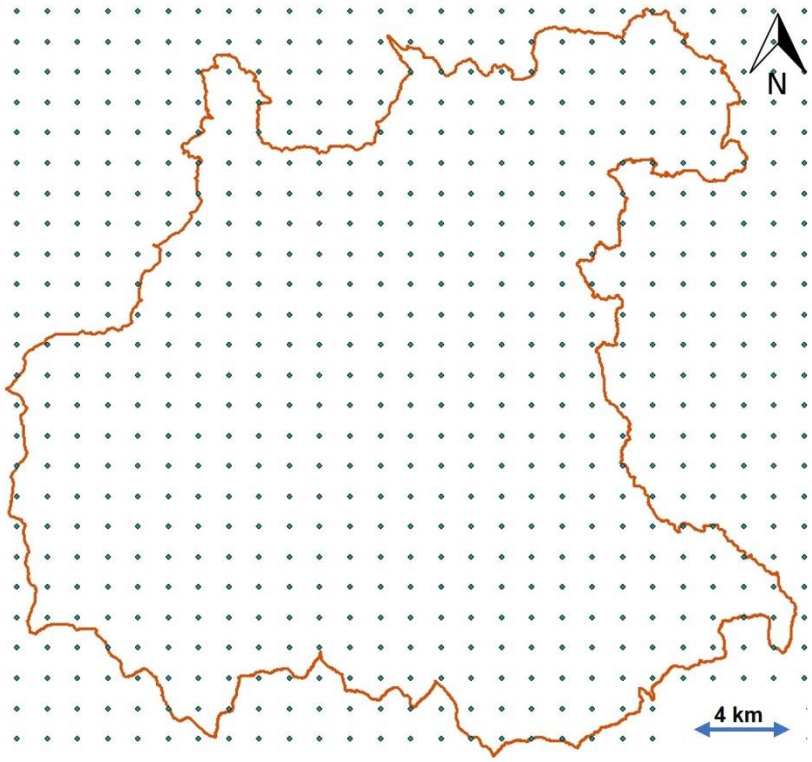

Figure 2.10 Gridded precipitation extracted for SWAT model input as point vector at 1km x 1km spatial resolution.

2.3.5 Temperature

The temperature parameter can broadly modify physical, chemical, and biological processes at the catchment scale. It significantly influences river catchment hydrology since the temperature can change transpiration rate by controlling humidity in the atmosphere, melting snow cover, and soil surface temperature. Hence, the inclusion of measured temperature can improve the

model results, and therefore it is highly recommended to include observed temperature records (Koczot et al., 2011; Remesan and Holman, 2015; Naseer et al., 2019).

In the Eamont catchment, the temperature dataset is accessed from the Centre for Environmental data analysis dataset named "HadUK-Grid Gridded Climate Observations on a 12 km grid" for the year between 1862 and 2015 (in recent time data is available beyond 2015) (Hollis et al., 2019). The dataset represents maximum, minimum air temperature recorded at 1.5m height above ground. The dataset was produced by interpolating the irregular distribution of weather observation stations. The interpolation uses Inverse distance weighting (IDW), and it is performed on the irregularly distributed gauging station to create uniform coverage for the U.K. Based on mentioned recommendations and data properties, the daily temperature minimum and maximum values are provided as gridded data to the SWAT model (in degree centigrade units).

2.4 Weather generator simulated weather parameters

A weather generator is meant to synthesise missing weather records based on long term observed weather stats (Williams et al., 1984; Sharpley and Williams, 1990), and it is an integrated functionality in the SWAT model. The Newton Rigg weather station (station id- 1073) falls within the Eamont river catchment at 54.67N, -2.78W at an elevation of 169m in the extreme northwest location within the Eamont river catchment. One weather station is located near Wet Sleddale Reservoir (UKCEH, 2018). However, it is not registered on the U.K. Met- Office website. These two weather stations do not reflect the spatial variability for weather parameters. However, Newton Rigg is an observed weather station site that serves as the primary station for deriving weather data statistics, which is required to simulate other climatic parameters in a weather generator tool. The weather generator requires 20 years of climate records prepared for WGN inside a climate statistics calculation tool named 'WGN parameters estimation tool' (Essenfelder, 2016; Neitsch et al., 2011, pp. 65–87). The hydrological model's weather generator database updated with the statistics is calculated from Newton Rigg's observed weather dataset.

2.4.1 Relative humidity

The relative humidity serves as an input for potential evapotranspiration estimation and is routinely required by evapotranspiration equations (*e.g.,* Penman-Monteith or Priestley-Taylor equations). These models require relative humidity at the daily frequency for each sub-catchment. Hence daily relative humidity values are simulated from the 'Centre for Environment Data Analysis dataset MIDAS: UK's hourly weather observation data that has provided dew point temperature for the *Newton Rigg* weather station (Met Office, 2006). Furthermore, dew point temperature is converted to the monthly relative humidity in weather generator by the following equations (Neitsch et al., 2011, pp. 81–82):

$$R_{hmon} = \frac{e_{mon}}{e^{o}_{mon}} \qquad 2.2$$

In equation 2.2, R_{hmon} is average relative humidity, e_{mon} is actual vapour pressure and e^{o}_{mon} saturation vapour pressure.

Additionally, the actual vapour pressure is present in the atmosphere at the dew point temperature is equal to saturation vapour pressure. The following equation calculates the actual vapour pressure:

$$e_{mon} = exp\left[\frac{16.78 * \mu dew_{mon} - 116.9}{\mu dew_{mon} + 237.3}\right] \qquad 2.3$$

The saturated vapour pressure is related to monthly air temperature and calculated by the following equation:

$$e^{o}_{mon} = exp\left[\frac{16.78 * \mu mp_{mon} - 116.9}{\mu mp_{mon} + 237.3}\right] \qquad 2.4$$

In equation 2.3 and 2.4, μdew_{mon} is monthly dew point temperature, and μmp_{mon} mean air temperature for the month.

With equations 2.3 & 2.4, dew point temperature data is converted to relative humidity. The daily relative humidity is simulated based on monthly average dew temperature values provided to the weather generator an application called "WGN Parameters Estimation Tool" (Essenfelder, 2016). As earlier mentioned, a single ground observation station would not represent the spatial weather variability in the river catchment. Therefore, the weather generator simulates

daily relative humidity for all sub-catchments with a continuity equation that uses dry and wet conditions for the month based on the triangular distribution (Neitsch et al., 2011, p. 83).

2.4.2 Wind velocity

The airflow over the plants or tree canopy can change the rate of transpiration. Accordingly, the wind speed variable plays a vital role since high wind speed can change the humidity produced by the plant and compensate that plant or tree will transpire more. The wind speed information is also a crucial input for the Penman-Monteith equation for calculating potential evapotranspiration.

In the Eamont catchment study area, the wind speed variable is selected from the 'Climate hydrology and ecology research support system (CHESS)' meteorology dataset for Great Britain (Robinson et al., 2016). The input wind speed data has a 1km x 1km grid resolution. A proximate grided point data has been used to update the *Newton Rigg* and stats calculated within the WGN parameter estimation tool.

2.4.3 Solar radiation

Incoming solar radiation to the earth's surface is the primary energy source to the atmosphere, and it controls the local temperature, soil surface temperature, and snow melting processes. The inclusion of measured solar radiation records can also improve the radiation-induced catchment scale sub-processes in the model. The hydrological model takes solar radiation as one of the weather variables.

In the Eamont river catchment, the downwelling solar radiation (W m^{-2}) at 1km x 1km resolution gridded dataset is selected and accessed from 'Climate Hydrology and Ecology research Support System: CHESS' (Robinson et al., 2017). The solar radiation data is supplied with unit *watt per* m^2 (W m^{-2}), although the selected hydrological model accepts solar radiation in the unit *megajoule per square metre per day* (M.J. m^{-2} day^{-1}). Therefore a conversion factor (0.0864) has been applied to the whole solar radiation records (FAO, 2019). The solar radiation variable dataset is available between 1961 and 2015, and average monthly solar radiation values were extracted from solar radiation data to update the weather generator (Robinson et al., 2017).

2.5 River hydro-geomorphological data

River's hydro-geomorphological state and its abstracted information provide crucial input for modelling algorithm and physical process related equations. For instance, reach length, slope, the river width and in-stream & overland roughness are expressed as manning's "n" value (Arcement and Schneider, 1989). This information has been provided in the two modelling tools selected for addressing the thesis objectives. The river's geomorphological information is processed and extracted from a digital elevation model (DEM) in a model. To enhance and avoid any accidental errors that are included in the model due to DEM inaccuracy and resolution limitations. The river's physical characteristics are verified with Google Earth imagery and GPS field data. Conspicuously, the network has remained identical for both models. Thus, catchments boundary conditions are maintained identical regarding the river's physical characteristics.

At the catchment scale, the discharge response is attenuated by reservoir and dam operation, an open Lake and ponds. Therefore, pond and reservoir characteristics related to storage, overflow value or emergency spillway information are added to the model. Groundwater plays a vital role in catchment hydrology, particularly in summer. Hence, aquifer characteristics and groundwater table are prerequisites at the stage of model parametrisation.

However, regardless of how familiar and experienced a modeller is, the catchment environment's physical process parameter and availability cannot be ensured for every single parameter considered in the model. Sometimes, the different agencies capture the data and measurements with various sensitivity range types of equipment. In other words, a physical process is monitored with two different sets of equipment, and an operator may get two different responses, which may not be identical. It is challenging to parametrise a highly parameterized model with every single parameter considered in the model. Practically, it is rare for a modeller to get all parameters considered in the model. Thus, the model's efficiency for predicting the actual hydrological response is often achieved with model calibration, and it can significantly reduce the model's uncertainty.

The water release data for Ullswater water, an open lake and Haweswater dam's daily gauge information is used for parametrising the model. The inclusion of controlled water release data has a fair influence in predicting a river catchment's hydrological response. Moreover, the Eamont river catchment's outlet location at the Udford gauge station is an observed hydrograph, and it has been used for the hydrological model's calibration and validation process Figure 2.11 (details of calibration is provided in 4.6).

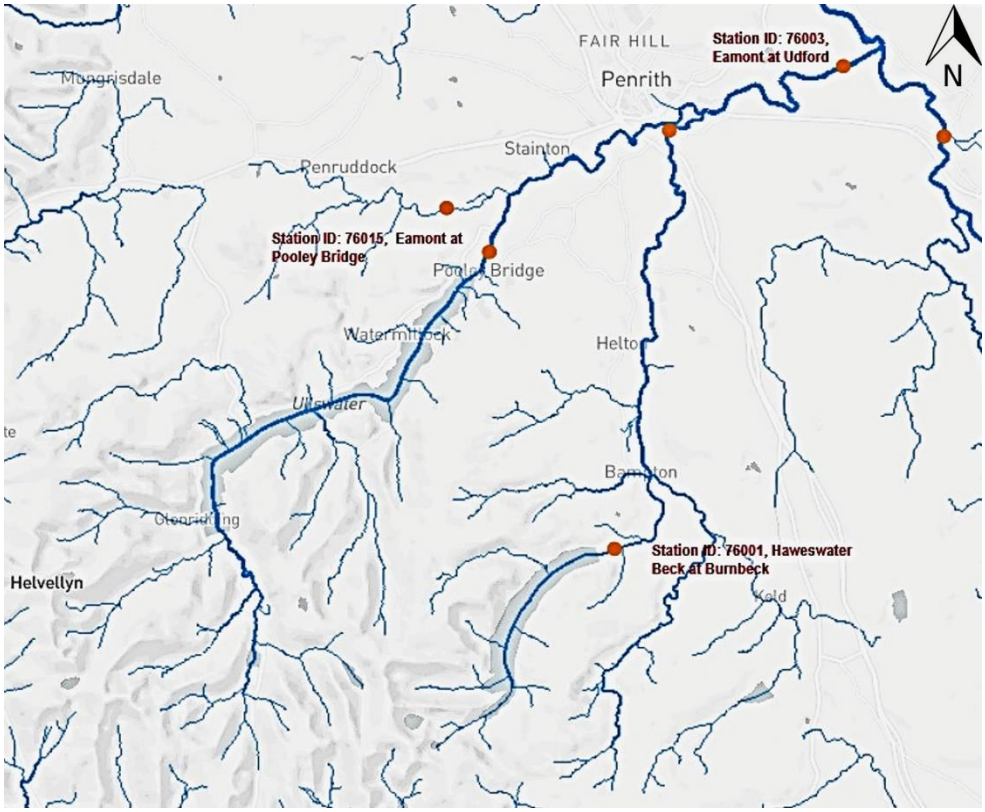

Figure 2.11 Gauge locations of open Lake and dams and Eamont River catchment's outlet.

2.6 Barrier locations and Trap efficiency input data

Since dam removal is a civil engineering activity, whether dam construction or dam removal, the river's response to dam removal on river geomorphic transformation is a progressive development process. It takes years to adapt to the new disequilibrium condition projected after the dam removal activity. Moreover, modelling is a preferred selection to solve such scientific problems. Nevertheless, model selection is based on its modelling structure and ability to

address scientific objectives. However, model parametrisation is equally valuable.

2.6.1 Weir & Dam location data

The Eamont river catchment has barely 396.2 Km^2, that consist of 22 dams and weirs, out of which 20 represent small weir structures, Figure 2.12. The location of the weirs is verified with the AMBER atlas. The AMBER atlas has also provided crucial information regarding their primary structure data (AMBER Consortium, 2020).

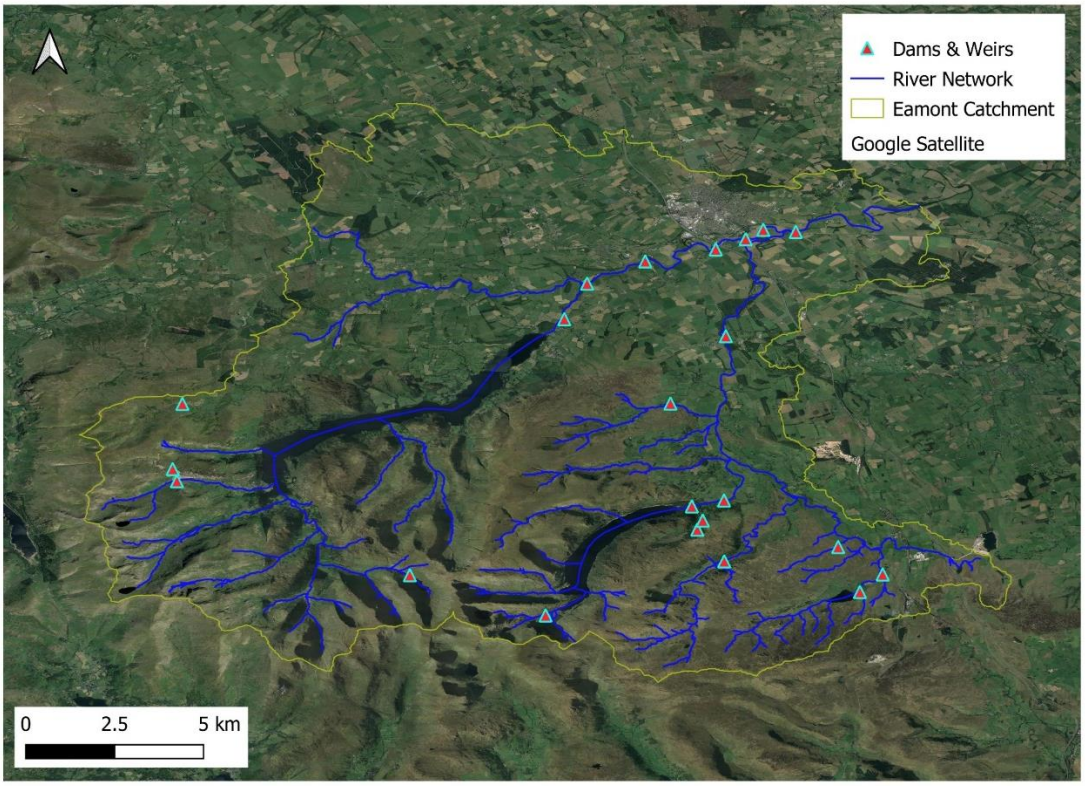

Figure 2.12 Dam and weir location on the Eamont river catchment.

One of the crucial inputs essential for estimating dam and weir's impact on river geomorphic conditions is trap efficiency. Since trap efficiency guides to the modeller for a dam or weir's impact on upstream rivers through trapped incoming sediments and consequent changes in the downstream river.

For this reason, it is recommended to estimate sediment trap efficiency (TE) and parametrise the model. Conversely, a model that lacks TE definition would represent a river network resembling pristine riverine conditions. Thus, TE

information is essential for the model's parametrisation and dam removal scenario development in the selected modelling environment.

2.6.2 Estimation of Sediment trap efficiency for Weirs and Dams

The volume of sediment trapped by a dam or weir structure is measured as sediment trap efficiency (equation 2.5).

$$TE = \frac{S_{inflow} - S_{outflow}}{S_{inflow}} = \frac{S_{settled}}{S_{inflow}} \qquad 2.5$$

Where S_{inflow} is sediment delivery, $S_{outflow}$ outflowing sediment from the reservoir, and $S_{settled}$ is the volume of sediments deposited in a reservoir. However, a dam or weir's sediment trap efficiency is influenced by many factors (discharge, reservoir, and incoming sediment characteristics), Figure 2.13.

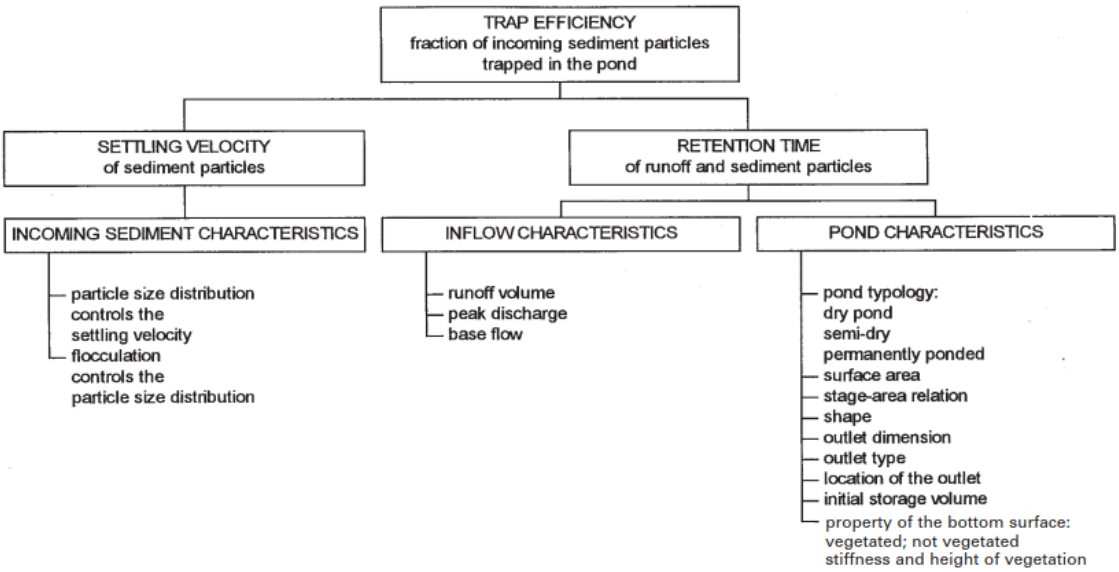

Figure 2.13 Factors impacting sediment trap efficiency of reservoirs or ponds (Verstraeten and Poesen, 2000).

However, data requirements regarding equation 2.5 are necessary to develop empirical relations and validate the theoretical models. Still, the required data is rarely available. Moreover, Brown (1943) and Brune (1953) presented two empirical methods for estimating sediment trap efficiency. Sediment trap efficiency method had been developed based on reservoir storage capacity C and catchment area W ratio and C/W ratio parameters expressed in the unit; $\mathrm{m3/Km^2}$, Brown (1943). Another method is based on capacity C – annual inflow

I ratio, which has both C/I parameters expressed in the same unit; m^3 / m^3) Brune (1953).

Equation 2.6 explained Brown's method based on the capacity – watershed area ratio and suggested a curve that indicates the relationship between trap efficiency and C/W ratio, which is developed from the data extracted for 15 reservoirs, Figure 2.14. The value of D ranges between 0.046 and 1, and mean value 0.1 (depends on characteristics of the reservoir) (Verstraeten and Poesen, 2000).

$$TE = 100 - (1 - \frac{1}{1+0.0021\,D\,\frac{C}{W}}) \qquad 2.6$$

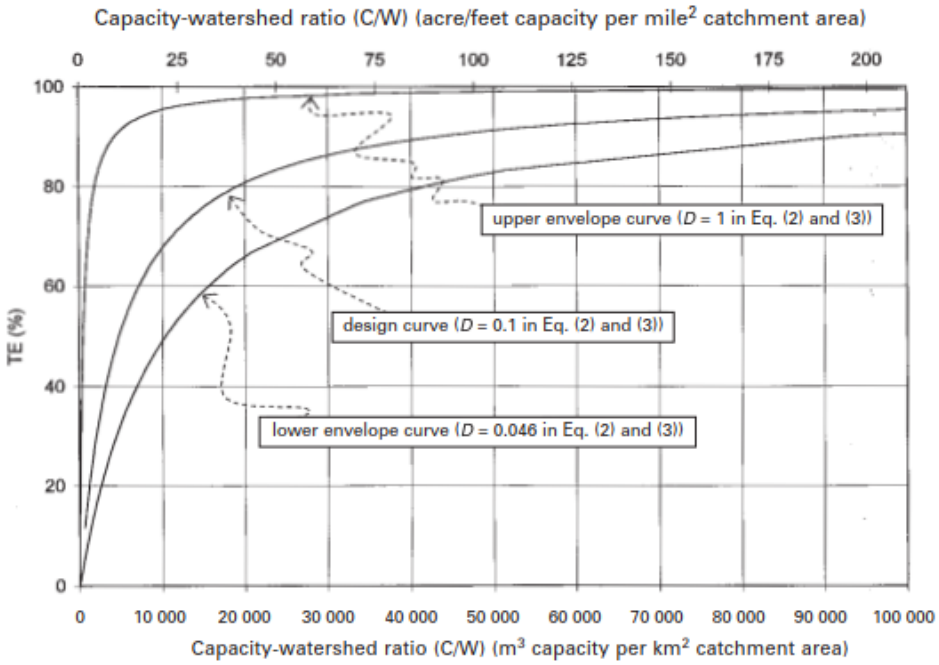

Figure 2.14 Trap efficiency related to capacity/watershed ratio - (C/W), Source: (Brown, 1943).

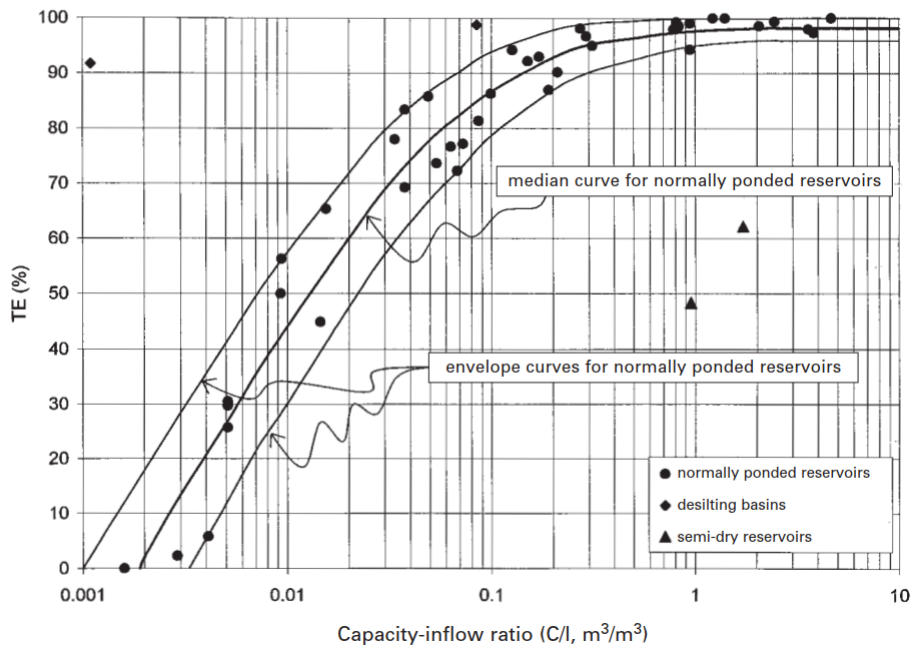

Figure 2.15 Sediment trap efficiency related to the capacity / annual inflow ratio - C/I (Brune, 1953).

Brune (1953) had suggested that reservoirs with a similar C/W ratio can have different TE's based on catchment's hydrological response and consequent runoff volume (Figure 2.15, runoff volume factor). However, a dam or weir sediment trap efficiency is not a fixed value, and it changes with time (years of cumulative deposited sediment reduces initial storage capacity). Heinemarm (1981) had proposed new relation for the estimation of sediment trap efficiency for small agricultural ponds based on C/I ratio and predicted that trap efficiency was lower than TE defined by Brune (1953).

In another study, Butcher et al. (1992) observed inflowing and outflowing sediment for two reservoirs in the southern Pennines (U.K.). They had estimated the TE for two reservoirs and evaluated TE predicted by Brown (1943), Brune (1953), Churchill (1948) and Heinemarm (1981) methods. The comparison with TE has resulted in a slight difference among other TE measurement methods. Based on the comparative findings of Butcher et al. (1992), they had stated that sediment trap efficiency predicted by Brown's method is the most suitable. Their statement was founded on the fact that the reservoirs had a similar hydrologic state as Brown used in his study. However, Brown's sediment trap efficiency method is the simplest among the other

empirical and theoretical methods. It is recommended to employ Brown's method of TE for small areas with requisite D factor estimation for the local area (equation 2.6).

Contrary to empirical models, sediment trap efficiency estimation with theoretical models is based on water particle sedimentation. Additionally, theoretical models require hydrodynamic conditions that define the quiescent or turbulent flow and whether steady (Camp, 1946) or variable discharge conditions (Ward et al., 1977; Haan et al., 1994). However, the theoretical models' requirements are high, including a sedigraph, compared to empirical models. Moreover, theoretical models for TE prediction are recommended over empirical models (Verstraeten and Poesen, 2000). Contrary to that, the implementation of theoretical models has significant constraints due to a lack of required information. Besides hydrodynamic information, discharge fluctuation measurement for a small structure is not straightforward for data-poor regions.

Furthermore, weirs vary in size and consequent discharge, leaving a weir structure that varies significantly. The discharge measurement for rectangular weir is measured with the following equation (Haan et al., 1994).

$$Q = CLH^{\frac{3}{2}} \qquad 2.7$$

In equation 2.7, Q is discharge, C is weir coefficient, L is weir length and H weir head. Where H is the difference between the lowest point of the weir crest and water surface or hydraulic head, including velocity head, this information is often unreported, and therefore discharge estimation is complicated. Although discharge equations vary based on weir structure, the v-notch weir discharge equation is based on the angle of the notch (Bentley, 2019; Haan et al., 1994, p. 147). Thus, sediment trap efficiency is measured with Brown's model for the Eamont river catchment, and catchment-wide weir and dams sediment trap efficiency is presented in Table 6.1.

Summary:

The Eamont river is a glacially carved valley in the northwest wettest part of the country. Thus, the landscape gives rise to many open and closed lakes. The

river catchment shows characteristics of a gravel-bed river. However, the river course is obstructed by two major dams and 20 weirs of various sizes. In addition to that, there is an inter-basin water transfer scheme. Hence, the Eamont catchment's hydrological response is influenced by dam structures and controlled water release in the downstream river. The current chapter has described the dataset required for the parametrisation of models, for example, DEM, land use, soil, climate data (simulated & observed), gauge data, and other non-spatial data to abstract the river catchment processes and their representation in the modelling environment. Finally, a river network-wide dataset is utilised for the model's parametrisation. Though, sediment amount stored or trapped because of the river barriers and dams is measured with sediment trap efficiency empirical model (lack of past sediment information restricted theoretical models). In conclusion, this chapter summarised the data requirement fulfilled with various sources to make model parametrisation. It ensured the seamless data exchange between the hydrological and sediment transport model at the river network scale, which has ultimately paved the way to resolve the solution for the thesis objectives.

Chapter 3: Fluvial Morphotypes and Grain Sizes: assessment and modelling implications.

3.1 River morphotypes

An excerpt of classifying river reaches into distinct morphotypes is discussed; the key is grain size distribution and water depth relationship in a given reach section. The theoretical relationship of grain size, channel depth and width are depicted in Figure 3.1. the schematic diagram depicts the river properties and their mutual relations. The resulting river morphologies are based on available sediment load (Qs) and transport capacity (Qc) in a river zone.

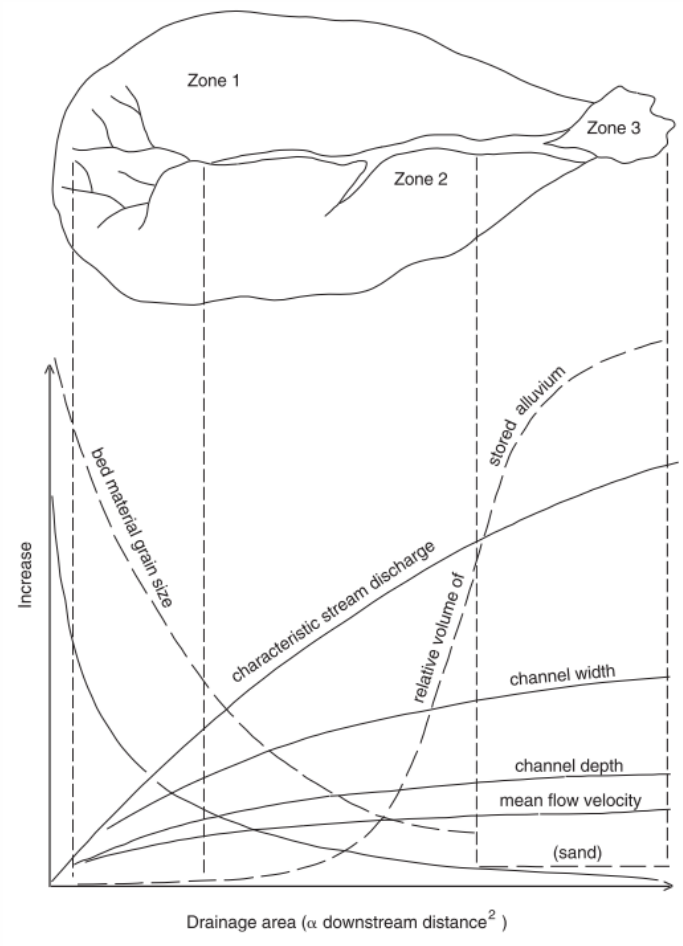

In broad terms, zones 1,2 & 3 represents sediment sources, transfer and deposition zones, respectively (based on the concept of (Schumm, 1977)

Figure 3.1 Schematic diagram of the variation in channel properties within a river catchment (Robert, 2003).

Given that grain size is a fundamental parameter for sediment transport equations, classifying a river network based on morphotype and their respective median grain

size values (D_{50}) can significantly improve modelling results. The grain size information in a river network reach, especially at the headwater region, is of prime importance because source reach provides sediment load and intermittent high-velocity discharge to the river, depending on the gradient, substrate, and channel form since erosive processes dominate the headwater region (Naiman et al., 2005).

The morphotype classification process uses remote sensing methods to classify a river based on hydro morphological characterisation at a network scale (Carbonneau and Piégay, 2012; Bizzi et al., 2016). Piegay et al. (2009) and Liébault (2003) had adopted the river morphotype classification for a braided river in the southeast part of France. They studied the geomorphology of a braided river and classified it into different morphotypes, which are characterised by respective D_{50} grain size information. In the case of the Eamont river, the morphological and mean particle size characteristics were identified on satellite and drone images, respectively, according to processed-based river classification (Brussock et al., 1985; Whiting and Bradley, 1993; Gordon et al., 2004). The classification process is followed based on Liébault (2003) river morphotypes; he had identified the following four significant morphotypes, ordered by finer GSD to coarse;

- A - riverbed with gravel river bars,
- B – riverbed with gravel flat bottom,
- C – riverbed with coarse flat bottom,
- D – riverbed with rocky bottom, (Figure 3.2).

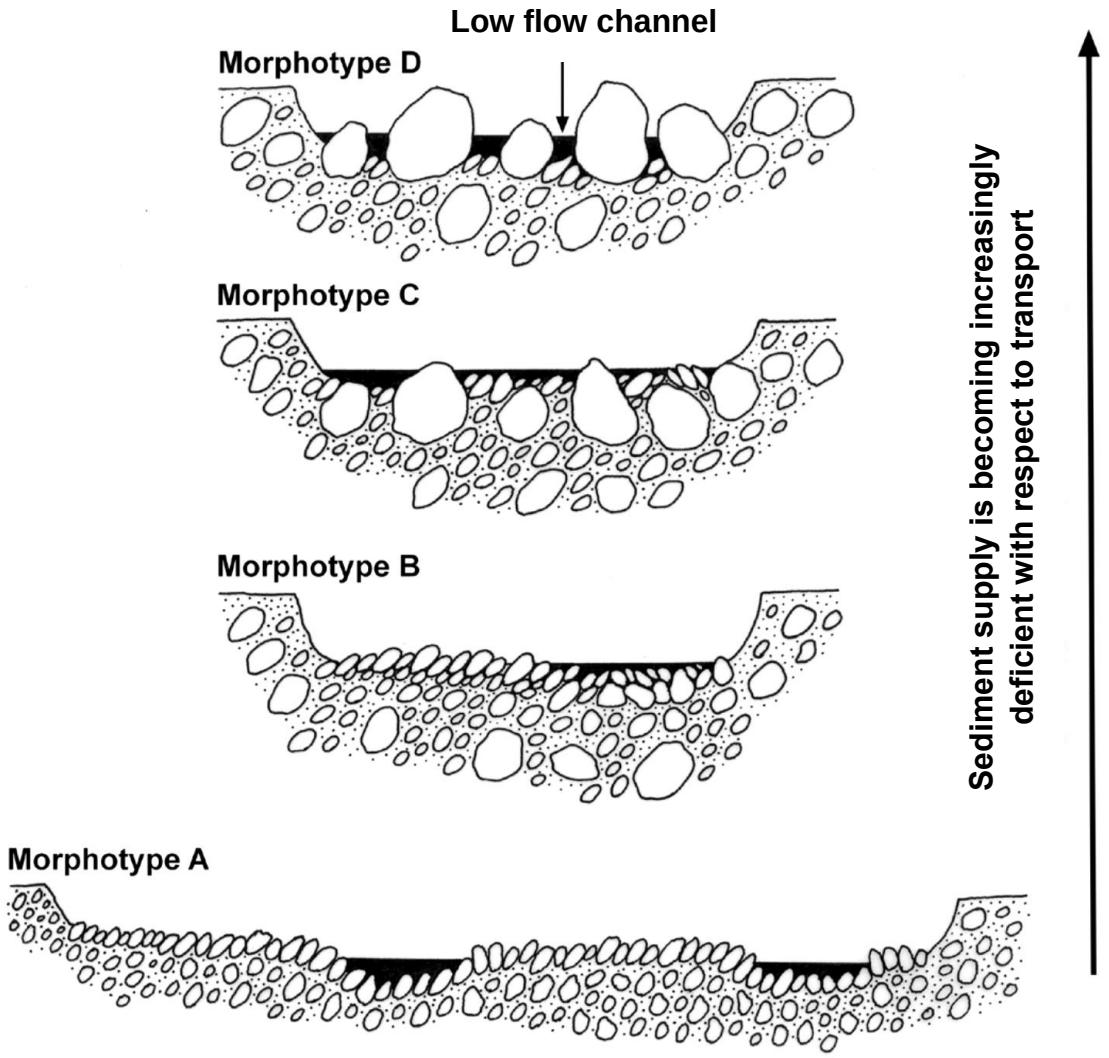

Figure 3.2 Schematic diagrams of different morphological types observed in drômoises mountains, illustrating an adjustment-based continuum balance sedimentary supply/transport capacity (Liébault, 2003).

The *morphotype D* is characterised by the high density of boulders at the bottom of the riverbed (particles have a diameter greater than 256mm). The river bottom marked by substantial irregularities suggests high hydraulic roughness and few pockets of gravel size grain either sheltered upstream of the river or downstream parts of the river. This morphotype is prevalent for the river section, which flows through gorges and often offers a low supply of sediments to the river network at low discharge conditions.

Morphotype C shows a coarse flat-bottomed riverbed, with fewer boulders emerging from the stream bed. The Riverbed bottom is composed of coarse gravel and stony filling. The width of the bed is always less than 20 meters.

Morphotype B shows flat bottom beds and the absence of boulder blocks on the river floor. This section is characterised by the absence of a large sedimentary form of storage. Morphological roughness is low, which indicate the low flow condition. The width of the current morphotype remains less than 20 meters.

Morphotype A has the main characteristic, in which beds rocky layer lies in conjunction with alluvial deposits (In Eamont river, gravels are dominant). These have a significant amount of deposition compared to previously mentioned morphotypes. The width of the reach can vary between 30 and 40 meters. Grain size distribution is homogeneous and occupied by gravels size sediments and often accumulated as patchy deposits.

Liébault (2003) described the D90, D50, D10 and D90/d values distribution in the different morphotypes, where d is the river's depth. The median grain size varies from morphotype A to D. However, the identification process of each morphotype on a river network based on particle size distribution is not straightforward compared to other morphometric variables. They analysed the grain size variable and found that the grain-size interquartile range threshold improved the morphotype classification process (Table 3.1). Thus, based on grain size interquartile threshold range, they found the following condition that discriminates one morphotype to another morphotype, and they are as follows:

a. When the value of D_{50} is beyond 60mm, it indicates that a probability of belonging to the morphotype C or D is highly likely.
b. If the value of D_{90} is higher than 140mm, then the possibility to classify the morphotype C or D is higher.
c. Lastly, if the D_{10} measured value is lower than 20mm, it suggests belongingness to morphotype A or B.
The variable relative roughness of the bed (D_{90}/d) significantly increases for the morphotype A to D. This is an indicator of energy decay of the transporting flow. Liébault (2003) presented the grain size analysis for D_{90}, D_{50} and D_{10}. The

interquartile range is presented in Table 3.1; a study on the Vjosa River basin had adopted these interquartile values to identify Morphotypes (Tangi, 2018).

D50 (mm)					
Morphotype	**Average**	**Standard Deviation**	**Minimum**	**Maximum**	**Interquartile range**
A	35.68	11.17	19.44	61.32	27.78; 40.87
B	43.76	13.99	20.91	72.84	33.06; 52.17
C	66.37	26.03	32.00	128.00	44.57; 79.43
D	84.35	23.05	47.12	132.61	63.29; 100.99
D90 (mm)					
Morphotype	**Average**	**Standard Deviation**	**Minimum**	**Maximum**	**Interquartile range**
A	94.83	38.49	40.71	184.77	63.12; 117.05
B	125.50	36.07	44.37	183.52	103.16; 146.49
C	206.65	83.42	85.21	384.00	135.15; 256.00
D	264.37	119.84	123.31	724.08	187.67; 298.68
D10 (mm)					
Morphotype	**Average**	**Standard Deviation**	**Minimum**	**Maximum**	**Interquartile range**
A	14.83	3.83	9.32	26.57	11.96; 17.00
B	15.20	3.89	9.86	22.19	11.74; 18.21
C	24.08	12.86	11.23	64.00	14.69; 32.11
D	25.41	9.68	11.31	43.43	18.22; 33.71

Table 3.1 Key size characteristics of Morphotypes (Liébault, 2003).

Morphotype A and D are distinctly different, while B and C are slightly differentiated as intermediate.

3.1.1 Classification of morphotypes in the Eamont catchment

The Eamont river is primarily a gravel-bed river. It originates in a glacial valley that is dominated by igneous and metamorphic bedrocks. The headwater section shows the presence of boulders and shallow water conditions similar to morphotype D. The low-lying area of the catchment depicts river conditions like morphotype A. Eamont catchment has distinct lake and pool existence. Moreover, the river flows through these deposition environments, disrupting the continuity of sediment refinement. Although, many tributaries also disrupt sediment size-refinement process because of varying grain size contributed at the confluence (Robert, 2003; Knighton, 2014). A few big dams or weirs are located in the

catchment, and they disturb the natural sediment refinement in context to the river continuum concept.

The Eamont river is classified into four distinct river morphotypes A - D. This is performed following depth, width, gradient, and mean sediment size information derived through photo-granulometry (discussed in section 3.4) performed at the reach scale. First, the identification process is based on google satellite images for river width and roughness measurement (Arcement and Schneider, 1989). Second, depth and gradient information were extracted from SWAT simulation software and 5m DTM data (Bluesky, 2014).

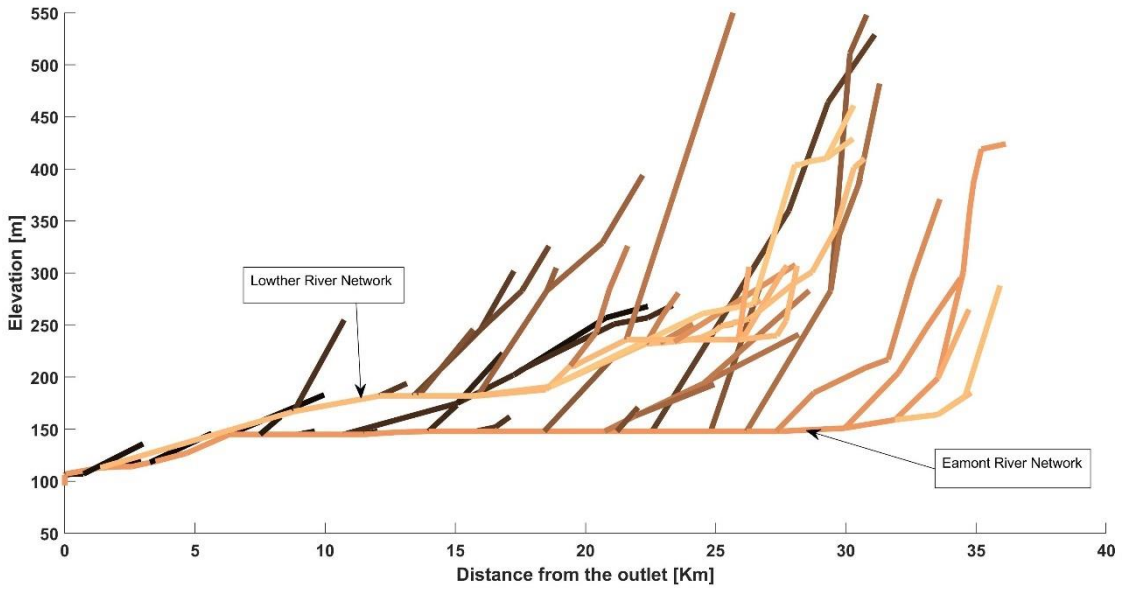

Figure 3.3 Eamont and its tributary river Lowther elevation profile.

Finally, river morphotype classification of headstream reaches were performed with respective depth, width, gradient, and median grain size information.

In the current study, it is essential to get grain size information for each reach because of the parametrization requirement of the CASCADE model. The Eamont and Lowther River network and their elevation profiles were analysed in Figure 3.3, and respective reach roughness factors were interpreted on google satellite and drone imagery, including other river parameters.

The interpolated grain fraction (D_{16}, D_{50} and D_{84}) values and their spatial distribution depicted on the Eamont river network (displayed in the CASCADE model environment (Figure 3.17), which is achieved with piecemeal linear

interpolation of photo-granulometric data between two nearest observations). The Eamont river network is fully parametrised, and morphological and topological attributes are presented in Appendix B**.**

3.2 Morphotypes associated with grain sizes

First, data is plotted for the sub-catchment area and river width information for validating divided river reach (satellite-based river morphological characterisation). Figure 3.4 shows the correlation between sub-catchment areas and the river width, and it supports reach division performed other than natural tributaries such as weir location and river geomorphology. Second, the median grain size (D_{50}) is plotted against the sub-catchments area of the Eamont river, and it has illustrated a fair correlation among the two, Figure 3.5.

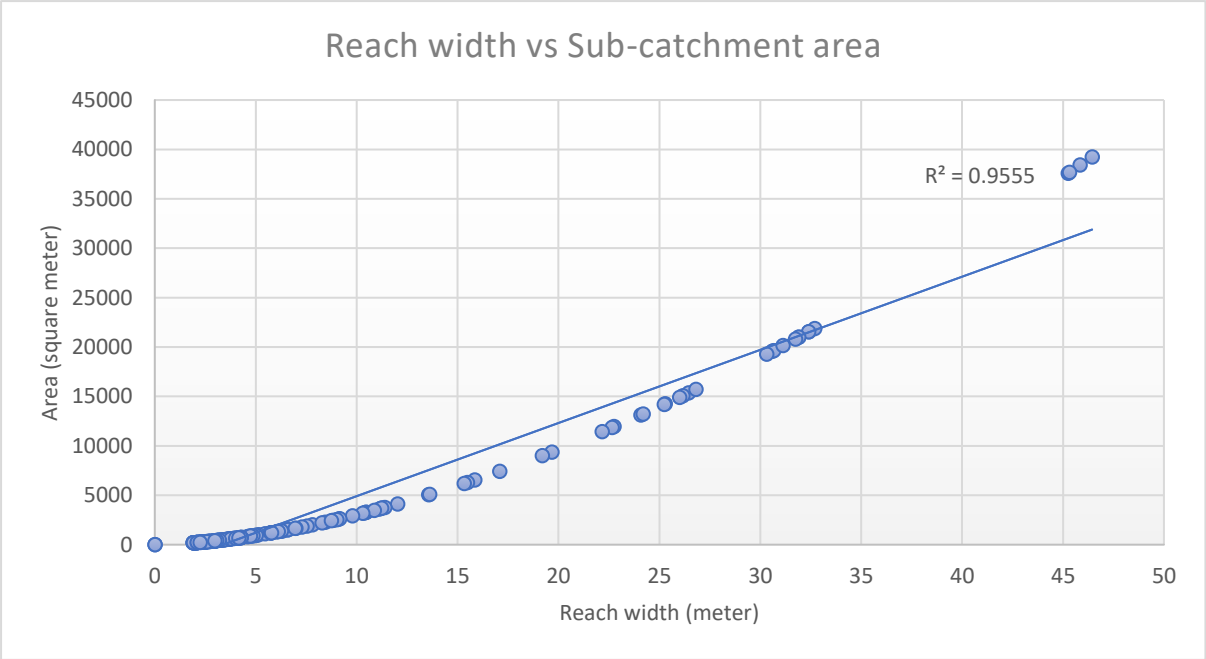

Figure 3.4 Reach width and sub-catchment area correlation for Eamont river catchment.

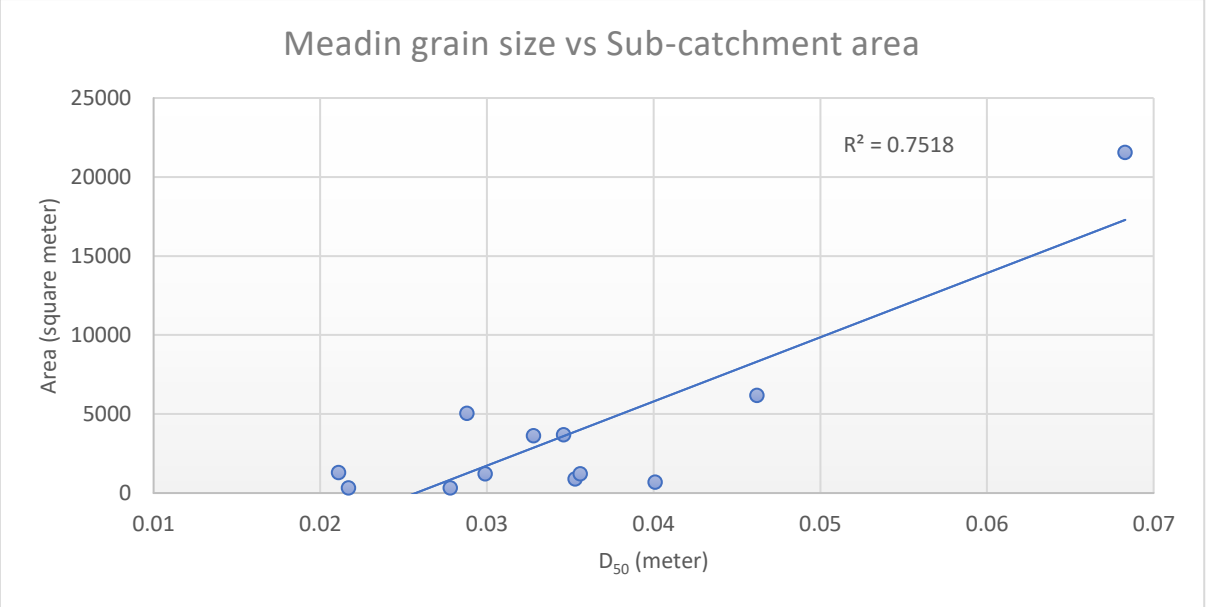

Figure 3.5 Median grain size (D50) measured on drone images and Eamont river sub-catchment area correlation.

The river reaches width and discharge relation progressively change in the downstream direction (Wolman and Brush, 1961), and change in the river width can influence the sediment flux leaving a river section under a variety of discharge conditions (Cook et al., 2017). Therefore, dividing the river into distinct morphological characteristics and respective grain distribution may significantly improve the sediment flux assessment. In a data-poor river catchment like the Eamont river, the Morphotype classification adoption becomes essential to develop the GSD at the river network scale.

3.2.1 Catchment-scale patterns

The grain size heterogeneity at the river catchment scale is established with grain size measurement (section 3.4.1) and river morphotype selection. The interpolated grain size result depicts a general trend that shows progressive refinement in the downstream direction, and at the few tributary confluence, the grain size varies abruptly, as evident in previous studies in the European region (Škarpich et al., 2019). Especially for grain size fractions D_{50} and D_{84}, it can be attributed to the fact that relatively bigger grain size would sink in the Ullswater lake depositional environment; therefore, it leaves the downstream river with a relatively dominant fraction of fine sediments. The presence of fine sediments is verified with the drone image analysis located at the Pooley Bridge (2°49'6.97"W,

54°37'1.88"N, station id 76015 - national river flow archive, U.K.), and at this site, grain size is finer than all the sample collected in the Eamont river headwater region (or Ullswater Lake's tributary catchments). Figure 3.17 depicts grain size fraction information which is established by linear interpolation; however, it cannot be treated as a replacement for actual sampling information.

3.2.2 Measurements of grain size

The grain size information is established by transforming low altitude hyperspatial images into orthorectified and scaled images, which are further processed for the grain size object detection to filter out individual grain (Detert and Weitbrecht, 2013). The grain data is generated digitally through a line sampling method proposed by Fehr (1987). The subsurface grain size fraction developed with the fuller curve estimation, Figure 3.12 & Figure 3.13. The detailed processing of orthorectification and object detection of gravel data development is explained in sections 3.5 and 3.6.

3.2.3 Measurement of bed-load transport

The difficulties in bedload transport measurement are linked to shear stress diversity across the river reach, which is not directly measured. Given transport rate dependence on grain size as defined for each reach, an inappropriate grain size assignment to transport formulae will lead to the wrong transport rate measurement. However, sediment is supplied through the riverbed and from the connected headwater region. Therefore, catchment-scale sediment supply and transport rate provide a means to evaluate the results (Wilcock et al., 2009). For direct bedload transport measurements, bulk samples are needed. However, it is difficult to collect such samples at the catchment scale (Kondolf and Piégay, 2003), and it is crucial to scrutinize the morphological characteristics of the river because river network can have a depositional environment that can ultimately impact catchment sediment flux or yield at the river outlet (Joyce et al., 2018, 2020). The mentioned limitations in bedload transport measurement are addressed in the CASCADE (Chapter 5:) tool that works on sediment connectivity fractional transport rate and models the hydro-morphological impacts for the sediment flux simulations. However, the model simulation is validated with an empirical relation because the catchment lacks sediment records.

3.3 Role of grain size in CASCADE

Sediment transport modelling provides insight regarding river dynamics, which helps immensely in river management and water resource exploitation planning (Kondolf et al., 2014a). However, bed-load sediment transport is complex, and accurate assessments remain difficult. There are bed-load transport equations and models; empirical (Du Boys, 1879), statistical (Einstein, 1942, 1950), mass-balance (Parker et al., 2000; Charru et al., 2004; Ancey et al., 2008), and lagrangian and particle dynamics (Heyman et al., 2016; Czuba, 2018). (Ancey, 2020a) has compared the various bed-load transport equation, models and he has enlisted reasons why bed-load transport prediction is complex: spatial-temporal variations due to flow dynamics, interaction of cascade processes, heterogeneity in bed material and flow conditions, poor knowledge of boundary condition, scale effects between field condition and laboratory, hysteresis.

In the CASCADE model (discussed in chapter 5), the riverbed grain size information plays a crucial role because the model estimates the available transport capacity in a river reach and redistribute the transport capacity among the sub-cascades. Each reach has 18 sub-cascades; thus, each river reach can have 18-grain classes mentioned in Krumbein (Φ) scale. The calculated transported capacity for river reach is redistributed among the sediment sub-cascades active within the same reach. The redistribution of the transport capacity is portioned with Wu – Molinas fractional transport rate computation (Molinas and Wu, 2000; Wu et al., 2003). Fractional transport rate enables the model to process different sub-cascades and their downstream direction journey, conditioned by transport capacity enough for the entrainment and transport of specific grain size.

On the other hand, if transport capacity in the reach is not enough for grain specific sub-cascade, then sediment flux gets deposited. Therefore, entrainment, transport, and deposition of a sediment load originating at the river sources are tracked for their respective sink. It becomes crucial information of sediment flux movement and reveals sediment connectivity and dis-connectivity. In conclusion, excessive erosion and deposition of sediment flux can provide insight into possible river morphological transformation sites. However, assigning the wrong grain size to the source reach and remaining reach can change the resulting sediment flux

under identical hydrologic, hydraulics, and river morphological boundary conditions. Although grain size distribution data is accessed with photo-granulometric technique, in the case of the Eamont river itself, it sets boundary conditions to a near-real grain size distribution but not the actual conditions.

3.4 Measurement of grains in the Eamont

The non-linear riverine behaviour of sediments has been established with flume, tracer, and sensor-based studies (Carré et al., 2007; Koiter et al., 2013; Houbrechts et al., 2015; Brambilla et al., 2018). Recent advancements have adopted sediment transport modelling and fractional transport formulae. In sediment transport studies, fractional sediment transport formulations are gaining credibility, and they are advocated in sediment transport modelling at the river network scale (Wilcock et al., 2001; Wilcock and Kenworthy, 2002; Wilcock and Crowe, 2003; Schmitt et al., 2018; Czuba, 2018; Tangi et al., 2019). It is crucial to obtain high-quality grain size distribution and hydraulics data to assess fractional sediment transport (Recking, 2016) because fractional sediment transport measurements are essential for river morpho-dynamics studies. However, the grain fraction data availability cannot ensure sediment transport estimates of practical accuracy (Wilcock et al., 2009).

At the regional scale, the grain size distribution in the river network reflects variations in available transport capacity in the reach section (Carey, 1985; Hubbell, 1987). Because processes such as sediment entrainment, deposition and transportation at reach scale are susceptible to hydrodynamic discharge and sediment types (Pitlick and Wilcock, 2001). A study has also revealed that the changes in bed-load grain size and its transport rate provide a better insight into downstream variations in distributed gain size and advanced textural composition (Shih and Komar, 1990a). In general, sediments get better sorted in the direction of sediment transfer (McLaren and Bowles, 1985; Rice and Church, 1998). The refinement in the size of sediment deposits attributed to grain specific sediment sorting (Ashworth and Ferguson, 1989; Lisle, 1995; Ferguson et al., 1996) has been verified in flume experiments (Paola et al., 1992).

Grain size-related parameters are correlated with the transport rate (Cudden and Hoey, 2003). Thus, in numerical modelling, distributed grain size information

would play an important role to predict sediment flux and yield. Grain size information at the river network and its predictive transported flux simulation can help formulate a sustainable river management plan (Clarke et al., 2003; Škarpich et al., 2019).

In order to enhance the weir removal study (present case), this section addresses the methodology of GSD (grain size distribution) information generation with a consumer-grade drone. The collected information serves as boundary condition data for improving model performance in the data-poor region (Eamont River catchment). In a montane river catchment like the Eamont, which has open lakes (depositional environment), their presence can abruptly impact sediment size on the river network scale.

The secondary objective is to develop GSD data at the network scale with sampled grain size data and assign GSD information to the unsampled river reach based on morphological similarities (morphotypes) with the sampled reach. Each reach at the river network will get grain size fraction data. The enhanced grain size information will help determine a better river cascading process within the CASCADE model. It is suggested that the geomorphological studies at the catchment scale would become more reliable if related studies include transport rate calculation at the local scale (Wilcock, 2001). Thus, an improvement in sediment transport flux information would be expected when a fractional transport rate formula is employed in a sediment transport model.

The distinct river morphologies emerge from a complex set of processes working on various parts of the river. At the reach scale, river morphology develops based on connected sediment source links, sediment transport capacities at a local scale, instream & riparian vegetation, and distribution of woody debris also impacts the flow conditions. Based on mountainous river catchment observations, river reach morphology shows a distinct slope, grain size, channel roughness pattern (Recking et al., 2016). Shear stress parameters have shown consistency to the channel roughness related to sediment supply and transport capacity at reach scale (Hey and Thorne, 1986; Montgomery and Buffington, 1997). Although discharge has a dominant role in carving out distinct river morphology, median grain size has the highest correlation with discharge (Hey and Thorne, 1986). The grain roughness is a dominant element indicator for flow resistance in a gravel-

bed river. The change in flow resistance depicts the variation in flow geometry between riffle and pool, local variation inflow condition, and the roughness of surface bed material (Hey, 1988, 1979).

In order to initialise the sediment movement, the amount of critical shear stress is exceeded by the flowing water for each sediment grain size (Shields, 1936a, 1936b).

$$\tau_* = \tau / g(\rho_s - \rho)D \qquad 3.1$$

The equation (3.1), τ_* is non-dimensional stress, and g gravitational force, ρ_s and ρ are sediment and water densities, respectively, D is the diameter of grain that is being mobilised.

In a steady uniform flow condition, shear stress is a function of stream depth and gradient of the stream. Equation (3.2), d is the flow depth and S is the energy gradient of the stream.

$$\tau = \rho g d S \qquad 3.2$$

The grain movement initiated when τ bed shear stress value exceeds the critical stress τ_c .

$$q_b = k(\tau - \tau_c)^n \qquad 3.3$$

In equation (3.3), q_b is the transport capacity in a channel where sediment supply is unlimited, k and n are empirical values (Du Boys, 1879; O'Brien and Rindlaub, 1934; Meyer-Peter and Müller, 1948; Buffington and Montgomery, 1999). However, the unequal mobility in gravel and sand weakly bimodal river, as analysis of fractional transport rate and grain size related to shear stress has suggested that gravel transport is size-selective and sand transport is close to unity (Wathen et al., 1995).

The elementary deterministic models have revealed that shear stress required to initialise sediment displacement depends on grain size (i.e. $\tau_c \propto D$), with additional factors like grain shape and degree of packing or imbrication (Knighton, 2014). Nevertheless, the grain size in a natural stream varies significantly, especially in the gravel-bed rivers. The grain mobility is influenced by pivoting angle (Komar and Li, 1986) degree of grain exposure (Fenton and Abbott, 1977), including sediment imbrication and bedform structure. Though shield number is

not a fixed value, it varies significantly if grain size > 8mm, irrespective of the loose or tightly packed river bed (Church, 1977). The experimental evidence has indicated that local mobility does not imply reach-averaged equal mobility if local variation in grain size exists (Paola and Seal, 1995). Thus, equal mobility to a grain mixture contradicts size-selective transport.

The perspective of river form-processes relationship changes from one scale to another. In a moderate-size catchment, a fluvial form can be depicted such as the following hierarchy, drainage network (>10^5 m) to river length (sequence of meanders), channel-reach (single meander), channel unit (pool, riffle), subunit (bars) and individual particle (<10^{-1} m) scales (Knighton, 2014). At each scale of river form-processes of the geomorphic unit get adjusted due to the dynamic movement of individual grain. Therefore grain size is recommended as a key-dependent variable in a numerical simulation of sediment transport models (Hoey and Ferguson, 1994). In a recent study, weir removal was performed with the sediment transport analysis in a numerical simulation model to access the impact of weir removal scenarios. It uses grain size as a basic functional unit to assess geomorphic change estimation following a removal case (Howard et al., 2017). Thus, grain size distribution in the river network scale within the modelling environment can bring out the geomorphic process & form information at a particular sample timescale. Hence, grain size is one of the most critical parameters advised for the sediment transport processes (Robert, 2003).

3.4.1 Optical granulometry

Optical granulometry is used to derive grain size information from vertical images. The derived information regarding grain size distribution reveals catchment hydro-geomorphic status and responsible process acting on the river (Parker et al., 1982; Andrews, 1983; Kirchner et al., 1990). The earliest adaptation of grain size estimation using the grid by number approach utilises photographs of sediments and grid of known interval (Ritter and Helley, 1968; Kellerhals and Bray, 1971; Iriondo, 1972; Adams, 1979). However, there were a few drawbacks: grain packing, shadow effect, scale distortion, and imbrication angle.

The digitisation of coarse grain edges was adopted to address this issue, and classification was performed based on an estimated ellipsoid (Ibbeken and

Schleyer, 1986; Diepenbroek and de Jong, 1994; Ibbeken et al., 1998). Recent advancements in remotely sensed optical imagery at a catchment scale can become valuable assets for extracting or mapping river parameters (Marcus and Fonstad, 2008). The early observer had shown ways to evade direct observation on-site (Fonstad and Marcus, 2005) and scaling up image-driven river environment characteristics at the catchment scale (Carbonneau et al., 2003, 2004, 2005a, 2005b, 2006; Carbonneau and Dietrich, 2017).

Optical image analysis primarily focused on gravel size information utilises digital image processing techniques, image grey-scale thresholding and image segmentation. Image processing techniques aim to sort out the individual grain and perform grain size measurements. The result obtained with optical granulometry was found accurate when compared with manually-identified measurements (Butler et al., 2001).

Optical granulometry techniques remove the need for labour-intensive fieldwork and careful sieve analysis in the lab environment. Most gravel-bed rivers often lack distributed grain size information (Verdú et al., 2005; Chávez et al., 2015), thus illustrating the need for fast grain size measurement with remote sensing. Recent advancements in UAVs and onboard sensors have opened a new hyperspatial remote sensing image domain. These two attributes of advanced consumer-grade UAVs have proven their importance in creating catchment scale distributed grain size information (Carbonneau et al., 2005a; Carbonneau and Dietrich, 2017; Langhammer et al., 2017; Carbonneau et al., 2018). In gravel-bed rivers, the entire size distribution information provides full spectrum for different parameters estimation; for example, D_{90} can be associated with channel roughness estimation, and D_{10} that makes the fair proportion of the river bed is essential for fish spawning habitat (Waters, 1995; Diplas et al., 2008). The resulting sediment transport models can exploit the entire range of distributed grain information for fractional transport rate calculation. Such models can act as sediment screening that determines sediment fate from source to sink. The models would have different transport rates at the reach section for specific grain size, this defines sediment transport and deposition pattern at the river network scale in a model like CASCADE.

3.4.2 BASEGRAIN: an overview

The BASEGRAIN is an automatic object detection tool that performs an optical granulometric analysis. It is suitable for top view or nadir images of non-cohesive sediments of gravel beds. It implements a five-step object detection algorithm to filter out grain edges, including separating interstices from grain area (Detert and Weitbrecht, 2013). Finally, a quasi-grain size is calculated from detected and filtered grain object's b-axis following the line-sampling method (Fehr, 1987).

The implementation of BASEGRAIN in this study was used to produce grain size distribution data for subsurface material. This feature of BASEGRAIN becomes crucial for providing distributed process and form information acting at a catchment scale, hydraulic and sediment transport modelling. Contrary to that, conventional laboratory techniques demand sample collection, transportation of samples to the lab facility and then performing sieving to get the weighted average results.

BASEGRAIN performs a few steps to refine grain size information (Detert and Weitbrecht, 2012). It implies a double grayscale threshold approach to separate grain area from interstices (Weichert et al., 2004; Graham et al., 2005a, 2005b). At first, BASEGRAIN identifies interstices between the single grains on the grayscale thresholding image. Second, interstices identification with morphological bottom-hat transformation. Third, the implementation of two gradient filtering techniques Sobel Method (MATLAB, 2018), for vital edge detection and this stage further employs the Canny edges method (Canny, 1986), enabling soft edge detection. Fourth, converge the previous steps of interstices detection to separate single grains by applying the watershed algorithm. Fifth, the ellipse's delineated grains are fitted to derive the grain size information by adjusting a-axis & b-axis (Plesiński et al., 2017).

Finally, Fehr’s line sampling methods produce surface grain size and prognosis to get sub-surface layer grain size information. The prognosis has been performed with the fuller curve estimation. Thus, it can provide the photographic sample undetected fine grains size information.

The input processed images must be rescaled for BASEGRAIN optical granulometry analysis. However, we note that optical granulometry is now moving towards deep learning methods, with applications such as SediNet (Buscombe, 2020) emerging in the very recent literature.

3.4.3 Morphotype identification on Google Images

In Figure 3.6, google satellite images depict river morphotypes present in the Eamont river catchment. After identifying morphotypes on Google images & their assignment to the river network, we assigned the respective mean grain size information. The missing reach grain size for remaining un-surveyed reaches get their respective D_{16}, D_{50} and D_{84} values based on linear interpolation performed in MATLAB, which are located between two successive photo-granulometric survey sites, Figure 3.16. Although linear interpolation can induce mathematical refinement of sediment size and avoid such unintended misinformation to the model, a careful approach is adopted. In this approach, a piecemeal linear interpolation has been performed. The interpolation is performed between two known samples sites (D_{16}, D_{50} and D_{84}) for which morphotypes are assigned. Such a piecemeal interpolation approach helps to generate continuous grain size distribution information on the Eamont river network. However, this cannot replace the actual sampled grain size information. This approach was previously used to initialise the CASCADE modelling performed for the Vjosa River (Tangi, 2018).

Morphotype D: on a source reach at the Eamont river network.

Morphotype C: Tributary River Lowther.

Morphotype B: Tributary River Lowther.

Morphotype A: Eamont river catchment outlet section.

Figure 3.6 Examples of Morphotypes identified on Google images for Eamont & Lowther River network.

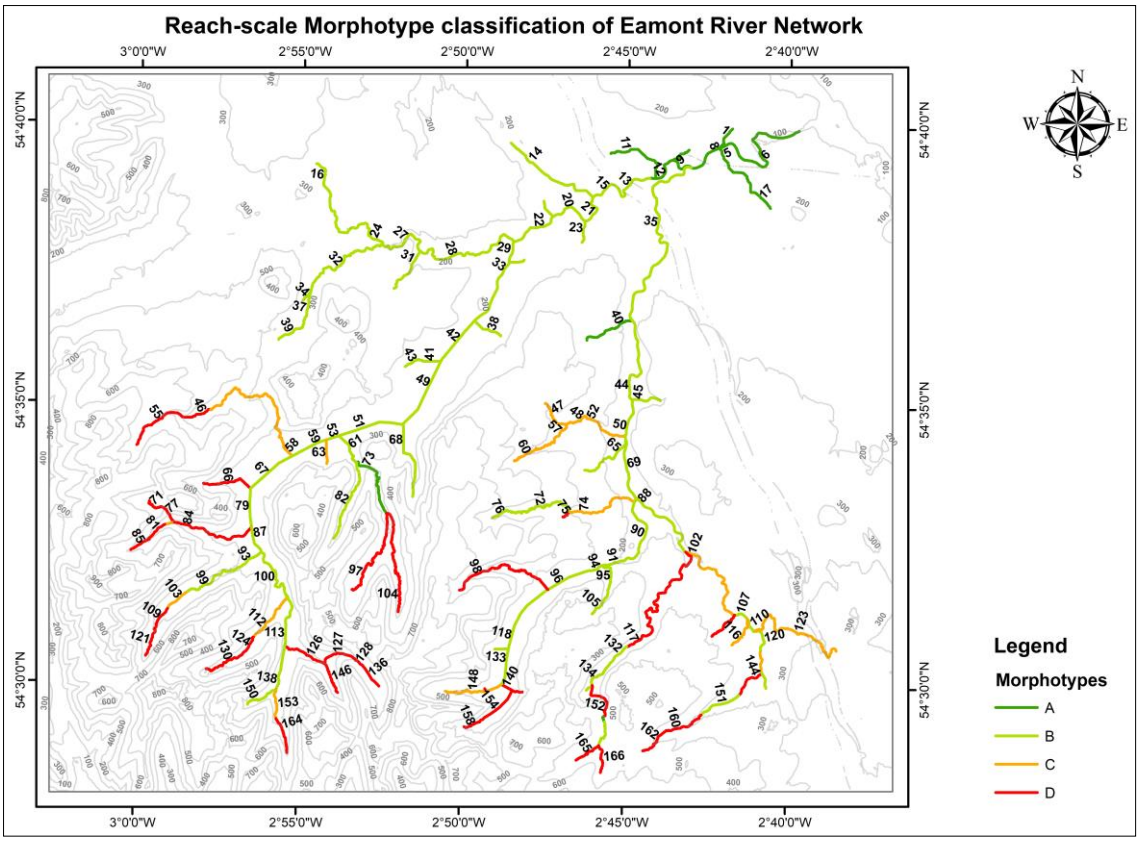

Figure 3.7 The morphotype classification of the Eamont river catchment.

3.5 Drone-derived hyperspatial image data

We have employed a DJI Phantom 4 drone equipped with a 12.4M pixel camera. It can produce high-resolution images, and its deployment for close-range image collection suits optical granulometry objectives. A three-axis (pitch, yaw, roll) gimbal keeps the onboard camera sensor stable to avoid any motion burr in the captured photographs. The pitch of the sensor is controllable within 0 – 90^0, and it enables piolet to collect multi-view images of the close-range gravel bed, suitable for fine-grain sediment under optical granulometry study.

Field surveys were completed in two subsequent field visits to the Lake District (April & June 2019). In these summer months, the river discharge was at the normal stage. A low water level ensures the maximum availability of exposed gravel bars. The consumer-grade quadcopter had gathered the exposed Eamont river gravel bed photographs. The drone allows access to an inaccessible part of the river gravel bar as the drone can maintain its position in mid-air against the wind. This suits for taking nadir photographs, including oblique photographs for optical granulometry.

Every sample site has at least 35 drone-captured images of gravel beds. The sampled images contain nadir as well as oblique images (± 30^0) of the sample site. The area of interest varies with the amount of exposed gravel bar in the river, and it varies between 2x2m and 5x5m. Images were taken following the photogrammetry rule, in which 60% side lap and 80% forward lap were secured. The onboard camera sensor has a field of view 94^0 that ensures a complete photographic imprint of the gravel bar. Albeit the wide-angle lens is prone to barrel shape lens distortion and impacts photographic impression, the central portion gets large scale, and corner parts of a photograph show low scale.

Moreover, scale difference is prominent in close range gravel images compared to high altitude images. Therefore, it is mandatory to resolve barrel distortion imprint on drone images (Aber et al., 2019, p. 86). Hence, drone images are processed in photogrammetric application software (AgiSoft: PhotoScan). Agisoft produces orthoimages, free from barrel distortion images.

The river flows through mid-altitude mountains in the catchment, and some river reaches are remote and inaccessible. The Eamont River joins Lowther River, a major tributary in the low-lying part of its catchment. The rive network is divided into 166 reaches in the hydrological modelling, based on distinct geomorphic parameters. Therefore, there is a requirement to get each geomorphic unit grain size sample as they are experiencing different stages of river development. The survey was planned to obtain a representative sample of each geomorphic type. Whether in headstream, river confluence, and at the outlet region of the catchment. Few image samples represent the change in grain sample at the immediate downstream section of the weir location on a river network. It is crucial to have representative GSD for all 166 reaches. However, it is not possible or practical with the photographic sample., Even it can be performed faster than the conventional procedure.

The river morphotype selections are based on (Liébault 2003), the morphological type ascertained before the detailed field visit. Four main geomorphic types were classified at the catchment scale with the help of Google Earth images.
The drone survey at a site consists of multiple images. The main objective of this exercise was to create high-resolution images that could provide better grain variability at the survey spot. The close-range images were captured at an altitude of 1 -2m height from the riverbed. Multi-view photos are recommended for better positional accuracy (Harwin and Lucieer, 2012; Bláha et al., 2012; Turner et al., 2014; Koci et al., 2017; Rossi et al., 2017; Carbonneau and Dietrich, 2017; Seifert et al., 2019). Although drone-captured images do not show much positional error for survey work, in grain size analysis, any deviation from sub-meter inaccuracy would progressively degrade the main objective of optical granulometry or photo-sieving. Thus, we have placed an object of a known length to rescale drone images at the post-processing stage or the BASEGRAIN application.

3.5.1 Post-processing of drone data

The site-specific images are loaded in Agisoft software as a separate processing chunk. Before further processing, image inspection must discard any accidental image introduction to blur images, which can hamper the quality of output images. Selecting an appropriate coordinate system is essential because the difference

between the image coordinate system and processing environment coordinate system would result in errors like the model's elevation.

3.5.1.a Alignment

Image alignment is a primary processing step that determines camera positions and image orientation. It virtualises the field drone locations in the model space. At this step, software shows the image's ground projection. The alignment process also builds a sparse point cloud model. Once camera data is imported and images projected in images space, the software performs common feature identification and matching among overlap parts of the projected images, resulting in spare point generation that visualises tie points in the 3D image space.

3.5.1.b Dense cloud

The dense cloud formed based on estimated depth information from the camera position of an individual camera. This depth information is stitched together for the formation of the dense cloud for each selected chunk. The density of dense points could be like a LIDAR point cloud based on the reconstruction parameter chosen. The *z*-information generated in dense cloud formation supplemented for digital elevation model creation.

3.5.1.c Mesh

A dense point cloud or a sparse point cloud provides base information that is utilised for polygonal mesh model creation. The mesh creation as an option as dense point cloud consists of better depth information than mesh dataset. Moreover, a dense point cloud is recommended to form a digital elevation model.

3.5.1.d Digital elevation model

The DEM is primarily a rasterised form of dense point cloud at regular grid size intervals, and its grid size is estimated from the source data. It provides base information for the orthorectification of drone capture images.

3.5.1.e Ortho-mosaic

The ortho-mosaic was created with an orthorectification process, including original drone capture images. The elevation information can be provided in the

form of a sparse cloud, mesh, or dense point cloud, which is used for the orthorectification process in gravel-bar images. The model projection system is set here to a projected coordinate in the UTM system, and the pixel value is set to a default value; the pixel values remain fine for high-resolution images (in cm).

3.6 BASEGRAIN: Eamont Rivers GSD data development

The drone images are converted to orthoimages in the photogrammetric suite. The orthoimages are analysed to derive the grain size information in the BASEGRAIN, and it reads the user input in the form of *mm/pix* value. The images are cropped for the recommended size of <~2500^2 pixels (BASEGRAIN 2.2 version).

Figure 3.8 SFM processed and scaled image of a gravel bar at the headwater section of river Eamont River.

The area under consideration for grain size distribution is processed in five sequential stages for interstices identification (Figure 3.9). It is based on a grayscale threshold and morphological bottom-hat transformation algorithm (edge detection). The extraction of interstices is controlled by multiple user inputs in the software user interface and can be fine-tuned based on on-screen visualisation. Although, the software's default setting produces satisfactory results. The grain edges are enhanced using gradient filtering. This stage also uses Sobel and Canny filters for strong and soft edge filtering, respectively (Figure 3.10).

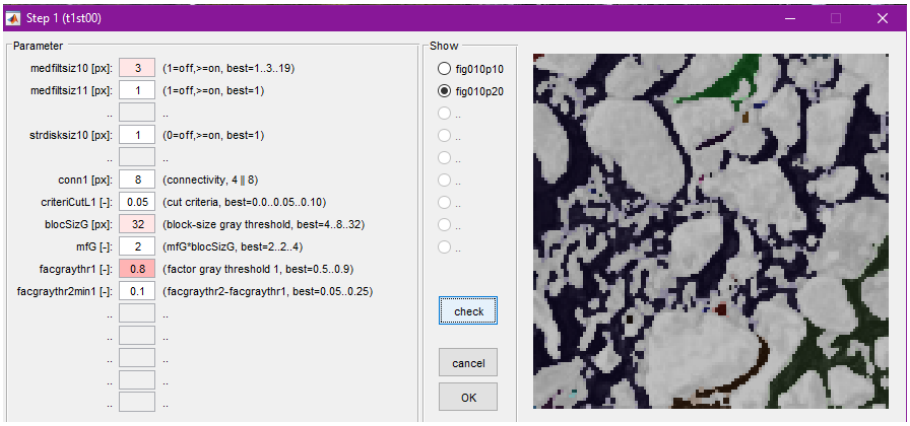

Figure 3.9 Scaled image undergoes digital image processing for edge filtering (BASEGRAIN).

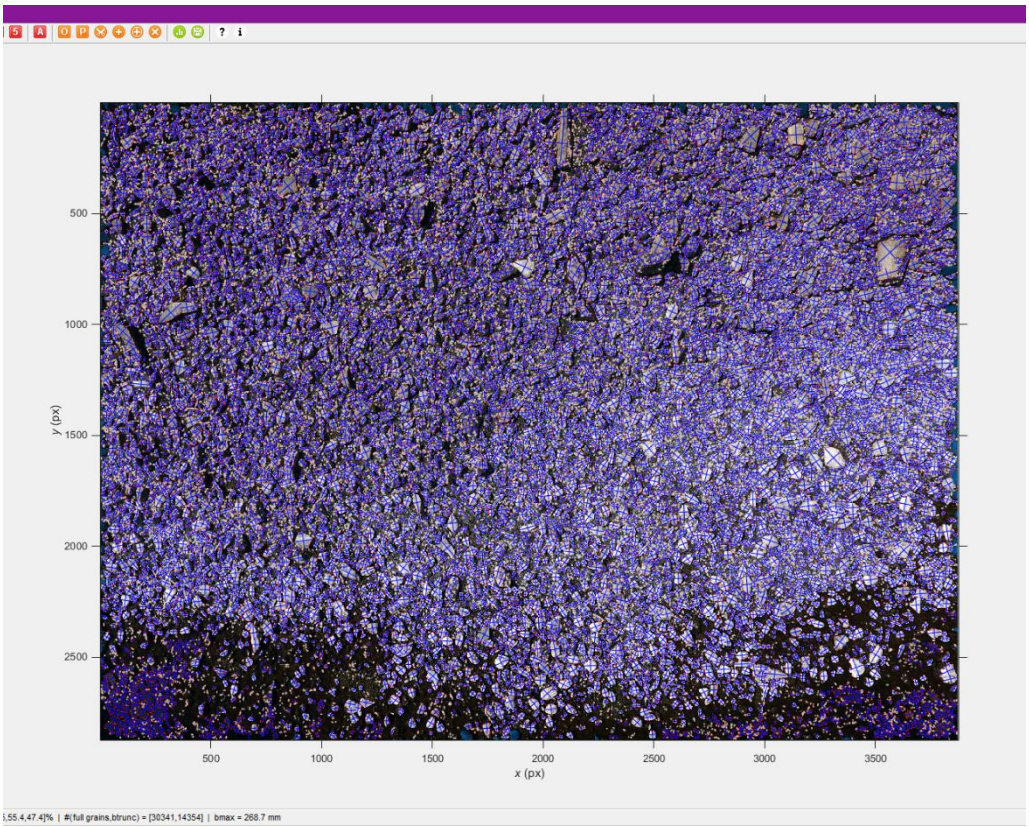

Figure 3.10 Pre-processing for automatic edge detection.

The extraction of individual grain objects formed while previous stages information converged, and watershed algorithm executed (Figure 3.10). Thus, formed grain objects analysed between switching between image and object view. Suppose there are a few discrepancies regarding grain size object formation. The whole process can be re-executed, or manual editing can be adopted.

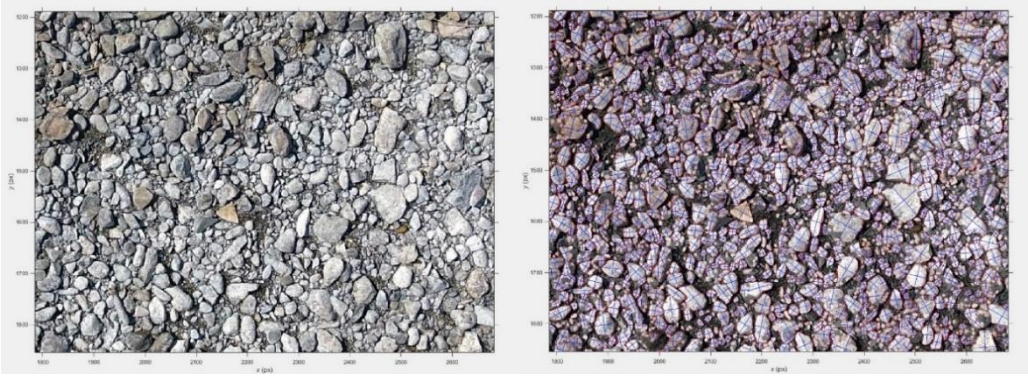

Figure 3.11 post-processing for manual editing.

When grain objects are of adequate size discerned in the final stage, ellipsoids are fitted to the newly formed grain objects and measure their a-axis & b-axis. Fehr's line sampling method, quasi area sampling, has separated grain size distribution within a gravel bed's photographic sample. Fehr's line sampling method provides fine grain size distribution prognosis by extending the grading curve (Figure 3.12 & Figure 3.13).

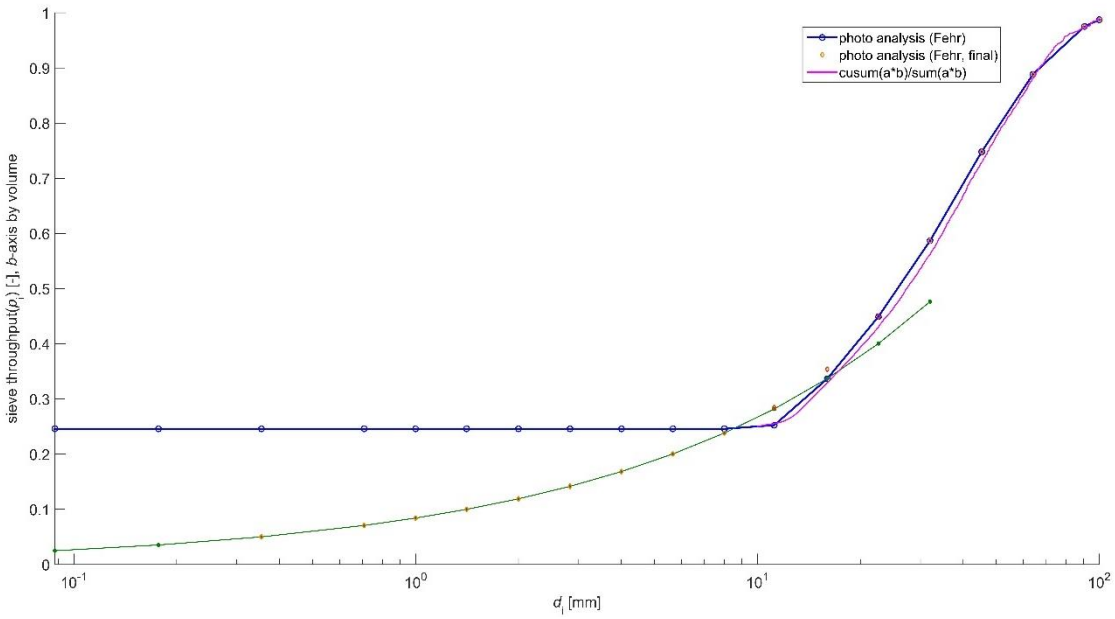

Figure 3.12 Grain size analysis, (b-axis truncation [10, 999: min, max], (semilogx plot, unit mm).

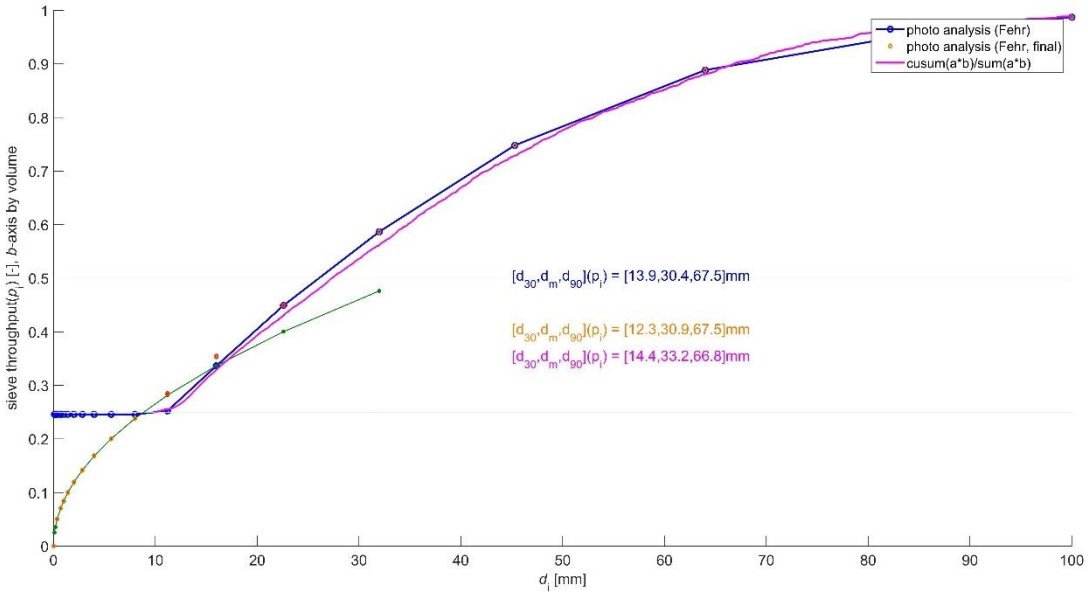

Figure 3.13 Grain size analysis (plotted Di limit 0:100 mm).

The grain size sample was collected on a different section of Eamont & its tributary river Lowther. The sampled images were collected so that each sample becomes a representative sample of four identified morphotypes. Figure 3.14 and Figure 3.15 explains the data collection for a representative morphotype C site on the river course of Eamont and grain size fraction generation with BASEGRAIN exported data Figure 3.16.

Figure 3.14 Low altitude drone flight location at Eamont headstream.

Figure 3.15 Gran size nadir image on Eamont River.

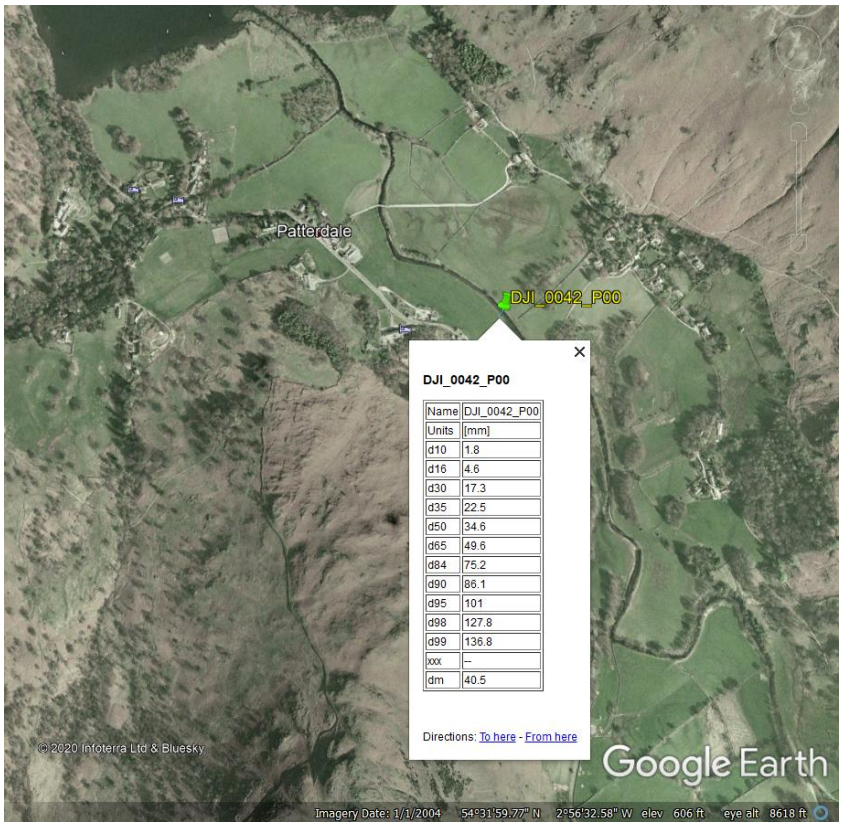

Figure 3.16 Grain size fraction results exported as KML file for display on Google Earth.

Figure 3.17 depicts piecemeal interpolated GSD data on the Eamont river network, which consist of 25 drone observations out of 166 reaches. The drone derived GSD sampled is distributed in the Headwater, mid-reach, and mouth region of Eamont and Lowther. Figure 3.18 demonstrates 25 drone sampled sites and remaining reaches assigned with piecemeal interpolated GSD data.

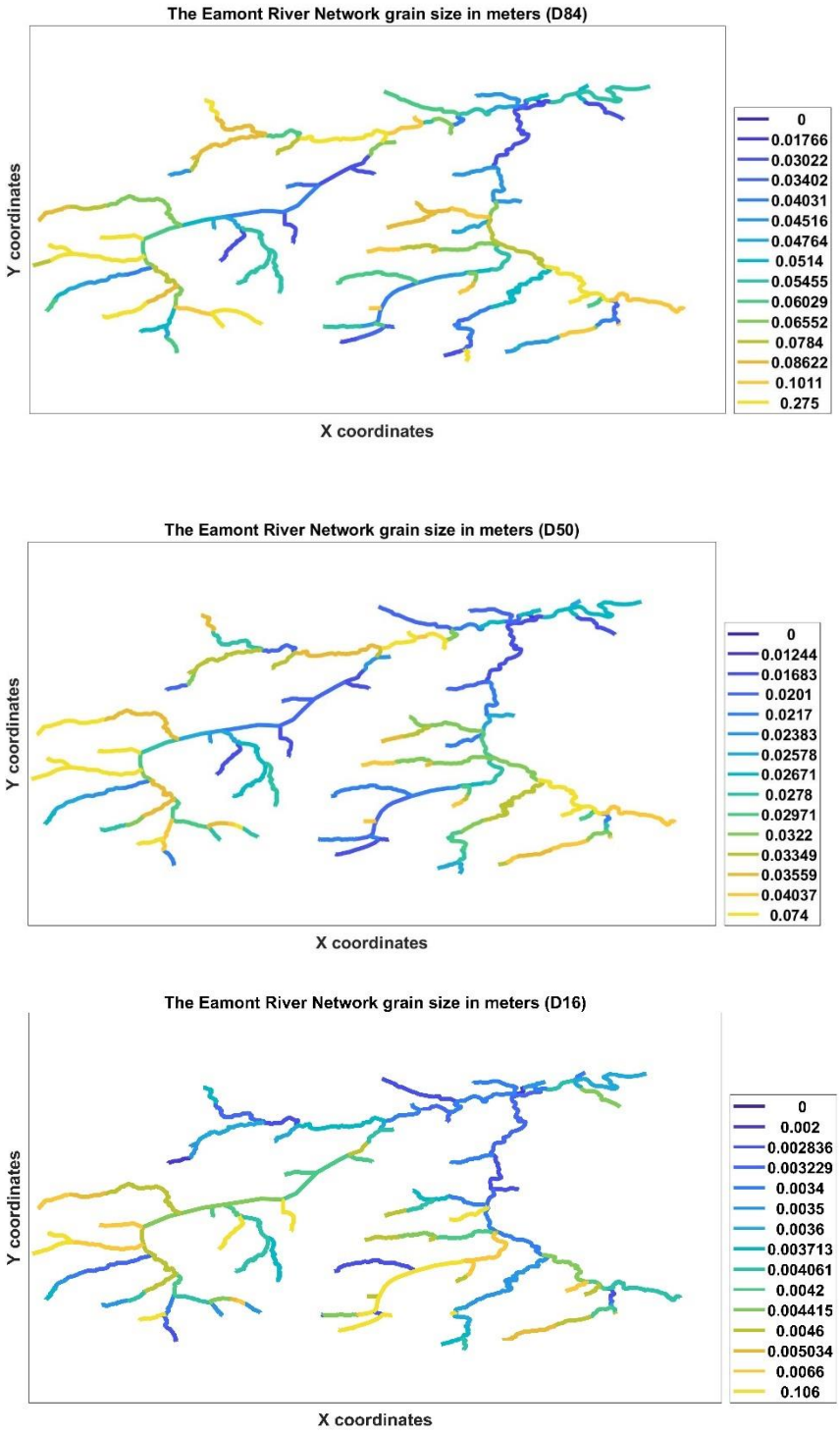

Figure 3.17 Grain size (D16, D50 and D84) fractional values on the Eamont river network.

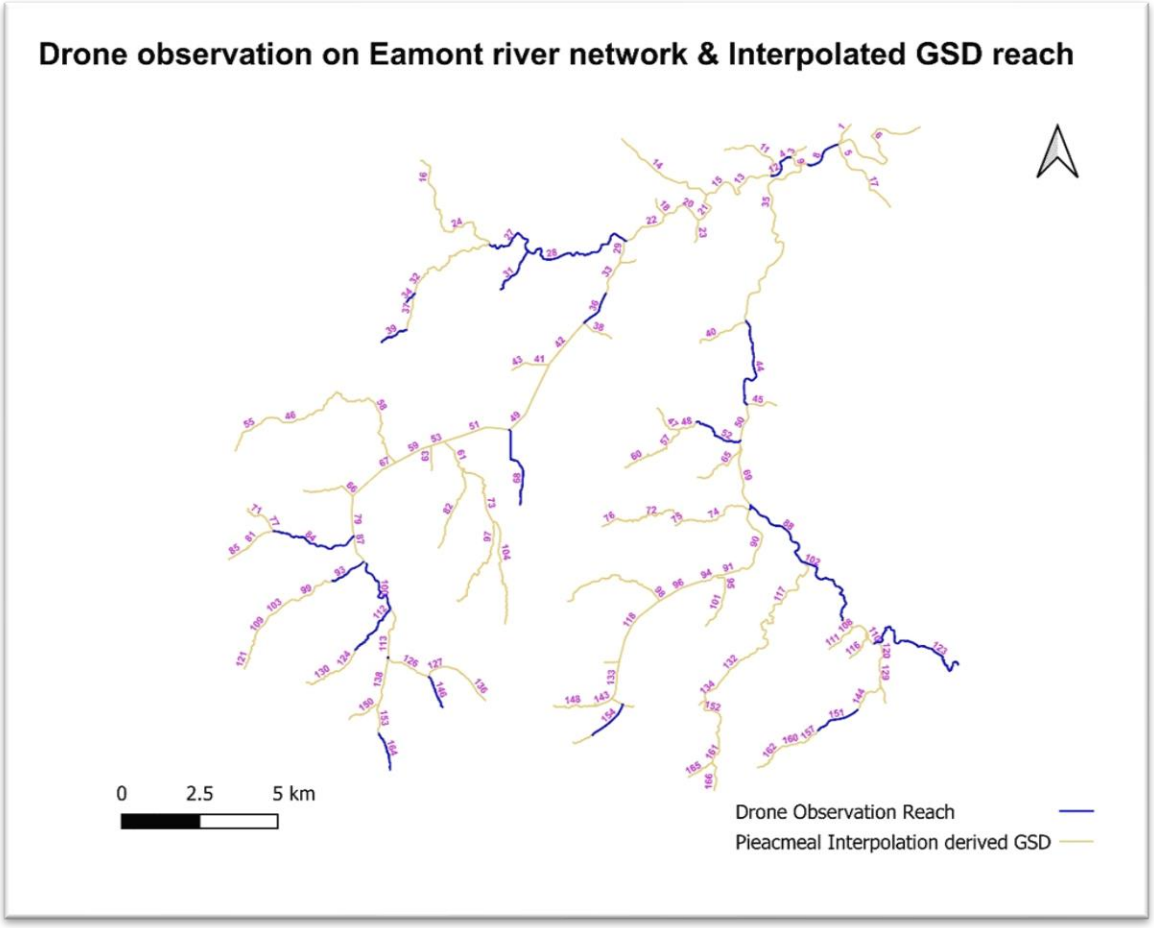

Figure 3.18 Drone sampled reach and piecemeal interpolated GSD reach on the Eamont & Lowther River network.

It is crucial to inform that all gravel bed photo-based grain size measurement software has shown limitations compared to manually measured GSDs. However, BASEGRAIN software provides reliable grain size measurement (Rüther et al., 2013; Westoby et al., 2015; Stahly et al., 2017), and a study reported that root mean square error for D_{50} did not exceed 13% (Chardon et al., 2022). However, in the current study, manual measurement of the river bed is not performed and therefore, deviation from the actual GSD measurement and software derived information is unreported.

Summary:

This chapter describes the approach to generate grain size distribution (GSD) information across the river network. The primary tool employed in this methodology is a consumer-grade drone to capture close rage hyper-spatial

resolution images and process them in photogrammetry software to get the scaled or ortho-photographs. The scaled images are processed for object detection software, in which their a & b axis gets measured, following that Fehr line sampling technique implemented to get the D_{16}, D_{50} & D_{84} information. This GSD information plays a vital role in initialising the CASCADE model, aiming to implement a fractional transport rate to gain a size-selective sediment flux estimate. Therefore, adopting and employing quick riverbed grain size sapling is the core of this part.

Grain size is an essential parameter for sediment transport processes and in simulation models. Moreover, it is an essential input for the CASCADE framework (requires D_{16}, D_{50} & D_{84} values in unit meter). The median grain size is strongly related to the catchment area and slope (Pike et al., 2010) for the Eamont river catchment, Figure 3.5. In sediment transport formulae, median grain size (D_{50}) values have always been utilised for “bulk” sediment transport that of sub-surface bed material or surface bed material (Burt and Allison, 2010). The size-selective sediment transport model and experimental studies were reported by (Parker et al., 1982) and (Wilcock 1993) and in a recent work, in which sediment transport model was presented for mixed-size sediment (sand /gravel). It exploits the sediment size of bed material rather than sub-surface bed material is capable of generating transient sediment transport estimates (Wilcock and Crowe, 2003). This model includes a hiding function refined compared to the earlier reported hiding functions. The model takes the full-size distribution of bed surface, including sand material, which makes it distinct. It has incorporated the nonlinear effect of sand content on gravel sediment transport. In this study, the CASCADE model was implemented for sediment transport study at the river network scale. It can utilise Wilcock and Crowe model along with other sediment formulas proposed (Engelund and Hansen, 1967; Yang, 1984; Wong and Parker, 2006). In the data-poor river catchment (Eamont), the model parameterisation becomes crucial with the maximum observed data available. The photo-granulometry is provided as an additional data for CASCADE model performance and prediction confidence.

Chapter 4: SWAT model simulation and its calibration analysis for long-term hydrological assessment in the Eamont catchment.

The current thesis aims to find weir and dam removal scenarios that offer the best possible sediment transport restoration at minimal costs. Adopting a modelling approach that uses the CASCADE model's simulation under different barrier removal scenarios will provide barriers impact on transported sediment flux. One of the critical limitations of CASCADE is its dependence on external distributed discharge data. In order to overcome this limitation, SWAT, a hydrological model, has been chosen to couple with CASCADE to simulate discharge inputs accurately. However, numerous hydrological models are available for modellers, and the selection of one model can be complex. Thus, the selection of a model must be based on the comparative analysis among various hydrological tools (1.3.2) to simulate the Eamont catchment's hydrological characteristics at the network scale.

4.1 SWAT Model: An introduction

SWAT is a physical, semi-distributed, process-based model that simulates river basin or catchment scale hydrology (Arnold et al., 1998; Gassman et al., 2007). The model was developed to predict water, sediment, chemical, and water exchange at daily or sub-daily frequencies for an extended period. SWAT requires detailed information of catchment-wide water interactions and accountable parameters that can affect the water quantification at the land, atmosphere, and river routing stages. Setting up the SWAT model with required inputs can be cumbersome, but once the model is parametrised, it can provide insight for planning and conservation practices and improve policy-making decisions (D. N. Moriasi et al., 2007).

Williams (1975) recommends the subdivision of catchments for effective sediment yield estimation. SWAT processes real-world information at a reduced scale by discretising the catchment into sub-catchment. HRU is the smallest unit for which hydrological and other associated catchment processes are simulated.

Hydrological response units (HRUs) are the lumped area of a sub-catchments spatial unit comprising land use, soil properties and land management information. The division of the catchment into sub-catchment provides a quantification of spatially distributed information on climate, hydrological response unit (HRUs), and water controlling or diversion schemes. The collective hydrological information of different land use and soil combinations and pond/reservoir, overland flow, groundwater flow, and streamflow are processed for each sub-catchment in the hydrological model (Neitsch et al., 2011). SWAT solves the water balance equation at the river catchment scale. Equation 4.5 explains the water balance in the model, and the schematic representation in Figure 4.1 explains the hydrologic cycle's component addressed in the model.

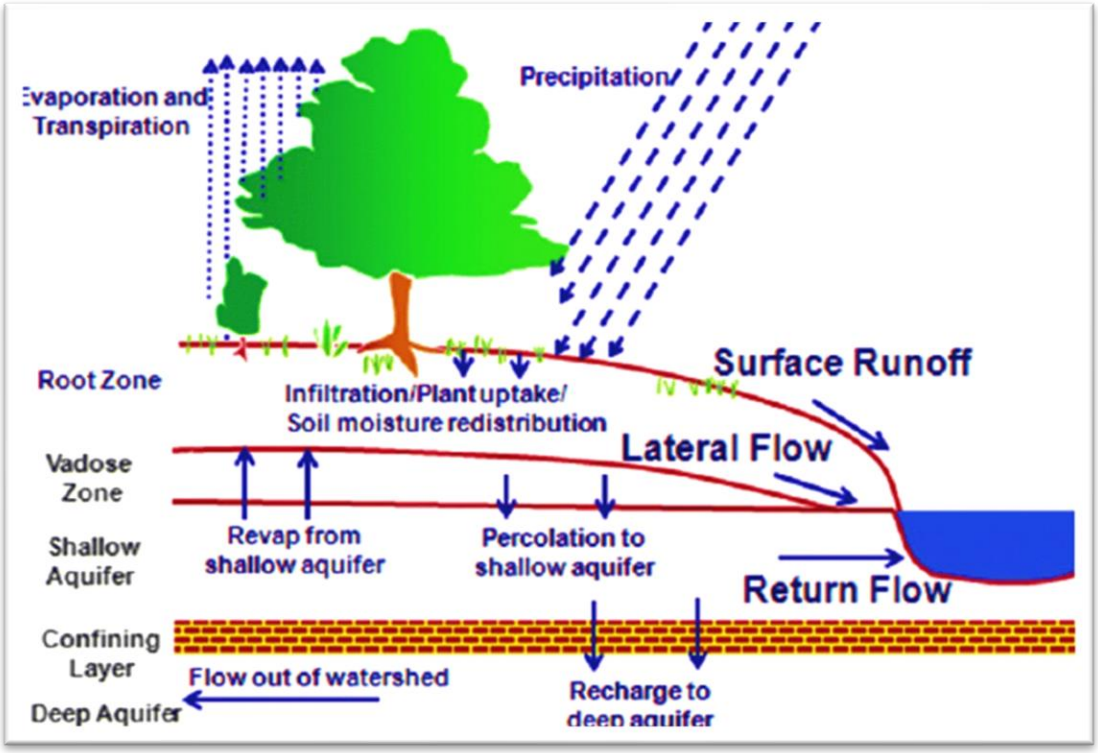

Figure 4.1 Schematic representation of Hydrologic cycle (Neitsch et al., 2011; Khayyun et al., 2019).

4.1.1 Land Phase

The land phase of the hydrological cycle consists of processes such as rainfall-runoff, evapotranspiration, and soil water (soil moisture, lateral flow and aquifer recharge) estimations. These water movement processes represent different pathways in which atmospheric water is converted to soil-water, surface, and

sub-surface water. The water loss is estimated for plant uptake and is modelled by evapotranspiration from land and rivers. Finally, the water is contributed to the river for the water routing process.

The land phase processing sequence in the model is depicted in Figure 4.2. It represents spatially distributed land phase processes primarily related to water exchange between land and the atmosphere. In the land phase, weather parameters play a crucial role in water availability and its movement back to the atmosphere based on rainfall vs temperature, humidity, and wind speed.

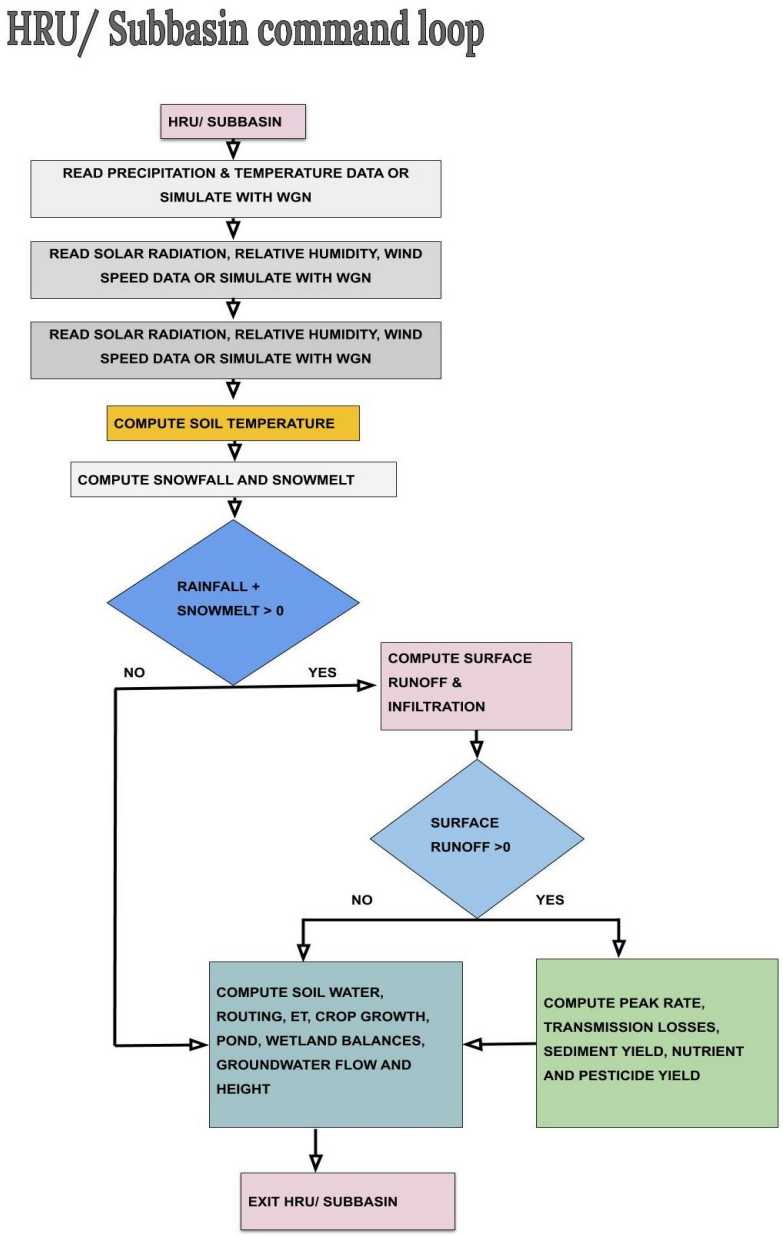

Figure 4.2 SWAT model's land phase processing loop in SWAT model's computer code.

Surface runoff occurs when soil moisture reaches saturation level, and no further infiltration occurs. In other words, the rainfall rate exceeds the rate of infiltration. An excess amount of rainfall and snowmelt can saturate the soil layers based on antecedent moisture conditions. This excess amount of water will become a part of surface runoff. Surface runoff and infiltration rate can be calculated with the SCS curve number (CN) (Cronshey, 1986) and Green and Ampt methods (Green and Ampt, 1911). In the current study, the curve number method is implemented. In the SCS curve number method, the excess rainfall is converted to runoff Q which is generated after meeting initial abstraction Ia (is the abstracted canopy amount of precipitation), and it is not going to be a part of runoff. Some part of runoff is absorbed by the soil $\boldsymbol{S}$. The following relation explains the SCS curve number method:

$$Q = \frac{(P - Ia)}{(P - Ia) + S} \qquad 4.1$$

In the equation, 4.1 $\boldsymbol{S}$ is potential maximum water retention. The amount of $\boldsymbol{S}$ is related to soil and land cover class in the catchment, which is represented as $\boldsymbol{CN}$ value. It ranges between 0 and 100, and the value of $\boldsymbol{CN}$ and $\boldsymbol{S}$ is related by following relation:

$$S = \frac{1000}{CN} - 10 \qquad 4.2$$

The CN value drops when soil approaches the wilting point condition. Contrary to that, the CN values become higher when the soil reaches its saturation stage (Neitsch et al., 2011, pp. 100–102). The runoff generation is highly dependent on the hydrological soil group and the antecedent soil moisture conditions. Hydrological soil group information consisting of CN values is accessed through the Harmonized world soil database (Batjes, 2009), while antecedent moisture conditions are modelled daily based on the rainfall data (Kumar et al., 2016).

The peak flow discharge in the model is computed with a modified rational method (eq. 4.3). Peak flow occurs at a given maximum rainfall in a day, and it is used to calculate erosion and sediment loss prediction.

$$Q_{peak} = \frac{\alpha_{tc} * Q * Area}{3.6 * t_{\text{cone}}} \qquad 4.3$$

In equation 4.3, the $\boldsymbol{Q_{peak}}$ is the peak discharge, $\boldsymbol{\alpha_{tc}}$ is amount of the rainfall that occur in a day at the time of concentration, $\boldsymbol{Q}$ is the surface runoff and $\boldsymbol{Area}$ is the sub catchment area, $\boldsymbol{t_{cone}}$ (hr) is time of concentration for a sub-catchment, 3.6 is a conversion factor (Neitsch et al., 2011, pp. 110–115).

Evapotranspiration is responsible for the loss of water from the land and water surfaces, and it collectively addresses the process of evaporation from plants and soil along with sublimation. In most rivers catchments, the evapotranspiration process exceeds the surface runoff (Dingman, 2015). Thus, its accurate measurements will be crucial for climate change and land-use alterations impacts water resources. The evapotranspiration process can be calculated based on Penman-Monteith (Monteith, 1965), Hargreaves (Hargreaves et al., 1985), and Priestley-Taylor (Priestley and Taylor, 1972). However, the Penman-Monteith method is often preferred and used in the current study (Vale and Holman, 2009; Holder et al., 2019). The inputs required for the penman-monteith method are solar radiation, air temperature, relative humidity, and wind speed (eq. 4.4).

$$\lambda E = \frac{\Delta\,(H_{net} - G) + \rho_{air}\, c_p [e_z^0 - e_z]\,/r_a}{\Delta + \gamma\left(1 + \frac{r_c}{r_a}\right)} \qquad 4.4$$

In equation 4.4, λE is the latent heat flux density (MJ m^{-2} d^{-1}), E is depth rate (mm d^{-1}), Δ is the slope of saturation vapour pressure-temperature curve, de/dT (kPa, $^0C^{-1}$), H_{net} is the net radiation (MJ m^{-2} d^{-1}), G is the heat flux density to the ground (MJ m^{-2} d^{-1}), ρ_{air} is the air density (kg m^{-3}), c_p is the specific heat at constant pressure (MJ kg^{-1} $^0C^{-1}$), e_z^0 is the saturation vapour pressure of air at height z (kPa), e_z is the water vapour pressure at the height z (kPa), γ is the psychrometric constant (kpa $^0C^{-1}$), r_c is the plant canopy resistance (s m^{-1}), and r_a is the diffusion resistance of the air layer (aerodynamic resistance) (s m^{-1}).

SWAT simulates saturated flow that is available after it surpasses the field capacity of the soil profile layer. The process for lateral flow is calculated with a kinematic storage model for subsurface flow (Sloan and Moore, 1984). The model then simulates subsurface flow in the two-dimensional cross-section flowing the gradient direction (Neitsch et al., 2011, pp. 160–162).

To summarise, the hydrological cycle-related processes that take place at the catchment is depicted in a simplified water balance equation, as follows:

$$\mathbf{SWt} = \mathbf{SWo} + \sum_{\mathbf{i=1}}^{\mathbf{t}} (\mathbf{Ri} - \mathbf{Qi} - \mathbf{ETi} - \mathbf{Pi} - \mathbf{Qri}) \quad 4.5$$

where SWt is final soil water content (mm H_2O), SWo is initial soil water content on day i (mm H_2O), t is Time (days), Ri is precipitation amount in a day i (mm H_2O), Qi is Surface runoff generated on the day i, ETi is evapotranspiration on day i, Pi is Percolation or seepage of water from the soil layer to subsoil layers vadose zone in a day i (mm H_2O), Qri = Return flow or groundwater recharge (Arnold et al., 1998; Neitsch et al., 2011, pp. 97–98).

Sediment routing in SWAT is a function of deposition and degradation and is performed for land and channel components. The land component model tracks the eroded particle from the land and route sediment particles to ponds, channels, and surface water bodies. Erosion is modelled with the entrainment, transport and deposition of soil particles by the erosive force of the raindrop and surface runoff. SWAT uses MUSLE (*Modified Universal Soil Loss Equation*), which is a modified version of USLE (*Universal Soil Loss Equation*) (Wischmeier and Smith, 1978). The runoff factor improves the prediction of sediment yield. One of the key advantages of implementing MUSLE is that it has replaced the rainfall factor (R) used for soil erosion in USLE replaced with runoff factor in MUSLE (Willams, 1975).

$$sed = \mathbf{11.8} * (\boldsymbol{Q_{surf}} * \boldsymbol{q_{peak}} * \boldsymbol{area_{hru}})^{\mathbf{0.56}} * K_{USLE} * LS_{USLE} * C_{USLE} * P_{USLE} * CFRG \quad 4.6$$

In MUSLE (equation 4.6), Q_{surf} is surface runoff volume, q_{peak} is peak discharge rate, $area_{hru}$ is the area of HRU. The K_{USLE} is the USLE soil erodibility factor, LS_{USLE} is the USLE topographic factor, C_{USLE} is the USLE cover and management factor, P_{USLE} is the USLE support practice factor and $CFRG$ is the coarse fragment factor. While sed is the sediment yield on the given day (metric tons). The coarse fragment factor $CFRG$ is calculated as per the following equation.

$$CFRG = exp(-0.053 * rock) \quad 4.7$$

In equation 4.7, $rock$ is the percent rock present in the first layer of the soil, and this information is accessed from the Harmonised world soil database (HWSD), Figure 2.6.

The land contribution of sediment to each given river reach is estimated from the detached (*i.e.* entrained*)* sediment size fraction from the primary particle size distribution of the soil (Foster et al., 1980). However, in the case of a significant catchment, the total amount of generated runoff from a storm event does not reach the main channel, only a fraction of it is available to the main channel. This lag in surface runoff is also reflected in the sediment delivery to the main channel. The amount of sediment reached to the main channel is calculated with the following equation.

$$sed = sed' + sed_{stor,i-1} - \left(1 - exp\left[\frac{-surlag}{t_{cone}}\right]\right) \quad 4.8$$

In the equation 4.8, sed is the amount of sediment delivered to the main channel of the catchment, sed' is the amount of sediment generated at the HRUs, sed_{stor} and is the amount of sediment stored or lagged. $surlag$ is the surface runoff lag coefficient, and t_{cone} is the time of concentration. The amount of sediment carried in the lateral flow and groundwater is modelled in SWAT.

$$\mathrm{sed_{lat}} = \frac{\left(\mathrm{Q_{lat}} + \mathrm{Q_{gw}}\right) * \mathrm{area_{hru}} * \mathrm{conc_{sed}}}{1000} \quad 4.9$$

In equation 4.9, $\mathrm{sed_{lat}}$ is the loading of sediment in the lateral and groundwater (metric tons), $\mathrm{Q_{lat}}$ and $\mathrm{Q_{gw}}$ are the lateral and groundwater flow in a given day (mm H_2O), $\mathrm{area_{hru}}$ is the area of the HRU, and $\mathrm{conc_{sed}}$ is the concentration of the sediments in lateral and groundwater flow (mg/L) (Neitsch et al., 2011, pp. 264–265).

4.1.2 Routing phase

The water in the leading river network is routed through Variable storage routing (Williams, 1969; Williams and Hann Jr, 1973), and it is a version of the kinematic wave model (T. V. Chow et al., 1988; Neitsch et al., 2011, pp. 428–435).

The outflow amount in the channel water balance equation 4.10 is subjected to transmission ($tloss$) and evapotranspiration losses (E_{ch}), bank storage (V_{bnk}) and water inflow and outflow can be impacted by irrigation and inter-basin water

transfer schemes (div), including amount of rain directly falling on the river section. SWAT can model all these scenarios, and it is subjected to model parametrisation (Neitsch et al., 2011).

$$V_{stored,2} = V_{stored,1} + V_{in} - V_{out} - tloss - E_{ch} + div + V_{bnk} \quad 4.10$$

In equation 4.10, V_{in} and V_{out} is the volume of water flowing into and flowing out of reach at the time step, $V_{stored,1}$ is the volume of the water in the reach at the beginning of the time step, and $V_{stored,2}$ is the volume of the water at the end of the time step. While other variables in the equation are transmission, evaporation, water diversion and bank storage, respectively (Neitsch et al., 2011, pp. 428 – 441).

4.1.3 Water and sediment routing from waterbodies

Reservoirs play a significant role in flood control and power generation.

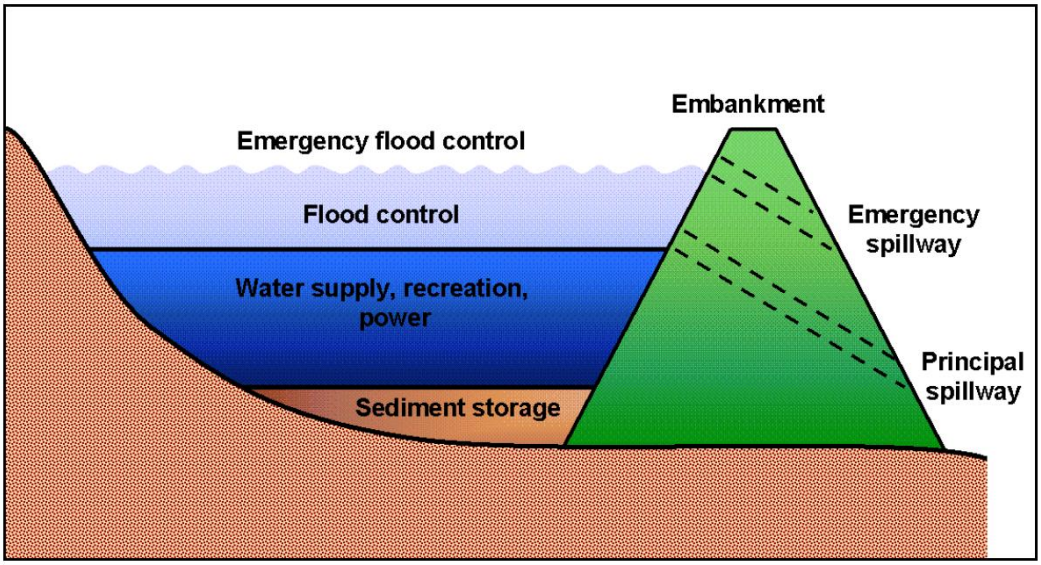

Figure 4.3 Components of a reservoir with floodwater detention features, source:(Neitsch et al., 2011).

$$V = V_{stored} + V_{flowin} - V_{flowout} + V_{pcp} - V_{evap} - V_{seep} \quad 4.11$$

The water balance associated with reservoirs is calculated with equation 4.11, where V_{stored} is the volume of water stored at the beginning of the day, V_{flowin}

volume of water flowing from the reservoir during the day, $V_{flowout}$ volume of water flowing out of the reservoir during the day, V_{pcp} , V_{evap} and V_{seep} are volume of precipitation falling on the reservoir area, the volume of water evaporated from the reservoir and volume of water lost through seepage from the reservoir. V is the volume of water in the reservoir at the end of the day. The mentioned variables in equation 4.11 are calculated as per mathematical relations mentioned in the SWAT manual (Neitsch et al., 2011, pp. 514–531). Reservoir outflow $V_{flowout}$ is defined as measured daily outflow rate.

Sediment routing in water bodies can be explained with a mass balance equation, eq. 4.12, where $sed_{wb,i}$ is the amount of sediment in the water body at the beginning of the time step (day), sed_{flowin} is the amount of the sediments flowing in the waterbody, sed_{stl} is the amount of the sediments lost by the settling process in the waterbody, $sed_{flowout}$ is the amount of sediment flowing out of the waterbody with the outflow, and sed_{wb} is the amount of sediments at the end of the time step. The mass balance components are calculated as per defined mathematical relations in the SWAT (Neitsch et al., 2011, pp. 534–537).

$$sed_{wb} = sed_{wb,i} + sed_{flowin} - sed_{stl} - sed_{flowout} \qquad 4.12$$

In equations 4.11 and 4.12, all the sub-components of water and sediment routing in a reservoir are calculated using the mathematics relations defined in the SWAT model manual (Neitsch et al., 2011, pp. 445).

The sediment routing in river channels can be performed with four different stream power models, namely 1). Simplified Bagnold equation, 2). Kodatie model, 3). Molinas and Wu model, 4). Yang sand and gravel model. The Bagnold model cannot track sediment yield of various sizes, and Kodatie, Molinas can process D_{50} value of 2mm, whereas the Yangs model can take D_{50} values between 2mm to 10mm.

4.2 SWAT model's sediment routing limitations for its utility in dam removal analysis

The unavailability of sediment yield for the Eamont river catchment has restricted the use of sediment routing and its calibration. In addition to that, there are a few reasons why SWAT may not be an appropriate model for solving the current research objective and the main rationales are; ***First***, SWAT is a continuous model, and its applications are suitable for more extended periods. In terms of hydrology, and sediment routing model requires initial conditions. Thus, the model requires a warmup period to start simulating results close to observed values and may require calibration later if there is any deviation between observed and simulated results. ***Second***, the model setup is static and therefore, for each model condition, there will be a unique model. In other words, removing a dam can impact the catchment hydrology because during model setup, observed daily release data is assigned to the dam. Therefore, the dam removal will impact the catchment hydrology. However, at the same time, the calibrated model parameter will lose their importance in such a scenario calibration performed when a dam is considered in the model setup during the simulation and calibration process. ***Third***, results generated by the model are massive and require a custom script to make them readable and meaningful. The purview of dam removal study and its impact on sediment transport will become cumbersome with limitations of SWAT models. ***Forth***, the model requires sediment concentration (mg/L) for waterbodies, HRU's and D_{50} values for the reservoir, which is not readily available for the catchment. ***Fifth***, the model can process grain size between 2mm and 10mm and limits its application for gravel river conditions.

The rationales mentioned above have hindered the application of SWAT for sediment routing in the Eamont river catchment. Furthermore, as earlier mentioned, sediment yield observed values for Eamont catchment are not available; therefore, SWAT model calibration for sediment yield is not performed. Still, the model has provided distributed hydrological data for the CASCADE model, surpassing the limitations mentioned above. Therefore, SWAT and CASCADE models are integrated into the current study to solve dam or weir

removal objectives. The details of CASCADE model processing and its working principles are explained in chapter 5. The chapter has highlighted that SWAT and CASCADE integration emerge as suitable integration to deal with mentioned limitations and resolve the multiple discharge scenario and dam removal impact on sediment flux at the catchment scale.

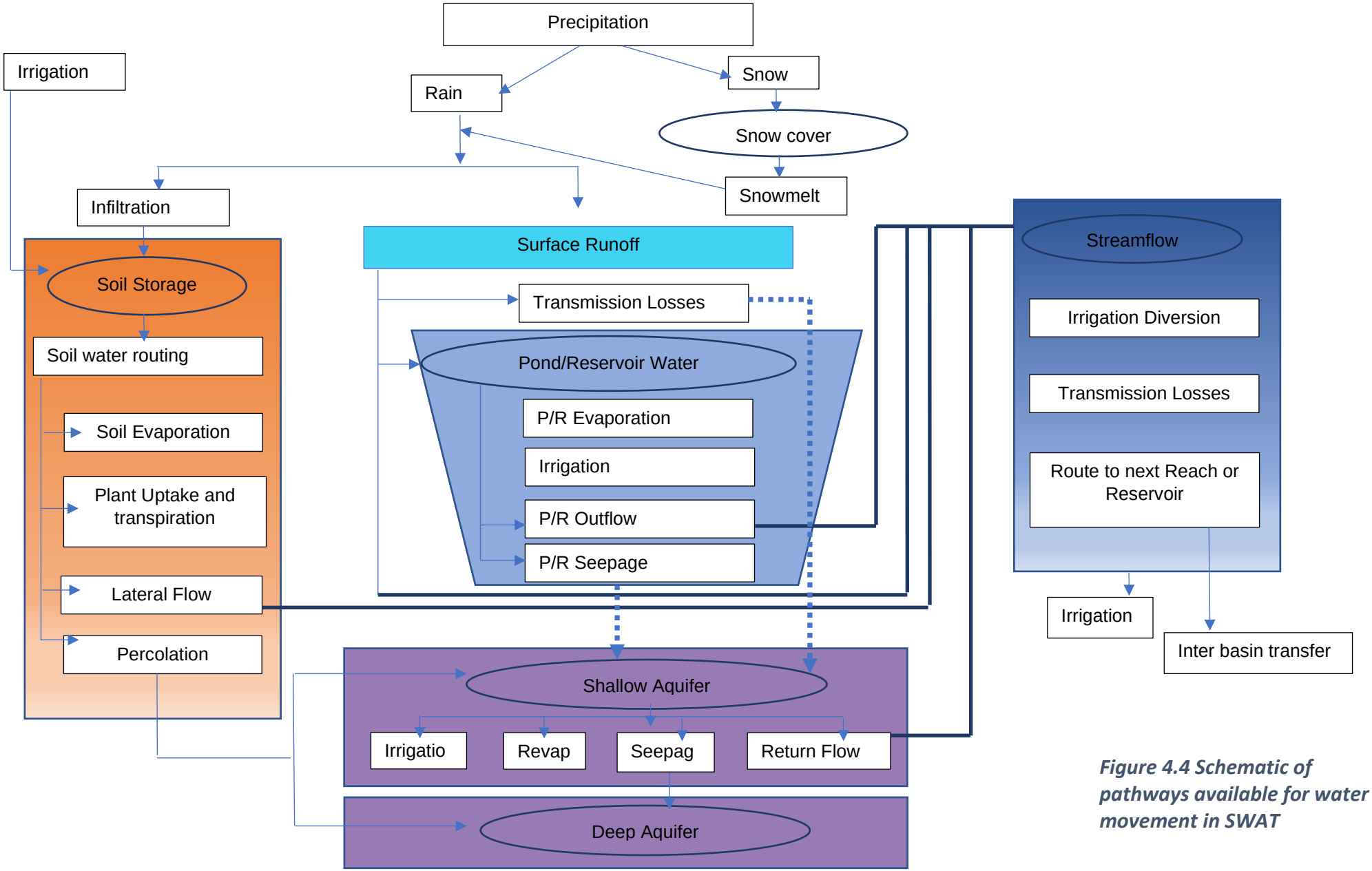

Figure 4.4 Schematic of pathways available for water movement in SWAT

4.3 Model calibration with SWAT-CUP (Calibration and Uncertainty Programs)

The objective of the calibration process of a model is to obtain a model state in which the following model characteristics can be achieved: *a)* model response to input state and model simulation performs a consistent pattern to the observed river catchment behaviour, *b)* Model prediction must be accurate with acceptable bias, *c)* uncertainty in the model's results should be less (Gupta et al., 2006).

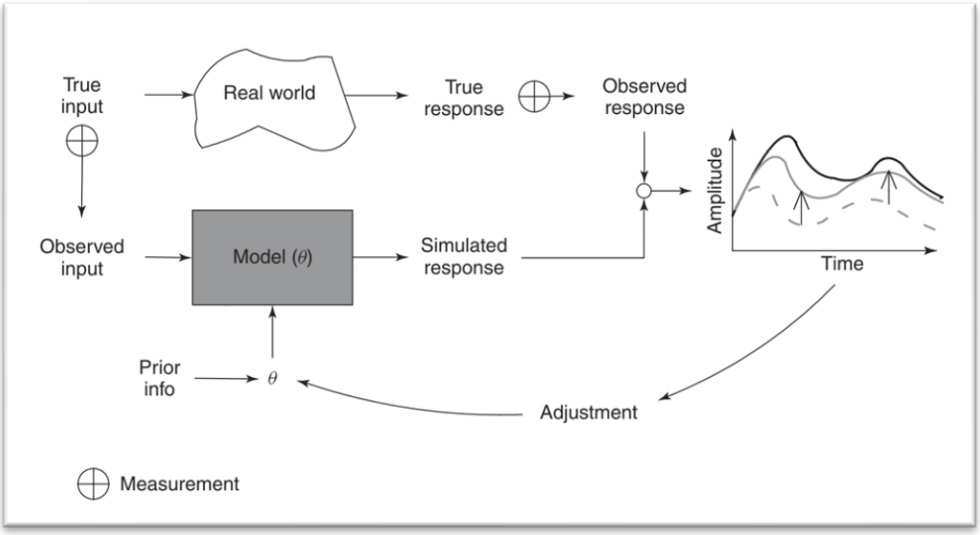

Figure 4.5 Graphic representation of model calibration procedure (Gupta et al., 2006).

A graphical representation of the model calibration process is briefly depicted in Figure 4.5. Model calibration is an iterative process that finds the optimal parameter values to reduce the uncertainty range between observed and simulated values. Calibration can be performed with a single parameter variation (Bathurst, 1986a, 1986b; Anderson and Woessner, 1992; Andersen et al., 2001) or multiple parameter values adjustments (Duan et al., 1994; Yapo et al., 1998; Duan, 2003).

SWAT-CUP is a computer programme designed & written for SWAT calibration. Any calibration model or programme that performs parameter adjustment to simulate and predict results similar to observed data is achieved with a recursive function. In the SWAT-CUP model, one of the calibration algorithms, SUFI-2 (a recursive algorithm), is selected (Abbaspour, 2011; Abbaspour et al., 1999).

However, the model has various other calibration algorithms apart from SUFI-2, such as GLUE, ParaSol, MCMC, and PSO (Abbaspour, 2011). The SUFI-2 algorithm's selection is based on its ability to address all kinds of uncertainty (Schuol and Abbaspour, 2006). SUFI-2 is an efficient algorithm for model calibration compared to GLUE and ParaSol. However, GLUE is a computation-intensive algorithm, and ParaSol is also efficient, yet it has limited ability to capture observed flow (Setegn et al., 2008; Teshager et al., 2016; Hallouz et al., 2018). Additionally, ParaSol requires a higher number of iterations compared to SUFI-2. The SUFI-2 algorithm maps all the uncertainty (parameter, conceptual model, and input) for the parameters expressed as distribution or range and captures most of the measured output within the 95% prediction uncertainty (95PPU) of the model (Figure 4.9). The 99PPU band can be compared (with measured discharge data) with the two factors, namely ***P*** and ***R*** factors (Abbaspour et al., 2004, 2007). The ***P*** factor is a measure of modelled data covered within the 95PPU envelope. ***P*** factor values vary between 0 and 1. Since model error can be reflected as (1 – ***P***) factor, thus recommended value for discharge is > 0.7 or 0.75. ***R*** factor is the wideness of the 95PPU envelope, and its value close to 1 is recommended.

The main reason for selecting SUFI-2 over other algorithms is that it is not complicated to implement and can calibrate the model with fewer iterations when compared with other algorithms. For example, the model calibration can be achieved with 1500 iterations with SUFI-2 whilst GLUE, ParaSol and MCMC necessitate 10,000, 7,500 and 5,000 iterations, respectively. In addition, an evaluation version of SWAT-CUP (version 5.2.1.1) is employed in the study, and it is locked for parallel processing. The number of iterations is limited to 2001. Thus, SUFI-2 becomes the first choice of SWAT model calibration.

Using SUFI-2, SWAT-CUP edits the SWAT model's parameters in an iterative pattern and estimates closeness between modelled output and observed catchment response with a Nash-Sutcliffe objective function. In the processing phase, the model iterates until it estimates the number of best simulations with adjusted parameter values while constantly improving the model's efficiency via objective function and two statistics (***P*** and ***R***). The model offers ten different objective functions; a few examples are coefficient of determination (R^2), Nash-

Sutcliffe efficiency (NSE), Percent bias (PBIAS), Modified Nash-Sutcliffe (MNS), Chi-square distribution (Chi2).

$$\mathrm{NS} = 1 - \frac{\sum_i |(Q_m - Q_s)_i|^2}{\sum_i (Q_{m,i} - \bar{Q_m})} \qquad 4.13$$

In equation 4.13, which is a Nash-Sutcliffe objective function (Nash and Sutcliffe, 1970), Q is discharge value (cms), while m and s are the measured and simulated discharge respectively. Although, there are other objective functions available for the calibration analysis, Nash-Sutcliffe objective function is recommended for the overall fit of a hydrograph (Servat and Dezetter, 1991), and NSE is preferred for the SUFI-2 algorithm in the current study area.

4.4 SWAT: Initial model simulation and its interpretation

The initial parametrised run of SWAT cannot be expected to deliver a perfect simulation of catchment hydrologic response. Therefore, the modeller is advised to interpret the initial model response with the observed and simulated hydrograph to provide the first estimate of model performance based on the simulated vs real hydrographs (Arnold et al., 2012).

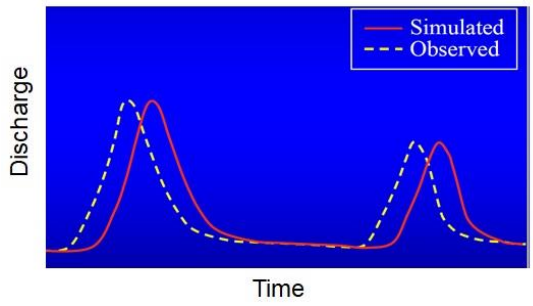	***Scenario 1*** Causes: • Time of concentration too long, • Overestimation of overland surface roughness, • Difference slope representation than actual catchment condition.
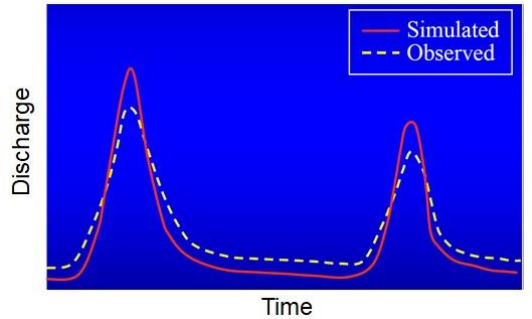	***Scenario 2*** Causes: • Low base flow, • High surface flow.

Figure 4.6 Difference in observed vs simulated hydrograph and relevant parameter adjustment techniques (SWAT, 2021).

Figure 4.7 depicts the initial predictions of SWAT. The mentioned figure shows that the initial SWAT model has runoff lag between observed and simulated hydrograph patterns, and along with that, it has over-predicted simulated discharge (Q) values. The following pattern had been ascertained. *First*, base flow is not captured well. *Second*, surface runoff is too high. *Third*, the runoff time of concentration is not accurately captured, and the response has an offset between simulated vs observed hydrograph. In order to calibrate the model, a few parameters were selected out from the numerous parameters that control the SWAT modelling environment. The parameters selected for sensitivity analysis and calibration are GW_DELAY, GWQMN, REVARMN, ALPH_BF, PNDEVCOFF, EVRSV, GWHT, RCHRAG_DP, and SURLAG. The description and details of the mentioned parameters are provided in section 4.5.

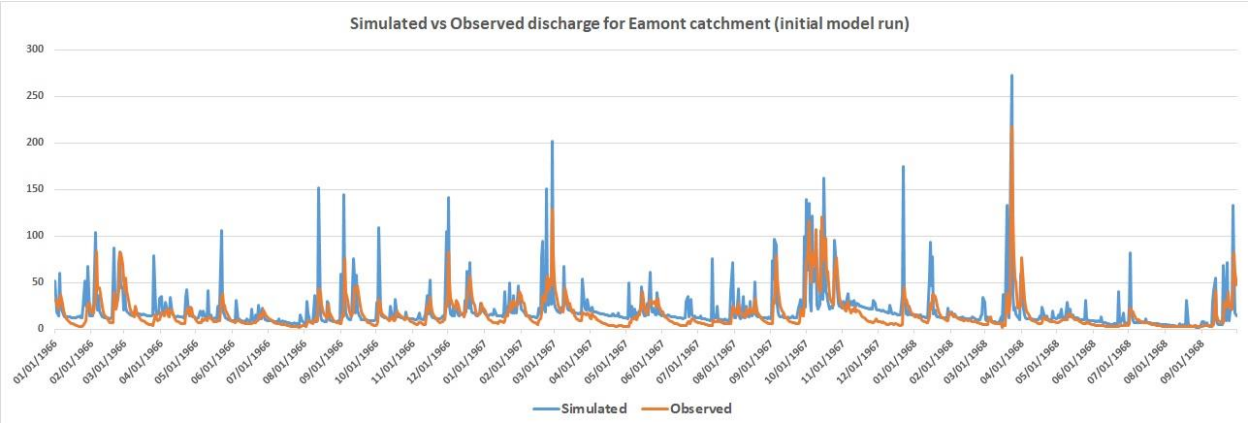

Figure 4.7 SWAT model's simulated vs observed hydrograph (initial model run).

4.5 SWAT-CUP: Sensitivity analysis for Eamont Catchment

The model's initial performance is tested for the observed river station site, depicted in Figure 4.7. Based on model result interpretations discussed in section 4.4 and guideline for model calibration & uncertainty analysis for the SWAT model (Abbaspour et al., 2017), the following model parameters have been shortlisted along with their boundary condition, absolute range (in case of boundary conditions are unknown and non-existent) (

Table 4.1).

Parameter Name	***Minimum value***	***Maximum value***
GW_DELAY (groundwater delay in days)	0	5
GWQMN (Threshold depth of water in the shallow aquifer required for return flow to occur in mm)	3000	5000
REVAPMN (Threshold depth of water in the shallow aquifer for "revap")	50	100
ALPHA_BF (Base flow alpha factor)	0	1
PNDEVCOFF (Pond evaporation coefficient)	0	5
EVRSV (Lake evaporation coefficient)	0	1
GWHT (Initial groundwater height in m)	47	55
RCHRG_DP (Deep aquifer percolation fraction)	0	1
SURLAG (Surface runoff lag coefficient)	0.05	4

Table 4.1 SWAT model parameters used for calibration and range of values considered for sensitivity & calibration.

The model calibration is proceeded by the assessment of parameter sensitivity. The most influencing parameters have been identified that control the catchment hydrology in the sensitivity analysis. The sensitivity analysis guides eliminating the wrong parameter based on the degree of sensitivity of the model to an individual parameter considered in the sensitivity analysis. The contributions of a parameter to achieve the best simulation of catchment hydrology is shown in Figure 4.8 and based on P-value test parameters, namely GW_DELAY, GWQMN, RCHRG_DP, ENRVS are found to be sensitive to the Eamont catchment hydrology compared to the other parameters considered, which are mentioned in

Table 4.1.

The sensitivity of the model parameters is analysed based on *p-value* and *t-stat* analysis. The *t*-stat is primarily a coefficient of a parameter derived from multiple regression, divided by the standard error. Thus, the indication of parameter sensitivity can be analysed by dividing the coefficient of parameter and standard error when the reminder is high. The high value of the parameter in the *t*-stat is an indicator of parameter sensitivity. However, ***t*-stat** and ***p*-value** are inextricably related to each other, and the *p*-value is used to test the null hypothesis. The low *p*-value for a model parameter shows that the parameter considered in the model is meaningful. On the other hand, a more significant *p*-value depicts that the model parameter does not influence the predictor variable

(discharge). Therefore, in the Eamont river catchment model, GW_DELAY, GWQMN, RCHARG_DP, ENRVS are sensitive to the predictor variable, while parameters such as REVAPMN, GWHT, SURLAG, PNDEVCOFF has low or no influence on the predictor variable.

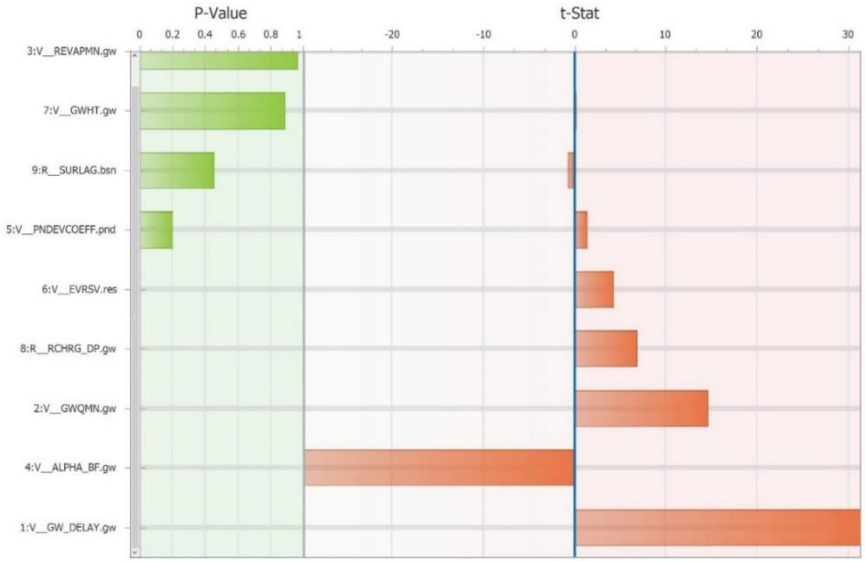

Figure 4.8 p and t-test for parameters considered in SWAT-CUP calibration programme.

Numerous natural phenomena or parameter information are not available; thus, the parameter valuations are ascertained with sensitivity and calibration. If boundary conditions are not well defined with credible information for the river catchment, the parameter's realistic value range is replaced with absolute range. This calibration process can lead to false value adjustment at the end of the calibration process for the best simulation. Thus model calibration process is often a case of equifinality (Beven, 1989, 1993). Though, the calibration process significantly reduces the model's uncertainty level. (Huang et al., 2020).

4.6 The calibration & validation process for the Eamont catchment

The core of the calibration process is to minimise the difference between simulation and observed variables by iteratively adjusting the natural process parameters. The simplification of this process is depicted in Figure 4.5. The model tries to simulate regional settings in the model versus existing natural conditions for a river catchment. The calibration process tries to improve the objective function Nash-Sutcliffe (in the Eamont catchment) (D. N. Moriasi et al.,

2007), and during the calibration process, other objective functions are also implemented because the single objective function may lead to calibration based on statistical nature (Gupta et al., 1998; Boyle et al., 2000).

Based on mentioned guidelines and procedures, calibration is performed for the Eamont river catchment. The calibration for the best model simulation selection with the SUFI-2 algorithm with NSE objective function is achieved at 1500 iterations, shown in Figure 4.9. The narrower 95PPU (green band in Figure 4.9) shows a lower difference between measured and simulated hydrographs. At the end of calibration analysis, the difference between measured and simulated hydrograph is progressively less prominent. Thereby, the calibration process helps determine the optimised parameter values in selecting the best simulation.

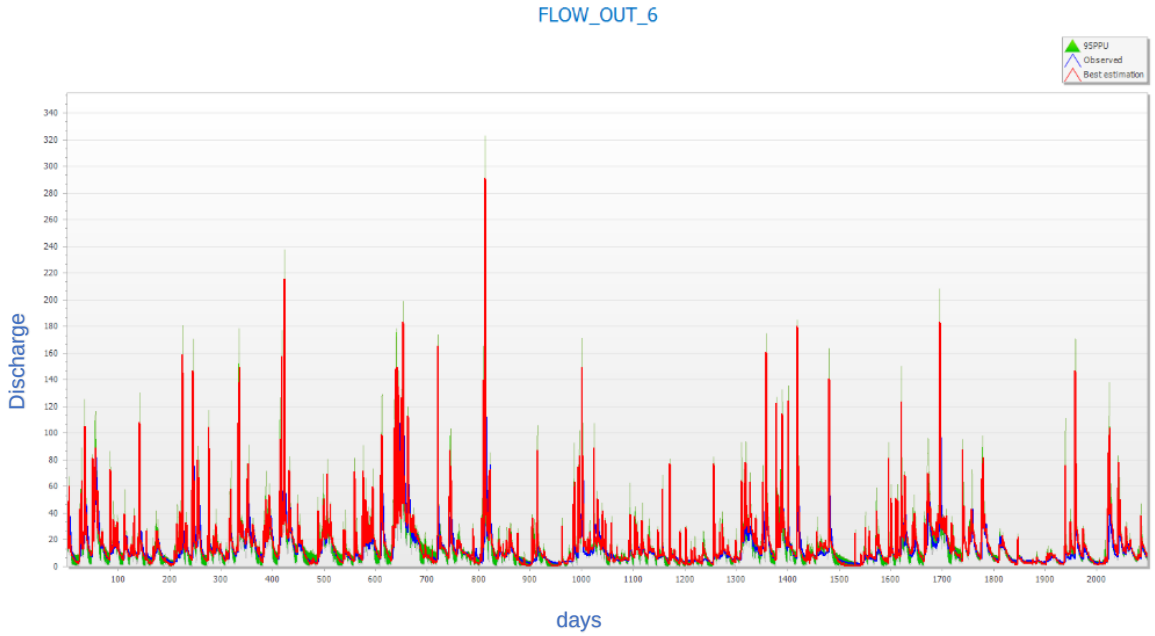

Figure 4.9 Best simulation 95PPU plot obtained after calibration process.

The fitted parameter values are established in the calibration stage (SWAT-CUP) and updated back to the SWAT model, and the model is executed for the remaining discharge period, which is reserved for the validation of the model. In other words, validation of a hydrological is a process that predicts the observed discharge for which model is not calibrated. The model validation process would be successfully achieved if a model can maintain the prediction consistency for unseen data.

The Eamont river catchments model simulation is divided into two timelines. Figure 2.11 depicts gauging stations and dam daily water release stations. The earlier one is used to calibrate the model, and the remaining time series (observed discharge) is used for models' validation. The following table shows adjusted or optimised parameter values achieved during the calibration process. The ***P*** & ***R*** factors for the model calibration (1960 – 1975, Table 4.3) are 0.74 and 0.65. Moreover, for the second calibration (1975 – 2000, Table 4.3) ***P*** & ***R*** factors are 0.70 and 0.59, respectively.

Parameter Name	***Fitted value***
GW_DELAY (groundwater delay in days)	0.71
GWQMN (Threshold depth of water in the shallow aquifer required for return flow to occur in mm)	4860
REVAPMN (Threshold depth of water in the shallow aquifer for "revap")	52.7
ALPHA_BF (Base flow alpha-factor)	0.087
PNDEVCOFF (Pond evaporation coefficient)	0.35
EVRSV (Lake evaporation coefficient)	0.20
GWHT (Initial groundwater height)	54.51
RCHRG_DP (Deep aquifer percolation fraction)	0.40
SURLAG (Surface runoff lag coefficient)	0.70

Table 4.2 SWAT model parameters adjusted values following calibration process.

However, it is recommended to employ an ensemble model calibration and validation approach (Velázquez et al., 2013) because the ensemble modelling approach offers better means to establish the model's uncertainty (input parameters) (Giuntoli et al., 2015; Strauch et al., 2012). Ensemble modelling can be established with the various data input in a single model or within different modelling environments (Aryal et al., 2019; Krysanova et al., 2017). Additionally, model performance or accuracy can be evaluated with multiple statistical methods (D. N. Moriasi et al., 2007). On the other hand, solving model uncertainty is a computation-intensive process and requires specific software and hardware or suitability to perform parallel processing (Tristram et al., 2014; Herrera et al., 2022).

In spite of the mentioned advantages of the ensemble modelling approach, the current hydrological modelling (Eamont catchment) and its calibration are established with the single parameter set. The main reason for this limitation is the unavailability of inter-basin water transfer discharge value. Firstly, in the catchment, inter-basin water transfer volume is close to 570 million litre water

per day (approximately), though the transferred water volume can fluctuate based on supply and demand. Thus, inter-basin water transfer volume changes the Eamont catchment response, and it turns catchment's natural processes of secondary nature. Hence, the inter-basin water transferred volume may induce high uncertainty in the model. Secondly, the SWAT-CUP model that is used for the SWAT model's calibration was an evaluation version, and it has restricted the ensemble modelling approach. The evaluation version was locked for running the model in parallel processing mode, and the maximum number of iterations permitted were 2000. Except for the SUFI-2 algorithm, the other calibration uncertainty procedures named GLUE, ParaSol (Parameter Solution), MCMC, PSO (Particle Swarm Optimization) take more than 2000 iterations to resolve the parameter uncertainty (Abbaspour, 2011, p. 15). Therefore, the current project uses a single parameter for the model calibration with the SUFI-2 algorithm.

4.7 Result and Discussion

In the Eamont river catchment models' calibration and validation stage, a few objective functions are considered R^2 and NSE. However, there are missing years for which dam daily release observed data is not available. Therefore, the models' calibration and validation processes are divided into two timelines. The daily calibration and validation process is divided as per the following Table 4.3, and relevant figures for calibration and validation period are depicted in Figure 4.10, Figure 4.11, Figure 4.12, and Figure 4.13.

Time-step	Process	Time step (excluding warmup period of 6 years)	R^2	NSE
1960 - 1975	Calibration	1966 - 1975	0.65	0.57
1970 - 1980	Validation	1976 - 1980	0.79	0.65
1975 - 2000	Calibration	1981 - 2000	0.63	0.68
1995 - 2015	Validation	2001 - 2015	0.77	0.71

Table 4.3 SWAT model calibration & validation statistics based on R^2 and Nash-Sutcliffe values.

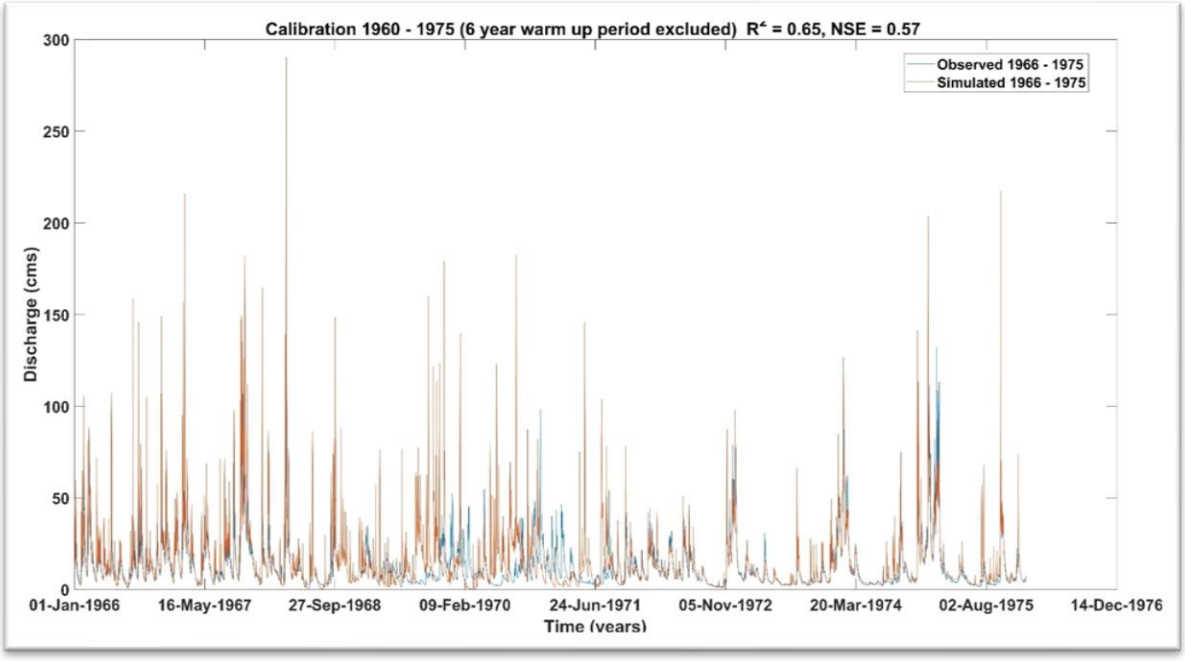

Figure 4.10 Calibration for the year 1960 to 1975 excluding six years as warmup period.

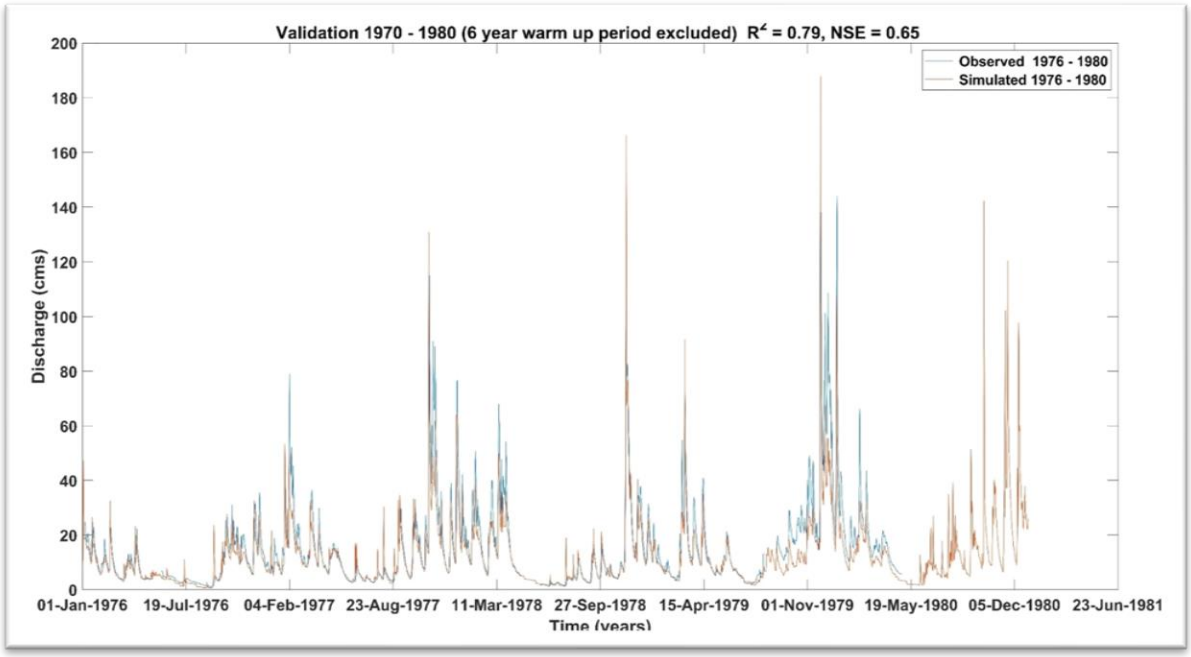

Figure 4.11 Validation for the year 1970 to 1980 excluding six years as warmup period.

Figure 4.10 & Figure 4.11 show calibration and validation of the model for the first 15 years for the Eamont river catchment between 1966 and 1980. The R^2 and NSE (Nash-Sutcliffe efficiency) for calibration and validation period are 0.65, 0.79 and 0.57, 0.65, respectively. The hydrographs for the first 15-year duration

shows the winter months peak discharge, and the peak value remained between 160 and 300cms.

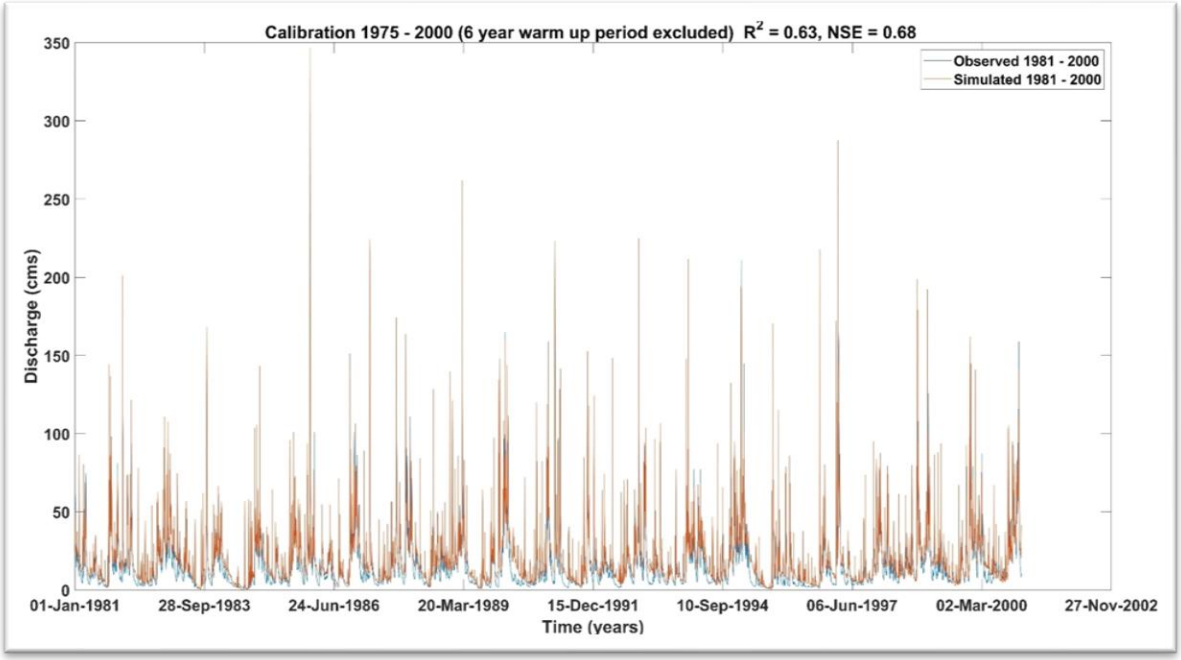

Figure 4.12 Calibration for the year 1975 to 2000 excluding six years as warmup period.

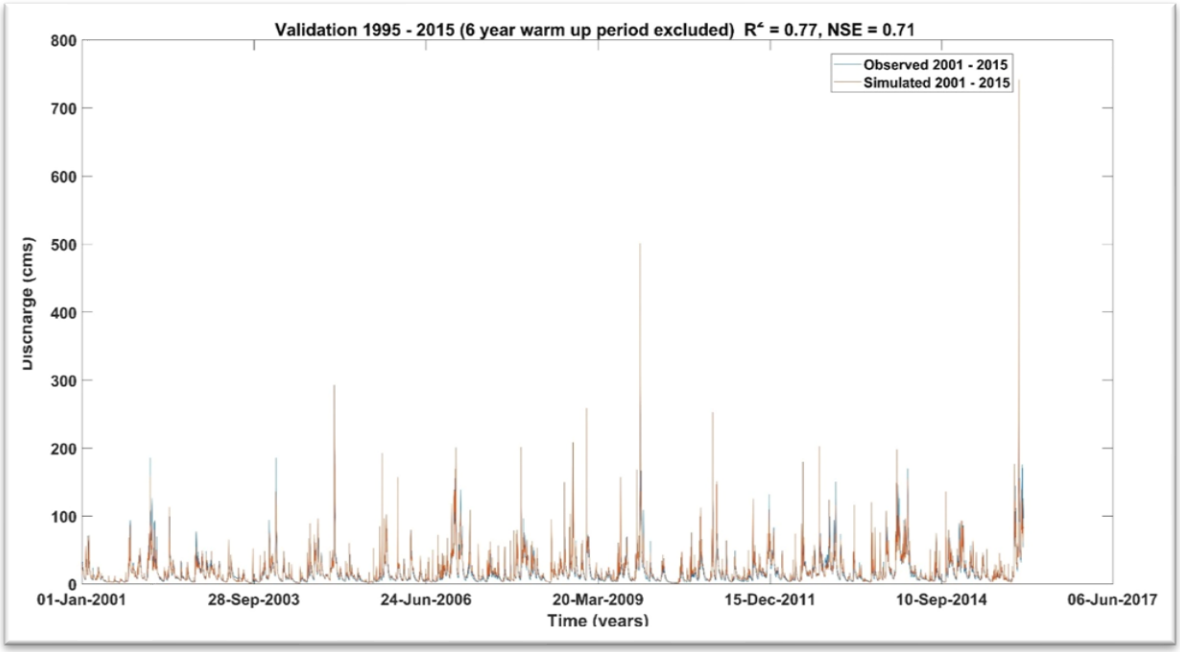

Figure 4.13 Validation for the year 1995 to 2015 excluding six years as warmup period.

Figure 4.12 and Figure 4.13 covers relatively longer duration as model calibration, and validation is performed for 20 and 15 years, respectively. The R^2

and NSE (Nash-Sutcliffe efficiency) for calibration and validation period are 0.63, 0.77 and 0.77, 0.71, respectively. Thus, the SWAT model has performed satisfactorily. Though, it has slightly over predicted the storm Desmond's discharge values.

The objective of the current study is *to find a spatial and temporal response to barrier removal in small rivers*. In order to solve the first objective, the SWAT model is implemented for distributed hydrological data development, and the model simulations were performed between the years 1960 and 2015 (excluding six years model warmup period).

The results of the distributed hydrological modelling and its calibration with SWAT-CUP programme provides catchments hydrological data, and it has indicated that hydrological findings have correlations with the previous hydro-climatic studies conducted for the Lake District region (Fowler et al., 2005; George et al., 2007; Wilby et al., 2008). The general trend of the hydrological data reveals a progressive trend in the hydrological response of the catchment, which shows the early years of 60 to 80s with normal peak discharge conditions, and the 90s decade was not much different from the early years. The peak discharge values were consistently below 300 (cms) for the mentioned period. Contrary to the 90s and previous decades, the hydrological event had shown significant changes in the next decade. The Eamont river catchment had experienced a few hydrological responses of high frequency and magnitude discharge between 2003 and 2015. Although, 2003-04, 2009-10 and 2015-16 had experienced exceptional storm events, which caused havoc to the region considering property and infrastructure damage (Stewart et al., 2012; Miller et al., 2013; van Oldenborgh et al., 2015; Barker et al., 2016). A storm event named Desmond had occurred between 4 and 6 December 2015, and within 48 hours, an unprecedented volume of the downpour was recorded (Glover, 2015; BBC, 2016). The approximate rainfall volume was estimated to be 1.5 trillion litres (Brown, 2020). A significant increase in peak discharge can disturb the equilibrium conditions attained in the past controlled discharge conditions and shift the sediment transport dynamics through water resources structures and their ability to trap sediments. It has emerged as a prime cause for geomorphic

change in such river catchment regions by shifting sediment transport and initiation of new sediment sources in the region.

However, northern England's regional hydrological pattern changes are interpreted due to climate change (Stahl et al., 2010; Bell et al., 2016). It is estimated that annual average damage across England due to flood or peak discharge events would increase by over 150% by 2075 (Richardson, 2002). The climatic change would possibly disturb the mass budget or sedimentary processes, thereby resulting in geomorphic changes (Dankers et al., 2007; Chalov et al., 2019), which can adversely impact the riverine physical habitat (Coulthard et al., 2012), and consequently turns freshwater ecosystem in a vulnerable state (Domisch et al., 2013; Field, 2014; Domisch et al., 2017). However, hydrology and sediment river connectivity plays a crucial role in geomorphic and habitat transformation. The concept of connectivity provides insight to interpret the river dynamics and helps formulate river restoration management practices in understanding climate-driven impacts on the river environment (Wohl et al., 2018).

Eamont River catchment receives the highest rainfall in the UK region and is known for the high frequency of peak discharge events (Black and Werritty, 1997). The catchment shows variations in the geomorphic setup characteristics: slope, width, riverbed, sub-catchment size, and open lakes or reservoir storage. The geomorphology of the catchment act as a significant control on the hydrological response (Beven, 1987). The various geomorphic, spatial conditions and seasonal variability are generally reflected in the catchment's hydrology and peak flow frequency. Although, the Eamont river catchment is also subjected to hydrological disturbances such as dams, weirs, inter-basin water transfer via an underground aqueduct. The Eamont river catchment's cumulative conditions, whether natural or manmade, brought the hydrological response of the catchment distinct than natural.

In such a condition, assessing the catchment outlet hydrograph would not serve as an indicator of a diverse hydrological condition within the river catchment, especially in the upland river tributaries region of a river catchment (Marks and Rutt, 1997). For example, a mountainous river that receives high orographic

rainfall and at varying slope conditions would characteristically facilitate an intermittent extreme discharge (Mayes et al., 2006). The high-intensity discharge conditions reflect high carrying capacity and would move significant sediment volume to the downstream direction. However, when a mountainous river merges with an open lake like Ullswater, the upland river experiences diminished hydrological potential because hydrological energy dissipates at Lake & River confluence zone, and thus, it impacts sediments carrying capacity. Consequently, these confluence zones form long-term sediment sink spots within a river catchment.

An enormous open lake like Ullswater that receives the intermittent high discharge from mountainous regions in the rainy season can tame the discharge fluctuations in the downstream river which is connected to the river. However, river tributaries that contribute significant discharge and sediments to the river system are located at the source region of the catchment and surpass the permanent sink like Ullswater. Moreover, sediment connectivity plays a significant role in sediment transport and geomorphic state of a river, where distributed hydrological conditions at river network scale act as an essential factor for dynamic equilibrium, and it is essential for geomorphological investigation for catchment management (Bracken and Wainwright, 2006; Bracken et al., 2013; Gurnell et al., 2016).

In addition to that, the presence of dam and weir changes the catchment area (sub-catchment area) that contributes runoff to river sections, for instance, river reach. In other words, deviation from the natural reach division based on the geomorphic and obstructions leads to change in contributing area for sub-catchment and resulting hydrological response at sub-catchment. Therefore, a semi-distributed hydrological model implementation that is parametrised with the high-resolution dataset and inclusion of known catchment processes would provide a better spatial-temporal hydrological behaviour, not just at the Eamont river catchment outlet but also its sub-catchments hydrological behaviour (Bouraoui et al., 2002; Leta et al., 2017).

The cumulative period of calibration and validation (divided into two parts, Table 4.3) of 50 years of hydrological simulation data is further used to find the

discharge percentile - Appendix A. for the CASCADE framework because it cannot process sediment transport at daily frequency data (CASCADE is of an instantaneous processing nature). However, based on the frequency of specific discharge scenarios, it can provide spatial-temporal variation in sediment transport and predict geomorphic change at the river network scale.

Summary:

The SWAT model has successfully established the Eamont River catchment's long-term hydrological assessment. The model parametrisation and its initial response are analysed for the model calibration process. The calibration is performed with SWAT-CUP, and a few model parameters emerge as sensitive to model in sensitivity analysis in the calibration process. They are GW_DELAY, GWQMN, RCHARG_DP, ENRVS (Table 4.2). The sensitivity of the parameters is analysed with a global approach along with ***t*** & ***p*** - test value comparison.

Moreover, the model calibration is performed with the SUFI-2 algorithm because the SUFI-2 algorithm requires fewer iterations than other available algorithms GLUE, ParaSOL and MCMC. The calibrated parameters are then tested for the model performance for the remaining hydrological timeline covering the model validation process. The calibrated model or best simulation is achieved with objective functions. For the Eamont river catchment best simulation selection has been performed with R^2 & Nash-Sutcliffe objective function. The values of R^2 & Nash-Sutcliffe are satisfactory for the calibration and validation period of the model (Table 4.3).

The chapter has highlighted the application of the distributed hydrological model and its calibration process for generating long term hydrographs at the river reach scale. The distributed hydrograph serves as a crucial input for CASCADE, which is integrated into the current project. The integration of the two models is based on SWAT models limitation (section 4.24.2) and CASCADE dependence on the external hydrological input data. This chapter is a progressive step for establishing and analysing dam or weir removal impacts at the river network scale.

Chapter 5: CASCADE Model: an introduction & its utility in weir removal analysis in a data-poor river catchment.

The emergence of science regarding dam removal is considered a viable option to restore riverine ecological status by improving morphology and biodiversity. Dam removal influences river status and can be progressed from degraded to the restored state by attaining natural discharge and sediment transport regime (Tullos et al., 2014). Though, not all dam removal scenarios can be considered because a dam removal scenario may lead to excessive sediment introduction to the river network. The high sediment introduction or recurring pattern following a dam demolition can change the morphology and physical habitat condition (Fuller and Death, 2018). In the case of multiple dams and weirs in a catchment, the restoration of natural hydrological, sediment regime and fish migration is still be affected by the dams left intact following a dam removal activity.

Regarding limited dam removal activity, dam removal benefits upstream-downstream geomorphic, hydrologic and habitat conditions (Birnie-Gauvin et al., 2018; Hill et al., 2019; Sun et al., 2021; Hermoso et al., 2021). In the long-term, dam removal would bring the river system to the natural state and alleviate regional economy and riverine biodiversity, but these positive responses are not immediate. Sometimes a significant change emerges between 5 and 10 years (Foley et al., 2017; Gough et al., 2018).

Since the longer time frame required to expect significant changes in the morphology of a river following a dam or weir removal. Therefore, modelling tools are employed to assess the prediction of likely change in the sediment transport pattern in a given river network (source to sink). In this research domain, the concept of connectivity in conjunction with sediment transport has provided additional insight for understanding connected sediment pathways and sediment dynamics (Pearson et al., 2020) and in muti-disciplinary domains (Turnbull et al., 2018). Keesstra et al. (2018) have suggested that the connectivity concept's implementation in the modelling environment provides better water and sediment regimes assessment.

In the earlier attempts to model landscape at the regional scale, for example, CAESAR -Community Surface Dynamic Modelling System (Coulthard, 2001; Van De Wiel et al., 2007; Coulthard et al., 2013) has paved the way for better process based sediment flux modelling. The CAESAR approach is based on cascading sediment flux transfer across the geomorphic subsystem connected in a hierarchical order (Schmidt and Preston, 2003). However, graph theory was not implemented in CAESAR (a landscape evolution model) to analyse the sediment flux transfer between geomorphic components. Other studies have adopted network analysis to explain sediment flux moment in a river basin as dynamic connections (Zaliapin et al., 2010; Czuba and Foufoula-Georgiou, 2014). They theorise the river network as nodes and edges represented sources and pathways to the outlet, attributed to geomorphic and hydraulic characteristics of the network to process water and sediment flux.

The dynamic pathways for sediment flux can reveal the places of excessive flux entrainment and flux deposition in parts of the river; therefore, it can highlight the possible geomorphic changes (Czuba and Foufoula-Georgiou, 2015). Czuba et al. (2017) developed a sediment routing model, which has performed in-channel sediment transport and storage dynamics while the network is conditioned for transport limited and supply-limited conditions. The model has highlighted how the river network will impact riverbed sediment thickness over time. The previous development of sediment transport model gives rise to the mixed-size sediment transport model, which has implemented a hiding function, thus prioritising coarse grain movement over sand grain. Czuba (2018) explained a Lagrangian framework to analyse sediment movement from source to sink perspective considering a mixture of grain sizes (developed in MATLAB software). Pfeiffer et al. (2020) adopted the lagrangian model developed by Czuba (2018) and translated it into a Python-based open-source package, “NetworkSedimentTransporter”, with the additional components that process sediment density, bed-material abrasion and active layer thickness.

However, many 2D & 3D models have limited capabilities at the network scales. For example, MIKE 21 is a non-cohesive sediment transport model; and its

application is regional and limited to tidal inlets, coastlines and man-made harbours bridges (Zavattero et al., 2016; DHI, 2021). Contrary, MIKE HYDRO (1D) model simulates bedload and suspended load calculations separately, and it needs a high amount of input parameters (DHI, 2022, pp. 245–246; Jahandideh-Tehrani et al., 2020). However, it is a proprietary tool and unsuitable for the data-poor region. FaSTMECH sediment transport and morphologic evolution model accounts for bedload and total load by applying a simple gravitational correction and conservation of sediment mass. The model predicts local erosion and deposition rate for riverbed evolution (Nelson et al., 2010; Zhang et al., 2018). Though, FaSTMECH cannot be applicable to the river catchment scale because it processes a limited extant river (reach). Similar to the mentioned 2D applications, Nays2DH works on a local scale (Shimizu et al., 2014; Takagi et al., 2019), and other as well, for example, Morph2D, NaysCUBE (3D), Mflow_02 (2D), EvaTRiP (Shimizu and Nelson, 2021). Although these 2D and 3D models cannot be held accountable for network scale sediment transport, they can be applicable for regional fish habitat conditions modelling.

In a recent development, a network scale model named “Sediment Routing and Floodplain Exchange (SeRFE)” has been developed (Gilbert and Wilcox, 2020). SeRFE can address sediment entrainment, transport and deposition over the river network, and sediment exchange performed with the channel/floodplain storage through capacity/supply and sediment balance. In addition, it can analyse interruptions caused by the artificial structure for sediment regime. However, SeRFE has not implemented a hiding function accountable for sand gravel and their mutual impact on sediment transport, and it lacks a size-selective sediment transport model (Wilcock and Crowe, 2003).

One of the critical advantages of network scale in-stream sediment transport models is that they can trace the source to sink sediment movement (mixed grain size). Thus, such models enable the modeller and decision-maker to strategize river restoration plans based on river network sediment dynamics. In addition to that, network scale, sediment transport model provides insight on the river confluence and its impact on sediment movement because much of the river confluence becomes a sediment storage zone that affects the habitat quality; thus,

sediment transport models in conjunction with sufficient ecological data can reveal network scale biodiversity controls (Rice, 2017).

In the present study, a river network scale model - CASCADE (**CA**tchment **S**ediment **C**onnectivity **A**nd **DE**livery) facilitates empirical sediment transport methods with *graph theory*; it provides network scale sediment connectivity. The selection of the CASCADE model is based on its parsimonious nature, which enables the modeller to simulate sediment dynamics in a data-poor region. Since the model is a 1D, CASCADE requires comparatively less data input than 2D & 3D models. Additionally, the model's source code is available to the modeller in the MATLAB environment, and it offers customisation for sediment routing equations. In the Eamont case study, CASCADE is integrated with the SWAT model for network pre-processing and input distributed hydrograph, while previous CASCADE studies relied on LISFLOOD and TopoToolBox for distributed hydrograph and river network extraction, respectively.

5.1 Introduction

The inception of the CASCADE model is rooted in the vital question linked to landscape evolution. Landscape evolutionary trends depend on aggradation degradation processes, and a landscape can be transformed based on the magnitude of transported sediments. However, sediment transport processes act on different spatial-temporal scales. Sediment connectivity in a riverine environment is influenced by the distance between source reach and connected sinks, the grain size of sediments in the source reach, river gradient, the hydrologic drag in different parts of the river network, sediment supply, and network topology. The concept of sediment connectivity at the river catchment scale is analysed using an individual cascading process termed "cascade " in the earliest version of the CASCADE- a sediment transport modelling framework developed by *Schmitt (2017)*. The CASCADE model extends the framework developed for sediment transport formulas in conjunction with graph theory, proposed by Czuba and Foufoula-Georgiou, (2014). By adopting and implementing the same principles, the CASCADE model performs sediment transport as an individual cascade, which is processed to provide insight for a specific source and connected

downstream sinks. The nature of entrained and transported sediment is controlled by transport capacity in different reaches. At the same time, aggregated information of sediments entering their respective sinks can elucidate sediment sorting, provenance, and magnitude of the sediment flux. Thus, interpreting sediment connectivity patterns among the source reaches, and multiple connected sediment sinks can also reveal sediment connectivity and dis-connectivity at the river network scale.

Later, the CASCADE model was evolved by Tangi, 2018; Tangi et al., 2019a. Contrary to the old version, the recent CASCADE model has replaced an individual cascade process that utilised single grain size, and it has transformed the framework structure with the implementation of sub-cascades (each sub-cascade is initialised with unique grain size) in each river reach. All the sub-cascades are processed downstream with the same grain size, and the fate of the sediment transport is measured with the transport capacity. Other sub-cascades influence the transport capacity in the river reach. Thus, the entrainment, transport and deposition of the specific grain size are decided based on the transport capacity, magnitude, and presence of other sub-cascades.

One of the novel advantages in the new CASCADE over earlier versions is that the grain size of sediments in the source reach or different parts of the river reach is defined by the user observed data. The field sampling methods or photo-granulometric techniques can be employed for grain size input in the model. Thus, collected information of grain size sets the boundary conditions for sediment distribution over the river network, reducing uncertainty in the modelling environment.

On the other hand, the previous version of CASCADE is implemented with a single gain per cascade determined by grain solver (Schmitt et al., 2016, pp. 19–20) (grain solver uses an empirical formula to determine the grain size under bankfull hydraulic conditions). A significant drawback of employing single grain size per cascade per reach is the overestimation of sediment flux since single grain size cannot represent grain size diversity in a reach. In other words, the assignment of finer grain size for a reach with higher transport capacity would result in sediment entrainment equal to transport capacity and overestimated the flux leaving the

reach. This shortcoming is addressed with a stochastic diagnosis of sediment supply, transport capacity and grain size for the initialisation of source reaches, with an inverse Monte Carlo approach (Schmitt, 2017, pp. 89–121). However, the importance of sediment size distribution has a significant influence on sediment transport process, and it has been proven in many studies (McLaren and Bowles, 1985; Best, 1988; Bridge, 1992; Guillou and Chapalain, 2010; Lepesqueur et al., 2019; Uchida et al., 2020).

The CASCADE model has been parametrised with a spatially distributed sampling of non-cohesive gravel bed derived GSD measurements in the present study. The measurement has been performed with the drone-based hyperspatial image analysis (see Chapter 3:). In the previous CASCADE studies, grain size values were based on random selection and refined with an inverse modelling approach. In the second case study, the CASCADE network grain size was initialised with the expert's opinion and sampled data (Liébault, 2003; Tangi, 2018, pp. 46–50). The present CASCADE implementation case for the analysis of weir and dams influence on sediment flux at the river network is implemented with observed grain size distribution.

CASCADE model: an introduction

CASCADE is a parsimonious model yet efficient enough to provide grain specific sediment flux at the river network. Additionally, the model determines the provenance of multiple sources of sediment and their contribution to the river network's various parts and the outlet. Thus, the model produces disaggregated entrainment, transport, and deposition information of sediments at the river network.

The CASCADE model represents sediment delivery of an individual sediment transport process represented as a cascade. The individual cascade is attributed and initialised with a specific sediment grain size and sediment flow at the source reach. A cascade can deposit or transport part of the sediment load downstream or ultimately exhaust its sediment load when it reaches the river outlet. Multiple sources are activated for an individual cascade during the CASCADE model execution, resulting in disaggregated grain-specific sediment load information

(each source has a specific grain size assignment). Thus, its distribution across the river network can be processed and analysed.

The graphical representation of the CASCADE model framework and the critical concept for the modelling approach is presented in Figure 5.1. The CASCADE modelling working concept begins at Figure 5.1A, which represents a river network of a case study catchment. The river network is presented as a direct acyclic graph consisting of river nodes and edges Figure 5.1B. An edge represents river reaches, and nodes are located at the confluence point, adjoining reaches, and at river sources. The river reaches, represented as edges in the CASCADE model, are assigned with a unique ID for each edge, and this ID becomes upstream node ID for each river edge (in case of outlet reach both upstream and downstream assigned with the same ID). The river network in the CASCADE model can be divided into equal-length based on a user-defined threshold or based on the geomorphological change in the river's characteristics at the network scale. At the beginning of the river network in the headwater region, the main or tributary river holds a source node and connected reach termed source reach. In an acyclic river network in Figure 5.1B, the source reaches can be identified as reach number 1 and reach 4, and respective source nodes are 1 and 4. The cascades have a distinct path that leads to a catchment outlet or end node of a river network. Multiple cascades in the downstream direction processing can remain active, shown in Figure 5.1D.

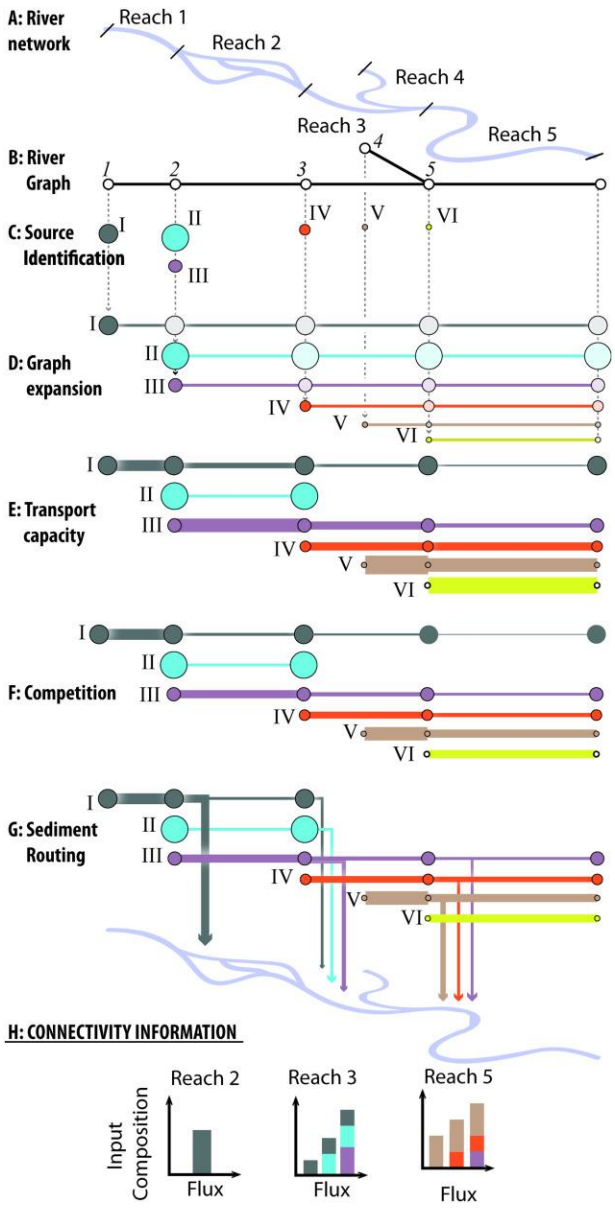

A. River network subdivision in reaches,

B. Graphic representation of the river network through nodes and edges,

C. Sediment source identification,

D. Graphic display of possible connected nodes,

E. Transport capacity represented for respective grain in the river reach through line width,

F. Competition corrected transport capacity,

G. Sediment routing at river network scale,

H. Sediment flux, provenance, sorting, and connectivity information is provided to each reach by an individual cascade flow through a crossing through a reach.

Figure 5.1 Graphical representation of CASCADE model framework (Schmitt et al., 2016)

The amount of sediment that a cascade can mobilise is ascertained by the transport capacity in the reach and the presence of other cascades in the same reach. The model uses two different standard sediment transport formulas, and a scaling function to process sediment multigraph into local-scale transport capacity (Czuba and Foufoula-Georgiou, 2014) for gravel (Wong and Parker, 2006) for sand (Engelund and Hansen, 1967) explained in equation 5.2 & 5.6. The model requires a calculation of the available transport capacity in a reach

estimated with *standard transport equations* and *geomorphic* and *hydrodynamic* conditions.

When transport capacity in the reach is limited, or the amount of sediment exceeds the required transport capacity, the cascade deposits the exceeding sediment load in the reach. Moreover, if grain size in a cascade cannot be entrained, then cascade can no longer contribute to sediment load downstream. On the other hand, when no new sediment load contributes to the reach section, sediment load will decline in the downstream direction Figure 5.1E (ii cascades).

Multiple cascades in a reach cause energy redistribution, and less energy will become available for a cascade. The competition forces cascade down-graph to lose their sediment load and initiate sediment load deposition (visual representation of progressively less energy in downstream, which depicts the occurrence of multiple cascades to initiate the competition, due to which sediment load gets reduced and it is represented with progressively reduced line width in the Figure 5.1E & F). The sediment entrainment and deposition information for each cascade at the network scale provides insight into sediment provenance, sediment sorting, network scale deposition, and transported sediment flux data (Figure 5.1G & H) by adopting graph theory in the model. Thus, the CASCADE model simulation provides sediment connectivity and dis-connectivity, which help determine the river fragmentation. The location of river erosion at river network scale with the incorporation and implementation of river obstructing structures has obstructed sediments' natural flow paths.

CASCADE produces sediment flux information for a given discharge scenario as the CASCADE model is instantaneous. Each reach in the river network gets a unique discharge (Q) value. Because discharge at a reach scale is a function of morphological, topographic, and climatic variables of the sub-catchments prevailing conditions. The simulated sediment flux is measured in *Kg/s,* and it is calculated for different Q scenarios to estimate the sediment flux under various Q conditions. The various Q discharge scenario-based CASCADE simulation is performed to estimate sediment flux fluctuation for average and peak flow conditions. This version (2018) of CASCADE has been successfully

implemented to analyse sand connectivity and hydropower generation by strategically planning dams in the Mekong river basin (Schmitt et al., 2018a).

5.2 Evolved CASCADE model

In the first CASCADE model, each reach at the river network acted as a potential sediment source for entrainment, deposition, and transportation. This CASCADE model could only be initialised with a single grain size for each source reach and remaining reaches in the river network. The grain size estimation & validation were carried out with the Monte Carlo approach – an inverse modelling approach (Schmitt, 2017). However, in the previous version of the CASCADE model, a reach with higher transport capacity initialised with possibly wrong grain size would result in a higher erosion rate since the model is transport capacity limited, not sediment supply limited. Hence single grain size assignment for reach level parametrisation would oppose the existence of multiple grain-size sediments (in natural condition) at reach scale, and sediment yield at river catchment scale becomes difficult to model. However, it is established with inverse modelling when catchment-wide observed sediment yield is available. This approach can lead to the application interpretation purely on statistical measures.

Addressing the mentioned issues with the older version of the CASCADE model, a few new changes are incorporated in the CASCADE model (2019 version) adopted to address the current research objectives. In the transformed version of the CASCADE model, the older approach of single grain assignment to a reach represented as a cascade is replaced with multiple grain-size sediment assignment to sub-cascades (Figure 5.2). Each sub-cascade has its specific grain size and sediment load, considering 18 sediment classes represented in Krumbein's phi (Φ) scale.

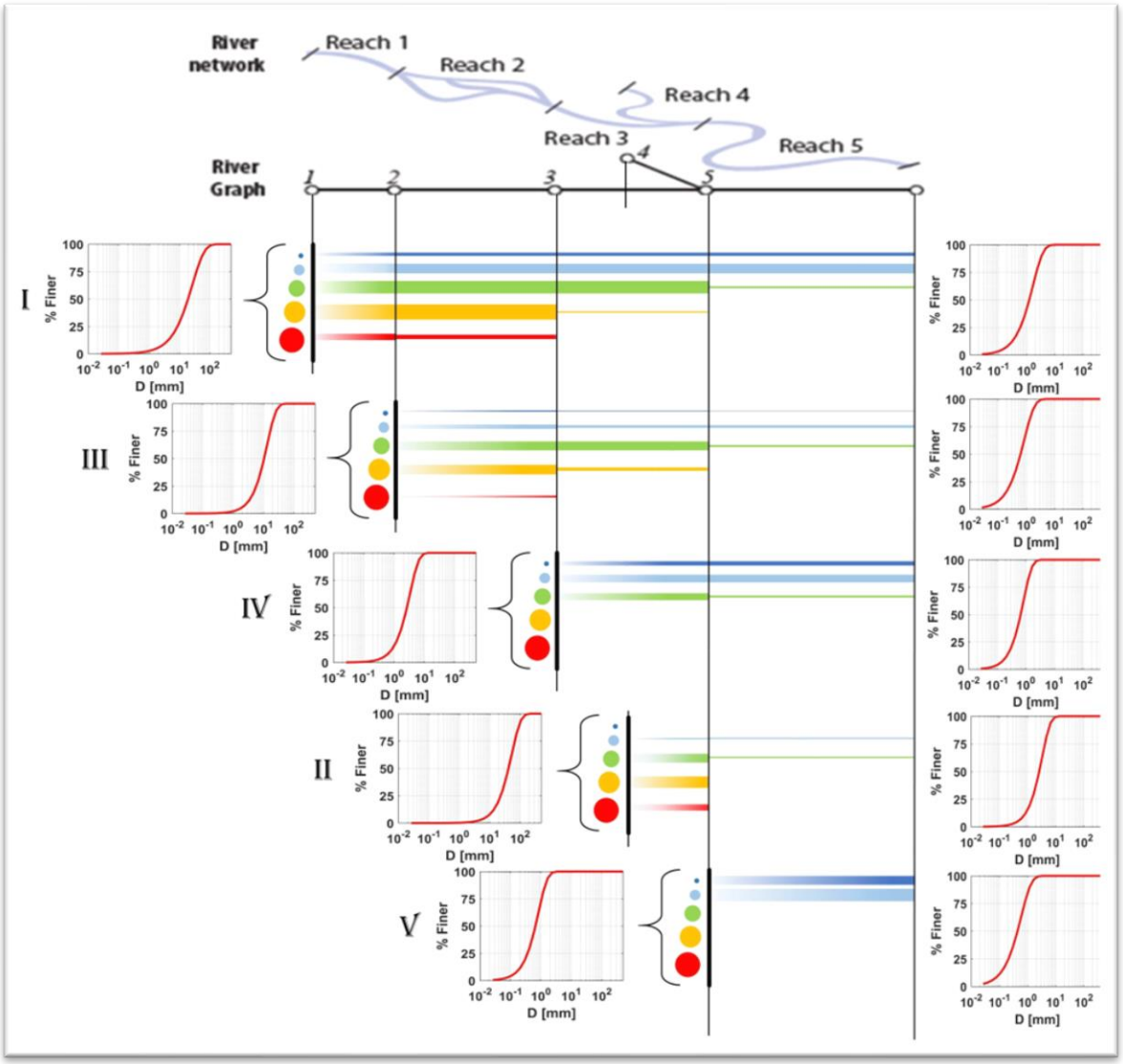

Figure 5.2 New CASCADE model processing framework's graphical representation (Tangi, 2018; Tangi et al., 2019b). Each cascade has sub-cascades with respective grain sizes.

The determination of grain size for source reaches, and the remaining network reach plays a significant role in the simulation of credible results, thereby contributing to the model's accuracy. For this reason, the current approach uses drone-based gravel bed images to perform granulometric analysis to extract and feed the grain size information in the new CASCADE model.

However, according to the prevailing hydrological conditions in each sub-cascade, other cascades' presence and magnitude can activate a new cascade. Though, at the same time, some sub-cascades may remain inactive. The activated sub-cascades process downstream, while each sub-cascade interacts

with the same grain size sub-cascade of the downstream reach, Figure 5.2. During downstream direction processing, sub-cascades can deposit their sediment load. If all sub-cascades cease to process downstream, then a cascade will stop.

The model uses the Wilcock and Crowe (2003) empirical fractional transport capacity calculation, which uses full-grain size distribution of bed surface grain, and grain size ranges between sand and gravel size fraction. Wilcock and Crowe's fractional transport capacity has an improved hiding function than the previously published; it incorporates the effects of sand content on gravel transport rate. A previous study had revealed that the critical shear stress required for the motion of the grain varies for uni-size and mixed-size sediments (Wilcock, 1993). Hence, the fractional transport capacity calculation formula that considers full grain size range and its interaction with the other sediments proves to be a better approach for sediment flux estimation at the network scale. The model expects grain size distribution information in the reaches, geomorphological and hydrological distributed information at each reach present in a river network.

The grain size classes considered in a sub-cascade get their transport capacity redistributed according to the incoming sediment load. For example, if incoming sediment load exceeds the transport capacity within a sub-cascade, then exceeding sediment loads gets deposits in that sub-cascade Figure 5.3 a. However, a cascade contains all grain sizes considered in its sub-cascades and cannot distinguish deposition process between grains of the same size entering from different sub-cascades. Therefore, the deposition process is distributed among the different grain sizes of the sub-cascade, and a sub-cascade will lose the same percentage of sediment load; as a consequence of that, a sub-cascade with a higher proportion of sediment load will deposit more than other sub-cascade in the reach, a graphic representation of this case is depicted in Figure 5.3. on the other hand, when transport capacity in the cascade is higher than the incoming sub-cascades, in such a situation, all the sub-cascades will cross the reach section without losing any sediment load, and sediment load will be equal to the remaining transport capacity, Figure 5.3b.

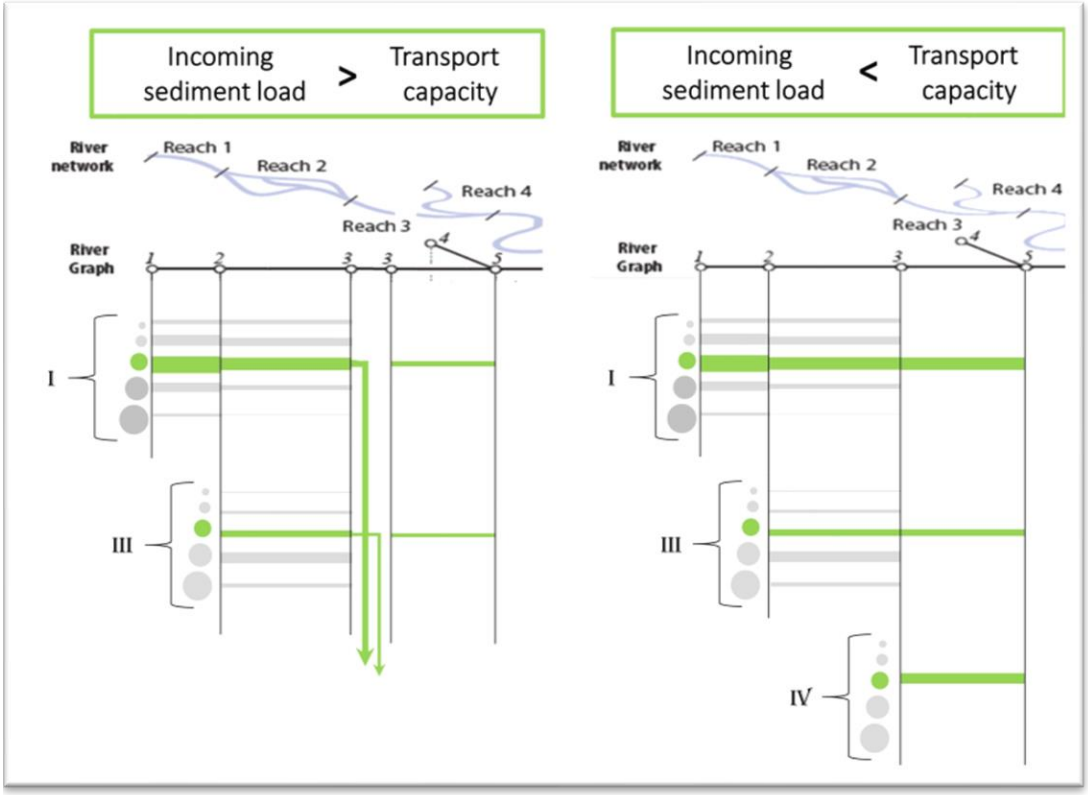

a) *Graphical representation of deposition process in sub-cascades, while incoming sediment loads exceed reaches available transport capacity.*

b) *Graphical representation of sediment entrainment process in sub-cascades, while transport capacity exceeds incoming sediment load.*

Figure 5.3 Graphical representation of sediment deposition and entrainment process in a sub-cascade in the revised CASCADE model framework (Tangi, 2018).

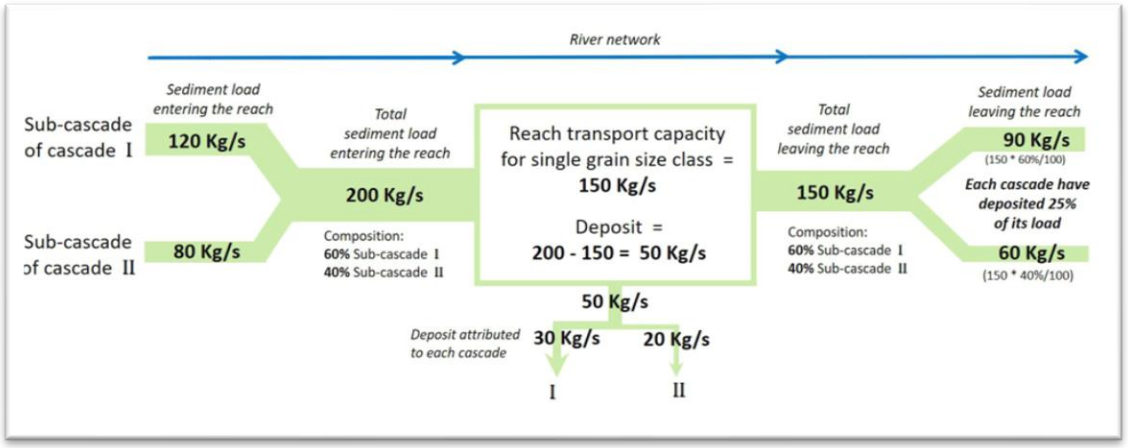

Figure 5.4 Depicting a numerical example describing sediment deposition to a sub-cascade transporting same grain size class is entering a downstream reach lower transporting capacity than total sediment load entering the reach section (Tangi, 2018).

Unlike the older version, the mobilisation of the sediment is not predetermined, where sediment classes were calculated with the inverse modelling. In contrast, the recent version establishes sediment mobilisation during the routing process, which includes reach's geomorphological attributes and incoming sediment flux. The model is transport capacity limited rather than supply limited; hence the non-supply limited nature of the model will continue to erode riverbed to supply sediments until available transport capacity is satisfied within a sub-cascade. Therefore, the sediment flux leaving a cascade is equivalent to available transport capacity in a sub-cascade, irrespective of cascade length or grain size distribution in the cascade. The transport capacity competition is evaluated among the active sub-cascades in the river reach, unlike the previous version, in which competition is calculated for specific grain size for a cascade (Tangi, 2018; Tangi et al., 2019b).

The new CASCADE model allows sediment modelling to be performed at the sub-cascade level, which enables tracking the grain specific load and its interaction with downstream and river confluence points. Hence, the model tracks down the parts of the river which has a high rate of entrainment and deposition that results in the identification of connected sediment sources and parts of the river, which is disconnected to the river network (Schmitt et al., 2016; Schmitt, 2017; Schmitt et al., 2018a; Tangi et al., 2019b).

The CASCADE model becomes a suitable tool for river restoration planning and tasks like gravel augmentation based on added advantages because the model provides insight regarding zones of extensive river erosion and deposition at river network scale by tracking the sediment connectivity and dis-connectivity caused by human interventions like dam and weir on the river course in an interactive software interface.

5.2.1 Transport capacity determination

The preferred transport capacity model was developed with mixed-size sediment transport of 48 flume runs using five different sand/ gravel sediment mixture sizes, and observations were made on sediment flow and transport. The model uses full-grain size distribution while the previous model has restricted sediment distribution to 2mm (Wilcock and Crowe, 2003) and measures the nonlinear

effect of sand presence on the bed of the river and its impacts on the gravel grain movement in the river. The gravel movement on the sand surface facilitates higher gavel movement in the river. Conversely, the sand movement on a gravel riverbed impedes sand grain movement because of the interstice space between gravels. The hiding function restricts the mobility of the smaller grain and increases coarser grains' mobility compared to the uni-size grain case. The hiding function implementation offers a variation of the reference shear stress that is a function of fractional grain size relative to the median size of the bed surface (Wilcock and Crowe, 2003).

The mixed sediment transport model is generated based on the fractional transport rates, as observed in a surface-based empirical model (Parker and Klingeman, 1982), which states that a low flow can move sediments of all sizes at the transport event in a gravel river bed condition. The Wilcock and Crowe equation is implemented at sub-cascade level; therefore, the equation is discretised for each reach for GSD available in the reach. The sediment flow Q_{bi} for sediment class i, and sediment flux calculated in unit Kg/s as the following relationship

:

$$Q_{bi} = \frac{\mathrm{F_i} W_i^* \left(\frac{\tau}{\rho}\right)^{1.5}}{(s-1)g} \rho_s W_{ac} \qquad 5.1$$

In equation 5.1, $\mathrm{F_I}$ is the proportion of size i on the riverbed surface in GSD; W_i^* is dimensionless transport rate for grain size fraction i, (5.2); τ is bed shear stress (5.5); ρ and ρ_s is density of water and sediment respectively values set to 1000 Kg/m^2 and 2650 Kg/m^2; g is gravity constant; s is the ratio of sediment to water density and $(s-1)$ is set to 1.65; g is gravity constant; W_{ac} is the active channel width of the reach represented for cascade and sub-cascade in the model (m).

The fractional transport rate W_i^* is derived from the following equation:

$$W_i^* = 11.2(1 - 0.853/\Phi^{0.5})^{4.5} \qquad 5.2$$

With $\Phi = \tau/\tau_{\mathrm{ri}}$, where τ_{ri} is the reference shear stress of size fraction i, the implementation of hiding function and calculation of shear stress τ_{ri} for grain fraction i , and shear stress for median grain size is τ_{rs50}. The equation used to solve the τ_{ri} is defined in the eq. 5.3. The gravel-bed river like Eamont and for

the presence of sand hiding factor γ is set to 0.005. The γ value depends on ratio of D_i/D_{s50} and it is calculated as per Wilcock and Crowe's suggested hiding function calculation equation.

$$\tau_{ri} = \tau_{rs50}\left(\frac{D_i}{D_{s50}}\right)^{\gamma} \quad 5.3$$

The shear stress formula for the median grain size τ_{rs50} is estimated with the mathematical relation suggested by Mueller et al. (2005):

$$\tau_{rs50} = (0.021 + 2.18\,S)\,(1650 * g * D_{s50}) \quad 5.4$$

In the eq. 5.4, S is the reach slope in meters (it should not be replaced with slope percentage, in case network processed outside the CASCADE model because most of the hydrological model uses slope percentage as slope unit even in SWAT).

Bed shear stress is derived from equation 5.5, where n is Manning's coefficient of the reach and Q is discharge for the reach section and related to the specific hydraulic condition.

$$\tau = \left(\rho g\left(\frac{nQ}{W_{ac}}\right)^{0.6} S^{0.7}\right) \quad 5.5$$

The adoption of graph theory and mixed sediment transport model like Wilcock and Crowe, which allows calculating fractional transport capacity for considered GSD in the river reach section, and along with hiding function that derives the required shear stress for considered grain i in the sub-cascade, which prioritise simulation of bedload over-sand. This is a big leap in the CASCADE model development and facilitates the end-user's analytical sediment transport simulation in a data-poor river catchment environment.

The other transport capacity function (Engelund and Hansen, 1967) is explained in 5.6, where W transport capacity, ρ_s and ρ are sediment density (kg/m3), W_{ac} is river width, v mean velocity (m3/s), q is discharge, S is slope of the river reach, R hydraulic radius, D_{50} is sediment diameter.

$$W = 0.05\rho_s + \frac{(W_{ac} * v)^2}{q}\frac{(S * R)^{\frac{3}{2}}}{\sqrt{g} * \left(\frac{\rho_s}{\rho} - 1\right)^2 * D_{50}} \quad 5.6$$

5.2.2 Grain size distribution in the river network

The vital information required to parametrise the CASCADE model is the grain size distribution information at the river network scale. Moreover, grain size distribution information should be established for each river reach in the modelled river network in an ideal case. However, collecting sampled grain size information for each river reach is not possible because it is a time-consuming and tedious process, whether physical measurement or a photographic analysis of the riverbed non-cohesive gravel beds.

In the previous CASCADE model approach, the grain size was estimated with inverse modelling (Schmitt et al., 2016), and the expert opinion-based GSD information used for modelling was performed at the catchment scale (Tangi, 2018). However, in the current CASCADE model execution, a consumer-grade quadcopter drone is employed to get the hyperspatial images of the non-cohesive gravel bed pictures taken at multiple heights from different angles, which is then processed in photogrammetric software capable of solving feature identification and the complex bundle stage with structure from motion (SFM) algorithm. It generates scaled images on which grain size measurements can be performed. Finally, an object identification software, BASEGRAIN (a MATLAB based tool), is used to perform digital image processing and edge detection filtering. Furthermore, a line sampling method is finally performed to develop the grain size fraction information for the sample image (Fehr, 1987). The technique and procedure are discussed in detail in chapter 5 for optical granulometric analysis for establishing GSD data at the river network scale.

5.2.3 Model inputs

The essential model input for the CASCADE model is a river network that should be a topologically corrected acyclic river network. The river network is further attributed with essential information to implement the *graph theory* and *sediment transport modelling*. For this reason, rivers characteristics such as geomorphological setup, observed or calibrated distributed hydrological information for each reach. Apart from the geomorphological and hydrological attributes, a few crucial inputs are supplied along the river network vector. The simplification of the river network for its interpretation and explanation, the river

network is represented. For example, it can have *N* number of reaches and considers *C* number of sediment classes.

Acyclic River Network

The river network representing an acyclic graph consists of reach node and edge, Figure 5.1B. In the MATLAB environment, the river network is identified as *ReachData* matrix*,* consisting of attributes represented as *Nx19 (N is the number of reaches and 19 depicts the geomorphological, hydrological and topological attributes).* Therefore, the matrix prepared for the CASCADE model processing is *Nx19* (N rows and 19 columns). The 19 columns represent the following river attributes: -

I. Unique reach identification code,
II. River upstream node identification code (***From node***),
III. Rivers downstream node identification code (***To node***),
IV. Rivers mean slope between upstream and downstream node (***m/m***),
V. Active river width for the reach section (***m***),
VI. Distributed hydrological information (Q) for each reach or water discharge scenarios representative of low, average and peak flow conditions ($\boldsymbol{m^3/s}$),
VII. Manning's n value for the reach,
VIII. River reach length (***Km***),
IX. East coordinate of the upstream node (***m***) (projected coordinate system),
X. East coordinate of the downstream node (***m***),
XI. North coordinate of the upstream node (***m***),
XII. North coordinate of the downstream node (***m***),
XIII. Elevation of the upstream *From node* (***m***),
XIV. Elevation of the downstream *To node* (***m***),
XV. D16 or sediment size range of the cumulative 16% (***m***),
XVI. D50 or sediment size range of the cumulative 50% (***m***),
XVII. D84 or sediment size range of the cumulative 84% (***m***),
XVIII. tr_limit or transport capacity limit (ranges between 0 and 1),
XIX. Ad or drainage catchment area of the river reach.

The river network that consists of all the above mentioned geomorphological and hydrological attributes, which has a node and reaches hierarchy defined, is suitable for CASCADE pre-processing and network hierarchy definition step.

Grain Size Frequency

The river network carries grain size fraction information mentioned in the attribute number XV, XVI, and XVII for D16, D50, and D84. The D_{16}, D_{50}, and D_{84} information are established as per the methodology defined in chapter 5.

However, grain fraction information transformed into sediment class 'C' (-9.5 to 7.5 on phi scale,

Table 5.1) using grain size distribution function, which transforms grain fraction (D16, D50 and D84) into grain size frequency within each reach according to sediment class in phi scale ($\boldsymbol{\Phi}$) (Krumbein and Aberdeen, 1937)**,** with the amplitude of 1 $\boldsymbol{\Phi}$.

$\mathbf{D}(\boldsymbol{\Phi})$	-9.5, -8.5, -7.5, -6.5	-5.5, -4.5, -3.5, -2.5, -1.5	-0.5, 0.5, 1.5, 2.5, 3.5	4.5, 5.5, 6.5, 7.5
Sediment type	Boulder	Gravel	Sand	Silt

Table 5.1 Sediment classes considered in the CASCADE model that belongs to Krumbein (Φ) scale.

The grain size frequency for sediment class C is based on median grain size fraction D50 with Rosin distribution (Shih and Komar, 1990b). The derived grain size frequency is used for transport capacity calculation for each sediment class. The Rosian distribution curve is implemented in the CASCADE model function as per the following equation:

$$F\ (\leq D) = 1 - \exp[-(D/k)^{s}] \qquad 5.7$$

In equation 5.7, k is the mode of GSD and s is an inverse measure of the curve spread around D_{50} (Tangi et al., 2019b). The grain size frequency for each reach is stored in the matrix called *Fi_r.* The *Fi_r* matrix helps calculate sediment transport capacity for each sub-cascade present in the river network's reach.

Although crucial yet optional inputs are mandatory for the model, external sediment flux information and its median grain size (in the case of landslide and sheet erosion information).

$\boldsymbol{Damdata}$ is Dx(C+1) matrix that contains the information for **D** dam in the river network for a node ID and contains the sediment trap efficiency for each sediment class.

$\boldsymbol{exdata}$ is an Sx3 matrix, where S is the external sediment flux. The three-matrix columns carry the following information: 1). Input reach node ID, 2). Sediment flux [Kg/s], and 3). Median grain size fraction information [D50].

Pre-processing

This pre-processing section explains the basic network processing requirements to run the CASCADE model. This involves the extraction of the *network* (struct) by processing fundamental data input matrix *ReachData*. The *network* (struct) contains information regarding the river network's connectivity. It stores upstream, downstream paths and distance between reach nodes, which creates a reach hierarchy for the river network. The network hierarchy determines the processing priority for each reach based on the number of nodes connected to upstream reach. Hierarchical information processed within a sub-function of the CASCADE model is named "*graph_preprocesing*".

Network Graph Processing

The *graph_preprocesing* function derive the topological characteristics of the network and saves the result into a struct array named *network,* and it provides the following network information (as an array & struct) to be utilised by the CASCADE model:

a) The struct array *Diatance_Upstream* stores each reach distance with other reaches and network sources; this information builds the hierarchal relationship within the river network.
b) The *Upstream_Node* struct array preserves the relationship of a reach with connected upstream nodes.
c) The array named *NH* stores reach node hierarchy, and it enlists reaches according to the number of farthest nodes.

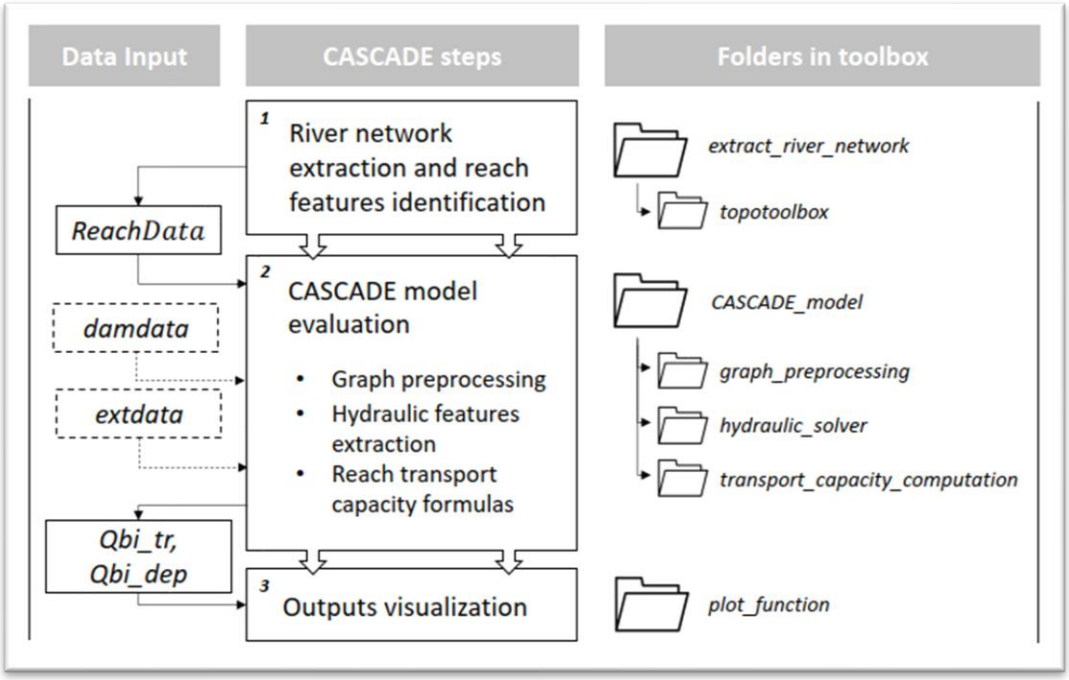

Figure 5.5 CASCADE model processing structure and folders contain model functions (Tangi et al., 2019b).

The processing step adds crucial information which is being exploited for the sub-cascade processing hierarchy, but it is also essential for tracking and storing sediment provenance details. Thus, source reaches contributing sediments can be traced for a specific reach or catchment outlet.

5.2.4 CASCADE sediment routing

The sediment routing in the river network is performed within the main function called “main_script_CASCADE”. The function performs a number of tasks in a series. First, it starts processing the river network as mentioned in Network graph processing. Secondly, network hierarchy ensures sediment routing in the remotest reach is processed first, and the processing continues downstream until the river outlet. This hierarchical processing is also maintained for source reaches; therefore, changes in the sediment flux can be reflected in sediment routing, caused by incoming flux from a tributary to river confluence and its impact on the catchment outlet.

Finally, in each river reach node, the amount of available sediment transport capacity is measured using the method and equations mentioned in section 5.2.1, and it implies transport capacity measurement with Engelund and

Hansen, (1967); Wong and Parker,(2006); Yang, (1984). The input for transport capacity calculation is provided by *ReachData* and *Fi_r* array matrix*,* which are river network and sediment frequency*.* However, the calculated transport capacity returns a single value, which is further processed to derive the fractional transport rate for the sediment classes considered. Finally, it is achieved with the fraction of total transport capacity available in reach by the Molinas formula (Molinas and Wu, 2000).

The calculated sediment transport capacity can activate a new cascade and its sub-cascades if sediment flux is equal to the transport capacity of each sediment class in the sub-cascade. At the time of sediment routing, the incoming sub-cascade interact with the same sediment class sub-cascade in the downstream reach, and according to the transport capacity in the reach, the sub-cascade continue to move towards the outlet direction or deposit the part of the sediment load in a condition when incoming sediment flux exceeds the transport capacity in the reach section, Figure 5.3 & Figure 5.4. The available transport capacity is influenced by geomorphological and hydrological features of the reach, and therefore it is crucial to run the CASCADE with multiple discharge scenarios. To access the sediment transport under various flow stages.

Moreover, impounding structures can also impact the sediment routing, and it is modelled as the capacity of an impounding structure to trap the sediment load (sediment trap efficiency ~ TE). Trap efficiency of a weir or dam structure can be established with the (Brune, 1953) or (Brown, 1943) and their proposed TE graph and mathematical relationships. The reason for selecting Brown's method in the current model is explained in the detailed section of chapter 2.

5.2.5 Model outputs

The CASCADE model returns disaggregated grain size-specific sediment flux information for entrained and deposited sediment for the river network. The various output is provided with the execution of CASCADE, and the following are the output data structure and the kind of information they contain.

Network is a scalar struct that contains river network related information such as network hierarchy, reach distance to outlet and connected sources.

ReachData is an *N*x1 struct matrix that contains *N* number of reach and hydro-geomorphological attributes.

$\boldsymbol{Qbi\_tr}$ is the 3-dimensional matrix composed of ***NxNxC***, where *C* is considered sediment class for reach *N*. A single cell-matrix cell contains sediment flux carried to Ny node by a sub-cascade originating at Nx node, specific sediment class *C*.

$\boldsymbol{Qbi_{dep}}$ is also a 3-dimensional matrix ***NxNxC*** contains deposited sediments in the reach *N*. In which sediment flux deposited in the node *Ny* by the sub-cascade originated at the node *Nx* for sediment class *C*.

$\boldsymbol{QB\_tr}$ is an *NxN* matrix, this matrix reports total sediment flux transported by each CASCADE to each node, and it is calculated from summing up all the sub-cascade in the $\boldsymbol{Qbi\_tr}$ matrix.

$\boldsymbol{QB\_dep}$ is an *NxN* matrix that reports the total sediment flux deposited by each CASCADE in each node. This is calculated by summing up all the sub-cascade in the $\boldsymbol{Qbi_{dep}}$.

$\boldsymbol{Fi\_r}$ is an *NxC* matrix addressing grain size frequency of the reach *N* for sediment class C. it is obtained by the subroutine 'GSDcurvefit.m' (Rosin curve function utilises D_{16}, D_{50} and D_{84} grain fraction information as an input).

The main outputs are produced with the execution of the primary function called "main_script_CASCADE.m". It calls a subroutine CASCADE function, as following MATLAB script function. The main inputs are *ReachData (matrix)* and *network (strut)*.

[Qbi_tr, Qbi_dep, QB_tr, QB_dep, Fi_r] = CASCADE_model (ReachData , Network);

5.3 Implementation of weir in CASCADE

The weir and dam impact the river processes at different scales considering the sheer size of hydropower project dam or diversion dam for agricultural requirements, which creates a massive reservoir and acts as an artificial sink in the river network. On the other hand, the high number of small dam structures present in Europe or elsewhere (small dams outnumber the massive dam

counts). For example, there are 630,000 small dams present in Europe, and the estimated number is beyond 1 million (Belletti et al., 2020; Zarfl and Lehner, 2020). The level of river fragmentation caused by small dams trap the moving sediments and act as a barrier for fish migration.

In contrast, numerous small dams, weir or other water resource engineering structures have never been reported on the continent-scale until AMBER - an EU funded by Horizon 2020 research and innovation project initiative that led to developing the first barrier such atlas for Europe. The AMBER atlas reveals river fragmentation in the UK (Jones et al., 2019) and Europe (AMBER Consortium, 2020). Though the development of this atlas and water resource engineering structure merely provides how much humans had tried to modify the natural river course and bring back the river to a natural condition, dam removal is gaining popularity among river restoration engineers and river ecologists (Wildman, 2013).

In the Eamont river catchment, the main structures that fragment the Eamont river and its main tributary, the Lowther River, are dam and weir structures. The hydro-morphological changes brought to the river system by small dam or weir by altering sediment regime, and sediment erosion and deposition pattern must be analysed with numerical modelling (Csiki and Rhoads, 2010, 2014). The current project is an effort to address these issues at the network scale with CASCADE, yet the crucial information which CASCADE uses to model the impacts of weir and dam on sediment regime by tracing grain specific sediment flux is sediment trap efficiency of the weir and dam structure.

The trap efficiency changes for different sediment sizes for a reservoir; hence, TE's value is adjusted for the Eamont river catchment weir and dams for the implications of a dam or weir removal scenario development and river fragmentation reduction. The CASCADE model would reflect the impact of the weir and dam removal in terms of erosion, deposition and entrainment following the removal or case of placement of a weir on the river network. The implementation of TE calculation and parametrisation of dam, weir TE values is discussed in 2.6.2. The details of CASCADE model implementation and results interpretation are covered in Chapter 6.

5.4 Model performance testing

The bedload sediment transport is variable and complicated to estimate in a modelling environment. It is not just bedload sediment transport modelling, but any natural environment in the physical model simulation requires high-quality data input and observed values, which can be used to assess model performance or model calibration. The observed results contribute to adjusting the model parameters for physical environmental parameters to attain a model state that can reasonably predict the simulated result proximate to the observed one.

The current study area is in northwest England, and its bedload and suspended sediment transport values are not available. There is no comprehensive sediment dataset available for British rivers (Walling and Collins, 2005). Therefore, model sensitivity and calibration with a reasonable confidence level in the CASCADE modelling is not direct. Thus, in the Eamont river catchment, GSD data is established with drone images. GSD data become a crucial input for the CASCADE parametrisation, which is the first time in the CASCADE implementation history that GSD data developed with extensive catchment hyperspatial images granulometric analysis. However, the model performance testing can only be validated with the observed values, or any past empirical model or equation for the basin is in concern. Providentially, an empirical bedload estimation relation is proposed by Sear and Newson (1991), and they had sampled many sites in England to formulate an empirical relationship. The relationship is used in the bedload transport studies (Wishart et al., 2008), and it is accepted for the river catchment more than 100km^2 for the English region.

$$Bed\ load\ (tonnes\ /year) = 2.5\ * a^{1.16} \qquad 5.8$$

The relationship eq. 5.8, where a catchment area and measured in unit Km^2. The emipirical relation is used to test the CASCADE model performance, and the model has never over predicted the bedload transport value even under extreme discharge conditions observed at the time of storm Desmond. Considering that bedload transport models are prone to overestimate the bed load values, the current CASCADE model parametrised with calibrated distributed discharge, drone-based GSD and network attribute proves to be

better conditioning the model for sediment flux fluctuation followed by weir removal under various Q scenarios.

Summary:

The proliferation of river course obstructing structures globally and Europe has degraded the river geomorphic and ecological sanctity to an extent where current ecological status reached an alarming stage. If the new dam construction continues to be promoted, which will put ecology and biodiversity at risk, there will be no return because the plant's biodiversity is declining at a staggering pace. However, despite the awareness of what kind of benefit biodiversity offers for the planet and humans, specifically, the freshwater ecosystem is most degraded at present, and it has been revealed by the living planet index survey and UN reports.

One of the primary reasons for the biodiversity declining trend in river fragmentation is also exposed in the AMBER barrier atlas and, according to AMBER assessment, which causes hydrological, sedimentological, and ecological imbalance (for example, barrier to migratory fish).

In recent times barrier or dam removal emerged as one of the fastest river restoration tools but not every barrier is economically suitable for removal activity. However, many barriers fall into the obsoleted category and pose a risk if not removed. *The question is which barrier should be removed on a priority basis of degradation they have brought to the freshwater ecosystem.* A possible solution is proposed in the current charter that has implemented a sediment transport modelling framework named CASCADE. The implementation of CASCADE facilitates sediment transport at the river network in a data-poor river catchment. Comparing it to the advanced sediment routing simulation models, the CASCADE model emerges as a better selection. One of the crucial rational to implement the CASCADE is the model's ability to combine empirical sediment transport formulas in conjunction with graph theory; thus, network scale sediment entrainment, transport and deposition of the sediment flux can be assessed. In addition to that, the CASCADE has considered the river reach as a cascading process, which in the recent version takes account of the Krumbein phi scale (ranging between silt and boulder and representing an 18-grain size fraction per reach, which is represented as sub-cascades in the

CASCADE modelling environment). Thus, the modelling environment facilitates a more realistic river reach sediment representation in the model compared to the previous version, which only considered the single grain size per cascade per reach. Finally, the model has preserved the river network hierarchy before and during the simulation. Thus, the model can deliver the grain specific sediment flux interacting with the river downstream hydro-morphological prevailing condition. This has resulted in sediment provenance and grain specific deposition and transport information. Weir and dam's presence on the river network can be analysed, which helps the modeller formulate strategic planning for the assessment of most damage causing river obstructing structure (it is discussed in chapter 6, which covers model execution in the Eamont River catchment).

This chapter has highlighted the parsimonious CASCADE model and its modelling framework with added advantages. Though, it also focused on the efforts being made compared to previous CASCADE models studies. It has two significant advancements regarding model parametrisation with the photo-granulometric data over the river network and its integration with the SWAT model for the hydrological input. On the other hand, the river network processed in each modelling environment is identical, which has the advantage of seamless data exchange between the two models, and it has bypassed the CASCADE models dependency on the toolbox called TopoToolBox. However, the TopoToolBox tool has its advantages when models like SWAT or other hydrological models are not utilized for the extraction of river network, for CASCADE model. In conclusion, integrating the two-modelling environment has proven its potential to deal with dam or weir removal strategic planning in the data-poor river catchments (for explanation and results, see chapter 6).

Chapter 6: The adaptive management approach for prioritising barrier removal with SWAT-CASCADE Model Simulations in the Eamont river catchment.

6.1 Introduction

Adaptive management is recommended for natural resource management and environmental decision making while the level of associated uncertainty is extreme (Walters, 2007). Climate change and its impact on biodiversity need urgent management strategies to reduce the expected ecosystem loss (Battin et al., 2007; Bálint et al., 2011; Jaeger et al., 2014; Pires et al., 2018; Kapoor, 2021). Globally, the adverse impacts of climate-driven disasters and ecosystem degradation are not common phenomena that can be overlooked. Human influences are posing significant adversity to the management solutions. In such conditions, adaptive management of natural resources and environment seems to be the way forward that is structured with a learning by doing approach (Peterson et al., 1997; Tompkins and Adger, 2003, 2004; Viney et al., 2007; Tanner-McAllister et al., 2017).

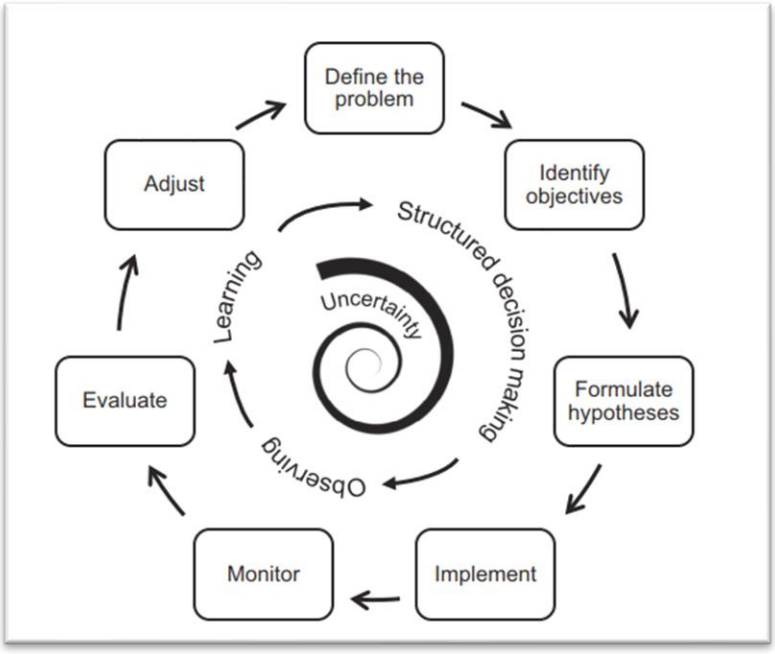

Figure 6.1 The iterative process of adaptive management characterised as 'Learning by doing', adopted from (Allen et al., 2011; Summers et al., 2015).

Adaptive management favours and focuses on adopting alternate methods hypotheses, implementing the solution and observing the finding to reduce the knowledge gap and improve the existing solutions. Thus, constant assessment of the implemented solutions and their feedback contributes to better research outcomes and policymaking.

Adaptive management's fundamental nature is learning by doing or observing actions; outcomes can sometimes be time-consuming. However, natural processes take years to indicate any significant outcome, especially in the riverine environment. Hence, it becomes challenging to adopt management approaches considering the research project's required time frame. In such cases, modelling can be a beneficial tool because models are based on abstracted reality and mathematical relations and algorithms explaining the physical environment. However, a decision-making approach based on adaptive management must be scrutinised based on the scientific justification; therefore, careful selection of the model's ability and its validation ensured further regional applicability and adaptability (McLain and Lee, 1996).

Dam or weir removal studies can take longer to reveal distinct geomorphology and ecological recovery (Mahan et al., 2021). Also, fish passage facilities on various dams are not always adequate; thus, dam or weir removal is gaining momentum that requires multiple years of monitoring (Poulos and Chernoff, 2021, p. 350; Wippelhauser, 2021). Sometimes ecological recovery is faster than geomorphic recovery following a dam removal (Tullos et al., 2014). In such uncertainty, ascertaining geomorphic changes following a barrier removal, a numerical model-based solution can significantly improve decision-making (Branco et al., 2014; Warrick et al., 2015; Foley et al., 2017; Schmitt et al., 2018a).

6.2 Sediment flux's spatial-temporal response scale in an impounded river network

Human impact on global sediment flux is enormous, and it distinctly puts the Anthropocene apart from other geological epochs (Syvitski and Kettner, 2011). In order to balance the negative impacts caused by human beings, it is recommended to restore sediment flux pathways and employ the modelling tools to restore the sediment and water connectivity (Zanandrea et al., 2021). In the

current analysis, we are trying to solve the same by addressing the first objective of the research project, "what are the temporal and spatial response scales of impounded channels to barrier removal". To formulate the analysis scenarios two different years had been selected that represent hydrograph information, each representing flood year and year of normal discharge conditions in 2015 and 2011, respectively. 2015 represents the extreme rainfall event experienced by the regional river catchments in the documented hydrological history. Hence the 2015 and 2011 hydrograph will represent transported sediment flux under the extreme discharge and standard conditions at the river network scale.

The yearly hydrographs are processed to get the q-percentile discharge scenarios because the CASCADE model is instantaneous and can process single discharge conditions at a single processing instance. Thus, the model has been executed for the q-percentile discharge class and the annual frequency of the class. Later, annual sediment flux is obtained by adding the values under each scenario (Tangi, 2018, pp. 26–28) with the CASCADE model's function *script_annual_simulation.m* (Tangi et al., 2019a).

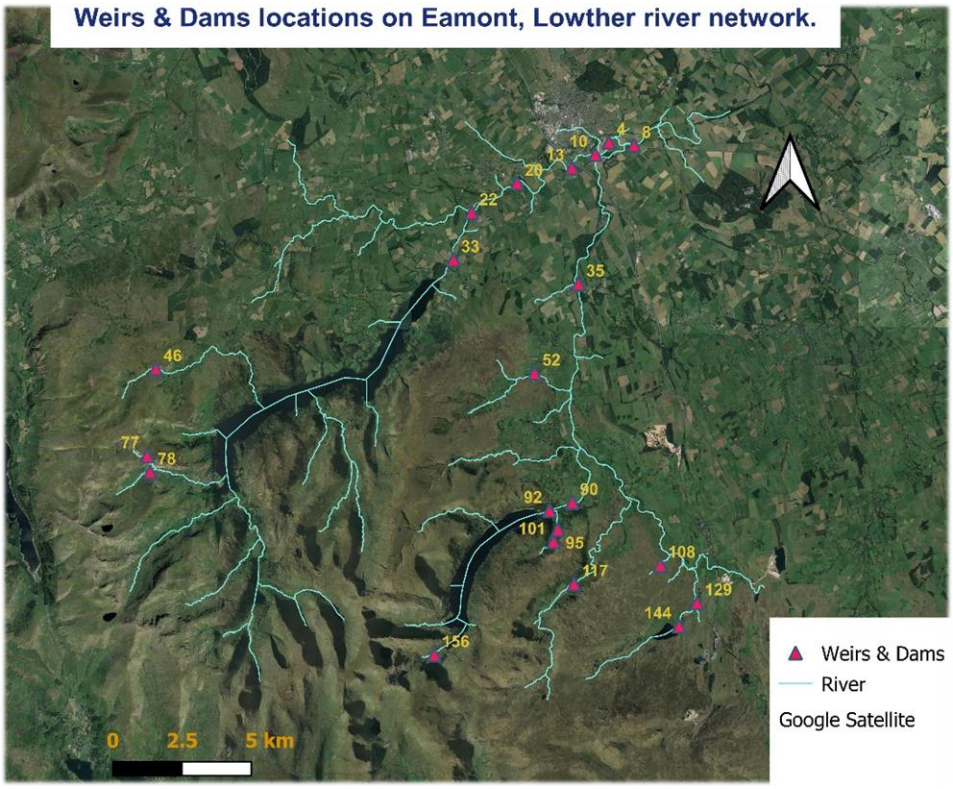

Figure 6.2 Dam and weirs locations on the river Eamont and Lowther.

Weir / Dam id	Cobble's TE (0.99%)	Gravel's TE (90%)	Sand's TE (70%)	Silt's TE (60%)	River
4	0.36	0.33	0.25	0.22	Eamont
8	0.59	0.53	0.41	0.35	Eamont
10	0.37	0.33	0.26	0.22	Eamont
13	0.69	0.62	0.48	0.41	Eamont
20	0.71	0.64	0.5	0.43	Eamont
22	0.49	0.44	0.35	0.30	Eamont
33	0.42	0.38	0.29	0.25	Eamont
35	0.19	0.17	0.13	0.11	**Lowther**
46	0.30	0.27	0.21	0.18	Eamont
52	0.82	0.74	0.57	0.49	**Lowther**
77	0.23	0.21	0.16	0.14	Eamont
78	0.41	0.37	0.28	0.24	Eamont
90	0.44	0.4	0.31	0.26	**Lowther**
92	0.99	0.99	0.99	0.99	**Lowther**
95	0.46	0.41	0.32	0.28	**Lowther**
101	0.55	0.49	0.38	0.33	**Lowther**
108	0.39	0.35	0.27	0.23	**Lowther**
117	0.95	0.86	0.67	0.57	**Lowther**
128	0.55	0.49	0.38	0.33	**Lowther**
129	0.33	0.30	0.23	0.20	**Lowther**
144	0.99	0.99	0.99	0.99	**Lowther**
156	0.16	0.14	0.11	0.09	**Lowther**

Table 6.1 Estimated Sediment Trap Efficiency for weir and dams in the Eamont River catchment, measured with Brown's equation.

During the simulation period, all dams and weirs are considered for their sediment trap efficiency and their location is depicted in Figure 6.2. The estimated sediment trap efficiency is reported in Table 6.1, and it is measured with Brown's equation in 2.6.2. Table 6.1 contains the weir id and measured trap efficiency of cobble, gravel, sand and silt particles. Brown's equation returns a single value for the bulk sediment trapped by a dam or weir structure. Therefore, an assumption is implied for the different grains trapped proportion. Thus, trap efficiency for cobble is assigned 99 per cent of the total estimated value, gravel 90 percent, sand 70 percent, and silt 60 percent, respectively. The percentage measure is the fraction of the total estimated trap efficiency. Hence, gravel sand and silt trap efficiencies proportion are inferred values. For example, in Table 6.1, weir id 95 depicts trap efficiency of 0.46 percent for cobbles that is equivalent to the total estimated, and its 60 percent value 0.28 assigned to the silt particle's trap efficiency. However,

trap efficiency values kept the same for different grain in the case of two big dams named Haweswater and Wet Sleddale dams, identified as 92 and 144, respectively, in Table 6.1.

The execution of the CASCADE model is performed with different transport capacity empirical formulas (Engelund and Hansen, 1967; Wilcock and Crowe, 2003; Wong and Parker, 2006; Yang, 1984) and hydraulic features estimation formulas (Manning et al., 1890), hydrologic solver (Schmitt et al., 2016). Especially in annual sediment flux estimation, multiple combinations of transport capacity formulas and hydraulic parameter estimation formulas have predicted higher values for sediment flux (transport, entrained and deposited). However, the combination of Yang's unit stream power equation and Manning – Strickler resulted in sediment flux estimates close to the empirical equation's derived sediment estimates for U.K. catchments (Sear and Newson, 1991), in Table 6.2. The Sear and Newson's had gathered different river catchments sediment data and proposed an empirical relation among the river catchment and sediment load, for UK's River catchment.

Equation 5.8, for the Eamont catchment, the value of a is 396.2 Km^2. Therefore, the estimated annual bedload of 2579 tonnes/year. The CASCADE model's performance is assessed based on the simulated sediment flux estimated under low and high discharge scenarios Table 6.2 & Table 6.3.

	Transport capacity formula				Hydraulic features estimation		Sediment Flux (kg/sec)		
All Weir/ Dams	Wilcock and Crowe	Engelung and Hansen	Yang	Wong and Parker	Manning - Strickler	Iterative hydraulic solver	Deposited Flux	Entrained Flux	Tranported Flux
✓	✓				✓		0.02	0	9.20
✓	✓					✓	139.49	0	1090.66
✓	✓	✓			✓		0.05	0	0.51
✓		✓				✓	30.26	0	276.69
✓			✓		✓		0.45	0	2.28
✓			✓			✓	1.85	0	9.67
✓				✓	✓		1.09	0	10.53
✓				✓		✓	132.51	0	620.74

Table 6.2 CASCADE simulation under low discharge. It justifies the combination of Yang's unit power equation and Manning-Strickler, which produces the sediment flux within the range predicted by Sear & Newson's equation.

All Weir/Dams	Wilcock and Crowe	Engelung and Hansen	Yang	Wong and Parker	Manning - Strickler	Iterative hydraulic solver	Deposited Flux	Entrained Flux	Transported Flux
✓			✓		✓		1189.45	0.00E+00	4520.60
✓			✓			✓	1185.7	0.00E+00	4607.08
✓				✓	✓		1086.79	0.00E+00	5969.47
✓		✓			✓		1441.72	0.00E+00	6999.03
✓				✓		✓	1465.44	0.00E+00	9077.65
✓	✓				✓		2.05E+03	0.00E+00	1.50E+04
✓		✓				✓	1.97E+03	0.00E+00	1.86E+04
✓	✓					✓	2.45E+03	0.00E+00	2.38E+04

Table 6.3 CASCADE simulation with different transport capacity formula and hydraulic feature estimation and its impact on sediment flux at the catchment outlet, while no weir/dams removed (simulation performed with peak flow conditions).

The execution of CASCADE for the 2011 hydrograph and generated results analysed for sediment flux transported, entrained, and deposited for gravel class (-5.5 to -1.5, Φ scale). The figures for sediment flux transported, entrained and deposited are depicted in Figure 6.3, Figure 6.4, and Figure 6.5, respectively. The tributary river Lowther has contributed a slightly higher amount of sediment flux in the entrainment and deposition stage, while the Eamont river system transported more sediment flux.

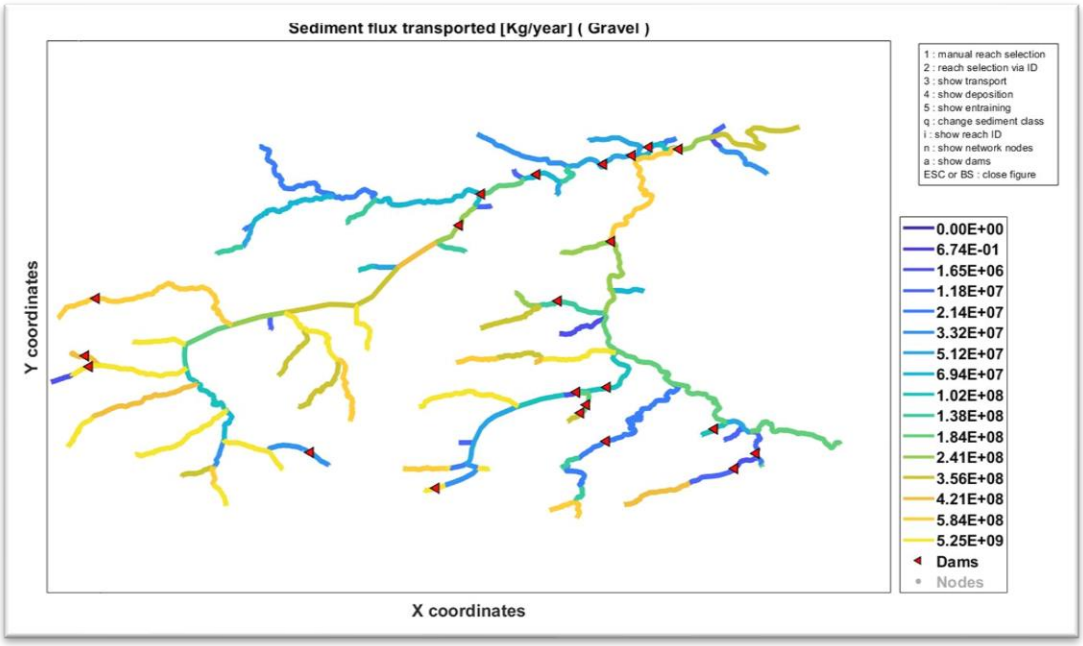

Figure 6.3 Annual sediment flux transported (Kg/year) at the Eamont river network in 2011.

The amount of sediment flux transported is higher for the headwater reaches for the Eamont and Lowther rivers, while the low relief parts of the catchment contributed less. The amount of sediment is similar in terms of entrained sediment flux because of the higher slope, narrower reaches and high transport capacity in those reaches.

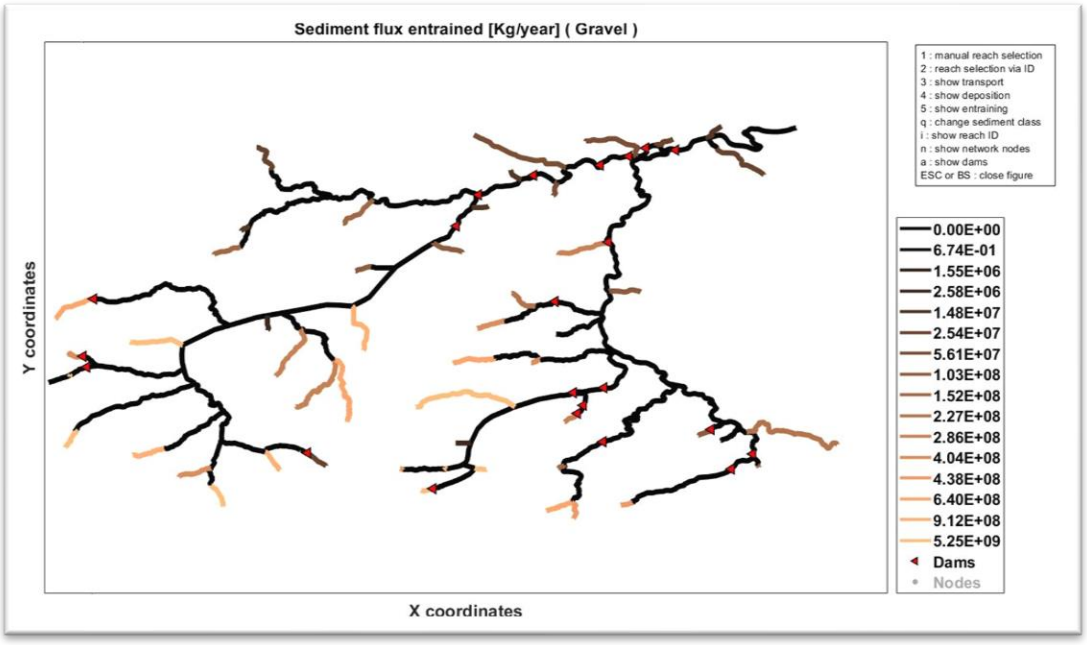

Figure 6.4 Annual sediment flux entrained (Kg/year) at the Eamont river network in 2011.

The high amount of deposited sediment flux occurred in lakes, reservoirs, and low relief areas. However, the location of dams and weirs on the river network has affected the deposition of sediment flux.

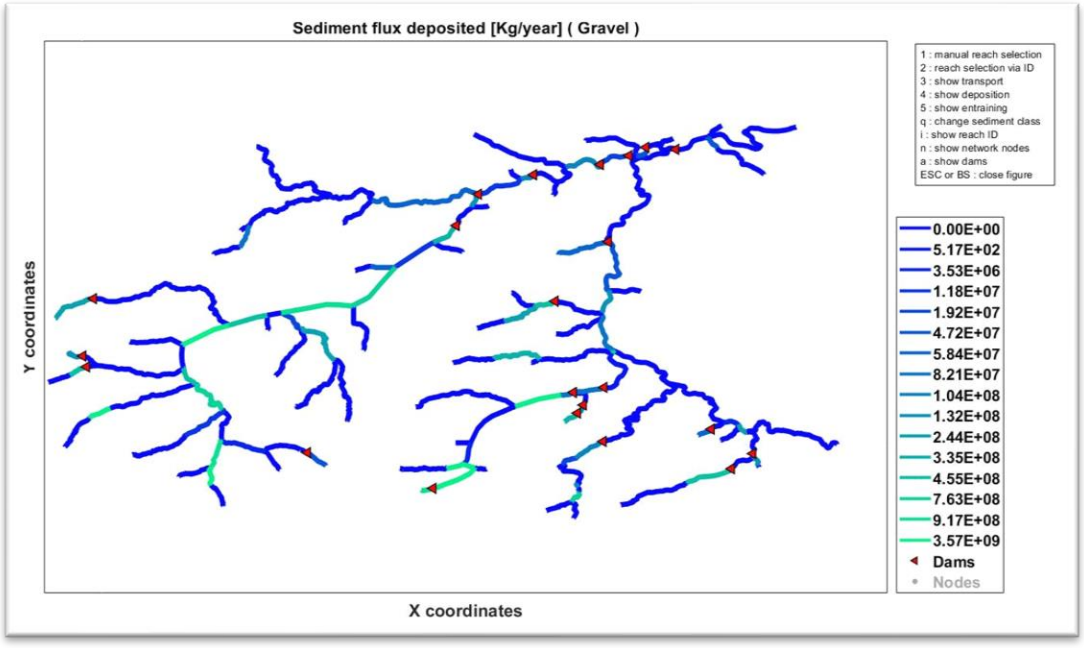

Figure 6.5 Annual sediment flux deposited (Kg/year) at the Eamont river network in 2011.

Second, annual sediment flux estimations were performed with the q-percentile hydrograph extracted from the yearly distributed simulation 2015 (SWAT output). Similar to the 2011 scenario, the 2015 results were extracted by the CASCADE function (*script_annual_simulation.m).* An identical sediment frequency matrix Fi_r is utilised in both cases, corresponding to the GSD for each grain class in the Φ scale. Thus, it ensures that under both q-percentile hydrographs, each reach has the same grain size.

The amount of transport, entrained, and deposited sediment flux for 2015 remained higher than in 2011, attributed to the extreme rainfall that led to the storm Desmond extracted q-percentile hydrograph (Figure 6.6, Figure 6.7 & Figure 6.8). However, a high amount of sediment flux cannot be verified because no validation sediment data is available for the catchment. In the annual sediment flux estimation process, CASCADE simulation has predicted a similar spatial trend of sediment flux movement under transport, entrained and deposited flux remained the same between 2011 & 2015.

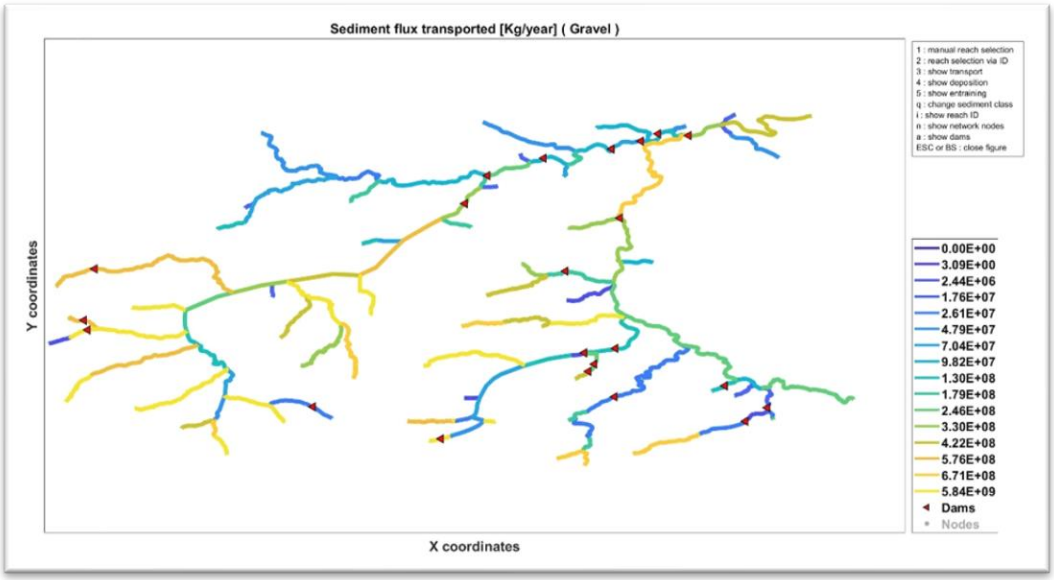

Figure 6.6 Annual sediment flux transported (Kg/year) at the Eamont river network in 2015.

The similar spatial distribution of sediments could be attributed to the enormous lake Ullswater on river Eamont, which acts as the ultimate sink for all the sediments carried by the headwater reach.

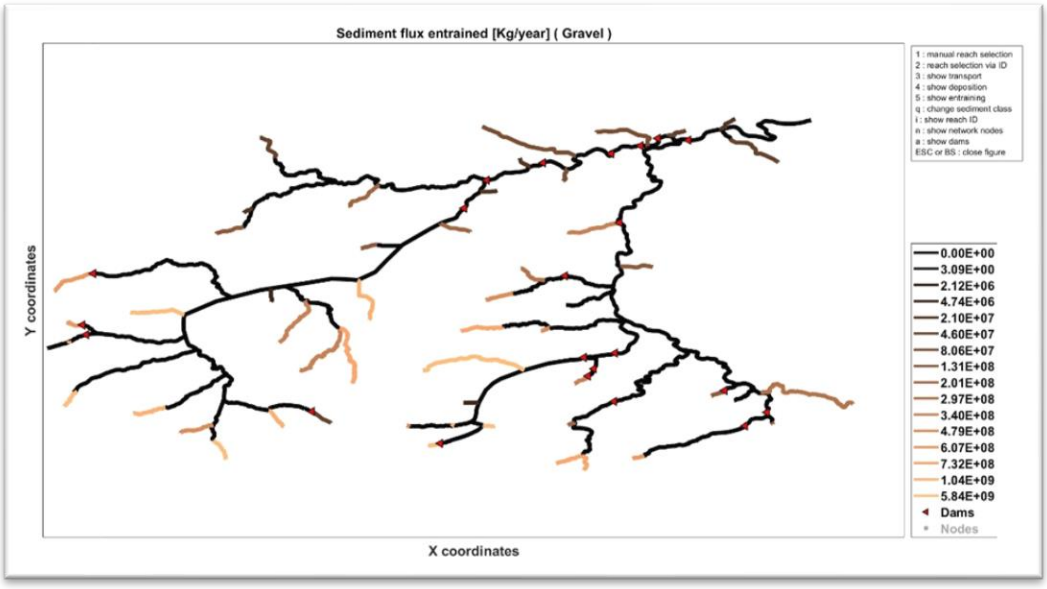

Figure 6.7 Annual sediment flux entrained (Kg/year) at the Eamont river network in 2015.

On the other hand, Lowther has a second big artificial lake or Haweswater reservoir in the catchment. It diverts the significant portion of runoff generated in the headwater region and relocates it to meet the Manchester city municipal and industrial water requirements. Lowther catchments low relief reaches originate at the relatively low slope region and have low transport capacity. Thus, under different hydrograph scenarios, catchment sediment flux has shown a similar spatial distribution of sediment flux pattern. However, all the dam and weirs present in the catchment were considered for the simulation 2011- & 2015-year's q-percentile hydrographs, which is the actual case scenario because, until 2016, no physical removal of the weir was performed. One of the weirs named *Carlton* had been removed in mid-2016 (B.B.C., 2016); it was located before the confluence of tributary Lowther and in the downstream part of the Ullswater lake, Figure 6.18.

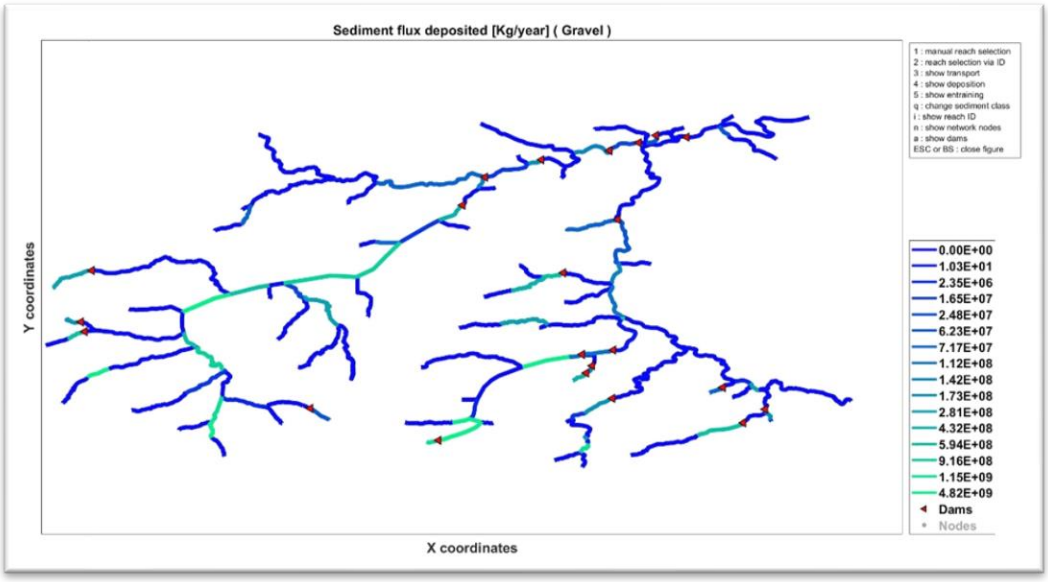

Figure 6.8 Annual sediment flux deposited (Kg/year) at the Eamont river network in 2015.

The sediment flux proportion contributed to the catchment outlet by River Eamont & tributary Lowther is slightly different for the annual simulation of the year 2011. Comparatively, the Lowther River has entrained and deposited more sediment flux than the Eamont river due to a higher river gradient than for the longest unobstructed river course in the catchment.

On the other hand, the river Eamont has transported a marginally higher sediment flux than Lowther. Because source reaches of the Eamont river contributes high flow and sediments from the peak elevation zone of the catchment. The geomorphic setup provides a high gradient compared to the remaining region of the catchment, and it ensures a fair share of transport capacity in the headwater reaches, for the Eamont river, depicted in Figure 3.3. The mentioned spatial pattern of sediment flux distribution and its proportion between Eamont & Lowther remained similar in the annual sediment flux estimates for the year 2015.

The CASCADE model has revealed the sediment flux transport, deposition and entrained at the network scale by analysing sediment connectivity established with varying transport capacity and competition among sub-cascades. However, predicted and observed sediment rates deviate at peak flow conditions, depending on competent discharge frequency or recurrence interval. In addition, river characteristics influence sediment transport rate (Nash, 1994), and the absence

of observed sediment data can hamper performing parameter sensitivity and model calibration analysis. An annual sediment flux assessment involves time-averaged sediment flux value addition. Therefore, to find the best weir removal scenario or removal prioritisation, it is better to rely on the CASCADE model's ability to process the instantaneous sediment flux movement along with sediment trapped by the structures. This analysis performs sediment routing for the whole range of sediment classes distributed in 18-grain sizes (-9.5 to 7.5 Φ) of the Krumbein phi (Φ) scale.

6.3 Prioritisation of barrier removal in the river network?

The project's second objective is to develop the barrier removal scenario in the European rivers, declared as the most fragmented rivers on the planet. Since the extent of the problem is enormous and it cannot be dealt with a site-specific modelling solution. However, a modelling approach that can analyse the catchment processes at the river network scale would serve as a case study for the region. One of the remarkable problems in the weir removal scenario development is that simply removing a weir may not produce expected results. Since a river network could be affected by the multiple cascades of weir structures, and thus weir removal scenarios must be accountable for the other weir or dams present on the river network and their mutual impact.

The current case study analyses sediment flux movement in the Eamont river catchment with multiple weirs and their ability to trap incoming sediment (trap efficiency) and the impacts they can cause downstream at the catchment outlet. The model simulation and sediment flux analysis were performed beyond one year's hydrograph (flood or drought year); thus, fifty years of hydrological information have been converted to a q-percentile hydrograph. It has represented the Q scenario recorded in the last fifty years for the Eamont river catchment.

The analysis of the weir removal is performed with switching between different weir combinations; the CASCADE model analyses instantaneous sediment flux movement and bedload transport that transforms the river morphology are episodic nature (Walling et al., 2000) suits the scenario development criteria. However, there are 22 weir and dams, and many combinations can be possible concerning their location in the catchment, Figure 6.9.

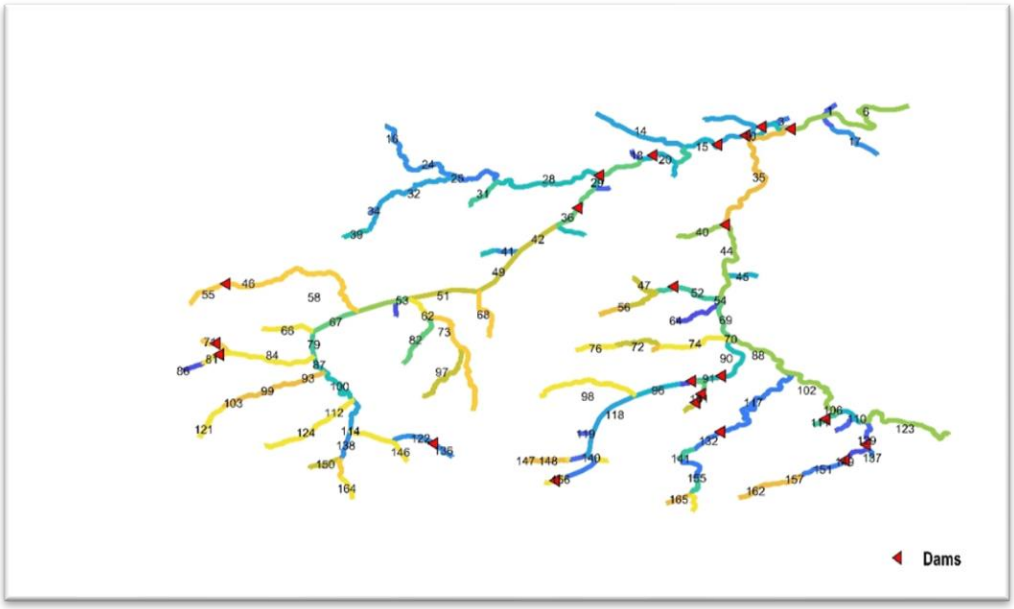

Figure 6.9 Locations of dams and weir considered in the CASCADE for the Eamont River Catchment and reach id.

To simplify the weir removal scenario and at the same time required the number of simulations to trace weirs accountability with spatial as well as their trap efficiency. Therefore, the river network is divided into quadrants based on the weirs' relative location in the Eamon River catchment. The *first quadrant* covers the Eamont rivers headwater regain located in the catchment's southwest part. The *second quadrant* covers the Lowther rivers headwater region, and it is in the Southeast. The *third & fourth quadrants* are in the Northwest and Northeast parts of the catchment, respectively (Figure 6.10), and they represent the low relief river course of the Eamont and Lowther rivers.

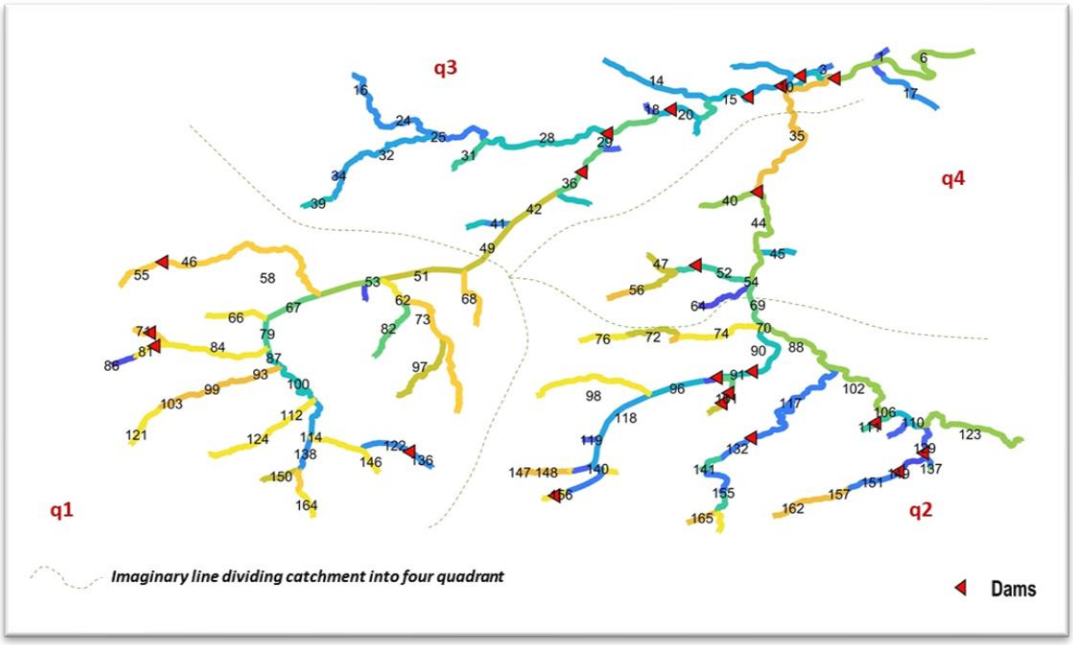

Figure 6.10 An imaginary line dividing the Eamont river catchment into four quadrants (q1, q2, q3 & q4).

Different weirs are analysed for their impact on catchment sediment flux by switching weir or virtual weir removal scenarios. Since weir removal combinations can be numerous thus, we started assessing the weir removal scenario for the different catchment quadrant (q1, q2, q3 & q4). In the first instance, the weir removal scenario is analysed for the Eamont river course downstream of the Ullswater lake region, represented by quadrant - q3. This quadrant has weirs situated between elevation 153 and 116m and has a flat gradient. The various weir removal scenarios for this quadrant have shown distinct sediment flux changes under each q-percentile discharge class, in Table 6.4. However, the weir in this region has low sediment trap efficiency.

Nevertheless, progressive removal of weirs discloses increased sediment flux transported at the outlet. A scenario representing complete removal of all five weirs (id 22, 20,13,10,4) has allowed maximum transported flux. However, the different weir removal scenarios show a significant change in sediment flux, but the optimal solution for quadrant 3 (q3) would be complete removal of weir id 22,20,13, 10 & 4 and leaving weir 33 in place; this combination provided the second-highest value for transported flux at the catchment outlet, Table 6.4. Thus,

it ensures maximum sediment connectivity for Eamont's downstream river section. Crucially, weir 33 is an important site that measures river gauge information and a critical hydrological analysis location that measures water release from Ullswater Lake.

Progressively, the Eamont river headwater region is considered for the weir removal scenario and the Ullswater lakes downstream river, representing the entire Eamont river course (q1 & q3, Figure 6.9) excluding tributary Lowther. By executing CASCADE under weir removal scenarios for this region. It has shown no distinct change in the sediment flux at the catchment outlet and follows transported flux pattern similar to the quadrant 3 (q3) weir removal scenarios. However, when all weirs are removed for quadrant id 1 and 3, it shows slightly increased flux at the outlet. Although, this could be attributed to the inability to fully parametrise the Ullswater lake depositional environment with an average depth of 25.3m, 14km length and water volume 219657965m^3. Ullswater Lake acts as the ultimate sink for sediments carried by Eamont river headwater reaches.

We further extended the weir removal scenarios to the tributary Lowther rivers headwater region, quadrant 2 (q2) represents it. In this region, two major dams are in operational status, and they store, divert a significant volume of water (*Haweswater* and *Wet Sleddale* Reservoirs represented by dam id 92 & 144 in CASCADE, respectively, in Table 6.1). Economic importance and cost involved for two dams; thus, it is impractical to propose the complete removal of two dams, while other weirs can be selected for removal as they offer means for improving sediment connectivity in the remaining river course of the Lowther River. To assess the weir removal scenario for the headwater region of Lowther, we kept the weirs in place for quadrants 3 & 1 or the Eamont river course.

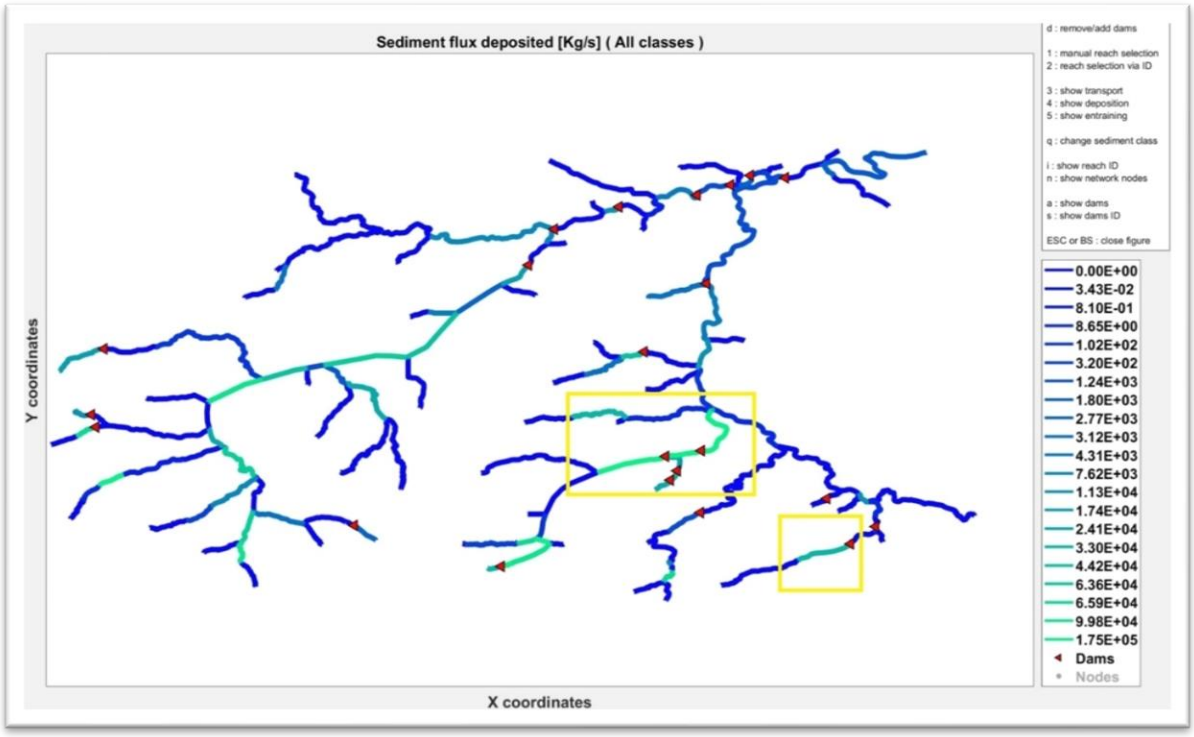

Figure 6.11 High deposition of sediment flux in the headwater region of the river Lowther, while all dams & weirs are in place.

Figure 6.11 depicts the sediment flux deposited during the simulation of CASCADE under peak flow conditions, and all the dams and weirs are considered at the time of CASCADE simulation. The high sediment flux deposited in the Haweswater, and Wet Sleddale reservoirs reach sections and the downstream river's immediate flat valley bottom.

In a different scenario, only Haweswater and Wet Sleddale were in place during the CASCADE simulation, excluding weirs in quadrant 2 (q2). The peak discharge scenario remained similar while all weir along with major dam analysed. Figure 6.12 shows the increase in the deposited flux; however, it has no impact on the transported flux to the catchment outlet (reach id 6).

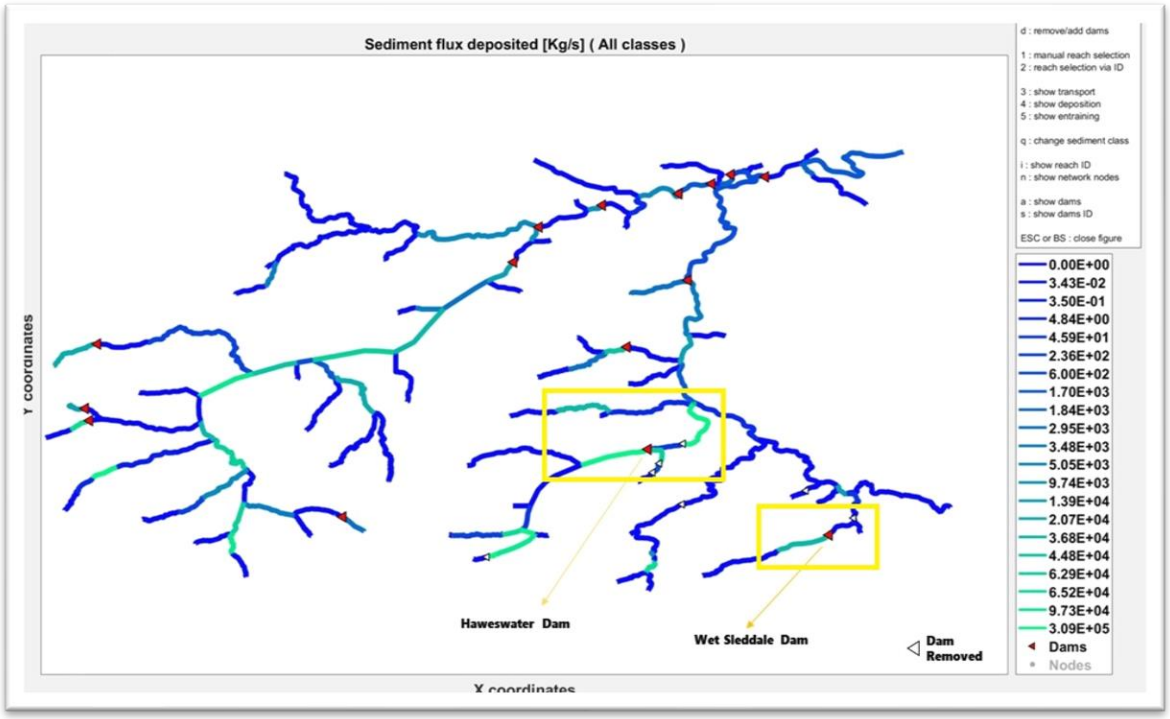

Figure 6.12 High deposition of sediment flux persisted, while all weirs removed and Haweswater, Wet Sleddale are considered in the CASCADE simulation.

The explanation for the weir removal scenarios depicted in Figure 6.11 & Figure 6.12 can be justified with the sediment connectivity (source to sink). The sediment delivery from the headwater region of river Lowther to the catchment outlet is low because of sediment dis-connectivity. Sediment connectivity in the Lowther River is depicted in Figure 6.13, which shows that the unobstructed headwater reach attains maximum sediment connectivity in the Lowther, and tributary reaches that joins the Lowther River in the low relief part of the catchment.

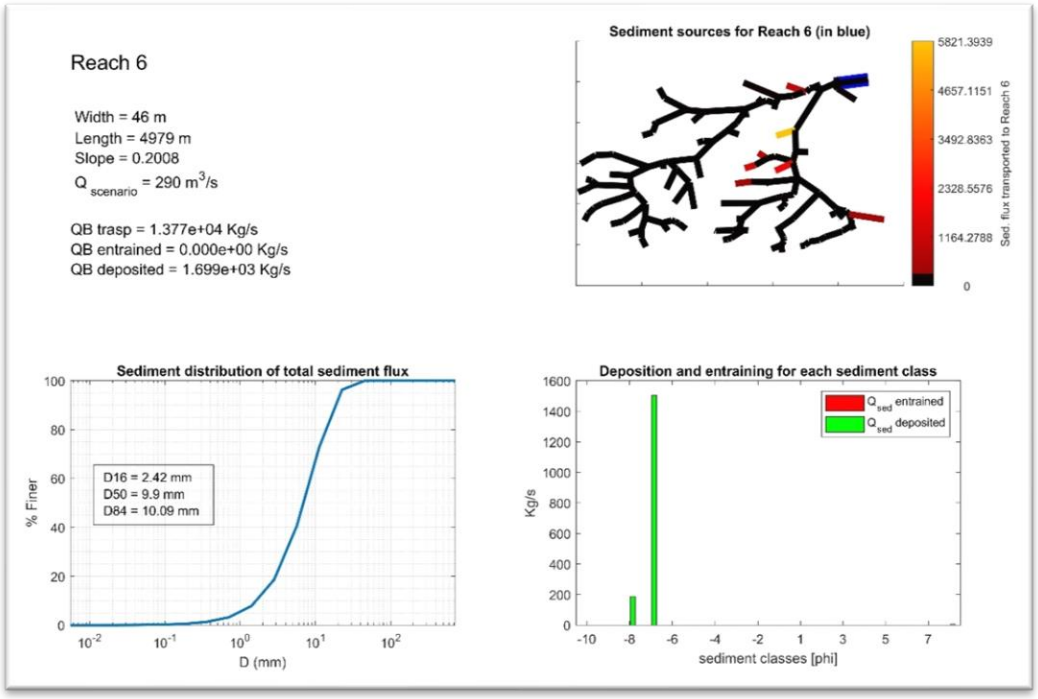

Figure 6.13 Source reaches supplying sediment flux to the catchment outlet (reach 6) under peak flow condition, sediment sources for reach 6 explains the sediment connectivity.

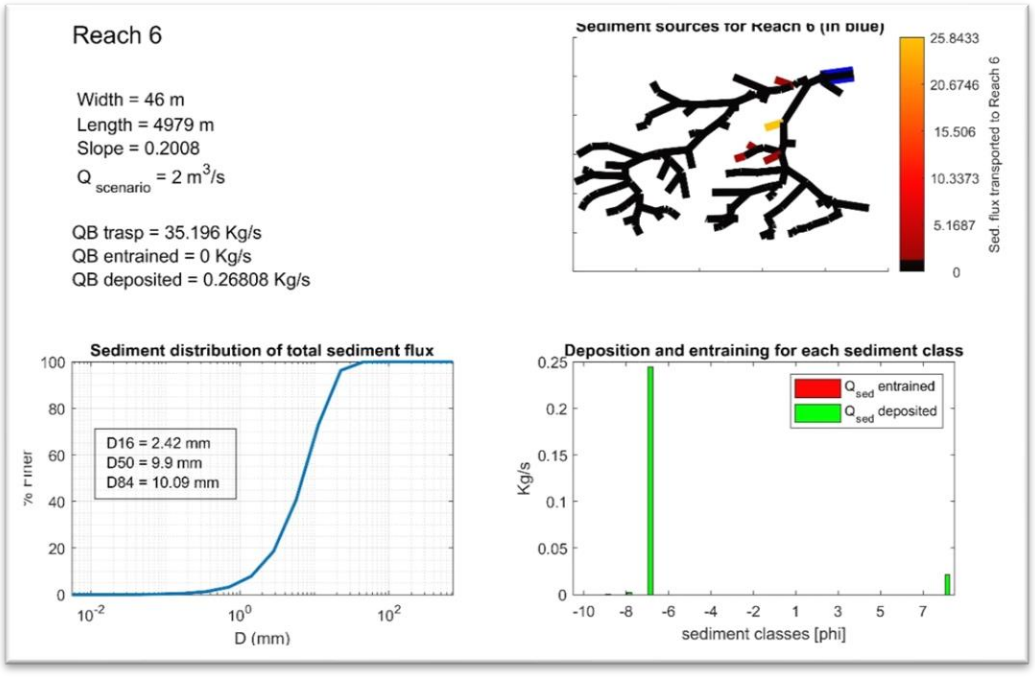

Figure 6.14 Source reaches supplying sediment flux to the catchment outlet (reach 6) under normal flow condition, while no weir or dam removed in CASCADE simulation.

Our analysis depicts the very high sediments flux transported and deposited at the catchment's outlet, Figure 6.13; however, it represents the CASCADE simulation under peak flow conditions. Contrary to that, sediment flux transported, entrained, and deposited under the normal discharge conditions shows reasonably good estimates Figure 6.14, which align well with an empirical relation proposed by Sear and Newson (1991). The resultant sediment flux is displayed in Table 6.4, which shows the impact of weir removal combinations at the river Eamont's outlet.

Before the quadrant 4 (q4) analysis, located in the low relief part of the Lowther River, the sediment connectivity (source to sink) has highlighted crucial information, which is depicted in Figure 6.13 & Figure 6.14, and illustrates sources supplying sediment flux to the outlet under peak and low discharge conditions, respectively, in which no weirs but Haweswater, Wet Sleddale dam considered. These figures outlined sediment connectivity in the figure's upper right parts, explaining the sediment connectivity.

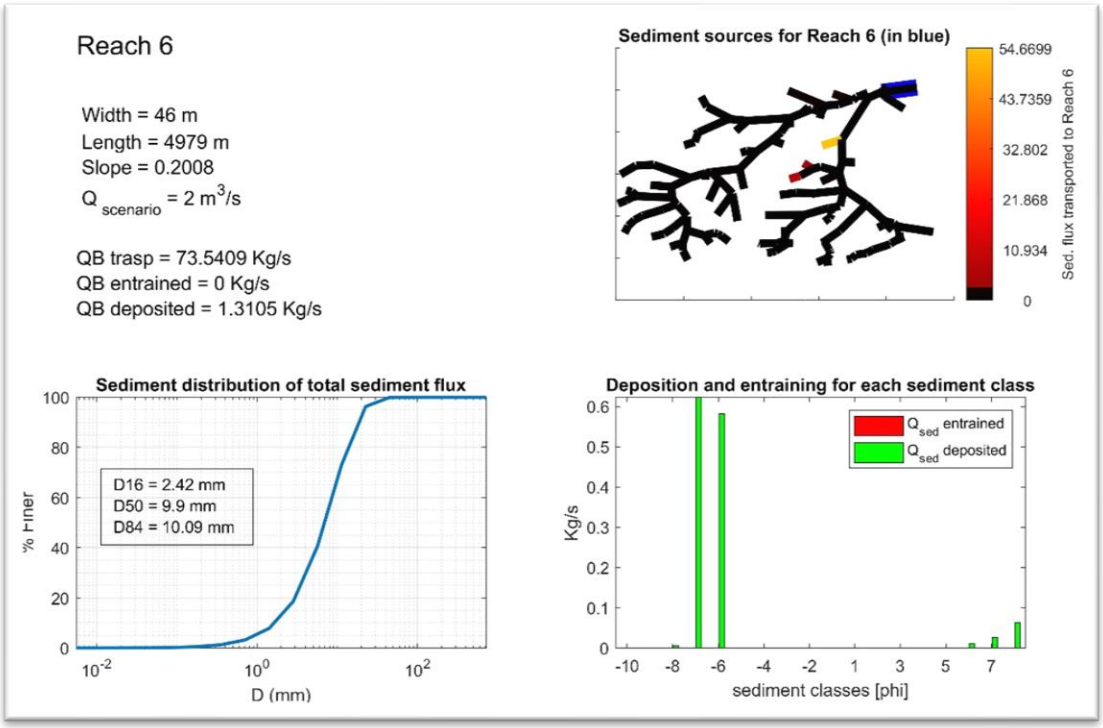

Figure 6.15 Sediment connectivity to the catchment outlet under low flow condition, all weirs removed.

Similarly, removing all weirs in the Eamont & Lowther catchments is executed in the CASCADE model at the low discharge condition, represented in Figure 6.15.

The last three weir removal and discharge scenarios (Figure 6.13, Figure 6.14 & Figure 6.15) analysis have set out a clear sediment connectivity pattern in the catchment. It has facilitated the weir removal scenario task by providing the fact that it is the Lowther tributary that contributes more sediments to the catchment outlet. Table 6.5 represents the weir removal analysis for the Lowther River.

We further extended this and scrutinised it under not just peak or low discharge but with the q-percentile (81.1%) discharge. The model execution shows whether it has a deviation from previous scenarios performed for the whole catchment along with q4. Figure 6.16 illustrates that discharge conditions beyond normal flow ensure sediment connectivity between distant tributaries and outlet reach. However, the below-normal discharge state in the CASCADE simulation has shown limited connectivity between the far end headwater region and outlet reach (Figure 6.14). The weir removal impacts for the quadrant q4 and q2 regions that cover the tributary Lowther River catchment, depicted in Table 6.5.

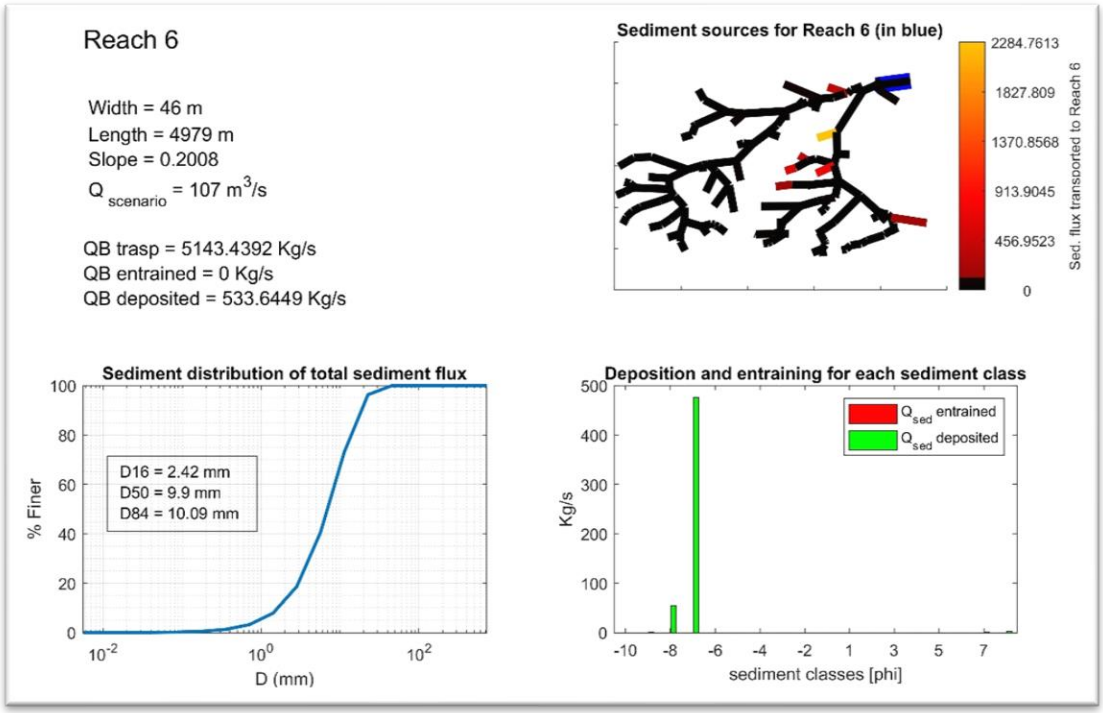

Figure 6.16 Sediment connectivity to the catchment outlet under peak flow condition, while all weirs were in place.

Unquestionably, many combinations of weir removals could be possible in conjunction with different transport capacity and hydraulic parameter estimation formulas. The earlier mentioned weir removal model execution that explains

connectivity alteration scenarios is performed with the CASCADE models script (connectivity_alteration_assessment.m), conditioned with transport capacity equation Wilcock and Crowe and hydraulic parameters estimated with Manning – Strickler formula.

Weir Removal Scenario (part 1)

Eamont river	Downstream Region	Discharge (m3/sec)								
		1.98	2.4	3.53	6.41	12.84	33.51	95.64	217.87	
Dam and Weir id's	33,22,20,13,10,4	3.73	6.46	17.3	58.25	180.18	719.74	2732	7045	Sediment Flux Deposited (Kg/s)
	33,22,20,13,10,4	3.73	6.46	17.3	58.25	180.18	719.74	2732	7045	
	33,22,20,13,10,4	3.73	6.46	17.3	58.25	170.82	719.74	2732	7045	
	33,22,20,13,10,4	3.73	6.46	17.3	57.55	124.78	577.46	2623.51	6632	
	33,22,20,13,10,4	3.73	6.46	17.3	48.49	103.48	496.66	2310.66	5959	
	33,22,20,13,10,4	3.73	6.46	17.3	46.64	99.11	480.09	2246.54	5821	
	33,22,20,13,10,4	3.73	6.46	17.3	43.64	91.94	453.14	2114.45	5.503E+10	
	33,22,20,13,10,4	3.73	6.46	17.3	50.99	109.23	518.73	2368.4	6050	
	33,22,20,13,10,4	3.73	6.46	17.3	58.25	154.64	714.06	2732.21	7042	
	33,22,20,13,10,4	3.73	6.46	17.3	55.52	122.15	563.47	2526.68	6367	
	33,22,20,13,10,4	3.73	6.46	17.3	44.89	96.83	475.7	2195.02	5733	
	33,22,20,13,10,4	3.73	6.46	17.3	46.62	99.79	481.31	2217.84	5717	
	33,22,20,13,10,4	3.73	6.46	17.3	47.71	101.5	489.4	2254.82	5806	

Table 6.4 Weir and Dam removal scenario for the Eamont River course – quadrant 3 (q3).

Weir Removal Scenario (part 2)

Dam and weir id's	Lowther River		Discharge (m3/sec)								
			2	2.4	3.5	6	13	33.51	95.6	217.9	
	(Headwater region)	(Downstream)									Sediment Flux Deposited (Kg/s)
	144,129,117,108,156,92,90,95,101	35,52	3.73	6.46	17.32	43.6	91.94	453.14	2114.45	5.50E+03	
	144,129,117,108,156,92,90,95,101	35,52	3.73	6.46	17.32	43.6	91.94	453.14	2114.45	5.50E+03	
	144,129,117,108,156,92,90,95,101	35,52	3.73	6.46	17.32	43.6	91.94	453.14	2114.45	5.50E+03	
	144,129,117,108,156,92,90,95,101	35,52	3.73	6.46	17.32	43.6	91.94	453.14	2114.45	5.50E+03	
	144,129,117,108,156,92,90,95,101	35,52	3.73	6.46	17.32	43.6	91.94	453.14	2114.45	5.50E+03	
	144,129,117,108,156,92,90,95,101	35,52	3.73	6.46	17.32	43.6	91.94	453.14	2114.45	5.50E+03	
	144,129,117,108,156,92,90,95,101	35,52	3.73	6.46	17.32	43.6	91.94	453.14	2114.45	5.50E+03	
	144,129,117,108,156,92,90,95,101	35,52	3.73	6.46	17.32	43.6	91.94	453.14	2114.45	5.50E+03	
	144,129,117,108,156,92,90,95,101	35,52	3.73	6.46	17.32	**58.3**	**91.94**	**580.0124**	**2523.7**	**6.50E+03**	
	144,129,117,108,156,92,90,95,101	35,52	3.73	6.46	17.32	**58.3**	**128.19**	**580.0124**	**2523.7**	**5.50E+03**	
	144,129,117,108,156,92,90,95,101	35,52	3.73	6.46	17.32	**43.6**	**128.19**	**580.0124**	**2114.4**	**5.50E+03**	

Table 6.5 Weir and Dam removal scenarios for the Lowther River headwater and downstream river course – quadrant 2, 4 (q2 & q4).

Index	
(purple)	Dam & weir included for scenario
(orange)	Dam & weir removed for scenario
(brown)	Deposited sediment flux
(blue)	Discharge scenario

6.4 Which removal scenarios can lead to predictable improvements?

Finding the solution to the predictable habitat improvement is not a straightforward solution. That is attributed to the uncertainty in the required time to have significant improvement in morphological and ecological conditions, and it requires repetitive monitoring for a longer duration. In the Eamont river catchment, a single weir named Carlton was proposed and taken out (B.B.C., 2016). Since the catchment had 22 weirs and dams before construction, the amount of trapped sediment by different structures over the years is not available. Therefore, the impact assessment on river morphology and physical changes cannot be direct. However, the low availability of fine sediments in the northwest river catchments in England shows riverine ecology suitability, while small weirs impact the river course (Quinlan et al., 2015).

The human impact on river characteristics are complex and may require monitoring at different spatial-temporal scale (Barquín Ortiz and Martinez-Capel, 2011). New technologies and their deployment at the river catchment scale may be preferred (Hedger et al., 2006; Woodget et al., 2015, 2017; Gracchi et al., 2021; Lang et al., 2021). Applying such technologies at the river network scale requires an extended research period. Moreover, technologies must address the multiple aspects of the river, which are hydrology, geomorphology, ecology, and biochemistry. Therefore, understanding the different aspects of rivers and their interdependence, including processing scale, plays a crucial role in river restoration planning (Polvi et al., 2020). The disparity between observed and modelled data at different scales as catchment, reach, and sub-reach may not directly facilitate river restoration.

Since in this research project, we have focused on catchment hydrology (SWAT model), grain size distribution analysis (Drone photogrammetry and BASEGRAIN), and sediment transport modelling by establishing the sediment connectivity & dis-connectivity pattern in an in-stream environment (CASCADE model). However, the lack of sediment records and spatial-temporal differences in the biological sampling (NFPD – national fish population database). Hence, it is preferred to rely on the concept of respective geomorphic diversity, river dynamics

& sediment dis-connectivity for river restoration planning (Brierley and Fryirs, 2009) as river connectivity ensures a healthy riverine ecosystem (Minshall et al., 1985; Kondolf et al., 2006; Nilsson et al., 2017). Sediment transport regime balance is beneficial for the riverine ecosystem (Wohl et al., 2015a). The negative impacts induced by the dam removal actions can release a hyper-concentrated pulse of sediment recovered in months or with years (Wilcox et al., 2014). However, a small weir in a gravel-bed river cannot release hyper-concentrated sediment pulse because of their limited trap efficiency, especially for fine-grain sediments, and it is evident in the present case study area.

The step required to restore habitat connectivity, sediment and hydrological, and lateral connectivity will improve instream habitat and nutrient and water quality improvement (Roni et al., 2008). The CASCADE model implementation has solved and provided the regions of dis-connectivity (Fryirs, 2013) due to natural and man-made conditions; however, the dis-connectivity addressed in the CASCADE model is of longitudinal dimension only. This seems to be a limitation in the 1D model, but at the same time, 1D models are efficient to process and solve the connectivity issue at limited data and computation power requirements. Adaptive management requires quick solutions to be tested and assessed their practical efficiency. We propose the CASCADE solution to access the sediment connectivity and delivery results to be implemented for habitat quality improvements.

The presence of two massive dams on river Lowther that provides maximum sediment flux to the catchment has undoubtedly changed the river process and forms, attaining former river condition impractical in the current situation (Dufour and Piégay, 2009). However, river restoration efforts should be directed towards better ecological conditions instead of past reference conditions. The river can self-maintain once it is allowed to flow free of river obstructing structure. For example, a part of the Mareit river in province Bozen-Bolzano, Italy, Figure 6.17 illustrates the benefits of freeing the river's course and preserving the longitudinal connectivity.

Figure 6.17 River restoration along the Mareit River, Italy. 2005 prior restoration (right), and 2010 after restoration (left). Source : (Wohl et al., 2015b).

The river restoration works must consider the catchment scale, not just the reach or part of the river section (Ogston et al., 2015; Wohl et al., 2015b). The process and methods must involve the restoration of longitudinal connectivity with the perspective of sediment delivery and their importance to reintroducing nutrients and grains that sustain the physical habitat for the benefit of the riverine ecosystem (Wilcock, 1997; Kondolf et al., 2006; Lane et al., 2008; Kondolf et al., 2014b). In general, river restoration works have been implemented to achieve specific goals (sediment management, physical habitat, water quality, flood protection), and implemented actions may have a fair amount of uncertainty, considering geographic, climatic diversity (Wohl and Merritts, 2007), though testing river restoration action will lead to improved scientific knowledge (Wheaton et al., 2008).

The lack of sufficient sediment and ecological monitoring data with the spatial-temporal resolution is a primary problem in the present case. Thus, it is preferred to extend the CASCADE driven sediment flux and delivery information to address the final objective of the research thesis that covers the fundamental driver (sediment delivery) of the river's physical habitat and ecological status. Since sediment delivery in terms of transport, entrainment, and deposition at suitable parts of the river environment establish suitable habitat distribution abundance (Wohl et al., 2015a).

Why it is necessary to maintain sediment connectivity for the longest stretch of the river course, and before barrier removal, the upstream and downstream barriers should be considered (network-scale assessment)?

In the previous paragraphs, it is learned that much of the sediment flux transported by the tributary river Lowther. However, a single physically removed Carlton weir was located on the Eamont river (before removal in 2016), Figure 6.18. In addition to that, Eamont rivers' transport flux gets deposited in the Ullswater lake. Thus, the lack of entrained and transported sediments depicted by the weirs situated in the low relief parts of the river, have an insignificant geomorphic footprint. Though, the low trap efficiency of downstream area weirs is an additional cause.

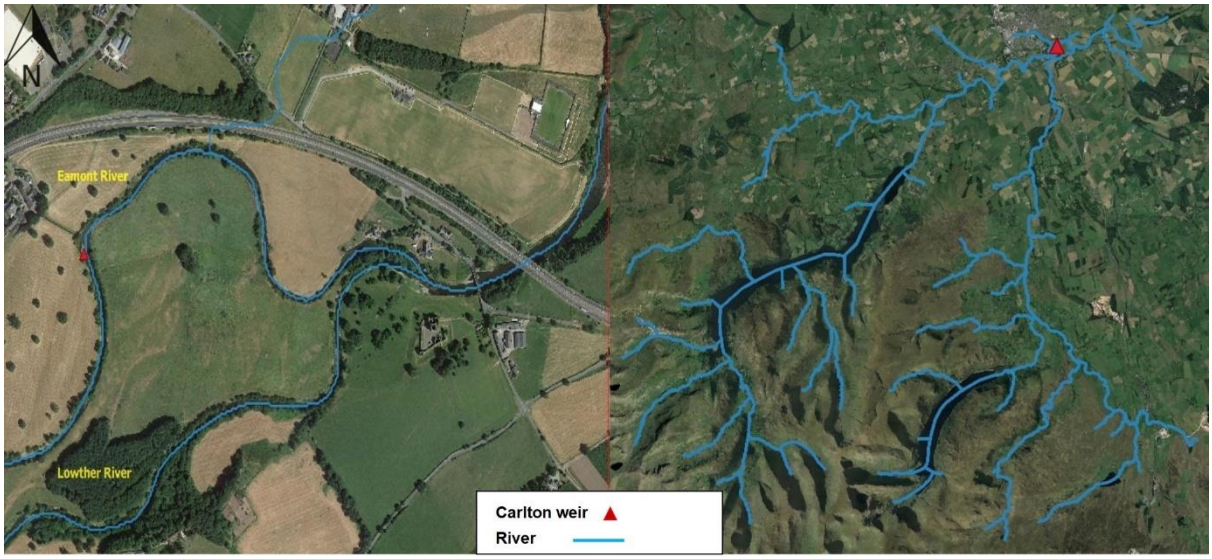

Figure 6.18 Carlton weir was located on river Eamont before the confluence with Lowther River.

In 2016 and previous years, the Carlton weir's backwater effect can be traced on satellite images until immediate upstream weir named Eamont weir (Figure 6.19). The backwater can affect a longer part of a river stretch because of two reasons flat river gradient and barrier height. The riverbed elevation difference between Carlton and Eamont weir is 4m, while the distance between the two weirs is 740m. Thus, it represents a flat riverbed and long backwater imprint.

Figure 6.19 The Carlton weir and an upstream Eamont weir in the year 2009.

However, following the removal of the Carlton weir in mid-2016, a few distinct geomorphic changes have occurred in the river course between the Carlton and Eamont weir sites. A mid-channel bar emerged at the Carlton weir removal site, and it could be attributed to the gravel and boulder accumulation in the immediate upstream stretch of the Carlton weir. However, there are places between the two-weir site where side channel bars have emerged due to lower water depth and relatively fast-moving water current (in the absence of any river obstruction till catchment outlet). Although there is no significant geomorphic change beyond the Eamont weir and upstream river because the river is under consistent flow (low fluctuation) conditions; thus, the same river forms persist, Figure 6.20.

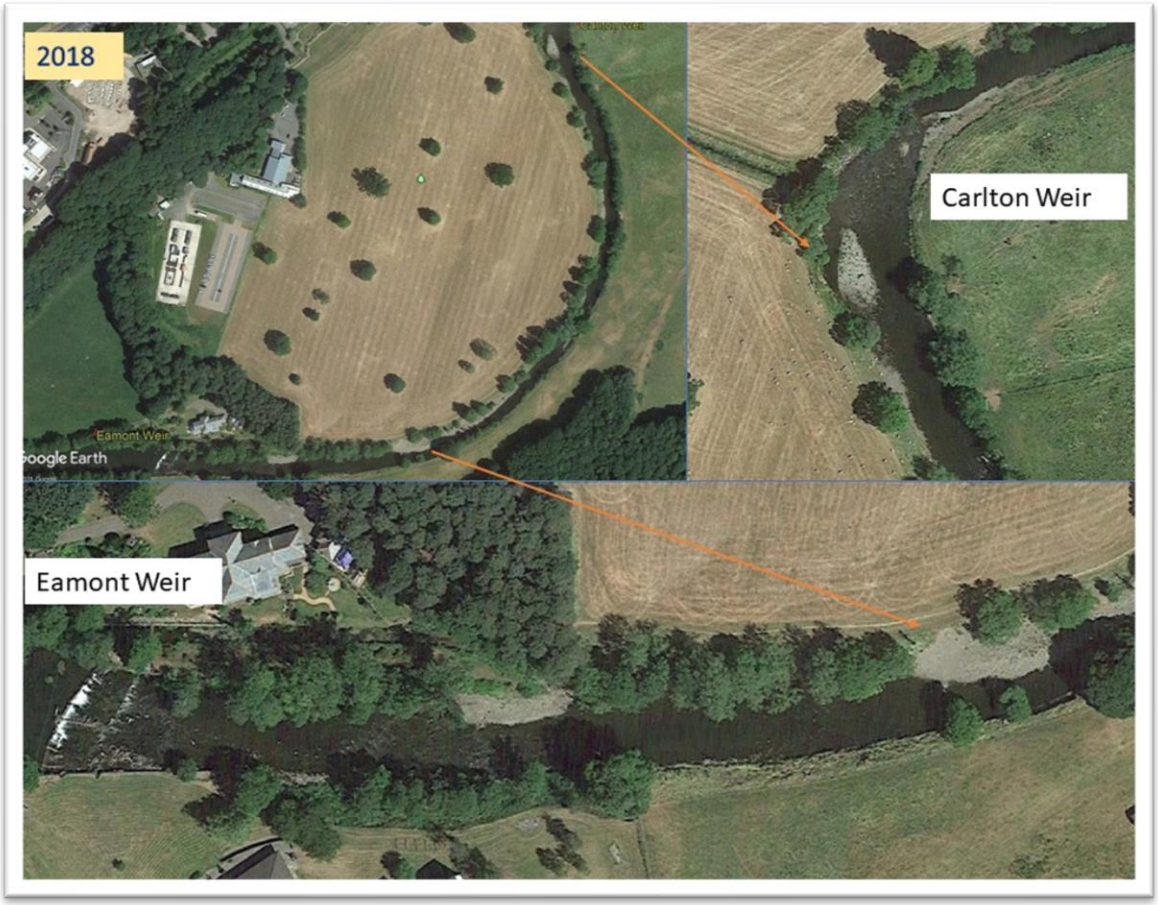

Figure 6.20 Illustrate that the Carlton weir was removed (in 2016), and geomorphic changes were observed in 2018.

The key finding of the image-based analysis illustrates and suggest that future barrier removal work should be executed with the consideration of weir position on the course of the river with respect to other barriers present in the river network. It is crucial because weir or dam demolition work is an economic, political, and social issue. Therefore, the most fragmented rivers in the European region and other parts of the world should execute dam or weir demolition with a goal "How to maximise the river restoration and ecological benefits?". This question will require detailed river hydrogeomorphic history and sediment transport modelling to find a reasonable answer in the different geographies and climatic regions.

Therefore, the Carlton weir removal scenario justification is simulated in the CASCADE model-based solution to find the sediment delivery fluctuation in pre and post removal scenarios. The model has been executed for two different cases,

first representing Carlton pre-removal scenario analysis in CASCADE Figure 6.21, and in second Carlton weir removal scenario analysed Figure 6.22.

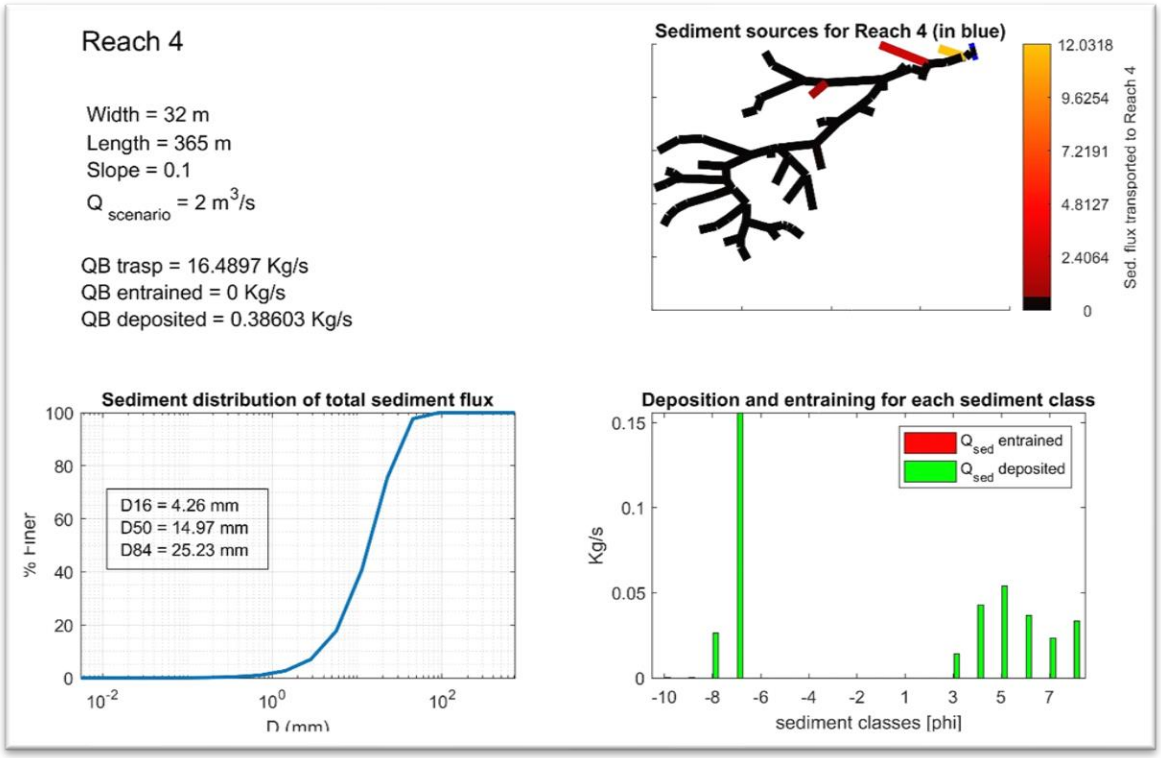

Figure 6.21 CASCADE model execution considering the existence of Carlton weir (pre-removal scenario).

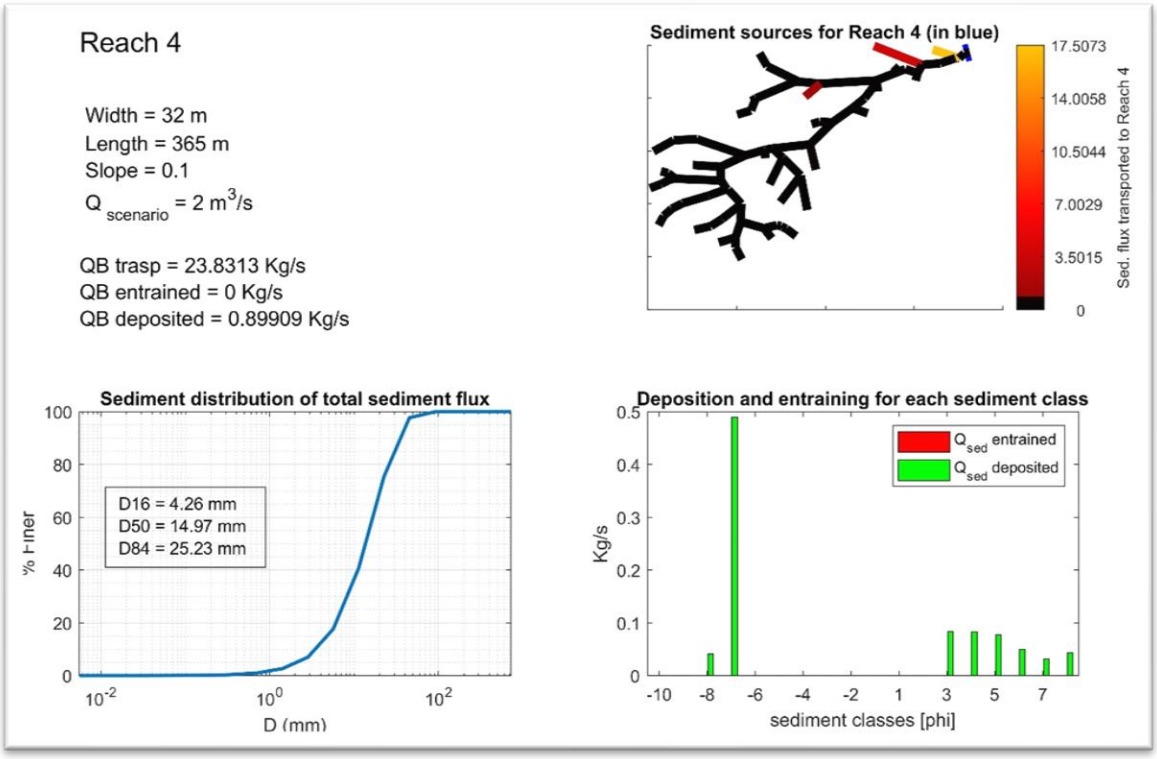

Figure 6.22 CASCADE model execution of Carlton weirs post-removal scenario.

Both Carlton weir pre-removal and removal cases show no major sediment flux transport or deposition changes; however, a significant contribution of sediments supplied by a tributary river 'Dacree Beck' in both scenarios.

The trap efficiency Table 6.1 and weir removal scenario Table 6.4 provide crucial information regarding which weirs would be considered for removal activity. However, the sediment flux at the catchment outlet remains constant under normal discharge conditions unless sediment routing and weir removal are performed under peak discharge. Weirs present at the confluence between Eamont and Lowther rivers obstruct the maximum volume of sediment under peak discharge simulation. The core reason for such an outcome can be attributed to the riverbed's low gradient and high roughness. Thus, the removal of the weirs located at the river confluence zone can be prioritised for the removal activity. Since this is region falls into the flood-prone zone; thus, a hydro-dynamic justification would empower this reasoning.

The sediment routing analysis performed in sections 6.3 and 6.4 is based on sediment grain size range between -5.5 and -1.5 Φ scale. However, the

CASCADE model performs sediment routing for the whole grain size defined at the time of model parametrization, while the model's UI can quantify the range of sediment modeller wants to analyse.

It is recommended that future river restoration or barrier removal cases be thoroughly analysed in sediment connectivity tools for removal case planning, and its execution emphasises freeing up the longest river stretch. Additionally, the impact of upstream and downstream barriers on the river network scale must be given utter importance. However, it is unscientific to discard the coherent research approach between biology and ecology. As our united approach is directed towards preserving the loss of diversity that is receding at an alarming rate, and if it continues to decline at the current rate, humans will get affected in the future too because we are just a part of Earth's ecosystem, and everything is intricately connected.

Summary:

This chapter can be summarised as an attempt to address sediment transport and spatial-temporal dimension within the Eamont river catchment. Though grain size is predominantly coarse grain gravel; thus, much of sediment transport is episodic. It is complicated to refine the temporal dimension in the bedload dominant sediment, however with the sediment connectivity tool, it is possible to infer the river reaches that are responsible for entrainment transport and deposition at the river catchment scale, under different discharge scenarios, representing low, average, and peak flow conditions. The second case represents an analysis of barrier removal prioritisation scenario development at the river network scale, which is impounded by the multiple barriers of various sediment trap efficiency. The CASCADE model was simulated for multiple scenarios to find which barrier is affecting maximum sediment flux moment, and on a priority basis, that barrier should be removed. An integrated approach that analyses biology, the water's ecology and chemistry should be adopted in an ideal case. However, those application requires more comprehensive monitoring, and it takes a longer time frame to find fruitful results. For the final objective, CASCADE is simulated to develop a removal scenario that will improve the physical habitat. A single physical removal in the catchment has provided information to test CASCADE models

efficiency. Through weir removal case, satellite image-based interpretation and cross-validation with the sediment connectivity and delivery tool, and CASCADE model simulation-based results recommend restoring the longer river course. In a nutshell, multiple-barrier impacts should be analysed at the river network scale. Model simulation finding has reaffirmed that any piecemeal river restoration efforts will go in vain unless the approach addresses catchment or network scale issues (Clarke et al., 2003).

The present case study recommends sediment connectivity tools to be implemented as an effective adaptive management planning tool; however, our model could not be calibrated and validated due to the lack of sediment data, though it should not be considered as a bottleneck issue (Czuba et al., 2017; Ancey, 2020b).

In reference to the CASCADE model calibration and validation perspective, it is complicated to perform validation with just an empirical equation. However, the models performance for its efficiency is tested and represented in Table 6.2 & Table 6.3. In low, average discharge conditions model has performed well within the limits of empirical equation estimates. On the other hand, sediment flux value deviation under peak flow conditions could have been validated if the observed data used for the formulation of the empirical equation were accessed for the catchment region.

Apart from the data limitation and its availability, a different approach could be used, which would be based on the single observed parameter that is grain size distribution data (drone derived information). The model calibration can be established with the inverse modelling approach, which is based on the assignment of different grain-size in an iterative fashion in a river network and continue to test model performance until the model performs well within the limits of empirical equation estimates. Similar approaches are reported for CASCADE model calibration. The model is initialized with a single grain assignment for a reach (Schmitt et al., 2016, 2018a), while multiple grain size assignment is used for a reach or sub-cascade (Tangi, 2018) by inverse stochastic characterization of sediment sources.

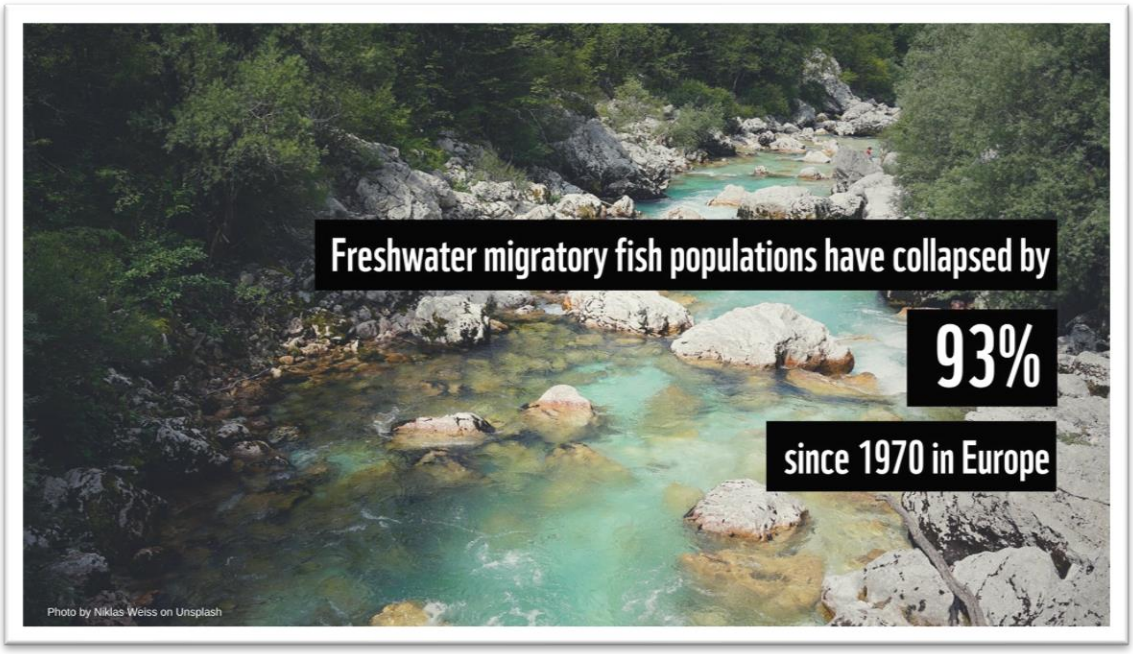

Figure 6.23 93% collapse in migratory freshwater fish populations in Europe - new report (W.W.F., 2021).

Chapter 7: Thesis summary and future perspectives

7.1 Future directions

An integrated current modelling approach is still far from providing the complete picture or answering all the issues regarding the impacts of multiple weirs and dams on river habitats. However, this research has provided some helpful insight for quantifying sediment transport in the river system subjected to intense human pressure.

7.1.1 Better hydrological quantification

As mentioned, the Eamont river catchment's hydrology is heavily impacted by river obstructing structures such as dams and weirs. The quantification of multiple weirs on hydrology should be modelled. However, the large variety of weirs and specific discharge measurement formulas limit relevant impact assessments. Similarly, the discharge of weirs has never been measured; thus, it is complex to establish their influence on the downstream river. Finally, the quality of the small dam's database required for such tasks has often been insufficient. A small dam database, the "AMBER atlas", has accomplished an enormous task to estimate the number of weirs in the European rivers, and it has provided crucial input for the CASCADE model.

The Eamont rivers' water is exploited via inter and intra basin transfer, which includes transferring water between the Ullswater lake, Haweswater Reservoir, Wet Sleddale reservoir to the Manchester city via underground aqueduct. A private company manages the inter-basin transfer scheme, and real-time water transfer data is unavailable in the public domain. If this data is accessible to the modeller, then a proprietary hydrological model would be adequate to access their hydrological footprint on the catchment hydrology. In the present case, the approximate daily water transfer values are used.

7.1.2 Improved GSD data

The current river catchment and most of the U.K. River catchments lack sediment records at the catchment outlet, including suspended and bedload quantification. However, the current study establishes the grain size distribution

information at the river network with a drone and optical granulometry implementation, which uses an indirect method to interpret the similar morphological condition at the river network scale. Thus, the sampled river morphotype's grain size data is assigned to the unknown or unsampled part of the river. The established grain size distribution information at the river network scale is subject to uncertainty. The reason for possible uncertainty in the GSD information is that unsampled river reach, which is assigned with the known sample and continuous data developed with an interpolation method, which is statistical nature. The development of GSD information for the Eamont river catchment (approximately 400Km^2) makes it challenging to map the entire river length with drone sampled images. Thus, it requires advancement in the GSD data development process (Bainbridge et al., 2021; Cabezas-Rabadán et al., 2021), and for that reason, it is crucial to bridge the gap between drone-based and satellite-based grain size assessment and efforts are being made (Marchetti et al., 2021). Thus, in future, we can expect model parametrization with the sampled river reach for its entire river course and anticipate more reliable modelling results.

7.1.3 CASCADE models limitations

The current project thesis tests the multi-model approach that addresses hydrology, river morphology, grain size data development across the river network, and sediment transport modelling. The mentioned modelling approach solves the size-selective sediment transport and grain specific sediment flux in conjunction with river scale connectivity and dis-connectivity of sediment transport pathways. It has provided crucial insight for the main objective of weirs removal strategies by evaluating their impact on sediment transport at the instream river network.

Though, a few things still require to be addressed in the CASCADE model. At present CASCADE model lacks sediment attrition process. Second, the model is one-dimensional; therefore, assessing two-dimensional geomorphic changes is complex. However, its dependence on external discharge input is solved with LISFLOOD (Tangi, 2018) and in the current research with the SWAT model. However, the integration of SWAT and CASCADE has improved a few things, such as the hydro-morphological conditions remains identical across the

modelling environment. It is possible because the SWAT-processed river network is imported into CASCADE; therefore, rivers topological and hydro-morphological attributes are identical. However, a hydraulic solver processes river hydraulics in the CASCADE model.

The objectivity of employing SWAT and CASCADE depends on the modeller's set target. Though, based on the complexity of the SWAT and parsimonious yet informative CASCADE can be summarised in a few peculiar differences in the two models. *First*, the SWAT model simulates the sediment transport for the overland and instream environment, whereas CASCADE produces sediment transport behaviour in an in-stream environment. However, if modellers have information about external sediment input for a river reach; in such case, external sediment input can be modelled in conjunction with sediment transport on the network scale (Tangi et al., 2019a, p. 402). Second, the SWAT model utilized USLE & MUSLE for the sediment yield represented in *metric tons.*

On the other hand, the CASCADE model reports sediment flux in *Kg/sec*. In addition to that, CASCADE offers various sediment transport capacity formulas, 5.2.4. *Third*, the CASCADE model offers more control on reach scale regarding transport limitation parameter (*tr_limit*) that controls the in-stream erosion. The erosion can be equal to transport capacity in the reach (*tr_limit* =1), and no sediment entrainment from the riverbed (*tr_limit* =0). *Third*, the SWAT model simulates discharge, sediment yield, nutrients, bacteria, evapotranspiration, and many other catchment parameters, while CASCADE reports sediment flux and sediment connectivity at the network. *Forth*, CASCADE offers interactive model simulation. However, comparing the two models would be inappropriate since the SWAT model is a complex semi-distributed model that requires enormous data to parameterise it. The CASCADE model is comparatively less complex yet provides crucial information regarding sediment connectivity and sediment flux dynamics.

The critical difference between the SWAT and CASCADE model is subject to sediment routing processing methods. *First,* the SWAT model estimates overland sediment erosion with modified universal soil loss equation (MUSLE) and then in-stream analysed by default Simplified Bagnold model (Bagnold,

1977). However, SWAT also provides four other stream power models (section 4.1.3), though grain size can be processed limited to a range <=2mm to 10mm. *Second*, the SWAT model simulates results for an extended simulation at a continuous time-step beyond the initial model warmup period (>= one year). The continuous-time-step simulation results in sediment yield (tonnes/hectare/year).

Conversely, the CASCADE model is instantaneous, and it simulates sediment flux (Kg/sec). *Third*, the CASCADE model processes the mixed gran size information as a separate cascade per reach and 18-grain size classes can remain active in a processed reach in the network. *Fourth*, the transport capacity distribution competition among the active cascade per reach (18-grain category) improves grain refinement. *Finally*, CASCADE simulates weir removal scenarios more rapidly based on UI's (user interface) ability to perform interactive sediment routing analysis. This UI trait has an advantage over the modelling tool that requires reset conditions for each simulation time step, which could be cumbersome.

In the current CASCADE version, sediment routing in the reservoir is not explicitly performed. In place of that dam or weirs impact on are analysed with dam and weirs sediment trap efficiency, and the method employed in the assessment of trap efficiency of weirs and dams because of lack of sediment records. Though a river is a multi-faceted system (hydrology, geomorphology, ecology, biogeochemistry), and it works on different processing scales: Catchment, Reach, and Sub-Reach scale (Polvi et al., 2020). The CASCADE lacks a methodology to report the ecosystem and habitat losses conditioned by sediment alteration (River network and reach scale data). Future development in this direction and better spatial coverage of sediment alteration data may provide means to assess habitat and biodiversity loss.

In this project, tools such as SWAT, Drone and CASCADE had provided insight for the selection and prioritization of small dam removal scenario development. The modelling had also justified that any piecemeal approach concerning the small dam or weir removal strategy would not yield expected geomorphic and ecological results. Based on modelling results, we have recommended that any

future removal or demolition of small dam, first assess their impact at the river network scale through sediment connectivity tools (in present case CASCADE).

The CASCADE implementation can be justified with single physical removal of a weir case in the catchment and its impact assessment on satellite images along with CASCADE based sediment alteration results. Thus, in the future, with the better grain size assessment exercise through satellite images, the combined use of SWAT to accurately model input hydrology and CASCADE to route sediment fluxes through the river network. Combining two models will provide a practical means to analyse the impact of multiple weirs or dams on sediment transport.

7.1.4 Future integration of ecological models with CASCADE

The process-based ecological models are recommended to manage the river network (Marcinkevage and Herricks, 2005). Since their ability to address spatial-temporal variability for the flow dynamics and ecological setups (physio-chemical conditions) is required for biodiversity at the network scale. However, processing scale in various ecological tools is restricted to reach length; on the contrary, lower scale changes may occur at the meso-habitat. The improvement in scale level in the process-based tools like SWAT that simulate flow conditions and nutrients may provide enhanced results. The CASCADE may produce slightly realistic results when the model's parameterization is based on a river network scale, similar to the monitoring performed at the recommended physical habitat survey.

The present limitations and availability of ecological data can be improved in the future with the assistance of remote sensing, citizen science and eDNA fingerprinting (Fan et al., 2020; Rinaldo et al., 2018). For an extended river network, ecological monitoring is still be preferred at the reach scale (Gansfort and Traunspurger, 2019; Kuemmerlen et al., 2019). The integrated ecological modelling system has proved the implication of the muti-model approach to address the ecological conditions (Johnston et al., 2017). The integrated approach had demonstrated the application of SWAT and models and tools such as Habitat Suitability Index (HSI), Bioaccumulation and Aquatic System

Simulator (BASS), and PiSCES (Piscine Stream Community Estimation System) applications to measure the stress on the fish community.

UK's National Fish Population data (NFPD) caters for a relational database of third-party electrofishing records for UK rivers (Environment Agency, 2021). It would be an excellent opportunity to exploit such a database to answer the ecological conditions of the river in conjunction with sediment routing and hydrological models in an integrated environment. River habitat survey - RHS (Costa and Vieira, 2021) can be applied in future applications along with an integrated modelling environment. It will provide ground-based observation to refine the CASCADE model or model's prediction to access the river conditions with RHS methods. This feedback mechanism can be applied to a limited stretch of the river as RHS methods cover a short distance (10m) with extensive ground observations. However, airborne LiDAR bathymetry and acoustic Doppler profiler (ADCP) can accelerate monitoring in-stream river conditions.

Regarding the EU Biodiversity Strategy for 2030 that aims to support free-flowing rivers, it advises selecting sites and finance to remove obsolete barriers in European rivers. Therefore, researchers may develop a more advanced modelling environment or integrated tool to free up European or other continental rivers in the coming years.

Appendix A : (q-percentile discharge for 166 reaches of Eamont Catchment)

Reach_id	Q1	Q2	Q3	Q4	Q5	Q6	Q7	Q8
1	0.00	0.01	0.01	0.02	0.02	0.05	0.11	0.34
2	0.70	1.53	3.20	6.29	12.99	31.34	88.77	211.80
3	0.00	0.01	0.01	0.02	0.02	0.05	0.15	0.45
4	0.16	0.40	1.86	3.98	8.71	21.60	58.38	135.16
5	0.01	0.01	0.02	0.03	0.06	0.10	0.37	1.21
6	0.71	1.56	3.23	6.34	13.06	31.45	89.01	212.28
7	0.69	1.50	3.17	6.24	12.91	31.25	88.42	211.02
8	0.69	1.51	3.17	6.25	12.93	31.25	88.46	211.10
9	0.16	0.42	1.87	4.00	8.75	21.65	58.51	135.42
10	0.15	0.38	1.83	3.95	8.66	21.50	58.07	134.38
11	0.01	0.01	0.02	0.03	0.04	0.10	0.42	1.10
12	0.16	0.40	1.86	3.98	8.70	21.60	58.38	135.14
13	0.15	0.38	1.83	3.95	8.66	21.50	58.07	134.38
14	0.01	0.01	0.02	0.03	0.04	0.11	0.37	0.98
15	0.15	0.37	1.83	3.93	8.64	21.46	57.96	134.12
16	0.01	0.02	0.03	0.05	0.09	0.22	0.61	1.54
17	0.00	0.01	0.01	0.01	0.02	0.04	0.13	0.50
18	0.00	0.01	0.01	0.02	0.03	0.08	0.28	0.77
19	0.13	0.32	1.76	3.84	8.50	21.17	57.08	132.00
20	0.13	0.32	1.77	3.84	8.51	21.18	57.13	132.14
21	0.14	0.35	1.80	3.88	8.57	21.32	57.52	133.10
22	0.13	0.30	1.75	3.81	8.47	21.09	56.83	131.40
23	0.01	0.01	0.01	0.02	0.03	0.09	0.32	0.90
24	0.04	0.05	0.08	0.13	0.24	0.58	1.62	3.95
25	0.09	0.13	0.21	0.35	0.64	1.54	4.58	11.46
26	0.05	0.08	0.12	0.21	0.39	0.95	2.98	7.53
27	0.09	0.14	0.21	0.36	0.66	1.60	4.76	11.93
28	0.12	0.17	0.27	0.46	0.82	1.99	6.03	15.26
29	0.01	0.02	1.42	3.27	7.55	19.13	51.80	119.28
30	0.01	0.01	0.01	0.02	0.03	0.08	0.31	0.83
31	0.01	0.01	0.02	0.03	0.06	0.15	0.48	1.26
32	0.05	0.08	0.12	0.20	0.37	0.91	2.84	7.18
33	0.00	0.01	1.48	3.21	7.50	19.06	51.54	118.54
34	0.01	0.01	0.02	0.04	0.07	0.17	0.54	1.40
35	0.53	0.82	1.25	2.13	3.90	9.98	33.70	82.98
36	0.76	1.18	1.89	3.43	6.63	17.85	55.43	136.46
37	0.03	0.04	0.07	0.11	0.21	0.50	1.55	3.94
38	0.01	0.01	0.01	0.02	0.04	0.10	0.35	0.96
39	0.01	0.02	0.03	0.05	0.10	0.24	0.71	1.77
40	0.01	0.01	0.02	0.03	0.05	0.12	0.40	1.17
41	0.01	0.02	0.03	0.05	0.09	0.24	0.80	2.15
42	0.74	1.15	1.84	3.36	6.53	17.58	54.55	133.90
43	0.01	0.01	0.02	0.03	0.05	0.13	0.42	1.14
44	0.51	0.78	1.17	2.02	3.72	9.63	32.58	79.95

45	0.01	0.01	0.02	0.04	0.06	0.15	0.54	1.47
46	0.04	0.05	0.08	0.16	0.29	0.79	2.38	6.00
47	0.01	0.01	0.02	0.04	0.07	0.18	0.56	1.55
48	0.04	0.06	0.09	0.16	0.31	0.78	2.70	7.15
49	0.71	1.09	1.75	3.23	6.29	17.05	52.79	128.86
50	0.49	0.74	1.11	1.92	3.57	9.29	31.45	76.97
51	0.67	1.02	1.63	3.03	5.92	16.11	49.52	120.02
52	0.05	0.07	0.11	0.19	0.36	0.90	3.15	8.30
53	0.55	0.83	1.34	2.49	4.89	13.34	40.38	96.99
54	0.43	0.66	0.98	1.71	3.16	8.32	28.22	68.54
55	0.03	0.05	0.07	0.14	0.26	0.69	2.11	5.31
56	0.01	0.01	0.02	0.03	0.07	0.16	0.58	1.58
57	0.03	0.05	0.07	0.11	0.22	0.56	2.00	5.27
58	0.08	0.12	0.18	0.33	0.63	1.58	4.90	12.20
59	0.53	0.80	1.30	2.42	4.76	13.02	39.32	94.16
60	0.02	0.02	0.03	0.06	0.12	0.31	1.11	2.80
61	0.10	0.15	0.23	0.43	0.85	2.40	8.01	19.55
62	0.00	0.00	0.00	0.00	0.00	0.00	0.00	0.00
63	0.01	0.01	0.02	0.04	0.08	0.20	0.70	1.76
64	0.01	0.01	0.02	0.03	0.05	0.14	0.48	1.26
65	0.01	0.02	0.03	0.05	0.10	0.25	0.89	2.28
66	0.02	0.04	0.06	0.11	0.21	0.55	1.77	4.38
67	0.45	0.67	1.09	2.04	4.05	11.30	34.16	80.60
68	0.02	0.04	0.05	0.10	0.19	0.52	1.87	4.73
69	0.42	0.64	0.94	1.65	3.05	8.08	27.37	66.48
70	0.08	0.13	0.19	0.33	0.64	2.09	8.92	22.61
71	0.02	0.02	0.04	0.07	0.14	0.38	1.14	2.77
72	0.03	0.05	0.07	0.11	0.22	0.59	2.19	5.49
73	0.07	0.10	0.16	0.30	0.60	1.69	5.62	13.59
74	0.05	0.06	0.10	0.17	0.33	0.88	3.30	8.24
75	0.01	0.01	0.02	0.04	0.07	0.20	0.78	1.92
76	0.03	0.04	0.05	0.10	0.19	0.51	1.87	4.70
77	0.02	0.03	0.04	0.08	0.15	0.43	1.31	3.16
78	0.04	0.06	0.10	0.18	0.36	1.06	3.17	7.35
79	0.41	0.60	0.99	1.85	3.68	10.39	31.34	73.18
80	0.40	0.59	0.96	1.80	3.58	10.15	30.55	71.15
81	0.04	0.05	0.10	0.18	0.35	1.03	3.09	7.14
82	0.03	0.04	0.06	0.11	0.22	0.64	2.19	5.41
83	0.01	0.02	0.03	0.06	0.13	0.38	1.15	2.62
84	0.08	0.11	0.19	0.35	0.69	1.98	5.98	14.07
85	0.02	0.02	0.04	0.07	0.15	0.46	1.39	3.24
86	0.01	0.02	0.03	0.06	0.12	0.36	1.08	2.51
87	0.32	0.47	0.77	1.45	2.89	8.17	24.65	57.07
88	0.33	0.50	0.73	1.29	2.32	5.76	19.60	46.42
89	0.24	0.34	0.56	1.05	2.09	5.91	17.91	40.78
90	0.04	0.06	0.08	0.15	0.29	1.07	6.36	18.18

91	0.03	0.04	0.06	0.10	0.20	0.82	5.91	17.24
92	0.00	0.00	0.00	0.01	0.01	0.15	5.04	15.71
93	0.08	0.12	0.20	0.37	0.75	2.16	6.51	15.50
94	0.00	0.00	0.00	0.01	0.01	0.14	4.92	15.68
95	0.02	0.03	0.04	0.07	0.14	0.38	1.43	3.39
96	0.21	0.30	0.47	0.89	1.70	4.85	16.12	37.32
97	0.03	0.05	0.07	0.13	0.26	0.74	2.43	5.75
98	0.04	0.05	0.08	0.15	0.28	0.80	2.83	6.79
99	0.07	0.10	0.17	0.32	0.65	1.90	5.65	13.51
100	0.24	0.34	0.56	1.05	2.09	5.91	17.91	40.78
101	0.02	0.02	0.04	0.07	0.13	0.34	1.27	3.01
102	0.18	0.26	0.38	0.67	1.21	2.93	10.04	24.64
103	0.05	0.07	0.12	0.24	0.49	1.45	4.32	9.83
104	0.03	0.05	0.07	0.13	0.28	0.79	2.66	6.39
105	0.02	0.02	0.03	0.06	0.11	0.30	1.11	2.61
106	0.17	0.24	0.36	0.63	1.14	2.74	9.38	22.95
107	0.15	0.23	0.33	0.58	1.05	2.53	8.65	21.18
108	0.01	0.01	0.03	0.04	0.08	0.21	0.69	1.65
109	0.04	0.05	0.10	0.18	0.38	1.12	3.31	7.57
110	0.14	0.21	0.30	0.53	0.96	2.29	7.82	19.08
111	0.01	0.01	0.02	0.04	0.07	0.19	0.63	1.53
112	0.06	0.08	0.14	0.26	0.53	1.53	4.59	10.71
113	0.17	0.24	0.38	0.73	1.46	4.12	12.50	27.99
114	0.15	0.21	0.35	0.67	1.33	3.78	11.41	25.39
115	0.01	0.01	0.02	0.03	0.06	0.15	0.57	1.42
116	0.01	0.01	0.03	0.04	0.08	0.19	0.74	1.85
117	0.14	0.21	0.31	0.56	1.02	2.65	8.75	20.21
118	0.16	0.23	0.37	0.70	1.35	3.88	12.66	28.82
119	0.01	0.02	0.03	0.05	0.11	0.34	1.15	2.68
120	0.11	0.16	0.24	0.43	0.77	1.84	6.38	15.44
121	0.02	0.04	0.06	0.11	0.24	0.71	2.06	5.08
122	0.03	0.04	0.06	0.11	0.22	0.63	1.99	4.42
123	0.03	0.04	0.05	0.09	0.18	0.45	1.40	3.50
124	0.05	0.07	0.11	0.21	0.43	1.27	3.77	8.79
125	0.03	0.04	0.06	0.10	0.21	0.61	1.93	4.28
126	0.06	0.08	0.14	0.26	0.52	1.51	4.67	10.35
127	0.03	0.04	0.07	0.13	0.27	0.78	2.45	5.47
128	0.02	0.03	0.04	0.09	0.17	0.51	1.61	3.55
129	0.11	0.16	0.23	0.41	0.74	1.79	6.12	14.89
130	0.03	0.04	0.06	0.12	0.26	0.79	2.33	5.50
131	0.11	0.15	0.22	0.40	0.71	1.71	5.90	14.23
132	0.12	0.16	0.24	0.44	0.81	2.14	7.11	16.12
133	0.12	0.17	0.27	0.52	1.01	2.92	9.27	20.64
134	0.10	0.13	0.20	0.37	0.66	1.79	5.85	13.22
135	0.01	0.01	0.02	0.03	0.07	0.18	0.65	1.67
136	0.02	0.03	0.04	0.08	0.16	0.47	1.48	3.26

137	0.01	0.01	0.02	0.03	0.07	0.17	0.62	1.60
138	0.09	0.13	0.21	0.40	0.80	2.26	6.75	15.23
139	0.00	0.00	0.00	0.00	0.00	0.00	0.00	0.00
140	0.07	0.10	0.16	0.30	0.58	1.68	5.23	11.49
141	0.01	0.02	0.03	0.05	0.09	0.25	0.90	2.07
142	0.01	0.02	0.03	0.06	0.11	0.32	1.07	2.46
143	0.04	0.06	0.10	0.18	0.36	1.06	3.39	7.61
144	0.09	0.14	0.19	0.36	0.64	1.52	5.25	12.58
145	0.02	0.02	0.03	0.07	0.12	0.34	1.17	2.66
146	0.02	0.03	0.04	0.09	0.18	0.53	1.60	3.47
147	0.01	0.02	0.03	0.06	0.14	0.44	1.39	3.07
148	0.03	0.04	0.06	0.11	0.22	0.67	2.12	4.69
149	0.09	0.13	0.19	0.35	0.63	1.49	5.11	12.21
150	0.03	0.04	0.07	0.14	0.28	0.79	2.38	5.43
151	0.09	0.12	0.17	0.32	0.57	1.38	4.75	11.34
152	0.07	0.10	0.15	0.28	0.50	1.35	4.31	9.73
153	0.05	0.06	0.11	0.21	0.41	1.18	3.52	7.91
154	0.05	0.07	0.11	0.22	0.44	1.29	3.95	8.56
155	0.07	0.09	0.14	0.25	0.46	1.24	3.90	8.79
156	0.03	0.05	0.07	0.15	0.29	0.89	2.65	5.67
157	0.07	0.09	0.13	0.25	0.45	1.10	3.74	8.83
158	0.03	0.04	0.06	0.12	0.25	0.76	2.26	4.82
159	0.07	0.09	0.14	0.25	0.45	1.23	3.85	8.68
160	0.06	0.07	0.11	0.21	0.38	0.96	3.26	7.66
161	0.06	0.08	0.13	0.25	0.44	1.19	3.73	8.39
162	0.04	0.05	0.07	0.14	0.24	0.62	2.11	4.93
163	0.04	0.05	0.07	0.13	0.23	0.59	1.99	4.65
164	0.02	0.03	0.05	0.09	0.19	0.53	1.60	3.54
165	0.04	0.05	0.07	0.14	0.26	0.71	2.20	4.89
166	0.02	0.03	0.05	0.09	0.15	0.41	1.29	2.97

Appendix B: CASCADE model input: "Reach Data" containing River's morphology, hydrology and topological attributes.

ReachData

166x1 struct with 23 fields

Fields	Ge	Bo	X	Y	reach_id	FromN	ToN	Slope	Wac	Q	n	Length	x_FN	x_TN	y_FN	y_TN	el_FN	el_TN	D16	D50	D84	tr_li	Ad
1	.ine'	[3.5...	1x30 double	1x30 double	1	1	6	0.3598	2.5269	0.3427	0.0350	833.7184	3.5508e+05	3.5467e+05	5.3040e+05	5.2976e+05	109	106	0.0017	0.0163	0.0295	1	306.6550
2	.ine'	[3.5...	[3.5464e+0...	[5.2975e+0...	2	2	6	2.9289	45.8500	238.7125	0.0350	34.1421	3.5464e+05	3.5467e+05	5.2975e+05	5.2976e+05	107	106	0.0017	0.0163	0.0295	0	3.8422e+04
3	.ine'	[3.5...	1x30 double	1x30 double	3	3	9	0.8177	2.5069	0.4450	0.0350	733.8047	3.5364e+05	3.5313e+05	5.2970e+05	5.2935e+05	120	114	0.0043	0.0149	0.0252	1	302.6375
4	.ine'	[3.5...	1x34 double	1x34 double	4	4	9	0.1000	32.4099	151.0563	0.0350	365.0610	3.5283e+05	3.5313e+05	5.2921e+05	5.2935e+05	114	114	0.0043	0.0150	0.0252	0	2.1552e+04
5	.ine'	[3.5...	1x28 double	1x28 double	5	5	2	0.1000	4.2467	1.2000	0.0350	689.2641	3.5494e+05	3.5464e+05	5.2919e+05	5.2975e+05	107	107	0.0043	0.0149	0.0252	0	728.5125
6	.ine'	[3.5...	1x424 dou...	1x424 dou...	6	6	6	0.2008	46.4426	239.6750	0.0350	4.9791e+03	3.5467e+05	3.5728e+05	5.2976e+05	5.3031e+05	106	96	0.0024	0.0099	0.0101	0	3.9253e+04
7	.ine'	[3.5...	[3.5370e+0...	[5.2911e+0...	7	7	8	0.1000	45.2560	237.4750	0.0350	12.0711	3.5370e+05	3.5371e+05	5.2911e+05	5.2910e+05	113	113	0.0017	0.0163	0.0295	0	3.7596e+04
8	.ine'	[3.5...	1x152 dou...	1x152 dou...	8	8	2	0.4542	45.3262	237.6250	0.0350	1.3209e+03	3.5371e+05	3.5464e+05	5.2910e+05	5.2975e+05	113	107	0.0038	0.0261	0.0517	0	3.7693e+04
9	.ine'	[3.5...	1x70 double	1x70 double	9	9	7	0.1203	32.7039	151.4563	0.0350	831.3351	3.5313e+05	3.5370e+05	5.2935e+05	5.2911e+05	114	113	0.0033	0.0124	0.0177	0	2.1878e+04
10	.ine'	[3.5...	1x11 double	1x11 double	10	10	12	0.4581	31.9130	150.2450	0.0350	218.2843	3.5233e+05	3.5254e+05	5.2876e+05	5.2875e+05	119	118	0.0033	0.0200	0.0404	0	2.1004e+04
11	.ine'	[3.5...	1x76 double	1x76 double	11	11	12	1.1787	3.4356	0.9488	0.0350	2.3756e+03	3.5104e+05	3.5254e+05	5.2958e+05	5.2875e+05	146	118	0.0033	0.0200	0.0404	1	511.7050
12	.ine'	[3.5...	1x60 double	1x60 double	12	12	4	0.5672	32.4027	151.0525	0.0350	705.2691	3.5254e+05	3.5283e+05	5.2875e+05	5.2921e+05	118	114	0.0020	0.0175	0.0328	0	2.1544e+04
13	.ine'	[3.5...	1x110 dou...	1x110 dou...	13	13	10	0.6687	31.9049	150.2412	0.0350	1.1964e+03	3.5148e+05	3.5233e+05	5.2828e+05	5.2876e+05	127	119	0.0033	0.0264	0.0460	0	2.0995e+04
14	.ine'	[3.4...	1x147 dou...	1x147 dou...	14	14	15	1.0447	3.0157	0.8200	0.0350	3.6375e+03	3.4774e+05	3.5045e+05	5.2993e+05	5.2813e+05	183	145	0.0022	0.0201	0.0555	1	411.7750
15	.ine'	[3.5...	1x133 dou...	1x133 dou...	15	15	13	1.0954	31.7417	149.9688	0.0350	1.6432e+03	3.5045e+05	3.5148e+05	5.2813e+05	5.2828e+05	145	127	0.0034	0.0213	0.0517	0	2.0816e+04
16	.ine'	[3.4...	1x89 double	1x89 double	16	16	24	0.6813	2.8758	1.5250	0.0350	1.6145e+03	3.4129e+05	3.4173e+05	5.2924e+05	5.2800e+05	268	257	0.0037	0.0338	0.1111	1	380.4375
17	.ine'	[3.5...	1x65 double	1x65 double	17	17	5	1.2668	2.5350	0.4813	0.0350	2.2893e+03	3.5633e+05	3.5494e+05	5.2776e+05	5.2919e+05	136	107	0.0043	0.0149	0.0252	1	308.2975
18	.ine'	[3.4...	1x15 double	1x15 double	18	18	19	0.4675	2.2885	0.5913	0.0350	641.7641	3.4883e+05	3.4913e+05	5.2801e+05	5.2749e+05	148	145	0.0034	0.0428	0.0985	1	259.9750
19	.ine'	[3.4...	1x46 double	1x46 double	19	19	20	0.1000	30.5884	147.7850	0.0350	506.6295	3.4913e+05	3.4950e+05	5.2749e+05	5.2773e+05	145	145	0.0032	0.0366	0.0517	0	1.9571e+04
20	.ine'	[3.4...	1x74 double	1x74 double	20	20	21	0.1000	30.6724	147.9400	0.0350	960.0357	3.4950e+05	3.5019e+05	5.2773e+05	5.2735e+05	145	145	0.0032	0.0417	0.0631	0	1.9661e+04
21	.ine'	[3.5...	1x108 dou...	1x108 dou...	21	21	15	0.1000	31.1354	148.9075	0.0350	1.1733e+03	3.5019e+05	3.5045e+05	5.2735e+05	5.2813e+05	145	145	0.0033	0.0315	0.0403	0	2.0158e+04
22	.ine'	[3.4...	1x156 dou...	1x156 dou...	22	22	19	0.1000	30.3132	147.2925	0.0350	1.7410e+03	3.4787e+05	3.4913e+05	5.2667e+05	5.2749e+05	145	145	0.0034	0.0428	0.0985	0	1.9278e+04
23	.ine'	[3.5...	1x28 double	1x28 double	23	23	21	2.1491	2.3369	0.6778	0.0350	791.0229	3.5008e+05	3.5019e+05	5.2664e+05	5.2735e+05	162	145	0.0032	0.0417	0.0631	1	269.2125
24	.ine'	[3.4...	1x288 dou...	1x288 dou...	24	24	25	1.5554	5.0145	3.7375	0.0350	3.5361e+03	3.4173e+05	3.4350e+05	5.2800e+05	5.2655e+05	257	202	0.0030	0.0270	0.0831	0	961.0050
25	.ine'	[3.4...	[3.4350e+0...	[5.2655e+0...	25	25	27	0.1000	8.8402	9.7225	0.0350	14.1421	3.4350e+05	3.4351e+05	5.2655e+05	5.2654e+05	202	202	0.0026	0.0235	0.0693	0	2.4724e+03
26	.ine'	[3.4...	1x24 double	1x24 double	26	26	25	1.7107	6.5797	6.2250	0.0350	292.2792	3.4326e+05	3.4350e+05	5.2652e+05	5.2655e+05	207	202	0.0036	0.0328	0.0784	0	1.5113e+03
27	.ine'	[3.4...	1x152 dou...	1x152 dou...	27	27	28	1.2562	9.1133	10.0625	0.0350	2.1494e+03	3.4351e+05	3.4472e+05	5.2654e+05	5.2635e+05	202	175	0.0022	0.0201	0.0555	0	2.6010e+03
28	.ine'	[3.4	1x349 dou...	1x349 dou...	28	28	22	0.6858	11.1157	12.5212	0.0350	4.3746e+03	3.4472e+05	3.4786e+05	5.2635e+05	5.2667e+05	175	145	0.0037	0.0338	0.1110	0	3.6217e+03

ReachData

166x1 struct with 23 fields

Fields	Ge	Bo	X	Y	reach_id	FromN	ToN	Slope	Wac	Q	n	Length	x_FN	x_TN	y_FN	y_TN	el_FN	el_TN	D16	D50	D84	tr_li	Ad
28	'Line'	[3.4...	1x349 dou...	1x349 dou...	28	28	22	0.6858	11.1157	12.5212	0.0350	4.3746e+03	3.4472e+05	3.4786e+05	5.2635e+05	5.2667e+05	175	145	0.0037	0.0338	0.1110	0	3.6217e+03
29	'Line'	[3.4...	1x57 double	1x57 double	29	29	22	0.1000	26.4454	137.2625	0.0350	786.6295	3.4767e+05	3.4787e+05	5.2598e+05	5.2667e+05	145	145	0.0035	0.0323	0.1047	0	1.5356e+04
30	'Line'	[3.4...	[3.4817e+0...	[5.2606e+0...	30	30	29	0.5665	2.1121	0.6538	0.0350	529.6016	3.4817e+05	3.4767e+05	5.2606e+05	5.2598e+05	148	145	0.0041	0.0235	0.0650	1	227.4525
31	'Line'	[3.4...	1x117 dou...	1x117 dou...	31	31	28	2.7720	2.4916	0.9200	0.0350	1.7316e+03	3.4385e+05	3.4472e+05	5.2512e+05	5.2635e+05	223	175	0.0036	0.0328	0.0784	1	299.5525
32	'Line'	[3.4...	1x311 dou...	1x311 dou...	32	32	26	1.2349	6.3392	5.9613	0.0350	3.5631e+03	3.4109e+05	3.4326e+05	5.2497e+05	5.2652e+05	251	207	0.0036	0.0328	0.0795	0	1.4204e+03
33	'Line'	[3.4...	1x111 dou...	1x111 dou...	33	33	29	0.1652	26.1703	136.7462	0.0350	1.2109e+03	3.4721e+05	3.4767e+05	5.2497e+05	5.2598e+05	147	145	0.0041	0.0236	0.0650	0	1.5090e+04
34	'Line'	[3.4...	1x37 double	1x37 double	34	34	32	0.4886	2.3434	1.1775	0.0350	409.3072	3.4084e+05	3.4109e+05	5.2471e+05	5.2497e+05	253	251	0.0035	0.0329	0.0806	1	270.4600
35	'Line'	[3.5...	1x604 dou...	1x604 dou...	35	35	7	0.7270	26.8176	98.8175	0.0350	7.4279e+03	3.5172e+05	3.5370e+05	5.2410e+05	5.2911e+05	167	113	0.0030	0.0166	0.0300	0	1.5718e+04
36	'Line'	[3.4...	1x127 dou...	1x127 dou...	36	36	33	0.0789	25.9999	117.9588	0.0350	1.2673e+03	3.4653e+05	3.4721e+05	5.2405e+05	5.2497e+05	148	147	0.0046	0.0150	0.0252	0	1.4927e+04
37	'Line'	[3.4...	1x89 double	1x89 double	37	37	32	0.4672	4.2538	3.3663	0.0350	1.2843e+03	3.4082e+05	3.4109e+05	5.2381e+05	5.2497e+05	257	251	0.0035	0.0317	0.0723	0	730.5475
38	'Line'	[3.4...	1x43 double	1x43 double	38	38	36	2.3076	2.0748	0.6713	0.0350	1.0834e+03	3.4739e+05	3.4653e+05	5.2354e+05	5.2405e+05	173	148	0.0041	0.0168	0.0302	1	220.7975
39	'Line'	[3.4...	1x33 double	1x33 double	39	39	37	1.2441	2.5383	1.6275	0.0350	964.5458	3.4003e+05	3.4082e+05	5.2343e+05	5.2381e+05	269	257	0.0020	0.0178	0.0433	1	308.9650
40	'Line'	[3.5...	1x103 dou...	1x103 dou...	40	40	35	4.5491	2.4992	0.8625	0.0350	1.9345e+03	3.5025e+05	3.5172e+05	5.2340e+05	5.2410e+05	255	167	0.0033	0.0200	0.0404	1	301.0750
41	'Line'	[3.4...	1x11 double	1x11 double	41	41	42	0.5391	3.0941	1.5663	0.0350	741.9239	3.4468e+05	3.4540e+05	5.2276e+05	5.2269e+05	152	148	0.0041	0.0178	0.0327	0	429.7725
42	'Line'	[3.4...	1x93 double	1x93 double	42	42	36	0.1000	25.2942	116.1925	0.0350	1.8231e+03	3.4540e+05	3.4653e+05	5.2269e+05	5.2405e+05	148	148	0.0041	0.0169	0.0302	0	1.4258e+04
43	'Line'	[3.4...	1x27 double	1x27 double	43	43	41	1.7929	2.1190	0.8387	0.0350	557.7691	3.4422e+05	3.4468e+05	5.2253e+05	5.2276e+05	162	152	0.0042	0.0188	0.0352	1	228.6775
44	'Line'	[3.5...	1x227 dou...	1x227 dou...	44	44	35	0.4555	25.2431	95.9238	0.0350	3.2933e+03	3.5174e+05	3.5172e+05	5.2143e+05	5.2410e+05	182	167	0.0026	0.0207	0.0424	0	1.4210e+04
45	'Line'	[3.5...	1x33 double	1x33 double	45	45	44	1.1393	2.9324	1.2975	0.0350	1.0533e+03	3.5268e+05	3.5174e+05	5.2139e+05	5.2143e+05	194	182	0.0028	0.0245	0.0417	1	392.9950
46	'Line'	[3.3...	1x58 double	1x58 double	46	46	58	6.8977	3.5935	5.8463	0.0350	1.5078e+03	3.3647e+05	3.3778e+05	5.2101e+05	5.2110e+05	464	360	0.0048	0.0423	0.0732	0	551.4950
47	'Line'	[3.4...	1x105 dou...	1x105 dou...	47	47	48	4.4037	2.3174	0.9675	0.0350	1.2716e+03	3.4887e+05	3.4956e+05	5.2130e+05	5.2061e+05	302	246	0.0037	0.0312	0.0862	1	265.4725
48	'Line'	[3.4...	1x70 double	1x70 double	48	48	52	2.5162	5.1443	4.1622	0.0350	755.1219	3.4956e+05	3.5014e+05	5.2061e+05	5.2087e+05	246	227	0.0037	0.0313	0.0862	0	1.0028e+03
49	'Line'	[3.4...	1x314 dou...	1x314 dou...	49	49	42	0.1000	24.0834	112.7287	0.0350	2.6198e+03	3.4413e+05	3.4540e+05	5.2061e+05	5.2269e+05	148	148	0.0042	0.0188	0.0352	0	1.3139e+04
50	'Line'	[3.5...	1x100 dou...	1x100 dou...	50	50	44	0.1000	24.2025	93.2325	0.0350	1.3038e+03	3.5153e+05	3.5174e+05	5.2026e+05	5.2143e+05	182	182	0.0030	0.0253	0.0650	0	1.3247e+04
51	'Line'	[3.4...	1x215 dou...	1x215 dou...	51	51	49	0.1000	22.7541	106.9650	0.0350	2.3216e+03	3.4203e+05	3.4413e+05	5.2023e+05	5.2061e+05	148	148	0.0042	0.0208	0.0402	0	1.1952e+04
52	'Line'	[3.5...	1x135 dou...	1x135 dou...	52	52	50	2.4577	5.7725	5.1613	0.0350	1.8310e+03	3.5014e+05	3.5153e+05	5.2087e+05	5.2026e+05	227	182	0.0034	0.0299	0.0876	0	1.2151e+03
53	'Line'	[3.4...	1x55 double	1x55 double	53	53	51	0.1000	19.6759	89.6900	0.0350	468.8478	3.4161e+05	3.4203e+05	5.2010e+05	5.2023e+05	148	148	0.0043	0.0228	0.0452	0	9.3808e+03
54	'Line'	[3.5...	1x17 double	1x17 double	54	54	50	0.1000	22.6528	87.7275	0.0350	194.4975	3.5154e+05	3.5153e+05	5.2008e+05	5.2026e+05	182	182	0.0031	0.0268	0.0664	0	1.1864e+04
55	'Line'	[3.3	1x78 double	1x78 double	55	55	46	3.6284	3.2824	5.1938	0.0350	1.7914e+03	3.3533e+05	3.3647e+05	5.1995e+05	5.2101e+05	529	464	0.0051	0.0492	0.0821	1	474.2375

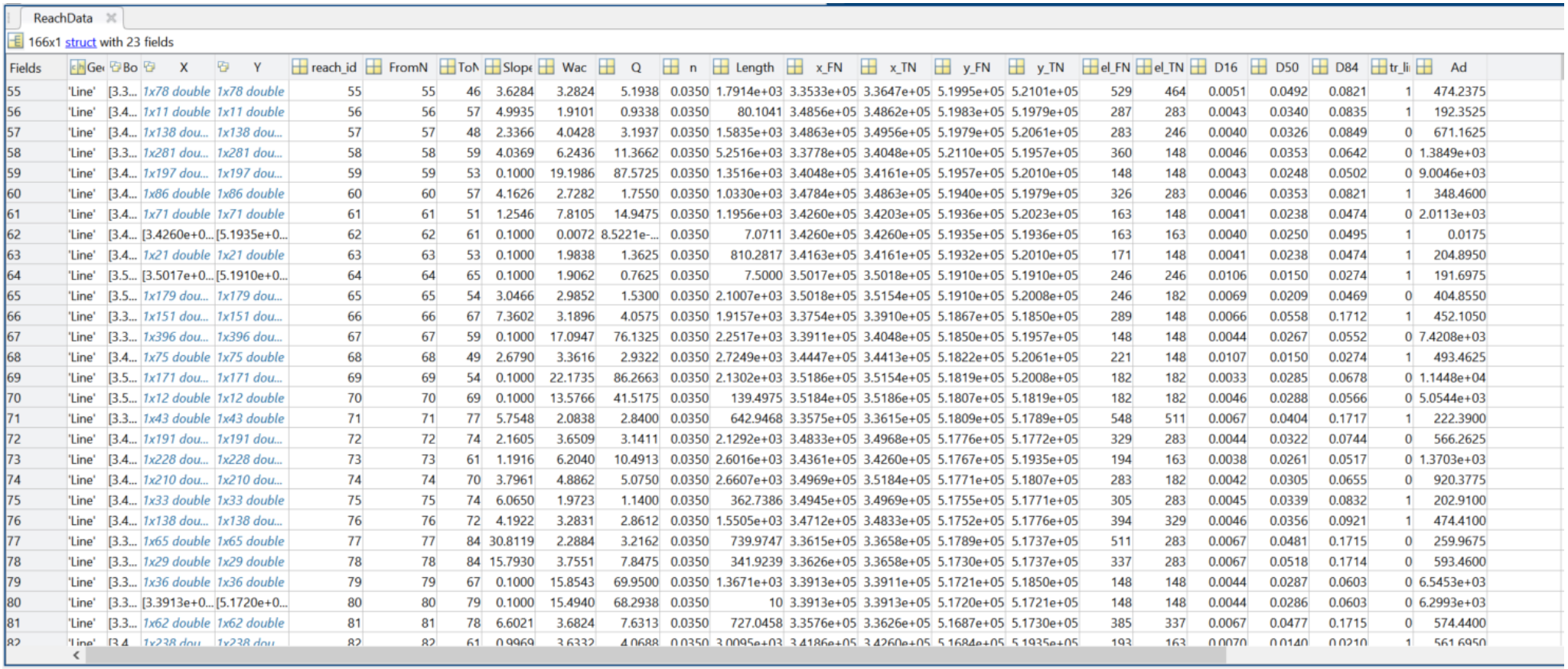

ReachData

166x1 struct with 23 fields

Fields	Ge	Bo	X	Y	reach_id	FromN	ToN	Slope	Wac	Q	n	Length	x_FN	x_TN	y_FN	y_TN	el_FN	el_TN	D16	D50	D84	tr_li	Ad
55	'Line'	[3.3...	1x78 double	1x78 double	55	55	46	3.6284	3.2824	5.1938	0.0350	1.7914e+03	3.3533e+05	3.3647e+05	5.1995e+05	5.2101e+05	529	464	0.0051	0.0492	0.0821	1	474.2375
56	'Line'	[3.4...	1x11 double	1x11 double	56	56	57	4.9935	1.9101	0.9338	0.0350	80.1041	3.4856e+05	3.4862e+05	5.1983e+05	5.1979e+05	287	283	0.0043	0.0340	0.0835	1	192.3525
57	'Line'	[3.4...	1x138 dou...	1x138 dou...	57	57	48	2.3366	4.0428	3.1937	0.0350	1.5835e+03	3.4863e+05	3.4956e+05	5.1979e+05	5.2061e+05	283	246	0.0040	0.0326	0.0849	0	671.1625
58	'Line'	[3.3...	1x281 dou...	1x281 dou...	58	58	59	4.0369	6.2436	11.3662	0.0350	5.2516e+03	3.3778e+05	3.4048e+05	5.2110e+05	5.1957e+05	360	148	0.0046	0.0353	0.0642	0	1.3849e+03
59	'Line'	[3.4...	1x197 dou...	1x197 dou...	59	59	53	0.1000	19.1986	87.5725	0.0350	1.3516e+03	3.4048e+05	3.4161e+05	5.1957e+05	5.2010e+05	148	148	0.0043	0.0248	0.0502	0	9.0046e+03
60	'Line'	[3.4...	1x86 double	1x86 double	60	60	57	4.1626	2.7282	1.7550	0.0350	1.0330e+03	3.4784e+05	3.4863e+05	5.1940e+05	5.1979e+05	326	283	0.0046	0.0353	0.0821	1	348.4600
61	'Line'	[3.4...	1x71 double	1x71 double	61	61	51	1.2546	7.8105	14.9475	0.0350	1.1956e+03	3.4260e+05	3.4203e+05	5.1936e+05	5.2023e+05	163	148	0.0041	0.0238	0.0474	0	2.0113e+03
62	'Line'	[3.4...	[3.4260e+0...	[5.1935e+0...	62	62	61	0.1000	0.0072	8.5221e-...	0.0350	7.0711	3.4260e+05	3.4260e+05	5.1935e+05	5.1936e+05	163	163	0.0040	0.0250	0.0495	1	0.0175
63	'Line'	[3.4...	1x21 double	1x21 double	63	63	53	0.1000	1.9838	1.3625	0.0350	810.2817	3.4163e+05	3.4161e+05	5.1932e+05	5.2010e+05	171	148	0.0041	0.0238	0.0474	1	204.8950
64	'Line'	[3.5...	[3.5017e+0...	[5.1910e+0...	64	64	65	0.1000	1.9062	0.7625	0.0350	7.5000	3.5017e+05	3.5018e+05	5.1910e+05	5.1910e+05	246	246	0.0106	0.0150	0.0274	1	191.6975
65	'Line'	[3.5...	1x179 dou...	1x179 dou...	65	65	54	3.0466	2.9852	1.5300	0.0350	2.1007e+03	3.5018e+05	3.5154e+05	5.1910e+05	5.2008e+05	246	182	0.0069	0.0209	0.0469	0	404.8550
66	'Line'	[3.3...	1x151 dou...	1x151 dou...	66	66	67	7.3602	3.1896	4.0575	0.0350	1.9157e+03	3.3754e+05	3.3910e+05	5.1867e+05	5.1850e+05	289	148	0.0066	0.0558	0.1712	1	452.1050
67	'Line'	[3.3...	1x396 dou...	1x396 dou...	67	67	59	0.1000	17.0947	76.1325	0.0350	2.2517e+03	3.3911e+05	3.4048e+05	5.1850e+05	5.1957e+05	148	148	0.0044	0.0267	0.0552	0	7.4208e+03
68	'Line'	[3.4...	1x75 double	1x75 double	68	68	49	2.6790	3.3616	2.9322	0.0350	2.7249e+03	3.4447e+05	3.4413e+05	5.1822e+05	5.2061e+05	221	148	0.0107	0.0150	0.0274	1	493.4625
69	'Line'	[3.5...	1x171 dou...	1x171 dou...	69	69	54	0.1000	22.1735	86.2663	0.0350	2.1302e+03	3.5186e+05	3.5154e+05	5.1819e+05	5.2008e+05	182	182	0.0033	0.0285	0.0678	0	1.1448e+04
70	'Line'	[3.5...	1x12 double	1x12 double	70	70	69	0.1000	13.5766	41.5175	0.0350	139.4975	3.5184e+05	3.5186e+05	5.1807e+05	5.1819e+05	182	182	0.0046	0.0288	0.0566	0	5.0544e+03
71	'Line'	[3.3...	1x43 double	1x43 double	71	71	77	5.7548	2.0838	2.8400	0.0350	642.9468	3.3575e+05	3.3615e+05	5.1809e+05	5.1789e+05	548	511	0.0067	0.0404	0.1717	1	222.3900
72	'Line'	[3.4...	1x191 dou...	1x191 dou...	72	72	74	2.1605	3.6509	3.1411	0.0350	2.1292e+03	3.4833e+05	3.4968e+05	5.1776e+05	5.1772e+05	329	283	0.0044	0.0322	0.0744	0	566.2625
73	'Line'	[3.4...	1x228 dou...	1x228 dou...	73	73	61	1.1916	6.2040	10.4913	0.0350	2.6016e+03	3.4361e+05	3.4260e+05	5.1767e+05	5.1935e+05	194	163	0.0038	0.0261	0.0517	0	1.3703e+03
74	'Line'	[3.4...	1x210 dou...	1x210 dou...	74	74	70	3.7961	4.8862	5.0750	0.0350	2.6607e+03	3.4969e+05	3.5184e+05	5.1771e+05	5.1807e+05	283	182	0.0042	0.0305	0.0655	0	920.3775
75	'Line'	[3.4...	1x33 double	1x33 double	75	75	74	6.0650	1.9723	1.1400	0.0350	362.7386	3.4945e+05	3.4969e+05	5.1755e+05	5.1771e+05	305	283	0.0045	0.0339	0.0832	1	202.9100
76	'Line'	[3.4...	1x138 dou...	1x138 dou...	76	76	72	4.1922	3.2831	2.8612	0.0350	1.5505e+03	3.4712e+05	3.4833e+05	5.1752e+05	5.1776e+05	394	329	0.0046	0.0356	0.0921	1	474.4100
77	'Line'	[3.3...	1x65 double	1x65 double	77	77	84	30.8119	2.2884	3.2162	0.0350	739.9747	3.3615e+05	3.3658e+05	5.1789e+05	5.1737e+05	511	283	0.0067	0.0481	0.1715	0	259.9675
78	'Line'	[3.3...	1x29 double	1x29 double	78	78	84	15.7930	3.7551	7.8475	0.0350	341.9239	3.3626e+05	3.3658e+05	5.1730e+05	5.1737e+05	337	283	0.0067	0.0518	0.1714	0	593.4600
79	'Line'	[3.3...	1x36 double	1x36 double	79	79	67	0.1000	15.8543	69.9500	0.0350	1.3671e+03	3.3913e+05	3.3911e+05	5.1721e+05	5.1850e+05	148	148	0.0044	0.0287	0.0603	0	6.5453e+03
80	'Line'	[3.3...	[3.3913e+0...	[5.1720e+0...	80	80	79	0.1000	15.4940	68.2938	0.0350	10	3.3913e+05	3.3913e+05	5.1720e+05	5.1721e+05	148	148	0.0044	0.0286	0.0603	0	6.2993e+03
81	'Line'	[3.3...	1x62 double	1x62 double	81	81	78	6.6021	3.6824	7.6313	0.0350	727.0458	3.3576e+05	3.3626e+05	5.1687e+05	5.1730e+05	385	337	0.0067	0.0477	0.1715	0	574.4400
82	'Line'	[3.4	1x238 dou...	1x238 dou...	82	82	61	0.9969	3.6332	4.0688	0.0350	3.0095e+03	3.4186e+05	3.4260e+05	5.1684e+05	5.1935e+05	193	163	0.0070	0.0140	0.0210	1	561.6950

ReachData

166x1 struct with 23 fields

Fields	Ge	Bo	X	Y	reach_id	FromN	ToN	Slope	Wac	Q	n	Length	x_FN	x_TN	y_FN	y_TN	el_FN	el_TN	D16	D50	D84	tr_li	Ad
82	'Line'	[3.4...	1x238 dou...	1x238 dou...	82	82	61	0.9969	3.6332	4.0688	0.0350	3.0095e+03	3.4186e+05	3.4260e+05	5.1684e+05	5.1935e+05	193	163	0.0070	0.0140	0.0210	1	561.6950
83	'Line'	[3.3...	[3.3575e+0...	[5.1681e+0...	83	83	81	7.6006	1.9292	2.7750	0.0350	65.7843	3.3575e+05	3.3576e+05	5.1681e+05	5.1687e+05	390	385	0.0068	0.0449	0.0559	1	195.5825
84	'Line'	[3.3...	1x308 dou...	1x308 dou...	84	84	80	4.1822	5.7727	14.4750	0.0350	3.2279e+03	3.3658e+05	3.3913e+05	5.1737e+05	5.1720e+05	283	148	0.0066	0.0558	0.1712	0	1.2152e+03
85	'Line'	[3.3...	1x90 double	1x90 double	85	85	81	11.9884	2.2975	3.5263	0.0350	809.1169	3.3514e+05	3.3576e+05	5.1647e+05	5.1687e+05	482	385	0.0068	0.0517	0.0657	0	261.6750
86	'Line'	[3.3...	[3.3513e+0...	[5.1647e+0...	86	86	85	0.1000	1.9555	2.7463	0.0350	10.6066	3.3513e+05	3.3514e+05	5.1647e+05	5.1647e+05	482	482	0.0107	0.0740	0.0900	1	200.0425
87	'Line'	[3.3...	1x123 dou...	1x123 dou...	87	87	80	0.1000	13.6239	54.4500	0.0350	1.1421e+03	3.3945e+05	3.3913e+05	5.1638e+05	5.1720e+05	148	148	0.0045	0.0307	0.0652	0	5.0838e+03
88	'Line'	[3.5...	1x241 dou...	1x241 dou...	88	88	69	0.3038	15.3278	44.2613	0.0350	2.9626e+03	3.5352e+05	3.5186e+05	5.1638e+05	5.1819e+05	191	182	0.0034	0.0301	0.0692	0	6.1870e+03
89	'Line'	[3.3...	1x24 double	1x24 double	89	89	87	0.1000	11.2431	38.7425	0.0350	150	3.3954e+05	3.3945e+05	5.1633e+05	5.1638e+05	148	148	0.0045	0.0326	0.0702	0	3.6911e+03
90	'Line'	[3.5...	1x235 dou...	1x235 dou...	90	90	70	0.2283	12.0319	36.4525	0.0350	2.6276e+03	3.5159e+05	3.5184e+05	5.1618e+05	5.1807e+05	188	182	0.0053	0.0274	0.0538	0	4.1328e+03
91	'Line'	[3.5...	1x83 double	1x83 double	91	91	90	2.4605	11.4036	34.9587	0.0350	934.7666	3.5077e+05	3.5159e+05	5.1594e+05	5.1618e+05	211	188	0.0059	0.0259	0.0511	0	3.7794e+03
92	'Line'	[3.5...	1x15 double	1x15 double	92	92	91	1.0264	10.4784	31.7162	0.0350	97.4264	3.5068e+05	3.5077e+05	5.1591e+05	5.1594e+05	211	210	0.0066	0.0245	0.0483	0	3.2823e+03
93	'Line'	[3.3...	1x188 dou...	1x188 dou...	93	93	87	2.5634	6.0172	15.2488	0.0350	1.4434e+03	3.3845e+05	3.3945e+05	5.1578e+05	5.1638e+05	185	148	0.0029	0.0211	0.0394	0	1.3022e+03
94	'Line'	[3.5...	1x32 double	1x32 double	94	94	92	1.3481	10.4607	31.6688	0.0350	445.0610	3.5031e+05	3.5068e+05	5.1577e+05	5.1591e+05	216	210	0.0073	0.0230	0.0456	0	3.2730e+03
95	'Line'	[3.5...	1x48 double	1x48 double	95	95	91	3.2338	2.7275	2.4322	0.0350	989.5584	3.5098e+05	3.5077e+05	5.1523e+05	5.1594e+05	243	211	0.0055	0.0291	0.0648	0	348.2975
96	'Line'	[3.4...	1x204 dou...	1x204 dou...	96	96	94	0.1000	10.3890	28.8012	0.0350	1.6089e+03	3.4896e+05	3.5031e+05	5.1514e+05	5.1577e+05	236	216	0.0079	0.0216	0.0428	0	3.2357e+03
97	'Line'	[3.4...	1x276 dou...	1x276 dou...	97	97	73	1.2856	3.5166	4.5563	0.0350	3.6560e+03	3.4246e+05	3.4361e+05	5.1515e+05	5.1767e+05	241	194	0.0037	0.0267	0.0528	1	531.9750
98	'Line'	[3.4...	1x317 dou...	1x317 dou...	98	98	96	7.6690	3.7447	4.4637	0.0350	4.0944e+03	3.4602e+05	3.4895e+05	5.1512e+05	5.1514e+05	550	236	0.0028	0.0217	0.0563	1	590.7100
99	'Line'	[3.3...	1x171 dou...	1x171 dou...	99	99	93	1.2076	5.4713	13.4625	0.0350	1.9874e+03	3.3696e+05	3.3845e+05	5.1505e+05	5.1578e+05	209	185	0.0031	0.0225	0.0434	0	1.1113e+03
100	'Line'	[3.3...	1x256 dou...	1x256 dou...	100	100	89	0.1213	11.2411	38.7387	0.0350	2.4742e+03	3.4027e+05	3.3954e+05	5.1498e+05	5.1633e+05	151	148	0.0046	0.0346	0.0752	0	3.6901e+03
101	'Line'	[3.5...	1x40 double	1x40 double	101	101	95	8.0838	2.5048	2.2638	0.0350	519.5584	3.5080e+05	3.5098e+05	5.1479e+05	5.1523e+05	285	243	0.0050	0.0324	0.0784	0	302.2175
102	'Line'	[3.5...	1x296 dou...	1x296 dou...	102	102	88	1.1282	10.8771	24.3063	0.0350	3.1910e+03	3.5480e+05	3.5352e+05	5.1453e+05	5.1638e+05	227	191	0.0044	0.0462	0.1206	0	3.4930e+03
103	'Line'	[3.3...	1x84 double	1x84 double	103	103	99	0.9243	4.5962	10.4463	0.0350	865.5382	3.3635e+05	3.3696e+05	5.1452e+05	5.1505e+05	217	209	0.0033	0.0239	0.0474	0	831.1625
104	'Line'	[3.4...	1x342 dou...	1x342 dou...	104	104	73	2.1955	3.9462	4.9163	0.0350	4.0537e+03	3.4399e+05	3.4361e+05	5.1441e+05	5.1767e+05	283	194	0.0036	0.0272	0.0539	1	644.6375
105	'Line'	[3.5...	1x54 double	1x54 double	105	105	101	5.9388	2.2584	1.9575	0.0350	690.3732	3.5042e+05	3.5080e+05	5.1434e+05	5.1479e+05	326	285	0.0046	0.0356	0.0921	1	254.3000
106	'Line'	[3.5...	1x48 double	1x48 double	106	106	102	1.1344	10.2980	22.7150	0.0350	440.7716	3.5513e+05	3.5480e+05	5.1430e+05	5.1453e+05	232	227	0.0043	0.0447	0.1143	0	3.1886e+03
107	'Line'	[3.5...	1x32 double	1x32 double	107	107	106	0.1821	9.8013	21.0387	0.0350	549.0559	3.5557e+05	3.5513e+05	5.1415e+05	5.1430e+05	233	232	0.0042	0.0432	0.1081	0	2.9364e+03
108	'Line'	[3.5...	1x60 double	1x60 double	108	108	106	4.2098	2.1387	1.5575	0.0350	665.1219	3.5476e+05	3.5512e+05	5.1391e+05	5.1430e+05	260	232	0.0054	0.0495	0.1396	0	232.2375
109	'Line'	[3.3	1x84 double	1x84 double	109	109	103	8.4985	3.8986	8.1238	0.0350	906.0408	3.3591e+05	3.3635e+05	5.1384e+05	5.1452e+05	294	217	0.0035	0.0253	0.0514	0	631.7250

ReachData

166x1 struct with 23 fields

Fields	Ge	Bo	X	Y	reach_id	FromN	ToN	Slope	Wac	Q	n	Length	x_FN	x_TN	y_FN	y_TN	el_FN	el_TN	D16	D50	D84	tr_li	Ad
109	'Line'	[3.3...	1x84 double	1x84 double	109	109	103	8.4985	3.8986	8.1238	0.0350	906.0408	3.3591e+05	3.3635e+05	5.1384e+05	5.1452e+05	294	217	0.0035	0.0253	0.0514	0	631.7250
110	'Line'	[3.5...	1x46 double	1x46 double	110	110	107	0.1834	9.1598	18.9788	0.0350	545.2691	3.5581e+05	3.5557e+05	5.1377e+05	5.1415e+05	234	233	0.0041	0.0416	0.1018	0	2.6232e+03
111	'Line'	[3.5...	1x46 double	1x46 double	111	111	108	3.5468	2.0307	1.4462	0.0350	592.0889	3.5438e+05	3.5476e+05	5.1360e+05	5.1391e+05	281	260	0.0066	0.0558	0.1712	1	213.0300
112	'Line'	[3.3...	1x176 dou...	1x176 dou...	112	112	100	2.5814	4.7911	10.3413	0.0350	2.0531e+03	3.3920e+05	3.4027e+05	5.1357e+05	5.1498e+05	204	151	0.0046	0.0353	0.0821	0	890.7150
113	'Line'	[3.4...	1x132 dou...	1x132 dou...	113	113	100	0.4163	9.0154	26.6538	0.0350	1.9218e+03	3.4024e+05	3.4027e+05	5.1332e+05	5.1498e+05	159	151	0.0041	0.0296	0.0616	0	2.5546e+03
114	'Line'	[3.4...	[3.4024e+0...	[5.1331e+0...	114	114	113	0.1000	8.4430	24.3513	0.0350	10	3.4024e+05	3.4024e+05	5.1331e+05	5.1332e+05	159	159	0.0036	0.0246	0.0479	0	2.2901e+03
115	'Line'	[3.5...	[3.5504e+0...	[5.1331e+0...	115	115	116	0.1000	1.9047	1.3700	0.0350	7.5000	3.5504e+05	3.5505e+05	5.1331e+05	5.1331e+05	251	251	0.0200	0.0225	0.0284	1	191.4550
116	'Line'	[3.5...	1x106 dou...	1x106 dou...	116	116	107	1.4177	2.3058	1.7033	0.0350	1.2697e+03	3.5505e+05	3.5557e+05	5.1331e+05	5.1415e+05	251	233	0.0046	0.0288	0.0566	0	263.2600
117	'Line'	[3.5...	1x447 dou...	1x447 dou...	117	117	88	1.2033	8.2948	18.2850	0.0350	5.8171e+03	3.5156e+05	3.5352e+05	5.1325e+05	5.1638e+05	261	191	0.0034	0.0335	0.0479	0	2.2234e+03
118	'Line'	[3.4...	1x242 dou...	1x242 dou...	118	118	96	0.1000	8.7478	23.1637	0.0350	2.5984e+03	3.4764e+05	3.4896e+05	5.1318e+05	5.1514e+05	236	236	0.0085	0.0201	0.0400	0	2.4295e+03
119	'Line'	[3.4...	[3.4719e+0...	[5.1317e+0...	119	119	118	0.1000	2.0664	1.9050	0.0350	456.6421	3.4719e+05	3.4764e+05	5.1317e+05	5.1318e+05	236	236	0.0046	0.0356	0.0921	1	219.2950
120	'Line'	[3.5...	1x90 double	1x90 double	120	120	110	0.3885	7.5440	15.2450	0.0350	1.0296e+03	3.5598e+05	3.5582e+05	5.1306e+05	5.1377e+05	238	234	0.0025	0.0213	0.0308	0	1.8982e+03
121	'Line'	[3.3...	1x78 double	1x78 double	121	121	109	7.1416	2.9613	5.1700	0.0350	1.0782e+03	3.3562e+05	3.3591e+05	5.1297e+05	5.1384e+05	371	294	0.0037	0.0267	0.0554	1	399.4650
122	'Line'	[3.4...	1x25 double	1x25 double	122	122	127	23.6389	2.9938	4.1075	0.0350	262.2792	3.4249e+05	3.4227e+05	5.1289e+05	5.1298e+05	363	301	0.0049	0.0395	0.1239	0	406.8000
123	'Line'	[3.5...	1x394 dou...	1x394 dou...	123	123	110	1.5888	4.1342	3.8150	0.0350	4.6575e+03	3.5850e+05	3.5582e+05	5.1310e+05	5.1377e+05	308	234	0.0040	0.0401	0.0955	1	696.6375
124	'Line'	[3.3...	1x97 double	1x97 double	124	124	112	3.9880	4.1541	8.5675	0.0350	1.1033e+03	3.3855e+05	3.3920e+05	5.1288e+05	5.1357e+05	248	204	0.0041	0.0316	0.1027	0	702.2150
125	'Line'	[3.4...	1x14 double	1x14 double	125	125	122	17.4658	2.9414	3.9812	0.0350	143.1371	3.4259e+05	3.4249e+05	5.1280e+05	5.1289e+05	388	363	0.0055	0.0450	0.1397	0	395.0125
126	'Line'	[3.4...	1x151 dou...	1x151 dou...	126	126	114	2.4271	5.0273	9.8250	0.0350	1.6480e+03	3.4155e+05	3.4024e+05	5.1269e+05	5.1331e+05	199	159	0.0038	0.0287	0.0924	0	965.1150
127	'Line'	[3.4...	1x81 double	1x81 double	127	127	126	10.4917	3.4204	5.0738	0.0350	972.1930	3.4227e+05	3.4155e+05	5.1298e+05	5.1269e+05	301	199	0.0044	0.0341	0.1081	0	507.9425
128	'Line'	[3.4...	1x23 double	1x23 double	128	128	125	10.5806	2.6650	3.3562	0.0350	292.9899	3.4280e+05	3.4259e+05	5.1264e+05	5.1280e+05	419	388	0.0060	0.0504	0.1554	0	335.0975
129	'Line'	[3.5...	1x39 double	1x39 double	129	129	120	1.1327	7.2890	14.6425	0.0350	529.7056	3.5600e+05	3.5598e+05	5.1258e+05	5.1306e+05	244	238	0.0030	0.0269	0.0337	0	1.7925e+03
130	'Line'	[3.3...	1x117 dou...	1x117 dou...	130	130	124	3.6392	3.0275	5.2938	0.0350	1.2915e+03	3.3763e+05	3.3855e+05	5.1252e+05	5.1288e+05	295	248	0.0035	0.0278	0.1232	1	414.4600
131	'Line'	[3.5...	1x23 double	1x23 double	131	131	129	2.1181	6.9964	13.9425	0.0350	236.0660	3.5604e+05	3.5600e+05	5.1238e+05	5.1258e+05	249	244	0.0035	0.0268	0.0355	0	1.6742e+03
132	'Line'	[3.5...	1x103 dou...	1x103 dou...	132	132	117	0.4636	6.6044	14.5375	0.0350	1.2941e+03	3.5076e+05	3.5156e+05	5.1234e+05	5.1325e+05	267	261	0.0035	0.0313	0.0373	0	1.5208e+03
133	'Line'	[3.4...	1x74 double	1x74 double	133	133	118	0.1000	6.9640	17.6538	0.0350	1.2653e+03	3.4741e+05	3.4764e+05	5.1201e+05	5.1318e+05	236	236	0.0093	0.0187	0.0373	0	1.6613e+03
134	'Line'	[3.5...	1x56 double	1x56 double	134	134	132	0.4601	5.7309	11.7750	0.0350	651.9848	3.5042e+05	3.5076e+05	5.1197e+05	5.1234e+05	270	267	0.0035	0.0288	0.0333	0	1.2006e+03
135	'Line'	[3.5...	1x53 double	1x53 double	135	135	131	0.4174	2.3491	1.6288	0.0350	479.2031	3.5614e+05	3.5604e+05	5.1196e+05	5.1238e+05	251	249	0.0041	0.0312	0.0337	0	271.5500
136	'Line'	[3.4	1x77 double	1x77 double	136	136	128	0.5354	2.5483	3.1013	0.0350	933.9266	3.4335e+05	3.4280e+05	5.1195e+05	5.1264e+05	424	419	0.0035	0.0278	0.1232	1	311.0150

ReachData

166x1 struct with 23 fields

Fields	Ge	Bo	X	Y	reach_id	FromN	ToN	Slope	Wac	Q	n	Length	x_FN	x_TN	y_FN	y_TN	el_FN	el_TN	D16	D50	D84	tr_li	Ad
140	'Line'	[3.4...	1x67 double	1x67 double	140	140	133	0.1000	4.8684	10.3487	0.0350	440.7716	3.4776e+05	3.4741e+05	5.1181e+05	5.1201e+05	236	236	0.0099	0.0172	0.0345	0	914.7975
141	'Line'	[3.5...	1x28 double	1x28 double	141	141	134	1.4314	1.9634	1.8013	0.0350	279.4544	3.5022e+05	3.5042e+05	5.1181e+05	5.1197e+05	274	270	0.0240	0.0275	0.0370	1	201.3800
142	'Line'	[3.4...	1x13 double	1x13 double	142	142	143	6.0721	1.9087	1.8737	0.0350	115.2817	3.4686e+05	3.4693e+05	5.1186e+05	5.1178e+05	243	236	0.0060	0.0202	0.0468	1	192.1300
143	'Line'	[3.4...	1x69 double	1x69 double	143	143	133	0.1000	3.7753	6.2163	0.0350	582.3402	3.4692e+05	3.4741e+05	5.1177e+05	5.1201e+05	236	236	0.0076	0.0190	0.0428	0	598.7900
144	'Line'	[3.5...	1x93 double	1x93 double	144	144	131	0.6445	6.2762	12.2825	0.0350	1.0860e+03	3.5536e+05	3.5604e+05	5.1176e+05	5.1238e+05	256	249	0.0041	0.0322	0.0373	0	1.3969e+03
145	'Line'	[3.4...	1x48 double	1x48 double	145	145	140	17.2191	2.0985	2.2900	0.0350	406.5254	3.4811e+05	3.4776e+05	5.1176e+05	5.1181e+05	306	236	0.0099	0.0172	0.0345	1	225.0100
146	'Line'	[3.4...	1x103 dou...	1x103 dou...	146	146	126	5.5482	2.6048	3.4200	0.0350	1.1896e+03	3.4199e+05	3.4155e+05	5.1174e+05	5.1269e+05	265	199	0.0035	0.0278	0.1232	1	322.5825
147	'Line'	[3.4...	1x11 double	1x11 double	147	147	148	2.8038	2.1092	2.6375	0.0350	106.9975	3.4555e+05	3.4562e+05	5.1178e+05	5.1173e+05	307	304	0.0028	0.0217	0.0563	1	226.9325
148	'Line'	[3.4...	1x148 dou...	1x148 dou...	148	148	143	4.2041	2.7942	3.9913	0.0350	1.6175e+03	3.4562e+05	3.4692e+05	5.1173e+05	5.1177e+05	304	236	0.0044	0.0209	0.0515	0	362.6150
149	'Line'	[3.5...	1x14 double	1x14 double	149	149	144	1.8726	6.1143	11.9163	0.0350	160.2082	3.5528e+05	3.5536e+05	5.1164e+05	5.1176e+05	259	256	0.0042	0.0323	0.0647	0	1.3374e+03
150	'Line'	[3.3...	1x118 dou...	1x118 dou...	150	150	138	1.6422	3.1177	5.0888	0.0350	1.2787e+03	3.3900e+05	3.3994e+05	5.1134e+05	5.1181e+05	185	164	0.0344	0.0413	0.0500	1	435.2500
151	'Line'	[3.5...	1x139 dou...	1x139 dou...	151	151	149	0.1000	5.7828	11.0200	0.0350	1.5456e+03	3.5403e+05	3.5528e+05	5.1099e+05	5.1164e+05	290	259	0.0046	0.0356	0.0921	0	1.2187e+03
152	'Line'	[3.5...	1x113 dou...	1x113 dou...	152	152	134	8.3740	4.6541	8.7375	0.0350	1.6002e+03	3.5079e+05	3.5042e+05	5.1093e+05	5.1197e+05	404	270	0.0036	0.0292	0.0399	0	848.6675
153	'Line'	[3.3...	1x91 double	1x91 double	153	153	138	1.7060	4.1906	7.5225	0.0350	1.0551e+03	3.3994e+05	3.3994e+05	5.1088e+05	5.1181e+05	182	164	0.0031	0.0389	0.0458	0	712.5525
154	'Line'	[3.4...	1x126 dou...	1x126 dou...	154	154	140	0.1000	4.0114	7.8438	0.0350	1.4714e+03	3.4679e+05	3.4776e+05	5.1084e+05	5.1181e+05	240	236	0.0106	0.0158	0.0318	0	662.4825
155	'Line'	[3.5...	1x23 double	1x23 double	155	155	152	0.1000	4.3136	7.8488	0.0350	205.2082	3.5082e+05	3.5079e+05	5.1076e+05	5.1093e+05	404	404	0.0036	0.0269	0.0326	0	747.7275
156	'Line'	[3.4...	1x30 double	1x30 double	156	156	154	3.9895	3.0139	5.3300	0.0350	350.9188	3.4652e+05	3.4679e+05	5.1070e+05	5.1084e+05	254	240	0.0112	0.0143	0.0290	0	411.3650
157	'Line'	[3.5...	1x60 double	1x60 double	157	157	151	1.5573	4.7316	8.3025	0.0350	706.3351	3.5356e+05	3.5403e+05	5.1059e+05	5.1099e+05	301	290	0.0047	0.0352	0.0459	0	872.3600
158	'Line'	[3.4...	1x35 double	1x35 double	158	158	156	12.3907	2.6903	4.5513	0.0350	427.7386	3.4617e+05	3.4652e+05	5.1061e+05	5.1070e+05	307	254	0.0119	0.0129	0.0262	1	340.4300
159	'Line'	[3.5...	1x27 double	1x27 double	159	159	155	0.9644	4.2745	7.7488	0.0350	311.0660	3.5085e+05	3.5082e+05	5.1048e+05	5.1076e+05	407	404	0.0036	0.0273	0.0323	0	736.4700
160	'Line'	[3.5...	1x71 double	1x71 double	160	160	157	4.5049	4.2720	7.1400	0.0350	910.1219	3.5277e+05	3.5356e+05	5.1039e+05	5.1059e+05	342	301	0.0047	0.0355	0.0427	0	735.7575
161	'Line'	[3.5...	1x59 double	1x59 double	161	161	159	0.4431	4.1630	7.4738	0.0350	676.9848	3.5063e+05	3.5085e+05	5.0998e+05	5.1048e+05	410	407	0.0037	0.0275	0.0323	0	704.7475
162	'Line'	[3.5...	1x58 double	1x58 double	162	162	160	8.4643	3.1984	4.4788	0.0350	697.0458	3.5243e+05	3.5277e+05	5.0994e+05	5.1039e+05	401	342	0.0048	0.0385	0.0457	0	454.1850
163	'Line'	[3.5...	1x30 double	1x30 double	163	163	162	2.1806	3.0775	4.0378	0.0350	412.7386	3.5209e+05	3.5243e+05	5.0980e+05	5.0994e+05	410	401	0.0048	0.0327	0.0445	1	425.9325
164	'Line'	[3.3...	1x104 dou...	1x104 dou...	164	164	153	7.9335	2.5927	3.3450	0.0350	1.3361e+03	3.4030e+05	3.3994e+05	5.0974e+05	5.1088e+05	288	182	0.0028	0.0217	0.0563	1	320.0800
165	'Line'	[3.4...	1x98 double	1x98 double	165	165	161	1.8316	2.9825	4.3687	0.0350	1.0374e+03	3.4988e+05	3.5063e+05	5.0949e+05	5.0998e+05	429	410	0.0037	0.0244	0.0283	1	404.2575
166	'Line'	[3.5...	1x90 double	1x90 double	166	166	161	4.7978	2.2481	2.6238	0.0350	1.0630e+03	3.5069e+05	3.5063e+05	5.0908e+05	5.0998e+05	461	410	0.0039	0.0239	0.2750	1	252.3675
167																							

References:

Abbasi, T., Abbasi, S.A., 2011. Small hydro and the environmental implications of its extensive utilization. Renewable and Sustainable Energy Reviews 15, 2134–2143. https://doi.org/10.1016/j.rser.2010.11.050

Abbaspour, C.K., 2008. SWAT Calibrating and Uncertainty Programs. A User Manual. Eawag Zurich, Switzerland.

Abbaspour, K., Vaghefi, S., Srinivasan, R., 2017. A Guideline for Successful Calibration and Uncertainty Analysis for Soil and Water Assessment: A Review of Papers from the 2016 International SWAT Conference. Water 10, 6. https://doi.org/10.3390/w10010006

Abbaspour, K.C., 2011. SWAT-CUP4: SWAT calibration and uncertainty programs–a user manual. Swiss Federal Institute of Aquatic Science and Technology, Eawag.

Abbaspour, K.C., Johnson, C.A., Van Genuchten, M.T., 2004. Estimating uncertain flow and transport parameters using a sequential uncertainty fitting procedure. Vadose Zone Journal 3, 1340–1352.

Abbaspour, K.C., Rouholahnejad, E., Vaghefi, S., Srinivasan, R., Yang, H., Kløve, B., 2015. A continental-scale hydrology and water quality model for Europe: Calibration and uncertainty of a high-resolution large-scale SWAT model. Journal of Hydrology 524, 733–752. https://doi.org/10.1016/j.jhydrol.2015.03.027

Abbaspour, K.C., Sonnleitner, M.A., Schulin, R., 1999. Uncertainty in estimation of soil hydraulic parameters by inverse modeling: Example lysimeter experiments. Soil Science Society of America Journal 63, 501–509.

Abbaspour, K.C., Yang, J., Maximov, I., Siber, R., Bogner, K., Mieleitner, J., Zobrist, J., Srinivasan, R., 2007. Modelling hydrology and water quality in the pre-alpine/alpine Thur watershed using SWAT. Journal of Hydrology 333, 413–430. https://doi.org/10.1016/j.jhydrol.2006.09.014

Aber, J.S., Marzolff, I., Ries, J., Aber, S.E.W., 2019. Small-format aerial photography and UAS imagery: Principles, techniques and geoscience applications. Academic Press.

Adams, J., 1979. Gravel size analysis from photographs. Journal of the Hydraulics Division 105, 1247–1255.

Ahearn, D.S., Dahlgren, R.A., 2005. Sediment and nutrient dynamics following a low-head dam removal at Murphy Creek, California. Limnology and Oceanography 50, 1752–1762. https://doi.org/10.4319/lo.2005.50.6.1752

Albert, J.S., Destouni, G., Duke-Sylvester, S.M., Magurran, A.E., Oberdorff, T., Reis, R.E., Winemiller, K.O., Ripple, W.J., 2020. Scientists' warning to humanity on the freshwater biodiversity crisis. Ambio 1–10.

Alcamo, J., 2003. Ecosystems and human well-being: a framework for assessment.

Allan, J.D., Castillo, M.M., 2007. Stream ecology: structure and function of running waters. Springer Science & Business Media.

Allen, C.R., Fontaine, J.J., Pope, K.L., Garmestani, A.S., 2011. Adaptive management for a turbulent future. Journal of Environmental Management, Adaptive management for Natural Resources 92, 1339–1345. https://doi.org/10.1016/j.jenvman.2010.11.019

Allen, D.J., Newell, A.J., Butcher, A.S., 2010. Preliminary review of the geology and hydrogeology of the Eden DTC sub-catchments.

Almond, R.E.A., Grooten M, Petersen, T., 2020. Living Planet Report 2020: bending the curve of biodiversity loss.

AMBER Consortium, 2020. The AMBER Barrier Atlas. A Pan-European Database of Artificial Instream Barriers. Version 1, 29.

Amoros, C., Bornette, G., 2002. Connectivity and biocomplexity in waterbodies of riverine floodplains. Freshwater Biology 47, 761–776. https://doi.org/10.1046/j.1365-2427.2002.00905.x

Ancey, C., 2020a. Bedload transport: a walk between randomness and determinism. Part 1. The state of the art. Journal of Hydraulic Research 58, 1–17. https://doi.org/10.1080/00221686.2019.1702594

Ancey, C., 2020b. Bedload transport: a walk between randomness and determinism. Part 2. Challenges and prospects. Journal of Hydraulic Research 58, 18–33. https://doi.org/10.1080/00221686.2019.1702595

Ancey, C., Davison, A.C., Böhm, T., Jodeau, M., Frey, P., 2008. Entrainment and motion of coarse particles in a shallow water stream down a steep slope. Journal of Fluid Mechanics 595, 83–114.

Andersen, J., Refsgaard, J.C., Jensen, K.H., 2001. Distributed hydrological modelling of the Senegal River Basin—model construction and validation. Journal of hydrology 247, 200–214.

Anderson, D., Moggridge, H., Warren, P., Shucksmith, J., 2015. The impacts of 'run-of-river' hydropower on the physical and ecological condition of rivers. Water and Environment Journal 29, 268–276. https://doi.org/10.1111/wej.12101

Anderson, M.P., Woessner, W.W., 1992. The role of the postaudit in model validation. Advances in Water Resources 15, 167–173.

Andrews, E.D., 1983. Entrainment of gravel from naturally sorted riverbed material. Geological Society of America Bulletin 94, 1225–1231.

Ansar, A., Flyvbjerg, B., Budzier, A., Lunn, D., 2014. Should we build more large dams? The actual costs of hydropower megaproject development. Energy Policy 69, 43–56. https://doi.org/10.1016/j.enpol.2013.10.069

Arcement, G.J., Schneider, V.R., 1989. Guide for selecting Manning's roughness coefficients for natural channels and flood plains. US Government Printing Office Washington, DC.

Arias, M.E., Cochrane, T.A., Lawrence, K.S., Killeen, T.J., Farrell, T.A., 2011. Paying the forest for electricity: a modelling framework to market forest conservation as payment for ecosystem services benefiting hydropower generation. Environmental Conservation 473–484.

Arnold, J.G., Fohrer, N., 2005. SWAT2000: current capabilities and research opportunities in applied watershed modelling. Hydrological Processes 19, 563–572. https://doi.org/10.1002/hyp.5611

Arnold, J.G., Moriasi, D.N., Gassman, P.W., Abbaspour, K.C., White, M.J., Srinivasan, R., Santhi, C., Harmel, R.D., Van Griensven, A., Van Liew, M.W., 2012. SWAT: Model use, calibration, and validation. Transactions of the ASABE 55, 1491–1508.

Arnold, J.G., Srinivasan, R., Muttiah, R.S., Williams, J.R., 1998. LARGE AREA HYDROLOGIC MODELING AND ASSESSMENT PART I: MODEL DEVELOPMENT'. JAWRA Journal of the American Water Resources Association 34, 73–89. https://doi.org/10.1111/j.1752-1688.1998.tb05961.x

Arthington, A.H., Bunn, S.E., Poff, N.L., Naiman, R.J., 2006. The Challenge of Providing Environmental Flow Rules to Sustain River Ecosystems. Ecological

Applications 16, 1311–1318. https://doi.org/10.1890/1051-0761(2006)016[1311:TCOPEF]2.0.CO;2

Aryal, A., Shrestha, S., Babel, M.S., 2019. Quantifying the sources of uncertainty in an ensemble of hydrological climate-impact projections. Theor Appl Climatol 135, 193–209. https://doi.org/10.1007/s00704-017-2359-3

Ashley, J.T.F., Bushaw-Newton, K., Wilhelm, M., Boettner, A., Drames, G., Velinsky, D.J., 2006. The Effects of Small Dam Removal on the Distribution of Sedimentary Contaminants. Environ Monit Assess 114, 287–312. https://doi.org/10.1007/s10661-006-4781-3

Ashmore, P.E., Day, T.J., 1988. Spatial and temporal patterns of suspended-sediment yield in the Saskatchewan River basin. Canadian Journal of Earth Sciences 25, 1450–1463.

Ashmore, P.E., Rennie, C.D., 2013. Gravel-bed rivers: from particles to patterns. Earth Surface Processes and Landforms 38, 217–220.

Ashworth, P.J., Ferguson, R.I., 1989. Size-selective entrainment of bed load in gravel bed streams. Water Resources Research 25, 627–634.

Bagnold, R.A., 1977. Bed load transport by natural rivers. Water resources research 13, 303–312.

Bainbridge, Z., Lewis, S., Stevens, T., Petus, C., Lazarus, E., Gorman, J., Smithers, S., 2021. Measuring sediment grain size across the catchment to reef continuum: Improved methods and environmental insights. Marine Pollution Bulletin 168, 112339. https://doi.org/10.1016/j.marpolbul.2021.112339

Baker, T.J., Miller, S.N., 2013. Using the Soil and Water Assessment Tool (SWAT) to assess land use impact on water resources in an East African watershed. Journal of Hydrology 486, 100–111. https://doi.org/10.1016/j.jhydrol.2013.01.041

Bálint, M., Domisch, S., Engelhardt, C.H.M., Haase, P., Lehrian, S., Sauer, J., Theissinger, K., Pauls, S.U., Nowak, C., 2011. Cryptic biodiversity loss linked to global climate change. Nature climate change 1, 313–318.

Barbarossa, V., Schmitt, R.J., Huijbregts, M.A., Zarfl, C., King, H., Schipper, A.M., 2020. Impacts of current and future large dams on the geographic range connectivity of freshwater fish worldwide. Proceedings of the National Academy of Sciences 117, 3648–3655.

Barker, L., Hannaford, J., Muchan, K., Turner, S., Parry, S., 2016. The winter 2015/2016 floods in the UK: a hydrological appraisal. Weather 71, 324–333. https://doi.org/10.1002/wea.2822

Barker, P.A., Wilby, R.L., Borrows, J., 2004. A 200-year precipitation index for the central English Lake District. Hydrological Sciences Journal 49. https://doi.org/10.1623/hysj.49.5.769.55131

Bärlund, I., Kirkkala, T., Malve, O., Kämäri, J., 2007. Assessing SWAT model performance in the evaluation of management actions for the implementation of the Water Framework Directive in a Finnish catchment. Environmental Modelling & Software 22, 719–724.

Barquín Ortiz, J., Martinez-Capel, F., 2011. Preface: Assessment of physical habitat characteristics in rivers, implications for river ecology and management. Limnetica 30, 159–167.

Bathurst, J.C., 1986a. Physically-based distributed modelling of an upland catchment using the Systeme Hydrologique Europeen. Journal of hydrology 87, 79–102.

Bathurst, J.C., 1986b. Sensitivity analysis of the Systeme Hydrologique Europeen for an upland catchment. Journal of Hydrology 87, 103–123.

Batjes, N.H., 2009. Harmonized soil profile data for applications at global and continental scales: updates to the WISE database. Soil Use and Management 25, 124–127. https://doi.org/10.1111/j.1475-2743.2009.00202.x

Battin, J., Wiley, M.W., Ruckelshaus, M.H., Palmer, R.N., Korb, E., Bartz, K.K., Imaki, H., 2007. Projected impacts of climate change on salmon habitat restoration. Proceedings of the national academy of sciences 104, 6720–6725.

Bauwe, A., Kahle, P., Lennartz, B., 2019. Evaluating the SWAT model to predict streamflow, nitrate loadings and crop yields in a small agricultural catchment. Advances in Geosciences 48, 1–9.

Baxter, R.M., 1977. Environmental effects of dams and impoundments. Annual Review of Ecology and Systematics 8, 255–283.

BBC, 2016. One year on: Storm Desmond - BBC Weather Watchers [WWW Document]. URL https://www.bbc.co.uk/weatherwatchers/article/38206476/one-year-on-storm-desmond/ (accessed 5.20.21).

BBC, N., 2016. River Eamont weir removal proposed to prevent flooding [WWW Document]. URL https://www.bbc.co.uk/news/uk-england-cumbria-36607688 (accessed 7.17.21).

Beames, P., 2021. Map. Global Dam Watch. URL http://globaldamwatch.org/map/ (accessed 4.6.21).

Beechie, T.J., Sear, D.A., Olden, J.D., Pess, G.R., Buffington, J.M., Moir, H., Roni, P., Pollock, M.M., 2010. Process-based Principles for Restoring River Ecosystems. BioScience 60, 209–222. https://doi.org/10.1525/bio.2010.60.3.7

Bell, V.A., Kay, A.L., Davies, H.N., Jones, R.G., 2016. An assessment of the possible impacts of climate change on snow and peak river flows across Britain. Climatic Change 136, 539–553. https://doi.org/10.1007/s10584-016-1637-x

Belletti, B., Garcia de Leaniz, C., Jones, J., Bizzi, S., Börger, L., Segura, G., Castelletti, A., van de Bund, W., Aarestrup, K., Barry, J., Belka, K., Berkhuysen, A., Birnie-Gauvin, K., Bussettini, M., Carolli, M., Consuegra, S., Dopico, E., Feierfeil, T., Fernández, S., Fernandez Garrido, P., Garcia-Vazquez, E., Garrido, S., Giannico, G., Gough, P., Jepsen, N., Jones, P.E., Kemp, P., Kerr, J., King, J., Łapińska, M., Lázaro, G., Lucas, M.C., Marcello, L., Martin, P., McGinnity, P., O'Hanley, J., Olivo del Amo, R., Parasiewicz, P., Pusch, M., Rincon, G., Rodriguez, C., Royte, J., Schneider, C.T., Tummers, J.S., Vallesi, S., Vowles, A., Verspoor, E., Wanningen, H., Wantzen, K.M., Wildman, L., Zalewski, M., 2020. More than one million barriers fragment Europe's rivers. Nature 588, 436–441. https://doi.org/10.1038/s41586-020-3005-2

Belletti, B., Rinaldi, M., Bussettini, M., Comiti, F., Gurnell, A.M., Mao, L., Nardi, L., Vezza, P., 2017. Characterising physical habitats and fluvial hydromorphology: A new system for the survey and classification of river geomorphic units. Geomorphology 283, 143–157. https://doi.org/10.1016/j.geomorph.2017.01.032

Benda, L., Poff, N.L., Miller, D., Dunne, T., Reeves, G., Pess, G., Pollock, M., 2004. The Network Dynamics Hypothesis: How Channel Networks Structure Riverine Habitats. BioScience 54, 413. https://doi.org/10.1641/0006-3568(2004)054[0413:TNDHHC]2.0.CO;2

Bentley, 2019. Rectangular Weirs [WWW Document]. URL https://docs.bentley.com/LiveContent/web/Bentley%20StormCAD%20SS5-v1/en/GUID-545D2D7C36774BD6BB1DAB903E492CE1.html (accessed 7.7.19).

Best, J.L., 1988. Sediment transport and bed morphology at river channel confluences. Sedimentology 35, 481–498. https://doi.org/10.1111/j.1365-3091.1988.tb00999.x

Best, J.L., Rhoads, B.L., 2008. Sediment transport, bed morphology and the sedimentology of river channel confluences. River confluences, tributaries and the fluvial network 45–72.

Beven, K., 2006. On undermining the science? Hydrological Processes: An International Journal 20, 3141–3146.

Beven, K., 1993. Prophecy, reality and uncertainty in distributed hydrological modelling. Advances in Water Resources, Research Perspectives in Hydrology 16, 41–51. https://doi.org/10.1016/0309-1708(93)90028-E

Beven, K., 1989. Changing ideas in hydrology—the case of physically-based models. Journal of hydrology 105, 157–172.

Beven, K., 1987. Towards the use of catchment geomorphology in flood frequency predictions. Earth Surface Processes and Landforms 12, 69–82.

Beven, K., Binley, A., 1992. The future of distributed models: model calibration and uncertainty prediction. Hydrological processes 6, 279–298.

Beven, K.J., 2012. Rainfall-runoff modelling: the primer, 2nd ed. ed. Wiley-Blackwell, Chichester, West Sussex ; Hoboken, NJ.

Beven, K.J., 1990. A Discussion of Distributed Hydrological Modelling, in: Abbott, M.B., Refsgaard, J.C. (Eds.), Distributed Hydrological Modelling. Springer Netherlands, Dordrecht, pp. 255–278. https://doi.org/10.1007/978-94-009-0257-2_13

Birk, S., Chapman, D., Carvalho, L., Spears, B.M., Andersen, H.E., Argillier, C., Auer, S., Baattrup-Pedersen, A., Banin, L., Beklioğlu, M., Bondar-Kunze, E., Borja, A., Branco, P., Bucak, T., Buijse, A.D., Cardoso, A.C., Couture, R.-M., Cremona, F., de Zwart, D., Feld, C.K., Ferreira, M.T., Feuchtmayr, H., Gessner, M.O., Gieswein, A., Globevnik, L., Graeber, D., Graf, W., Gutiérrez-Cánovas, C., Hanganu, J., Işkın, U., Järvinen, M., Jeppesen, E., Kotamäki, N., Kuijper, M., Lemm, J.U., Lu, S., Solheim, A.L., Mischke, U., Moe, S.J., Nõges, P., Nõges, T., Ormerod, S.J., Panagopoulos, Y., Phillips, G., Posthuma, L., Pouso, S., Prudhomme, C., Rankinen, K., Rasmussen, J.J., Richardson, J., Sagouis, A., Santos, J.M., Schäfer, R.B., Schinegger, R., Schmutz, S., Schneider, S.C., Schülting, L., Segurado, P., Stefanidis, K., Sures, B., Thackeray, S.J., Turunen, J., Uyarra, M.C., Venohr, M., von der Ohe, P.C., Willby, N., Hering, D., 2020. Impacts of multiple stressors on freshwater biota across spatial scales and ecosystems. Nat Ecol Evol 4, 1060–1068. https://doi.org/10.1038/s41559-020-1216-4

Birnie-Gauvin, K., Candee, M.M., Baktoft, H., Larsen, M.H., Koed, A., Aarestrup, K., 2018. River connectivity reestablished: E ffects and implications of six weir removals on brown trout smolt migration. River Research and Applications 34, 548–554.

Birnie-Gauvin, K., Larsen, M.H., Nielsen, J., Aarestrup, K., 2017. 30 years of data reveal dramatic increase in abundance of brown trout following the removal of a small hydrodam. Journal of Environmental Management 204, 467–471. https://doi.org/10.1016/j.jenvman.2017.09.022

Biswas, A.K., Tortajada, C., 2001. Development and Large Dams: A Global Perspective. International Journal of Water Resources Development 17, 9–21. https://doi.org/10.1080/07900620120025024

Bizzi, S., Demarchi, L., Grabowski, R.C., Weissteiner, C.J., Van de Bund, W., 2016. The use of remote sensing to characterise hydromorphological properties of European rivers. Aquatic Sciences 78, 57–70. https://doi.org/10.1007/s00027-015-0430-7

Black, A.R., Werritty, A., 1997. Seasonality of flooding: a case study of North Britain. Journal of Hydrology 195, 1–25. https://doi.org/10.1016/S0022-1694(96)03264-7

Bláha, M., Eisenbeiss, H., Grimm, D., Limpach, P., 2012. Direct Georeferencing of UAVs. Int. Arch. Photogramm. Remote Sens. Spatial Inf. Sci. XXXVIII-1/C22, 131–136. https://doi.org/10.5194/isprsarchives-XXXVIII-1-C22-131-2011

Bloschl, G., Sivapalan, M., 1995. Scale issues in hydrological modelling: A review. Hydrol. Process. 9, 251–290. https://doi.org/10.1002/hyp.3360090305

Bluesky, L., 2014. Bluesky 5m resolution Digital Terrain Model (DTM) for England and Wales. NERC Earth Observation Data Centre.

Bohn, B.A., Kershner, J.L., 2002. Establishing aquatic restoration priorities using a watershed approach. Journal of Environmental Management 64, 355–363.

Bolland, J.D., Nunn, A.D., Lucas, M.C., Cowx, I.G., 2012. The Importance of Variable Lateral Connectivity Between Artificial Floodplain Waterbodies and River Channels. River Research and Applications 28, 1189–1199. https://doi.org/10.1002/rra.1498

Boorman, D.B., 2003. Climate, Hydrochemistry and Economics of Surface-water Systems (CHESS): adding a European dimension to the catchment modelling experience developed under LOIS. Science of the total environment 314, 411–437.

Borah, D.K., Bera, M., 2004. Watershed-scale hydrologic and nonpoint-source pollution models: Review of applications. Transactions of the ASAE 47, 789.

Boulton, A.J., 2007. Hyporheic rehabilitation in rivers: restoring vertical connectivity. Freshwater Biology 52, 632–650. https://doi.org/10.1111/j.1365-2427.2006.01710.x

Bouraoui, F., Galbiati, L., Bidoglio, G., 2002. Climate change impacts on nutrient loads in the Yorkshire Ouse catchment (UK). Hydrology and Earth System Sciences 6, 197–209. https://doi.org/10.5194/hess-6-197-2002

Boyle, D.P., Gupta, H.V., Sorooshian, S., 2000. Toward improved calibration of hydrologic models: Combining the strengths of manual and automatic methods. Water Resources Research 36, 3663–3674.

Bracken, L.J., Croke, J., 2007. The concept of hydrological connectivity and its contribution to understanding runoff-dominated geomorphic systems. Hydrological Processes 21, 1749–1763. https://doi.org/10.1002/hyp.6313

Bracken, L.J., Turnbull, L., Wainwright, J., Bogaart, P., 2015. Sediment connectivity: a framework for understanding sediment transfer at multiple scales. Earth Surf. Process. Landforms 40, 177–188. https://doi.org/10.1002/esp.3635

Bracken, L.J., Wainwright, J., 2006. Geomorphological equilibrium: myth and metaphor? Transactions of the Institute of British Geographers 31, 167–178. https://doi.org/10.1111/j.1475-5661.2006.00204.x

Bracken, L.J., Wainwright, J., Ali, G.A., Tetzlaff, D., Smith, M.W., Reaney, S.M., Roy, A.G., 2013. Concepts of hydrological connectivity: Research approaches, pathways and future agendas. Earth-Science Reviews 119, 17–34. https://doi.org/10.1016/j.earscirev.2013.02.001

Brambilla, D., Papini, M., Longoni, L., 2018. Temporal and Spatial Variability of Sediment Transport in a Mountain River: A Preliminary Investigation of the

Caldone River, Italy. Geosciences 8, 163. https://doi.org/10.3390/geosciences8050163

Branco, P., Segurado, P., Santos, J.M., Ferreira, M.T., 2014. Prioritizing barrier removal to improve functional connectivity of rivers. Journal of Applied Ecology 51, 1197–1206. https://doi.org/10.1111/1365-2664.12317

Bridge, J.S., 1992. A revised model for water flow, sediment transport, bed topography and grain size sorting in natural river bends. Water Resources Research 28, 999–1013. https://doi.org/10.1029/91WR03088

Brierley, G.J., Fryirs, K.A., 2005. Geomorphology and river management: applications of the river styles framework. Blackwell Pub, Malden, MA.

Brooks, A.J., Haeusler, T.I.M., Reinfelds, I., Williams, S., 2005. Hydraulic microhabitats and the distribution of macroinvertebrate assemblages in riffles. Freshwater Biology 50, 331–344.

Brown, C.B., 1943. Discussion of" Sedimentation in reservoirs", in: Proceedings of the American Society of Civil Engineers.

Brown, J., 2020. Cumbria hit by 1.15 trillion litres of rainfall in 48 hours [WWW Document]. News and Star. URL https://www.newsandstar.co.uk/news/18919447.storm-desmond-cumbria-hit-1-15-trillion-litres-rainfall-48-hours/ (accessed 5.20.21).

Brune, G.M., 1953. Trap efficiency of reservoirs. Eos, Transactions American Geophysical Union 34, 407–418. https://doi.org/10.1029/TR034i003p00407

Brussock, P.P., Brown, A.V., Dixon, J.C., 1985. Channel Form and Stream Ecosystem Models 1. JAWRA Journal of the American Water Resources Association 21, 859–866.

Buendia, C., Gibbins, C.N., Vericat, D., Batalla, R.J., Douglas, A., 2013. Detecting the structural and functional impacts of fine sediment on stream invertebrates. Ecological Indicators 25, 184–196. https://doi.org/10.1016/j.ecolind.2012.09.027

Buffington, J.M., Montgomery, D.R., 1999. Effects of hydraulic roughness on surface textures of gravel-bed rivers. Water Resources Research 35, 3507–3521. https://doi.org/10.1029/1999WR900138

Bunn, S.E., Arthington, A.H., 2002. Basic principles and ecological consequences of altered flow regimes for aquatic biodiversity. environmental management 30, 492–507. https://doi.org/10.1007/S00267-002-2737-0

Burgess, O.T., Pine, W.E., Walsh, S.J., 2013. Importance of Floodplain Connectivity to Fish Populations in the Apalachicola River, Florida. River Research and Applications 29, 718–733. https://doi.org/10.1002/rra.2567

Burt, T.P., Allison, R.J. (Eds.), 2010. Sediment cascades: an integrated approach. Wiley, Chichester ; Hoboken, NJ.

Buscombe, D., 2020. SediNet: A configurable deep learning model for mixed qualitative and quantitative optical granulometry. Earth Surface Processes and Landforms 45, 638–651.

Bushaw-Newton, K.L., Hart, D.D., Pizzuto, J.E., Thomson, J.R., Egan, J., Ashley, J.T., Johnson, T.E., Horwitz, R.J., Keeley, M., Lawrence, J., 2002. AN INTEGRATIVE APPROACH TOWARDS UNDERSTANDING ECOLOGICAL RESPONSES TO DAM REMOVAL: THE MANATAWNY CREEK STUDY 1. JAWRA Journal of the American Water Resources Association 38, 1581–1599.

Butcher, D.P., Claydon, J., Labadz, J.C., Pattinson, V.A., Potter, A.W.R., White, P., 1992. Reservoir sedimentation and colour problems in southern Pennine reservoirs. Water and Environment Journal 6, 418–430.

Butler, J.B., Lane, S.N., Chandler, J.H., 2001. Automated extraction of grain-size data from gravel surfaces using digital image processing. Journal of Hydraulic Research 39, 519–529.

Cabezas-Rabadán, C., Pardo-Pascual, J.E., Palomar-Vázquez, J., 2021. Characterizing the Relationship between the Sediment Grain Size and the Shoreline Variability Defined from Sentinel-2 Derived Shorelines. Remote Sensing 13, 2829.

Calle, M., Alho, P., Benito, G., 2017. Channel dynamics and geomorphic resilience in an ephemeral Mediterranean river affected by gravel mining. Geomorphology 285, 333–346. https://doi.org/10.1016/j.geomorph.2017.02.026

Camp, T.R., 1946. Sedimentation and the Design of Settling Tanks. Transactions of the American Society of Civil Engineers 111, 895–936. https://doi.org/10.1061/TACEAT.0005912

Canny, J., 1986. A computational approach to edge detection. IEEE Transactions on pattern analysis and machine intelligence 679–698.

Cantelli, A., Wong, M., Parker, G., Paola, C., 2007. Numerical model linking bed and bank evolution of incisional channel created by dam removal. Water Resources Research 43.

Carbonneau, P., Piégay, H., 2012. Fluvial remote sensing for science and management. John Wiley & Sons.

Carbonneau, P.E., Bergeron, N., Lane, S.N., 2005a. Automated grain size measurements from airborne remote sensing for long profile measurements of fluvial grain sizes: size measurements of fluvial grain sizes. Water Resources Research 41. https://doi.org/10.1029/2005WR003994

Carbonneau, P.E., Bergeron, N.E., Lane, S.N., 2005b. Texture-based image segmentation applied to the quantification of superficial sand in salmonid river gravels. Earth Surface Processes and Landforms: The Journal of the British Geomorphological Research Group 30, 121–127.

Carbonneau, P.E., Bizzi, S., Marchetti, G., 2018. Robotic photosieving from low-cost multirotor sUAS: a proof-of-concept. Earth Surface Processes and Landforms 43, 1160–1166.

Carbonneau, P.E., Dietrich, J.T., 2017. Cost-effective non-metric photogrammetry from consumer-grade sUAS: implications for direct georeferencing of structure from motion photogrammetry. Earth Surf. Process. Landforms 42, 473–486. https://doi.org/10.1002/esp.4012

Carbonneau, P.E., Lane, S.N., Bergeron, N., 2006. Feature based image processing methods applied to bathymetric measurements from airborne remote sensing in fluvial environments. Earth Surface Processes and Landforms: The Journal of the British Geomorphological Research Group 31, 1413–1423.

Carbonneau, P.E., Lane, S.N., Bergeron, N.E., 2004. Catchment-scale mapping of surface grain size in gravel bed rivers using airborne digital imagery. Water resources research. 40, W07202. https://doi.org/10.1029/2003WR002759

Carbonneau, P.E., Lane, S.N., Bergeron, N.E., 2003. Cost-effective non-metric close-range digital photogrammetry and its application to a study of coarse gravel river beds. International Journal of Remote Sensing 24, 2837–2854.

Cardinale, B.J., Duffy, J.E., Gonzalez, A., Hooper, D.U., Perrings, C., Venail, P., Narwani, A., Mace, G.M., Tilman, D., Wardle, D.A., 2012. Biodiversity loss and its impact on humanity. Nature 486, 59–67.

Carey, W.P., 1985. VARIABILITY IN MEASURED BEDLO AD-TRANSPORT RATES 1. JAWRA Journal of the American Water Resources Association 21, 39–48.

Carré, D.M., Biron, P.M., Gaskin, S.J., 2007. Flow dynamics and bedload sediment transport around paired deflectors for fish habitat enhancement: a field study in the Nicolet River. Can. J. Civ. Eng. 34, 761–769. https://doi.org/10.1139/l06-083

Casserly, C.M., Turner, J.N., O'Sullivan, J.J., Bruen, M., Bullock, C., Atkinson, S., Kelly-Quinn, M., 2020. Impact of low-head dams on bedload transport rates in coarse-bedded streams. Science of The Total Environment 716, 136908. https://doi.org/10.1016/j.scitotenv.2020.136908

Cavalli, M., Trevisani, S., Comiti, F., Marchi, L., 2013. Geomorphometric assessment of spatial sediment connectivity in small Alpine catchments. Geomorphology 188, 31–41.

Cavalli, M., Vericat, D., Pereira, P., 2019. Mapping water and sediment connectivity. Science of The Total Environment 673, 763–767. https://doi.org/10.1016/j.scitotenv.2019.04.071

Chalov, S., Golosov, V., Li, R., Tsyplenkov, A. (Eds.), 2019. Climate Change Impacts on Hydrological Processes and Sediment Dynamics: Measurement, Modelling and Management: The Proceedings of The Second International Young Scientists Forum on Soil and Water Conservation and ICCE symposium 2018, 27–31 August, 2018, Moscow, Springer Proceedings in Earth and Environmental Sciences. Springer International Publishing, Cham. https://doi.org/10.1007/978-3-030-03646-1

Chardon, V., Piasny, G., Schmitt, L., 2022. Comparison of software accuracy to estimate the bed grain size distribution from digital images: A test performed along the Rhine River. River Research and Applications 38, 358–367. https://doi.org/10.1002/rra.3910

Charlton, R., 2010. Fundamentals of fluvial geomorphology, Repr. ed. Routledge, London.

Charru, F., Mouilleron, H., Eiff, O., 2004. Erosion and deposition of particles on a bed sheared by a viscous flow. Journal of Fluid Mechanics 519, 55.

Chaubey, I., Cotter, A.S., Costello, T.A., Soerens, T.S., 2005. Effect of DEM data resolution on SWAT output uncertainty. Hydrol. Process. 19, 621–628. https://doi.org/10.1002/hyp.5607

Chávez, G.M., Sarocchi, D., Santana, E.A., Borselli, L., 2015. Optical granulometric analysis of sedimentary deposits by color segmentation-based software: OPTGRAN-CS. Computers & Geosciences 85, 248–257.

Chow, T.V., Maidment, D.R., Mays, L.W., 1988. Applied hydrology. Water Resources Handbook; McGraw-Hill: New York, NY, USA.

Chow, V.T., Maidment, D.R., Mays, L.W., 1988. Applied hydrology.

Church, M., 1977. Palaeohydrological reconstructions from a Holocene valley fill.

Church, M., Ham, D., Hassan, M., Slaymaker, O., 1999. Fluvial clastic sediment yield in Canada: scaled analysis. Canadian Journal of Earth Sciences 36, 1267–1280.

Churchill, M.A., 1948. Discussion of analysis and use of reservoir sedimentation data, in: Proceedings of the Federal Interagency Sedimentation Conference. Bureau of Reclamation, US Department of the Interior, Washington, DC. pp. 139–140.

Cienciala, P., Nelson, A.D., Haas, A.D., Xu, Z., 2020. Lateral geomorphic connectivity in a fluvial landscape system: Unraveling the role of confinement, biogeomorphic interactions, and glacial legacies. Geomorphology 354, 107036. https://doi.org/10.1016/j.geomorph.2020.107036

Clarke, S.J., Bruce-Burgess, L., Wharton, G., 2003. Linking form and function: towards an eco-hydromorphic approach to sustainable river restoration. Aquatic Conservation: Marine and Freshwater Ecosystems 13, 439–450. https://doi.org/10.1002/aqc.591

Connor-Streich, G., Henshaw, A.J., Brasington, J., Bertoldi, W., Harvey, G.L., 2018. Let's get connected: A new graph theory-based approach and toolbox for understanding braided river morphodynamics. WIREs Water 5. https://doi.org/10.1002/wat2.1296

Cook, K., Turowski, J., Hovius, N., 2017. Effect of channel width variation on sediment transport in mixed alluvial-bedrock rivers-from case study to concept, in: EGU General Assembly Conference Abstracts. p. 17197.

Cooley, S.W., Ryan, J.C., Smith, L.C., 2021. Human alteration of global surface water storage variability. Nature 591, 78–81. https://doi.org/10.1038/s41586-021-03262-3

Cools, J., Broekx, S., Vandenberghe, V., Sels, H., Meynaerts, E., Vercaemst, P., Seuntjens, P., Van Hulle, S., Wustenberghs, H., Bauwens, W., Huygens, M., 2011. Coupling a hydrological water quality model and an economic optimization model to set up a cost-effective emission reduction scenario for nitrogen. Environmental Modelling & Software, Thematic Issue on Science to Improve Regional Environmental Investment Decisions 26, 44–51. https://doi.org/10.1016/j.envsoft.2010.04.017

Cooper, J.R., Wainwright, J., Parsons, A.J., Onda, Y., Fukuwara, T., Obana, E., Kitchener, B., Long, E.J., Hargrave, G.H., 2012. A new approach for simulating the redistribution of soil particles by water erosion: A marker-in-cell model. J. Geophys. Res. 117, F04027. https://doi.org/10.1029/2012JF002499

Cossart, É., Fressard, M., 2017. Assessment of structural sediment connectivity within catchments: insights from graph theory. Earth Surface Dynamics 5, 253–268. https://doi.org/10.5194/esurf-5-253-2017

Coulthard, T.J., 2001. Landscape evolution models: a software review. Hydrological Processes 15, 165–173. https://doi.org/10.1002/hyp.426

Coulthard, T.J., Neal, J.C., Bates, P.D., Ramirez, J., de Almeida, G.A., Hancock, G.R., 2013. Integrating the LISFLOOD-FP 2D hydrodynamic model with the CAESAR model: implications for modelling landscape evolution. Earth Surface Processes and Landforms 38, 1897–1906.

Coulthard, T.J., Ramirez, J., Fowler, H.J., Glenis, V., 2012. Using the UKCP09 probabilistic scenarios to model the amplified impact of climate change on drainage basin sediment yield. Hydrol. Earth Syst. Sci. 16, 4401–4416. https://doi.org/10.5194/hess-16-4401-2012

Couto, T.B., Olden, J.D., 2018. Global proliferation of small hydropower plants – science and policy. Frontiers in Ecology and the Environment 16, 91–100. https://doi.org/10.1002/fee.1746

Covino, T., 2017. Hydrologic connectivity as a framework for understanding biogeochemical flux through watersheds and along fluvial networks. Geomorphology 277, 133–144.

Cronshey, R., 1986. Urban hydrology for small watersheds. US Dept. of Agriculture, Soil Conservation Service, Engineering Division.

Csiki, S., Rhoads, B.L., 2010. Hydraulic and geomorphological effects of run-of-river dams. Progress in Physical Geography: Earth and Environment 34, 755–780. https://doi.org/10.1177/0309133310369435

Csiki, S.J., Rhoads, B.L., 2014. Influence of four run-of-river dams on channel morphology and sediment characteristics in Illinois, USA. Geomorphology 206, 215–229. https://doi.org/10.1016/j.geomorph.2013.10.009

Cudden, J.R., Hoey, T.B., 2003. The causes of bedload pulses in a gravel channel: the implications of bedload grain-size distributions. Earth Surface Processes and Landforms 28, 1411–1428. https://doi.org/10.1002/esp.521

Cui, Y., Parker, G., 2005. Numerical model of sediment pulses and sediment-supply disturbances in mountain rivers. Journal of Hydraulic Engineering 131, 646–656.

Czuba, J.A., 2018. A Lagrangian framework for exploring complexities of mixed-size sediment transport in gravel-bedded river networks. Geomorphology 321, 146–152. https://doi.org/10.1016/j.geomorph.2018.08.031

Czuba, J.A., Foufoula-Georgiou, E., 2015. Dynamic connectivity in a fluvial network for identifying hotspots of geomorphic change. Water Resources Research 51, 1401–1421. https://doi.org/10.1002/2014WR016139

Czuba, J.A., Foufoula-Georgiou, E., 2014. A network-based framework for identifying potential synchronizations and amplifications of sediment delivery in river basins. Water Resources Research 50, 3826–3851. https://doi.org/10.1002/2013WR014227

Czuba, J.A., Foufoula-Georgiou, E., Gran, K.B., Belmont, P., Wilcock, P.R., 2017. Interplay between spatially explicit sediment sourcing, hierarchical river-network structure, and in-channel bed material sediment transport and storage dynamics: Sediment Dynamics On River Networks. Journal of Geophysical Research: Earth Surface 122, 1090–1120. https://doi.org/10.1002/2016JF003965

D. N. Moriasi, J. G. Arnold, M. W. Van Liew, R. L. Bingner, R. D. Harmel, T. L. Veith, 2007. Model Evaluation Guidelines for Systematic Quantification of Accuracy in Watershed Simulations. Transactions of the ASABE 50, 885–900. https://doi.org/10.13031/2013.23153

Dankers, R., Christensen, O.B., Feyen, L., Kalas, M., de Roo, A., 2007. Evaluation of very high-resolution climate model data for simulating flood hazards in the Upper Danube Basin. Journal of Hydrology 347, 319–331. https://doi.org/10.1016/j.jhydrol.2007.09.055

Darby, S., Sear, D.A. (Eds.), 2008. River restoration: managing the uncertainty in restoring physical habitat. Wiley, Chichester.

de Leaniz, C.G., 2020. Broken rivers: ground-truthing the world's most fragmented rivers. Authorea Preprints.

de Leaniz, C.G., O'Hanley, J., 2021. Best practices for selecting barriers within European catchments.

Detert, M., Weitbrecht, V., 2013. User guide to gravelometric image analysis by BASEGRAIN. Advances in science and research 1789–1795.

Detert, M., Weitbrecht, V., 2012. Automatic object detection to analyze the geometry of gravel grains–a free stand-alone tool, in: River Flow. Taylor & Francis Group London, pp. 595–600.

Devi, G.K., Ganasri, B.P., Dwarakish, G.S., 2015. A Review on Hydrological Models. Aquatic Procedia 4, 1001–1007. https://doi.org/10.1016/j.aqpro.2015.02.126

DHI, S., 2021. MIKE 21 ST [WWW Document]. MIKE 21 ST : MIKE2017MIKE 21 STNon-Cohesive Sediment Transport Module. URL https://manuals.mikepoweredbydhi.help/2017/Coast_and_Sea/m21st.pdf

DHI, W.& E., 2022. MIKE HYDRO River User Guide. DHI Water & Environment Hørsholm.

Di Luzio, M., Arnold, J.G., Srinivasan, R., 2005. Effect of GIS data quality on small watershed stream flow and sediment simulations. Hydrol. Process. 19, 629–650. https://doi.org/10.1002/hyp.5612

Dias, M.S., Tedesco, P.A., Hugueny, B., Jézéquel, C., Beauchard, O., Brosse, S., Oberdorff, T., 2017. Anthropogenic stressors and riverine fish extinctions. Ecological indicators 79, 37–46.

Diepenbroek, M., de Jong, C., 1994. Quantification of textural particle characteristics by image analysis of sediment surfaces—examples from active and paleo-surfaces in steep, coarse-grained mountain environments, in: Dynamics and Geomorphology of Mountain Rivers. Springer, pp. 301–314.

Dile, Y.T., Srinivasan, R., 2014. Evaluation of CFSR climate data for hydrologic prediction in data-scarce watersheds: an application in the Blue Nile River Basin. JAWRA Journal of the American Water Resources Association 50, 1226–1241. https://doi.org/10.1111/jawr.12182

Dilks, C.F., Dunn, S.M., Robert, C.F., 2003. Benchmarking models for the Water Framework Directive: evaluation of SWAT for use in the Ythan catchment, UK., in: 2003 International SWAT Conference. p. 201.

Dingman, S.L., 2015. Physical hydrology. Waveland press.

Diplas, P., Kuhnle, R., Gray, J., Glysson, D., Edwards, T., 2008. Sediment transport measurements. Sedimentation Engineering: Theories, Measurements, Modeling, and Practice. ASCE Manuals and Reports on Engineering Practice 110, 165–252.

Djokic, D., Ye, Z., 2000. DEM preprocessing for efficient watershed delineation. Hydrologic and Hydraulic Modelling Support with Geographic Information Systems 65, 84.

Domisch, S., Araújo, M.B., Bonada, N., Pauls, S.U., Jähnig, S.C., Haase, P., 2013. Modelling distribution in European stream macroinvertebrates under future climates. Global Change Biology 19, 752–762. https://doi.org/10.1111/gcb.12107

Domisch, S., Portmann, F.T., Kuemmerlen, M., O'Hara, R.B., Johnson, R.K., Davy-Bowker, J., Bækken, T., Zamora-Muñoz, C., Sáinz-Bariáin, M., Bonada, N., Haase, P., Döll, P., Jähnig, S.C., 2017. Using streamflow observations to estimate the impact of hydrological regimes and anthropogenic water use on European stream macroinvertebrate occurrences. Ecohydrology 10, e1895. https://doi.org/10.1002/eco.1895

Dore, A.J., Choularton, T.W., Brown, R., Blackall, R.M., 1992. Orographic rainfall enhancement in the mountains of the Lake District and Snowdonia. Atmospheric Environment. Part A. General Topics 26, 357–371. https://doi.org/10.1016/0960-1686(92)90322-C

Downs, P.W., Cui, Y., Wooster, J.K., Dusterhoff, S.R., Booth, D.B., Dietrich, W.E., Sklar, L.S., 2009. Managing reservoir sediment release in dam removal projects: An approach informed by physical and numerical modelling of non-cohesive sediment. International Journal of River Basin Management 7, 433–452.

Doyle, M.W., Stanley, E.H., Harbor, J.M., 2003. Channel adjustments following two dam removals in Wisconsin. Water Resources Research 39. https://doi.org/10.1029/2002WR001714

Doyle, M.W., Stanley, E.H., Harbor, J.M., 2002. Geomorphic Analogies for Assessing Probable Channel Response to Dam Removal1. JAWRA Journal of the American Water Resources Association 38, 1567–1579.

Doyle, M.W., Stanley, E.H., Orr, C.H., Selle, A.R., Sethi, S.A., Harbor, J.M., 2005. Stream ecosystem response to small dam removal: Lessons from the Heartland. Geomorphology, Dams in Geomorphology 71, 227–244. https://doi.org/10.1016/j.geomorph.2004.04.011

Du Boys, M.P., 1879. Le Rhone et les rivieres a lit affouillable: Mem. Doc. Ann. Pont et Chaussees, Ser 5.

Duan, Q., 2003. Global optimization for watershed model calibration. Calibration of watershed models 6, 89–104.

Duan, Q., Sorooshian, S., Gupta, V.K., 1994. Optimal use of the SCE-UA global optimization method for calibrating watershed models. Journal of hydrology 158, 265–284.

Dudgeon, D., Arthington, A.H., Gessner, M.O., Kawabata, Z.-I., Knowler, D.J., Lévêque, C., Naiman, R.J., Prieur-Richard, A.-H., Soto, D., Stiassny, M.L.J., Sullivan, C.A., 2006. Declining biodiversity can alter the performance of ecosystems. Biological Reviews 81, 163–182. https://doi.org/10.1017/S1464793105006950

Duffy, J.E., 2009. Why biodiversity is important to the functioning of real-world ecosystems. Frontiers in Ecology and the Environment 7, 437–444.

Dufour, S., Piégay, H., 2009. From the myth of a lost paradise to targeted river restoration: forget natural references and focus on human benefits. River Research and Applications 25, 568–581. https://doi.org/10.1002/rra.1239

Dufour, S., Rollet, A.J., Chapuis, M., Provansal, M., Capanni, R., 2017. On the political roles of freshwater science in studying dam and weir removal policies: A critical physical geography approach. Water Alternatives 10, 853.

Easton, Z.M., Fuka, D.R., Walter, M.T., Cowan, D.M., Schneiderman, E.M., Steenhuis, T.S., 2008. Re-conceptualizing the soil and water assessment tool (SWAT) model to predict runoff from variable source areas. Journal of Hydrology 348, 279–291. https://doi.org/10.1016/j.jhydrol.2007.10.008

Einstein, H.A., 1950. The bed-load function for sediment transportation in open channel flows. Washington DC: US Department of Agriculture.

Einstein, H.A., 1942. Formulas for the transportation of bed load. Transactions of the American Society of civil Engineers 107, 561–577.

El-Nasr, A.A., Arnold, J.G., Feyen, J., Berlamont, J., 2005. Modelling the hydrology of a catchment using a distributed and a semi-distributed model. Hydrological Processes: An International Journal 19, 573–587.

Engelund, F., Hansen, E., 1967. A monograph on sediment transport in alluvial streams. Technical University of Denmark 0stervoldgade 10, Copenhagen K.

Environment Agency, U., 2021. Freshwater fish surveys (NFPD) [WWW Document]. URL https://data.gov.uk/dataset/823e7de7-33a2-4fc6-9a79-4c7672130094/freshwater-fish-surveys-nfpd (accessed 2.22.22).

Essenfelder, A.H., 2016. SWAT Weather Database: A Quick Guide. Version: v.0.16.07. https://doi.org/doi: 10.13140/RG.2.1.4329.1927.

European Environment Agency, 2021. Tracking barriers and their impacts on European river ecosystems [WWW Document]. URL https://www.eea.europa.eu/themes/water/european-waters/water-use-and-environmental-pressures/tracking-barriers-and-their-impacts (accessed 4.19.21).

European Environment Agency., 2018. European waters: assessment of status and pressures 2018. Publications Office, LU.

European Environment Agency, 2011. Vulnerability and adaptation to climate change in Europe. Publications Office of the European Union, Luxembourg.

Evans, D.J., 2020. Lake District, in: Landscapes and Landforms of England and Wales. Springer, pp. 483–513.

Evans, R., 2006. Land use, sediment delivery and sediment yield in England and Wales., in: Owens, P.N., Collins, A.J. (Eds.), Soil Erosion and Sediment Redistribution in River Catchments: Measurement, Modelling and Management. CABI, Wallingford, pp. 70–84. https://doi.org/10.1079/9780851990507.0070

Falkenmark, M., 1986. Fresh water: Time for a modified approach. Ambio 192–200.

Fan, J., Wang, S., Li, H., Yan, Z., Zhang, Y., Zheng, X., Wang, P., 2020. Modeling the ecological status response of rivers to multiple stressors using machine learning: A comparison of environmental DNA metabarcoding and morphological data. Water Research 183, 116004. https://doi.org/10.1016/j.watres.2020.116004

FAO, 2021. Harmonized world soil database v1.2 [WWW Document]. URL http://webarchive.iiasa.ac.at/Research/LUC/External-World-soil-database/HWSD_Data/HWSD.mdb (accessed 4.25.21).

FAO, 2019. Annex 1. Units and symbols [WWW Document]. URL http://www.fao.org/3/X0490E/x0490e0i.htm (accessed 4.16.21).

FAO/IIASA/ISRIC/ISSCAS/JRC, 2012. Harmonized World Soil Database (version 1.2) [WWW Document]. URL http://webarchive.iiasa.ac.at/Research/LUC/External-World-soil-database/HTML/index.html?sb=1 (accessed 9.22.18).

Fehr, R., 1987. Einfache Bestimmung der Korngrössenverteilung von Geschiebematerial mit Hilfe der Linienzahlanalyse. Verlags-AG der akademischen, technischen Vereine. https://doi.org/10.5169/seals-76710

Fencl, J.S., Mather, M.E., Costigan, K.H., Daniels, M.D., 2015. How Big of an Effect Do Small Dams Have? Using Geomorphological Footprints to Quantify Spatial Impact of Low-Head Dams and Identify Patterns of Across-Dam Variation. PLoS One 10. https://doi.org/10.1371/journal.pone.0141210

Ferguson, R., Hoey, T., Wathen, S., Werritty, A., 1996. Field evidence for rapid downstream fining of river gravels through selective transport. Geology 24, 179–182.

Ferrer-Boix, C., Martín-Vide, J.P., Parker, G., 2014. Channel evolution after dam removal in a poorly sorted sediment mixture: Experiments and numerical model. Water Resources Research 50, 8997–9019.

Ficklin, D.L., 2018. Hydroclimatology lab - Indiana University [WWW Document]. Hydroclimatology lab - Indiana University. URL http://dficklin.weebly.com/uploads/2/5/0/8/25084583/matlab_netcdf_to_ascii_swat2013.m (accessed 12.29.18).

Ficklin, D.L., Barnhart, B.L., 2014a. SWAT hydrologic model parameter uncertainty and its implications for hydroclimatic projections in snowmelt-dependent watersheds. Journal of Hydrology 519, 2081–2090. https://doi.org/10.1016/j.jhydrol.2014.09.082

Ficklin, D.L., Barnhart, B.L., 2014b. SWAT hydrologic model parameter uncertainty and its implications for hydroclimatic projections in snowmelt-dependent watersheds. Journal of Hydrology 519, 2081–2090. https://doi.org/10.1016/j.jhydrol.2014.09.082

Field, C.B., 2014. Climate change 2014–Impacts, adaptation and vulnerability: Regional aspects. Cambridge University Press.

Fisher, W.L., Bozek, M.A., Vokoun, J.C., Jacobson, R.B., 2012. Freshwater aquatic habitat measurements. Fisheries techniques, 3rd edition. American Fisheries Society, Bethesda, Maryland 101–161.

Fitzpatrick, F.A., 1998. Revised methods for characterizing stream habitat in the National Water-Quality Assessment Program. US Department of the Interior, US Geological Survey.

Fjeldstad, H.-P., Barlaup, B.T., Stickler, M., Gabrielsen, S.-E., Alfredsen, K., 2012. Removal of weirs and the influence on physical habitat for salmonids in a norwegian river: removal of weirs in a norwegian river. River Research and Applications 28, 753–763. https://doi.org/10.1002/rra.1529

Foley, M.M., Bellmore, J.R., O'Connor, J.E., Duda, J.J., East, A.E., Grant, G.E., Anderson, C.W., Bountry, J.A., Collins, M.J., Connolly, P.J., 2017. Dam removal: Listening in. Water Resources Research 53, 5229–5246.

Fonstad, M.A., Marcus, W.A., 2005. Remote sensing of stream depths with hydraulically assisted bathymetry (HAB) models. Geomorphology 72, 320–339.

Foster, G.R., Lane, L.J., Nowlin, J.D., Laflen, J.M., Young, R.A., 1980. A model to estimate sediment yield from field-sized areas: development of model.

Foster, I.D.L., Boardman, J., Evans, J.L., Copeland-Phillips, R., Vadher, A.N., Wright, S., Collins, A.L., Manning, C., 2021. Anthropogenic sediment traps and network dislocation in a lowland UK river. Earth Surf. Process. Landforms esp.5235. https://doi.org/10.1002/esp.5235

Fowler, H.J., Ekström, M., Kilsby, C.G., Jones, P.D., 2005. New estimates of future changes in extreme rainfall across the UK using regional climate model integrations. 1. Assessment of control climate. Journal of Hydrology 300, 212–233.

Fowler, H.J., Kilsby, C.G., Stunell, J., 2007. Modelling the impacts of projected future climate change on water resources in north-west England. Hydrology and Earth System Sciences 11, 1115–1126.

Francesconi, W., Srinivasan, R., Pérez-Miñana, E., Willcock, S.P., Quintero, M., 2016. Using the Soil and Water Assessment Tool (SWAT) to model ecosystem services: A systematic review. Journal of Hydrology 535, 625–636. https://doi.org/10.1016/j.jhydrol.2016.01.034

Freeman, M.C., Pringle, C.M., Jackson, C.R., 2007. Hydrologic Connectivity and the Contribution of Stream Headwaters to Ecological Integrity at Regional Scales1. JAWRA Journal of the American Water Resources Association 43, 5–14. https://doi.org/10.1111/j.1752-1688.2007.00002.x

Fressard, M., Cossart, E., 2019. A graph theory tool for assessing structural sediment connectivity: Development and application in the Mercurey vineyards (France). Science of The Total Environment 651, 2566–2584. https://doi.org/10.1016/j.scitotenv.2018.10.158

Freyhof, J., Brooks, E., 2011. European red list of freshwater fishes. Publications Office of the European Union Luxembourg.

Frissell, C.A., Liss, W.J., Warren, C.E., Hurley, M.D., 1986. A hierarchical framework for stream habitat classification: Viewing streams in a watershed context. Environmental Management 10, 199–214. https://doi.org/10.1007/BF01867358

Fryirs, K.A., Brierley, G.J., Preston, N.J., Kasai, M., 2007. Buffers, barriers and blankets: The (dis)connectivity of catchment-scale sediment cascades. CATENA 70, 49–67. https://doi.org/10.1016/j.catena.2006.07.007

Fryirs, K.A., Wheaton, J.M., Brierley, G.J., 2016. An approach for measuring confinement and assessing the influence of valley setting on river forms and processes. Earth Surface Processes and Landforms 41, 701–710. https://doi.org/10.1002/esp.3893

Fujita, H., 1977. Influence of water level fluctuations in a reservoir on slope stability. Bulletin of the International Association of Engineering Geology-Bulletin de l'Association Internationale de Géologie de l'Ingénieur 16, 170–173.

Fuka, D.R., Walter, M.T., MacAlister, C., Degaetano, A.T., Steenhuis, T.S., Easton, Z.M., 2014. Using the Climate Forecast System Reanalysis as weather input data for watershed models. Hydrological Processes 28, 5613–5623. https://doi.org/10.1002/hyp.10073

Fuller, I.C., Death, R.G., 2018. The science of connected ecosystems: What is the role of catchment-scale connectivity for healthy river ecology? Land Degradation & Development 29, 1413–1426. https://doi.org/10.1002/ldr.2903

Galia, T., Škarpich, V., Ruman, S., 2021. Impact of check dam series on coarse sediment connectivity. Geomorphology 377, 107595. https://doi.org/10.1016/j.geomorph.2021.107595

Gansfort, B., Traunspurger, W., 2019. Environmental factors and river network position allow prediction of benthic community assemblies: A model of nematode metacommunities. Sci Rep 9, 14716. https://doi.org/10.1038/s41598-019-51245-2

Gartner, J.D., Magilligan, F.J., Renshaw, C.E., 2015. Predicting the type, location and magnitude of geomorphic responses to dam removal: Role of hydrologic and geomorphic constraints. Geomorphology, Emerging geomorphic approaches to guide river management practices 251, 20–30. https://doi.org/10.1016/j.geomorph.2015.02.023

Gaskell, P., 2021. Weirs, barriers and hydropower [WWW Document]. Wild Trout Trust. URL https://www.wildtrout.org/content/weirs-culverts-and-barriers (accessed 4.12.21).

Gassman, P.W., M. R. Reyes, C. H. Green, J. G. Arnold, 2007. The Soil and Water Assessment Tool: Historical Development, Applications, and Future Research Directions. Transactions of the ASABE 50, 1211–1250. https://doi.org/10.13031/2013.23637

George, G., Hurley, M., Hewitt, D., 2007. The impact of climate change on the physical characteristics of the larger lakes in the English Lake District. Freshwater Biology 52, 1647–1666.

Gilbert, J.T., Wilcox, A.C., 2020. Sediment Routing and Floodplain Exchange (SeRFE): A Spatially Explicit Model of Sediment Balance and Connectivity Through River Networks. Journal of Advances in Modeling Earth Systems 12, e2020MS002048. https://doi.org/10.1029/2020MS002048

Giller, P.S., Giller, P., Malmqvist, B., 1998. The biology of streams and rivers. Oxford University Press.

Giuntoli, I., Vidal, J.-P., Prudhomme, C., Hannah, D.M., 2015. Future hydrological extremes: the uncertainty from multiple global climate and global hydrological models. Earth Syst. Dynam. 6, 267–285. https://doi.org/10.5194/esd-6-267-2015

Glavan, M., Pintar, M., 2012. Strengths, weaknesses, opportunities and threats of catchment modelling with Soil and Water Assessment Tool (SWAT) model. Water Resources Management and Modeling 39–64.

Glavan, M., White, S., Holman, I.P., 2011. Evaluation of river water quality simulations at a daily time step–Experience with SWAT in the Axe Catchment, UK. CLEAN–Soil, Air, Water 39, 43–54.

Glover, M., 2015. Chaos in Cumbria: floods turn lives upside down in Lake District [WWW Document]. the Guardian. URL http://www.theguardian.com/uk-news/2015/dec/07/chaos-cumbria-floods-lake-district-turn-lives-upside-down (accessed 5.20.21).

Gordon, N.D., McMahon, T.A., Finlayson, B.L., Gippel, C.J., Nathan, R.J., 2004. Stream hydrology: an introduction for ecologists. John Wiley and Sons.

Gough, P., Fernández Garrido, P., Van Herk, J., 2018. Dam Removal: A viable solution for the future of our European rivers [WWW Document]. Dam Removal Europe. URL https://damremoval.eu/wp-content/uploads/2018/07/Dam-Removal-Europe-Report-2018-DEF-1.pdf

Gracchi, T., Rossi, G., Stefanelli, C.T., Tanteri, L., Pozzani, R., Moretti, S., 2021. Tracking the Evolution of Riverbed Morphology on the Basis of UAV Photogrammetry. Remote Sensing 13, 829.

Graf, W.L., 2006. Downstream hydrologic and geomorphic effects of large dams on American rivers. Geomorphology, 37th Binghamton Geomorphology Symposium 79, 336–360. https://doi.org/10.1016/j.geomorph.2006.06.022

Graham, D.J., Reid, I., Rice, S.P., 2005a. Automated sizing of coarse-grained sediments: image-processing procedures. Mathematical geology 37, 1–28.

Graham, D.J., Rice, S.P., Reid, I., 2005b. A transferable method for the automated grain sizing of river gravels. Water Resources Research 41.

Granata, T., Cheng, F., Nechvatal, M., 2008. Discharge and suspended sediment transport during deconstruction of a low-head dam. Journal of Hydraulic Engineering 134, 652–657.

Grant, G.E., Marr, J.D.G., Hill, C., Johnson, S., Campbell, K., Mohseni, O., Wallick, J.R., Lewis, S.L., O'Connor, J.E., Major, J.J., Burkholder, B.K., 2008. Experimental and Field Observations of Breach Dynamics Accompanying Erosion of Marmot Cofferdam, Sandy River, Oregon 1–10. https://doi.org/10.1061/40976(316)350

Grant, G.E., Schmidt, J.C., Lewis, S.L., 2013. A Geological Framework for Interpreting Downstream Effects of Dams on Rivers, in: O'Connor, J.E., Grant, G.E. (Eds.), Water Science and Application. American Geophysical Union, Washington, D. C., pp. 203–219. https://doi.org/10.1029/007WS13

Green, W.H., Ampt, G.A., 1911. Studies on soil physics. The Journal of Agricultural Science 4, 1–24.

Greimann, B., 2013. Prediction of sediment erosion after dam removal using. The Challenges of Dam Removal and River Restoration 21, 59.

Grill, G., Lehner, B., Thieme, M., Geenen, B., Tickner, D., Antonelli, F., Babu, S., Borrelli, P., Cheng, L., Crochetiere, H., Macedo, H.E., Filgueiras, R., Goichot, M., Higgins, J., Hogan, Z., Lip, B., McClain, M.E., Meng, J., Mulligan, M., Nilsson, C., Olden, J.D., Opperman, J.J., Petry, P., Liermann, C.R., Sáenz, L., Salinas-Rodríguez, S., Schelle, P., Schmitt, R.J.P., Snider, J., Tan, F., Tockner, K., Valdujo, P.H., Soesbergen, A. van, Zarfl, C., 2019. Mapping the world's free-flowing rivers. Nature 569, 215–221. https://doi.org/10.1038/s41586-019-1111-9

Grizzetti, B., Pistocchi, A., Liquete, C., Udias, A., Bouraoui, F., van de Bund, W., 2017. Human pressures and ecological status of European rivers. Scientific Reports 7, 205. https://doi.org/10.1038/s41598-017-00324-3

Grusson, Y., Anctil, F., Sauvage, S., Sánchez Pérez, J., Grusson, Y., Anctil, F., Sauvage, S., Sánchez Pérez, J.M., 2017a. Testing the SWAT Model with Gridded Weather Data of Different Spatial Resolutions. Water 9, 54. https://doi.org/10.3390/w9010054

Grusson, Y., Anctil, F., Sauvage, S., Sánchez Pérez, J.M., 2017b. Assessing the climatic and temporal transposability of the SWAT model across a large contrasted watershed. Journal of Hydrologic Engineering 22, 04017004.

Guillou, N., Chapalain, G., 2010. Numerical simulation of tide-induced transport of heterogeneous sediments in the English Channel. Continental Shelf Research 30, 806–819.

Gupta, H.V., Beven, K.J., Wagener, T., 2006. Model calibration and uncertainty estimation. Encyclopedia of hydrological sciences.

Gupta, H.V., Sorooshian, S., Yapo, P.O., 1998. Toward improved calibration of hydrologic models: Multiple and noncommensurable measures of information. Water Resources Research 34, 751–763. https://doi.org/10.1029/97WR03495

Gurnell, A.M., Rinaldi, M., Belletti, B., Bizzi, S., Blamauer, B., Braca, G., Buijse, A.D., Bussettini, M., Camenen, B., Comiti, F., Demarchi, L., Jalón, D.G. de, Tánago, M.G. del, Grabowski, R.C., Gunn, I.D.M., Habersack, H., Hendriks, D., Henshaw, A.J., Klösch, M., Lastoria, B., Latapie, A., Marcinkowski, P., Martínez-Fernández, V., Mosselman, E., Mountford, J.O., Nardi, L., Okruszko, T., O'Hare, M.T., Palma, M., Percopo, C., Surian, N., Bund, W. van de, Weissteiner, C., Ziliani, L., 2016. A multi-scale hierarchical framework for developing understanding of river behaviour to support river management. Aquat Sci 78, 1–16. https://doi.org/10.1007/s00027-015-0424-5

Haan, C.T., Barfield, B.J., Hayes, J.C., 1994. Design hydrology and sedimentology for small catchments. Elsevier.

Habets, F., Molénat, J., Carluer, N., Douez, O., Leenhardt, D., 2018. The cumulative impacts of small reservoirs on hydrology: A review. Science of the Total Environment 643, 850–867.

Hallouz, F., Meddi, M., Mahé, G., Alirahmani, S., Keddar, A., 2018. Modeling of discharge and sediment transport through the SWAT model in the basin of Harraza (Northwest of Algeria). Water Science 32, 79–88. https://doi.org/10.1016/j.wsj.2017.12.004

Hamman, J.J., Nijssen, B., Bohn, T.J., Gergel, D.R., Mao, Y., 2018. The Variable Infiltration Capacity model version 5 (VIC-5): infrastructure improvements for new applications and reproducibility. Geosci. Model Dev. 11, 3481–3496. https://doi.org/10.5194/gmd-11-3481-2018

Hargreaves, G.L., Hargreaves, G.H., Riley, J.P., 1985. Agricultural Benefits for Senegal River Basin. Journal of Irrigation and Drainage Engineering 111, 113–124. https://doi.org/10.1061/(ASCE)0733-9437(1985)111:2(113)

Hart, D.D., Johnson, T.E., Bushaw-Newton, K.L., Horwitz, R.J., Bednarek, A.T., Charles, D.F., Kreeger, D.A., Velinsky, D.J., 2002. Dam Removal: Challenges and Opportunities for Ecological Research and River RestorationWe develop a risk assessment framework for understanding how potential responses to dam removal vary with dam and watershed characteristics, which can lead to more effective use of this restoration method. BioScience 52, 669–682. https://doi.org/10.1641/0006-3568(2002)052[0669:DRCAOF]2.0.CO;2

Harwin, S., Lucieer, A., 2012. An Accuracy Assessment of Georeferenced Point Clouds Produced Via Multi-View Stereo Techniques Applied to Imagery Acquired Via Unmanned Aerial Vehicle. Int. Arch. Photogramm. Remote Sens.

Spatial Inf. Sci. XXXIX-B7, 475–480. https://doi.org/10.5194/isprsarchives-XXXIX-B7-475-2012

Hauer, C., Leitner, P., Unfer, G., Pulg, U., Habersack, H., Graf, W., 2018. The Role of Sediment and Sediment Dynamics in the Aquatic Environment, in: Schmutz, S., Sendzimir, J. (Eds.), Riverine Ecosystem Management: Science for Governing Towards a Sustainable Future, Aquatic Ecology Series. Springer International Publishing, Cham, pp. 151–169. https://doi.org/10.1007/978-3-319-73250-3_8

Heckmann, T., Schwanghart, W., 2013. Geomorphic coupling and sediment connectivity in an alpine catchment—Exploring sediment cascades using graph theory. Geomorphology 182, 89–103.

Heckmann, T., Schwanghart, W., Phillips, J.D., 2015. Graph theory—Recent developments of its application in geomorphology. Geomorphology 243, 130–146. https://doi.org/10.1016/j.geomorph.2014.12.024

Hedger, R.D., Dodson, J.J., Bourque, J.-F., Bergeron, N.E., Carbonneau, P.E., 2006. Improving models of juvenile Atlantic salmon habitat use through high resolution remote sensing. Ecological Modelling 197, 505–511. https://doi.org/10.1016/j.ecolmodel.2006.03.028

Heinemarm, H.G., 1981. A NEW SEDIMENT TRAP EFFICIENCY CURVE FOR SMALL RESERVOIRS. J Am Water Resources Assoc 17, 825–830. https://doi.org/10.1111/j.1752-1688.1981.tb01304.x

Heino, J., Virkkala, R., Toivonen, H., 2009. Climate change and freshwater biodiversity: detected patterns, future trends and adaptations in northern regions. Biological Reviews 84, 39–54. https://doi.org/10.1111/j.1469-185X.2008.00060.x

Helfman, G.S., 2007. Fish conservation: a guide to understanding and restoring global aquatic biodiversity and fishery resources. Island Press.

Hermoso, V., Clavero, M., Filipe, A.F., 2021. An accessible optimisation method for barrier removal planning in stream networks. Science of The Total Environment 752, 141943.

Herrera, P.A., Marazuela, M.A., Hofmann, T., 2022. Parameter estimation and uncertainty analysis in hydrological modeling. WIREs Water 9. https://doi.org/10.1002/wat2.1569

Hey, R.D., 1988. Bar form resistance in gravel-bed rivers. Journal of Hydraulic Engineering 114, 1498–1508.

Hey, R.D., 1979. Flow resistance in gravel-bed rivers. Journal of the Hydraulics Division 105, 365–379.

Hey, R.D., Thorne, C.R., 1986. Stable channels with mobile gravel beds. Journal of Hydraulic engineering 112, 671–689.

Heyman, J., Bohorquez, P., Ancey, C., 2016. Entrainment, motion, and deposition of coarse particles transported by water over a sloping mobile bed. J. Geophys. Res. Earth Surf. 121, 1931–1952. https://doi.org/10.1002/2015JF003672

Hill, G., Maddock, I., Bickerton, M., 2008. River habitat mapping: are surface flow type habitats biologically distinct?

Hill, N., Trueman, J., Prévost, A., Fraser, D., Ardren, W., Grant, J., 2019. Effect of dam removal on habitat use by spawning Atlantic salmon. Journal of Great Lakes Research 45. https://doi.org/10.1016/j.jglr.2019.01.002

Hoey, T.B., Ferguson, R., 1994. Numerical simulation of downstream fining by selective transport in gravel bed rivers: Model development and illustration. Water resources research 30, 2251–2260.

Holder, A.J., Rowe, R., McNamara, N.P., Donnison, I.S., McCalmont, J.P., 2019. Soil & Water Assessment Tool (SWAT) simulated hydrological impacts of land use change from temperate grassland to energy crops: A case study in western UK [WWW Document]. GCB Bioenergy. https://doi.org/10.1111/gcbb.12628

Hollaway, M.J., Beven, K.J., Benskin, C.McW.H., Collins, A.L., Evans, R., Falloon, P.D., Forber, K.J., Hiscock, K.M., Kahana, R., Macleod, C.J.A., Ockenden, M.C., Villamizar, M.L., Wearing, C., Withers, P.J.A., Zhou, J.G., Barber, N.J., Haygarth, P.M., 2018. The challenges of modelling phosphorus in a headwater catchment: Applying a 'limits of acceptability' uncertainty framework to a water quality model. Journal of Hydrology 558, 607–624. https://doi.org/10.1016/j.jhydrol.2018.01.063

Hollis, D., McCarthy, M., Kendon, M., Legg, T., Simpson, I., 2019. HadUK-Grid gridded climate observations on a 1km grid over the UK, v1. 0.1. 0 (1862-2017). Centre for Environmental Data Analysis 14.

Hooke, J., 2003. Coarse sediment connectivity in river channel systems: a conceptual framework and methodology. Geomorphology 56, 79–94.

Horton, P., Schaefli, B., Kauzlaric, M., 2021. Why do we have so many different hydrological models? A review based on the case of Switzerland.

Houbrechts, G., Levecq, Y., Peeters, A., Hallot, E., Van Campenhout, J., Denis, A.-C., Petit, F., 2015. Evaluation of long-term bedload virtual velocity in gravel-bed rivers (Ardenne, Belgium). Geomorphology, Emerging geomorphic approaches to guide river management practices 251, 6–19. https://doi.org/10.1016/j.geomorph.2015.05.012

Hough, R.L., 2014. Biodiversity and human health: evidence for causality? Biodiversity and conservation 23, 267–288.

Howard, A.J., Coulthard, T.J., Knight, D., 2017. The potential impact of green agendas on historic river landscapes: Numerical modelling of multiple weir removal in the Derwent Valley Mills world heritage site, UK. Geomorphology 293, 37–52. https://doi.org/10.1016/j.geomorph.2017.05.009

Huang, S., Shah, H., Naz, B.S., Shrestha, N., Mishra, V., Daggupati, P., Ghimire, U., Vetter, T., 2020. Impacts of hydrological model calibration on projected hydrological changes under climate change—a multi-model assessment in three large river basins. Climatic Change 163, 1143–1164.

Hubbell, D.W., 1987. Bed load sampling and analysis. Sediment Transport in Gravel-Bed Rivers. John Wiley and Sons New York. 1987. p 89-118, 8 fig, 1 tab, 12 ref.

Hurrell, J.W., 1995. Decadal Trends in the North Atlantic Oscillation: Regional Temperatures and Precipitation. Science 269, 676–679. https://doi.org/10.1126/science.269.5224.676

Hurrell, J.W., Van Loon, H., 1997. Decadal Variations in Climate Associated with the North Atlantic Oscillation, in: Diaz, H.F., Beniston, M., Bradley, R.S. (Eds.), Climatic Change at High Elevation Sites. Springer Netherlands, Dordrecht, pp. 69–94. https://doi.org/10.1007/978-94-015-8905-5_4

Ibàñez, C., Prat, N., Canicio, A., 1996. Changes in the hydrology and sediment transport produced by large dams on the lower Ebro river and its estuary. Regulated Rivers: Research & Management 12, 51–62. https://doi.org/10.1002/(SICI)1099-1646(199601)12:1<51::AID-RRR376>3.0.CO;2-I

Ibbeken, H., Schleyer, R., 1986. Photo-sieving: A method for grain-size analysis of coarse-grained, unconsolidated bedding surfaces. Earth Surf. Process. Landforms 11, 59–77. https://doi.org/10.1002/esp.3290110108

Ibbeken, H., Warnke, D.A., Diepenbroek, M., 1998. Granulometric study of the Hanaupah Fan, Death Valley, California. Earth Surface Processes and Landforms: The Journal of the British Geomorphological Group 23, 481–492.

Ickes, B.S., Vallazza, J., Kalas, J., Knights, B., 2005. River floodplain connectivity and lateral fish passage: a literature review. US Fish and Wildlife Service, Mark Twain Wildlife Refuge Complex.

Ingram, J.A., 1978. The Permo-Triassic Sandstone Aquifers of North Cumbria. Hydrogeological Report No 19.

Iriondo, M.H., 1972. A rapid method for size analysis of coarse sediments. Journal of Sedimentary Research 42, 985–986.

Ishiyama, N., Ryo, M., Kataoka, T., Nagayama, S., Sueyoshi, M., Terui, A., Mori, T., Akasaka, T., Nakamura, F., 2018. Predicting the ecological impacts of large-dam removals on a river network based on habitat-network structure and flow regimes. Conservation Biology 32, 1403–1413.

Itsukushima, R., 2021. Relationship between watershed scale macroinvertebrate community and environmental factors in the Japanese archipelago. Limnologica 87, 125844. https://doi.org/10.1016/j.limno.2020.125844

Jaeger, K.L., Olden, J.D., Pelland, N.A., 2014. Climate change poised to threaten hydrologic connectivity and endemic fishes in dryland streams. Proceedings of the National Academy of Sciences 111, 13894–13899.

Jahandideh-Tehrani, M., Helfer, F., Zhang, H., Jenkins, G., Yu, Y., 2020. Hydrodynamic modelling of a flood-prone tidal river using the 1D model MIKE HYDRO River: calibration and sensitivity analysis. Environ Monit Assess 192, 97. https://doi.org/10.1007/s10661-019-8049-0

Jain, V., Tandon, S.K., 2010. Conceptual assessment of (dis)connectivity and its application to the Ganga River dispersal system. Geomorphology 118, 349–358. https://doi.org/10.1016/j.geomorph.2010.02.002

Janssen, J.A.M., Rodwell, J.S., Criado, M.G., Arts, G.H.P., Bijlsma, R.J., Schaminee, J.H.J., 2016. European red list of habitats: Part 2. Terrestrial and freshwater habitats. European Union.

Jarihani, A.A., Callow, J.N., McVicar, T.R., Van Niel, T.G., Larsen, J.R., 2015. Satellite-derived Digital Elevation Model (DEM) selection, preparation and correction for hydrodynamic modelling in large, low-gradient and data-sparse catchments. Journal of Hydrology 524, 489–506. https://doi.org/10.1016/j.jhydrol.2015.02.049

Jayakrishnan, R., Srinivasan, R., Santhi, C., Arnold, J.G., 2005. Advances in the application of the SWAT model for water resources management. Hydrological Processes: An International Journal 19, 749–762.

Jeong, J., Kannan, N., Arnold, J.G., Glick, R., Gosselink, L., Srinivasan, R., Harmel, R.D., 2011. Development of sub-daily erosion and sediment transport algorithms for SWAT. Transactions of the ASABE 54, 1685–1691.

Jodar-Abellan, A., Valdes-Abellan, J., Pla, C., Gomariz-Castillo, F., 2019. Impact of land use changes on flash flood prediction using a sub-daily SWAT model in five Mediterranean ungauged watersheds (SE Spain). Science of the Total Environment 657, 1578–1591.

Johnston, J.M., Barber, M.C., Wolfe, K., Galvin, M., Cyterski, M., Parmar, R., 2017. An integrated ecological modeling system for assessing impacts of multiple

stressors on stream and riverine ecosystem services within river basins. Ecological Modelling 354, 104–114. https://doi.org/10.1016/j.ecolmodel.2017.03.021

Jones, J., Börger, L., Tummers, J., Jones, P., Lucas, M., Kerr, J., Kemp, P., Bizzi, S., Consuegra, S., Marcello, L., 2019. A comprehensive assessment of stream fragmentation in Great Britain. Science of the total environment 673, 756–762.

Jones, J.I., Murphy, J.F., Collins, A.L., Sear, D.A., Naden, P.S., Armitage, P.D., 2012. The impact of fine sediment on macro-invertebrates. River research and applications 28, 1055–1071.

Joyce, H.M., Hardy, R.J., Warburton, J., Large, A.R.G., 2018. Sediment continuity through the upland sediment cascade: geomorphic response of an upland river to an extreme flood event. Geomorphology 317, 45–61. https://doi.org/10.1016/j.geomorph.2018.05.002

Joyce, H.M., Warburton, J., Hardy, R.J., 2020. A catchment scale assessment of patterns and controls of historic 2D river planform adjustment. Geomorphology 354, 107046.

Jungwirth, M., Muhar, S., Schmutz, S., 2000. Fundamentals of fish ecological integrity and their relation to the extended serial discontinuity concept. Hydrobiologia 422, 85–97.

Juracek, K.E., 1999. Geomorphic effects of overflow dams on the lower Neosho River, Kansas. US Department of the Interior, US Geological Survey.

Kapoor, K., 2021. Climate change and biodiversity loss must be tackled together - report [WWW Document]. Reuters. URL https://www.reuters.com/business/environment/climate-change-biodiversity-loss-must-be-tackled-together-report-2021-06-10/ (accessed 7.7.21).

Keesstra, S., Nunes, J.P., Saco, P., Parsons, T., Poeppl, R., Masselink, R., Cerdà, A., 2018. The way forward: Can connectivity be useful to design better measuring and modelling schemes for water and sediment dynamics? Science of The Total Environment 644, 1557–1572. https://doi.org/10.1016/j.scitotenv.2018.06.342

Keller, V.D.J., Tanguy, M., Prosdocimi, I., Terry, J.A., Hitt, O., Cole, S.J., Fry, M., Morris, D.G., Dixon, H., 2015. CEH-GEAR: 1 km resolution daily and monthly areal rainfall estimates for the UK for hydrological and other applications. Earth System Science Data 7, 143–155. https://doi.org/10.5194/essd-7-143-2015

Kellerhals, R., Bray, D.I., 1971. Sampling procedures for coarse fluvial sediments. Journal of the Hydraulics Division 97, 1165–1180.

Kerr, J.R., Vowles, A.S., Crabb, M.C., Kemp, P.S., 2021. Selective fish passage: Restoring habitat connectivity without facilitating the spread of a non-native species. Journal of Environmental Management 279, 110908. https://doi.org/10.1016/j.jenvman.2020.110908

Khan, S., Fryirs, K., Bizzi, S., 2021. Modelling sediment (dis) connectivity across a river network to understand locational-transmission-filter sensitivity for identifying hotspots of potential geomorphic adjustment. Earth Surface Processes and Landforms 46, 2856–2869.

Khayyun, T.S., Alwan, I.A., Hayder, A.M., 2019. Hydrological model for Hemren dam reservoir catchment area at the middle River Diyala reach in Iraq using ArcSWAT model. Applied Water Science 9, 1–15.

Kiesel, J., Guse, B., Bormann, H., 2019. Projecting the Consequences of Climate Change on River Ecosystems, in: Multiple Stressors in River Ecosystems. Elsevier, pp. 281–301. https://doi.org/10.1016/B978-0-12-811713-2.00016-9

King, S., O'Hanley, J.R., 2016. Optimal fish passage barrier removal—revisited. River Research and Applications 32, 418–428.

Kirchner, J.W., Dietrich, W.E., Iseya, F., Ikeda, H., 1990. The variability of critical shear stress, friction angle, and grain protrusion in water-worked sediments. Sedimentology 37, 647–672.

Kleinhans, M.G., Ferguson, R.I., Lane, S.N., Hardy, R.J., 2013. Splitting rivers at their seams: bifurcations and avulsion. Earth surface processes and landforms 38, 47–61.

Knighton, D., 2014. Fluvial forms and processes: a new perspective. Routledge.

Koci, J., Jarihani, B., Leon, J.X., Sidle, R.C., Wilkinson, S.N., Bartley, R., 2017. Assessment of UAV and Ground-Based Structure from Motion with Multi-View Stereo Photogrammetry in a Gullied Savanna Catchment. ISPRS International Journal of Geo-Information 6, 328. https://doi.org/10.3390/ijgi6110328

Koczot, K.M., Markstrom, S.L., Hay, L.E., 2011. Effects of baseline conditions on the simulated hydrologic response to projected climate change. Earth Interactions 15, 1–23.

Koiter, A.J., Owens, P.N., Petticrew, E.L., Lobb, D.A., 2013. The behavioural characteristics of sediment properties and their implications for sediment fingerprinting as an approach for identifying sediment sources in river basins. Earth-Science Reviews 125, 24–42. https://doi.org/10.1016/j.earscirev.2013.05.009

Kondolf, G.M., 1997. PROFILE: hungry water: effects of dams and gravel mining on river channels. Environmental management 21, 533–551.

Kondolf, G.M., Boulton, A.J., O'Daniel, S., Poole, G.C., Rahel, F.J., Stanley, E.H., Wohl, E., Bång, A., Carlstrom, J., Cristoni, C., 2006. Process-based ecological river restoration: visualizing three-dimensional connectivity and dynamic vectors to recover lost linkages. Ecology and society 11.

Kondolf, G.M., Gao, Y., Annandale, G.W., Morris, G.L., Jiang, E., Zhang, J., Cao, Y., Carling, P., Fu, K., Guo, Q., Hotchkiss, R., Peteuil, C., Sumi, T., Wang, H.-W., Wang, Z., Wei, Z., Wu, B., Wu, C., Yang, C.T., 2014a. Sustainable sediment management in reservoirs and regulated rivers: Experiences from five continents. Earth's Future 2, 256–280. https://doi.org/10.1002/2013EF000184

Kondolf, G.M., Gao, Y., Annandale, G.W., Morris, G.L., Jiang, E., Zhang, J., Cao, Y., Carling, P., Fu, K., Guo, Q., Hotchkiss, R., Peteuil, C., Sumi, T., Wang, H.-W., Wang, Z., Wei, Z., Wu, B., Wu, C., Yang, C.T., 2014b. Sustainable sediment management in reservoirs and regulated rivers: Experiences from five continents. Earth's Future 2, 256–280. https://doi.org/10.1002/2013EF000184

Kondolf, G.M., Piégay, H. (Eds.), 2003. Tools in fluvial geomorphology. J. Wiley, Hoboken, NJ, USA.

Krumbein, W.C., Aberdeen, E., 1937. The Sediments of Barataria Bay 15.

Krysanova, V., Vetter, T., Eisner, S., Huang, S., Pechlivanidis, I., Strauch, M., Gelfan, A., Kumar, R., Aich, V., Arheimer, B., Chamorro, A., van Griensven, A., Kundu, D., Lobanova, A., Mishra, V., Plötner, S., Reinhardt, J., Seidou, O., Wang, X., Wortmann, M., Zeng, X., Hattermann, F.F., 2017. Intercomparison of regional-scale hydrological models and climate change impacts projected for 12 large river basins worldwide—a synthesis. Environ. Res. Lett. 12, 105002. https://doi.org/10.1088/1748-9326/aa8359

Kuemmerlen, M., Reichert, P., Siber, R., Schuwirth, N., 2019. Ecological assessment of river networks: From reach to catchment scale. Science of The Total Environment 650, 1613–1627. https://doi.org/10.1016/j.scitotenv.2018.09.019

Kumar, S., Singh, A., Shrestha, D.P., 2016. Modelling spatially distributed surface runoff generation using SWAT-VSA: a case study in a watershed of the north-west Himalayan landscape. Modeling earth systems and environment 2.

“Land Cover Map-2015,” 2018. Great Britain Vector [ESRI Shapefile geospatial data] [WWW Document]. URL http://digimap.edina.ac.uk (accessed 4.16.21).

Lane, S.N., Reid, S.C., Tayefi, V., Yu, D., Hardy, R.J., 2008. Reconceptualising coarse sediment delivery problems in rivers as catchment-scale and diffuse. Geomorphology 98, 227–249.

Lang, N., Irniger, A., Rozniak, A., Hunziker, R., Wegner, J.D., Schindler, K., 2021. GRAINet: mapping grain size distributions in river beds from UAV images with convolutional neural networks. Hydrology and Earth System Sciences 25, 2567–2597. https://doi.org/10.5194/hess-25-2567-2021

Langhammer, J., Lendzioch, T., Miřijovský, J., Hartvich, F., 2017. UAV-based optical granulometry as tool for detecting changes in structure of flood depositions. Remote Sensing 9, 240.

Large, A.R., Boon, P.J., Raven, P.J., 2012. Current and future challenges in managing natural system variability for river conservation in European river basins. River Conservation and Management 381–401.

Leaniz, C.G. de, 2008. Weir removal in salmonid streams: implications, challenges and practicalities. Hydrobiologia 609, 83–96. https://doi.org/10.1007/s10750-008-9397-x

Lee, K.N., Lawrence, J., 1985. Adaptive management: learning from the Columbia River basin fish and wildlife program. Envtl. L. 16, 431.

Lehner, B., Liermann, C.R., Revenga, C., Vörösmarty, C., Fekete, B., Crouzet, P., Döll, P., Endejan, M., Frenken, K., Magome, J., Nilsson, C., Robertson, J.C., Rödel, R., Sindorf, N., Wisser, D., 2011. High-resolution mapping of the world’s reservoirs and dams for sustainable river-flow management. Frontiers in Ecology and the Environment 9, 494–502. https://doi.org/10.1890/100125

Lepesqueur, J., Hostache, R., Martínez-Carreras, N., Montargès-Pelletier, E., Hissler, C., 2019. Sediment transport modelling in riverine environments: on the importance of grain-size distribution, sediment density, and suspended sediment concentrations at the upstream boundary. Hydrol. Earth Syst. Sci. 23, 3901–3915. https://doi.org/10.5194/hess-23-3901-2019

Lesschen, J.P., Schoorl, J.M., Cammeraat, L.H., 2009. Modelling runoff and erosion for a semi-arid catchment using a multi-scale approach based on hydrological connectivity. Geomorphology 109, 174–183.

Leta, O.T., van Griensven, A., Bauwens, W., 2017. Effect of single and multisite calibration techniques on the parameter estimation, performance, and output of a SWAT model of a spatially heterogeneous catchment. Journal of Hydrologic Engineering 22, 05016036.

Lewis, L.H., Atkinson, A., 2020. Engineering Timelines - Haweswater Aqueduct [WWW Document]. URL http://www.engineering-timelines.com/scripts/engineeringItem.asp?id=888 (accessed 4.25.21).

Li, G., West, A.J., Densmore, A.L., Hammond, D.E., Jin, Z., Zhang, F., Wang, J., Hilton, R.G., 2016. Connectivity of earthquake-triggered landslides with the fluvial network: Implications for landslide sediment transport after the 2008 Wenchuan earthquake. Journal of Geophysical Research: Earth Surface 121, 703–724. https://doi.org/10.1002/2015JF003718

Liébault, F., 2003. Les rivières torrentielles des montagnes drômoises: évolution contemporaine et fonctionnement géomorphologique actuel (massifs du Diois et des Baronnies). Lyon 2.

Lisle, T.E., 1995. Particle size variations between bed load and bed material in natural gravel bed channels. Water Resources Research 31, 1107–1118.

Lisle, T.E., 1989. Sediment transport and resulting deposition in spawning gravels, north coastal California. Water resources research 25, 1303–1319.

Lisle, T.E., Hilton, S., 1992. The volume of fine sediment in pools: an index of sediment supply in gravel-bed streams1. JAWRA Journal of the American Water Resources Association 28, 371–383.

Logsdon, R.A., Chaubey, I., 2013. A quantitative approach to evaluating ecosystem services. Ecological Modelling 257, 57–65.

Lovgren, S., 2020. European rivers are stuffed with barriers, but a movement grows to remove them [WWW Document]. Environment. URL https://www.nationalgeographic.com/environment/article/european-rivers-littered-with-barricades-but-movement-grows-to-remove-them (accessed 4.6.21).

Lucas, M.C., Bubb, D.H., JANG, M.-H., Ha, K., Masters, J.E., 2009. Availability of and access to critical habitats in regulated rivers: Effects of low-head barriers on threatened lampreys. Freshwater Biology 54, 621–634.

Maddock, I., 1999. The importance of physical habitat assessment for evaluating river health. Freshwater Biology 41, 373–391. https://doi.org/10.1046/j.1365-2427.1999.00437.x

Madej, M.A., Sutherland, D.G., Lisle, T.E., Pryor, B., 2009. Channel responses to varying sediment input: A flume experiment modeled after Redwood Creek, California. Geomorphology 103, 507–519.

Magilligan, F.J., Graber, B.E., Nislow, K.H., Chipman, J.W., Sneddon, C.S., Fox, C.A., 2016. River restoration by dam removal: Enhancing connectivity at watershed scales. Elem Sci Anth 4, 000108. https://doi.org/10.12952/journal.elementa.000108

Magirl, C.S., Hilldale, R.C., Curran, C.A., Duda, J.J., Straub, T.D., Domanski, M., Foreman, J.R., 2015. Large-scale dam removal on the Elwha River, Washington, USA: Fluvial sediment load. Geomorphology 246, 669–686.

Mahan, D.C., Betts, J.T., Nord, E., Van Dyke, F., Outcalt, J.M., 2021. Response of benthic macroinvertebrates to dam removal in the restoration of the Boardman River, Michigan, USA. PLoS ONE 16, e0245030. https://doi.org/10.1371/journal.pone.0245030

Major, J.J., East, A.E., O'Connor, J.E., Grant, G.E., Wilcox, A.C., Magirl, C.S., Collins, M.J., Tullos, D.D., 2017. Geomorphic responses to dam removal in the United States–a two-decade perspective. Gravel-Bed Rivers: Processes and Disasters. Wiley and Sons 355–383.

Major, J.J., O'Connor, J.E., Podolak, C.J., Keith, M.K., Grant, G.E., Spicer, K.R., Pittman, S., Bragg, H.M., Wallick, J.R., Tanner, D.Q., 2012. Geomorphic response of the Sandy River, Oregon, to removal of Marmot Dam. US Geological Survey Reston, VA.

Malby, A.R., Whyatt, J.D., Timmis, R.J., Wilby, R.L., Orr, H.G., 2007. Long-term variations in orographic rainfall: analysis and implications for upland catchments. Hydrological Sciences Journal 52, 276–291. https://doi.org/10.1623/hysj.52.2.276

Manning, R., Griffith, J.P., Pigot, T., Vernon-Harcourt, L.F., 1890. On the flow of water in open channels and pipes.

Mao, L., Lenzi, M.A., 2007. Sediment mobility and bedload transport conditions in an alpine stream. Hydrological Processes: An International Journal 21, 1882–1891.

Mao, L., Surian, N., 2010. Observations on sediment mobility in a large gravel-bed river. Geomorphology 114, 326–337. https://doi.org/10.1016/j.geomorph.2009.07.015

Marchetti, G., Bizzi, S., Belletti, B., Lastoria, B., Mariani, S., Casaioli, M., Comiti, F., Carbonneau, P., 2021. Machine learning-based grain size mapping from satellite images, in: EGU General Assembly Conference Abstracts. pp. EGU21-14945.

Marcinkevage, A.C., Herricks, E.H., 2005. A Process-Based Ecological Model for River Network Management, in: Impacts of Global Climate Change. Presented at the World Water and Environmental Resources Congress 2005, American Society of Civil Engineers, Anchorage, Alaska, United States, pp. 1–11. https://doi.org/10.1061/40792(173)598

Marcus, W.A., Fonstad, M.A., 2008. Optical remote mapping of rivers at sub-meter resolutions and watershed extents. Earth Surface Processes and Landforms: The Journal of the British Geomorphological Research Group 33, 4–24.

Markovic, D., Carrizo, S.F., Kärcher, O., Walz, A., David, J.N., 2017. Vulnerability of European freshwater catchments to climate change. Global Change Biology 23, 3567–3580.

Marks, S.D., Rutt, G.P., 1997. Fluvial sediment inputs to upland gravel bed rivers draining forested catchments: potential ecological impacts. Hydrol. Earth Syst. Sci. 1, 499–508. https://doi.org/10.5194/hess-1-499-1997

Mayes, W.M., Walsh, C.L., Bathurst, J.C., Kilsby, C.G., Quinn, P.F., Wilkinson, M.E., Daugherty, A.J., O'Connell, P.E., 2006. Monitoring a flood event in a densely instrumented catchment, the Upper Eden, Cumbria, UK. Water and Environment Journal 20, 217–226. https://doi.org/10.1111/j.1747-6593.2005.00006.x

McCabe, D.J., 2010. Rivers and streams: Life in flowing water. Nature Education.

McCluney, K.E., Poff, N.L., Palmer, M.A., Thorp, J.H., Poole, G.C., Williams, B.S., Williams, M.R., Baron, J.S., 2014. Riverine macrosystems ecology: sensitivity, resistance, and resilience of whole river basins with human alterations. Frontiers in Ecology and the Environment 12, 48–58. https://doi.org/10.1890/120367

McCully, P., 1996. Silenced rivers: The ecology and politics of large dams. Zed Books.

McKay, S.K., Cooper, A.R., Diebel, M.W., Elkins, D., Oldford, G., Roghair, C., Wieferich, D., 2017. Informing watershed connectivity barrier prioritization decisions: a synthesis. River research and Applications 33, 847–862.

McKay, S.K., Schramski, J.R., Conyngham, J.N., Fischenich, J.C., 2013. Assessing upstream fish passage connectivity with network analysis. Ecological applications 23, 1396–1409.

McKie, R., 2019. 'To save our fish, we must first find ways to unblock UK's rivers,' say scientists [WWW Document]. the Guardian. URL http://www.theguardian.com/environment/2019/sep/01/to-save-fish-unblock-uk-rivers-swansea-university-scientists (accessed 4.6.21).

McLain, R.J., Lee, R.G., 1996. Adaptive management: promises and pitfalls. Environmental management 20, 437–448.

McLaren, P., Bowles, D., 1985. The Effects of Sediment Transport on Grain-Size Distributions. SEPM JSR Vol. 55. https://doi.org/10.1306/212F86FC-2B24-11D7-8648000102C1865D

Mellado-Díaz, A., Sánchez-González, J.R., Guareschi, S., Magdaleno, F., Toro Velasco, M., 2019. Exploring longitudinal trends and recovery gradients in macroinvertebrate communities and biomonitoring tools along regulated rivers. Science of The Total Environment 695, 133774. https://doi.org/10.1016/j.scitotenv.2019.133774

Met Office, 2006. MIDAS: UK Hourly Weather Observation Data. NCAS British Atmospheric Data Centre [WWW Document]. URL https://catalogue.ceda.ac.uk/uuid/916ac4bbc46f7685ae9a5e10451bae7c (accessed 4.16.21).

Meyer, J.L., Wallace, J.B., 2001. Lost linkages and lotic ecology: rediscovering small streams., in: Ecology: Achievement and Challenge: The 41st Symposium of the British Ecological Society Sponsored by the Ecological Society of America Held at Orlando, Florida, USA, 10-13 April 2000. Blackwell Science, pp. 295–317.

Meyer-Peter, E., Müller, R., 1948. Formulas for bed-load transport, in: IAHSR 2nd Meeting, Stockholm, Appendix 2. IAHR.

Milhous, R.T., 1973. Sediment transport in a gravel-bottomed stream.

Miller, J.D., Kjeldsen, T.R., Hannaford, J., Morris, D.G., 2013. A hydrological assessment of the November 2009 floods in Cumbria, UK. Hydrology Research 44, 180–197. https://doi.org/10.2166/nh.2012.076

Milliman, J.D., Meade, R.H., 1983. World-wide delivery of river sediment to the oceans. The Journal of Geology 91, 1–21.

Minshall, G.W., Cummins, K.W., Petersen, R.C., Cushing, C.E., Bruns, D.A., Sedell, J.R., Vannote, R.L., 1985. Developments in Stream Ecosystem Theory. Canadian Journal of Fisheries and Aquatic Sciences 42, 1045–1055. https://doi.org/10.1139/f85-130

Molinas, A., Wu, B., 2000. Comparison of fractional bed-material load computation methods in sand-bed channels. Earth Surface Processes and Landforms: The Journal of the British Geomorphological Research Group 25, 1045–1068.

Monteith, J.L., 1965. Evaporation and environment, in: Symposia of the Society for Experimental Biology. Cambridge University Press (CUP) Cambridge, pp. 205–234.

Montgomery, D.R., 1999. Process Domains and the River Continuum1. JAWRA Journal of the American Water Resources Association 35, 397–410. https://doi.org/10.1111/j.1752-1688.1999.tb03598.x

Montgomery, D.R., Abbe, T.B., Buffington, J.M., Peterson, N.P., Schmidt, K.M., Stock, J.D., 1996. Distribution of bedrock and alluvial channels in forested mountain drainage basins. Nature 381, 587–589.

Montgomery, D.R., Buffington, J.M., 1997. Channel-reach morphology in mountain drainage basins. Geological Society of America Bulletin 109, 596–611. https://doi.org/10.1130/0016-7606(1997)109<0596:CRMIMD>2.3.CO;2

Morita, K., Yamamoto, S., 2002. Effects of Habitat Fragmentation by Damming on the Persistence of Stream-Dwelling Charr Populations. Conservation Biology 16, 1318–1323. https://doi.org/10.1046/j.1523-1739.2002.01476.x

Moseley, F., 1986. Geology and Scenery in the Lake District. Macmillan International Higher Education.

Mueller, E.R., 2005. Morphologically based model of bed load transport capacity in a headwater stream. J. Geophys. Res. 110, F02016. https://doi.org/10.1029/2003JF000117

Mueller, E.R., Pitlick, J., Nelson, J.M., 2005. Variation in the reference Shields stress for bed load transport in gravel-bed streams and rivers. Water Resources Research 41. https://doi.org/10.1029/2004WR003692

Mueller, M., Pander, J., Geist, J., 2011. The effects of weirs on structural stream habitat and biological communities. Journal of Applied Ecology 48, 1450–1461. https://doi.org/10.1111/j.1365-2664.2011.02035.x

Mulligan, M., van Soesbergen, A., Sáenz, L., 2020. GOODD, a global dataset of more than 38,000 georeferenced dams. Sci Data 7, 31. https://doi.org/10.1038/s41597-020-0362-5

Mwangi, J.K., Shisanya, C.A., Gathenya, J.M., Namirembe, S., Moriasi, D.N., 2015. A modeling approach to evaluate the impact of conservation practices on water and sediment yield in Sasumua Watershed, Kenya. Journal of Soil and Water Conservation 70, 75–90.

Naiman, R.J., Decamps, H., McClain, M.E., Likens, G.E., 2005. Catchments and the physical template. Riparia: ecology, conservation, and management of streamside communities 19–48.

Naseer, A., Koike, T., Rasmy, M., Ushiyama, T., Shrestha, M., 2019. Distributed Hydrological Modeling Framework for Quantitative and Spatial Bias Correction for Rainfall, Snowfall, and Mixed-Phase Precipitation Using Vertical Profile of Temperature. Journal of Geophysical Research: Atmospheres 124, 4985–5009. https://doi.org/10.1029/2018JD029811

Nash, D.B., 1994. Effective Sediment-Transporting Discharge from Magnitude-Frequency Analysis. The Journal of Geology 102, 79–95.

Nash, J.E., Sutcliffe, J.V., 1970. River flow forecasting through conceptual models part I — A discussion of principles. Journal of Hydrology 10, 282–290. https://doi.org/10.1016/0022-1694(70)90255-6

National River Flow Archive, 2021. NRFA Station Data for 76003 - Eamont at Udford [WWW Document]. National River Flow Archive. URL https://nrfa.ceh.ac.uk/data/station/info/76003 (accessed 4.16.21).

Nazari-Sharabian, M., Taheriyoun, M., Karakouzian, M., 2020. Sensitivity analysis of the DEM resolution and effective parameters of runoff yield in the SWAT model: a case study. Journal of Water Supply: Research and Technology-Aqua 69, 39–54. https://doi.org/10.2166/aqua.2019.044

Neitsch, S.L., Arnold, J.G., Kiniry, J.R., Williams, J.R., 2011. Soil and water assessment tool theoretical documentation version 2009. Texas Water Resources Institute.

Nelson, J.M., Bennett, J.P., Wiele, S.M., 2003. Flow and sediment-transport modeling. Tools in fluvial geomorphology 539–576.

Nelson, J.M., Shimizu, Y., Takebayashi, H., McDonald, R.R., 2010. The international river interface cooperative: public domain software for river modeling, in: 2nd Joint Federal Interagency Conference, Las Vegas, June. Citeseer.

Neraas, L.P., Spruell, P., 2001. Fragmentation of riverine systems: the genetic effects of dams on bull trout (Salvelinus confluentus) in the Clark Fork River system. Molecular Ecology 10, 1153–1164. https://doi.org/10.1046/j.1365-294X.2001.01269.x

Newson, M., 2008. Land, water and development: sustainable and adaptive management of rivers. Routledge.

Newson, M.D., Clark, M.J., 2008. Uncertainty and the sustainable management of restored rivers. Wiley: Chichester, UK.

Newson, M.D., Newson, C.L., 2000. Geomorphology, ecology and river channel habitat: mesoscale approaches to basin-scale challenges. Progress in Physical Geography: Earth and Environment 24, 195–217. https://doi.org/10.1177/030913330002400203

Nguyen, H.H., Recknagel, F., Meyer, W., Frizenschaf, J., Ying, H., Gibbs, M.S., 2019. Comparison of the alternative models SOURCE and SWAT for predicting catchment streamflow, sediment and nutrient loads under the effect of land use changes. Science of The Total Environment 662, 254–265. https://doi.org/10.1016/j.scitotenv.2019.01.286

Nicholson, A.R., Wilkinson, M.E., O'Donnell, G.M., Quinn, P.F., 2012. Runoff attenuation features: a sustainable flood mitigation strategy in the Belford catchment, UK. Area 44, 463–469.

Nicholson, N., 2015. The Dambuilders - The Destruction of Mardale and the Building of the Haweswater Dam. Bookcase.

Nilsson, C., 2005. Fragmentation and Flow Regulation of the World's Large River Systems. Science 308, 405–408. https://doi.org/10.1126/science.1107887

Nilsson, C., Sarneel, J.M., Palm, D., Gardeström, J., Pilotto, F., Polvi, L.E., Lind, L., Holmqvist, D., Lundqvist, H., 2017. How do biota respond to additional physical restoration of restored streams? Ecosystems 20, 144–162.

Norman, L.M., Villarreal, M.L., Lara-Valencia, F., Yuan, Y., Nie, W., Wilson, S., Amaya, G., Sleeter, R., 2012. Mapping socio-environmentally vulnerable populations access and exposure to ecosystem services at the U.S.–Mexico borderlands. Applied Geography 34, 413–424. https://doi.org/10.1016/j.apgeog.2012.01.006

Norris, R.H., Thoms, M.C., 1999. What is river health? Freshwater Biology 41, 197–209. https://doi.org/10.1046/j.1365-2427.1999.00425.x

Null, S.E., Medellín-Azuara, J., Escriva-Bou, A., Lent, M., Lund, J.R., 2014. Optimizing the dammed: Water supply losses and fish habitat gains from dam removal in California. Journal of Environmental Management 136, 121–131. https://doi.org/10.1016/j.jenvman.2014.01.024

O'Brien, M.P., Rindlaub, B.D., 1934. The transportation of bed-load by streams. Eos, Transactions American Geophysical Union 15, 593–603.

Ogston, L., Gidora, S., Foy, M., Rosenfeld, J., 2015. Watershed-scale effectiveness of floodplain habitat restoration for juvenile coho salmon in the Chilliwack River, British Columbia. Canadian Journal of Fisheries and Aquatic Sciences 72, 479–490.

Ormerod, S.J., 2009. Climate change, river conservation and the adaptation challenge. John Wiley & Sons, Ltd. Chichester, UK.

Orr, C.H., Rogers, K.L., Stanley, E.H., 2006. Channel morphology and P uptake following removal of a small dam. Journal of the North American Benthological Society 25, 556–568.

Palmer, M.A., Bernhardt, E.S., Allan, J.D., Lake, P.S., Alexander, G., Brooks, S., Carr, J., Clayton, S., Dahm, C.N., Shah, J.F., Galat, D.L., Loss, S.G., Goodwin, P., Hart, D.D., Hassett, B., Jenkinson, R., Kondolf, G.M., Lave, R., Meyer, J.L., O'donnell, T.K., Pagano, L., Sudduth, E., 2005. Standards for ecologically successful river restoration. Journal of Applied Ecology 42, 208–217. https://doi.org/10.1111/j.1365-2664.2005.01004.x

Palmer, M.A., Reidy Liermann, C.A., Nilsson, C., Flörke, M., Alcamo, J., Lake, P.S., Bond, N., 2008. Climate change and the world's river basins: anticipating

management options. Frontiers in Ecology and the Environment 6, 81–89. https://doi.org/10.1890/060148

Paola, C., Parker, G., Seal, R., Sinha, S.K., Southard, J.B., Wilcock, P.R., 1992. Downstream fining by selective deposition in a laboratory flume. Science 258, 1757–1760.

Paola, C., Seal, R., 1995. Grain Size Patchiness as a Cause of Selective Deposition and Downstream Fining. Water Resources Research 31, 1395–1407. https://doi.org/10.1029/94WR02975

Parker, G., Dhamotharan, S., Stefan, H., 1982. Model experiments on mobile, paved gravel bed streams. Water Resources Research 18, 1395–1408.

Parker, G., Klingeman, P.C., 1982. On why gravel bed streams are paved. Water Resources Research 18, 1409–1423. https://doi.org/10.1029/WR018i005p01409

Parker, G., Paola, C., Leclair, S., 2000. Probabilistic Exner sediment continuity equation for mixtures with no active layer. Journal of Hydraulic Engineering 126, 818–826.

Passalacqua, P., 2017. The Delta Connectome: A network-based framework for studying connectivity in river deltas. Geomorphology 277, 50–62.

Patriadi, A., 2021. The Influence of Sembayat Weir on Sediment Transport Rate in The Estuary of Bengawan Solo River, Indonesia. GEOMATE 20. https://doi.org/10.21660/2021.81.j2072

Pattison, I., Lane, S.N., Hardy, R.J., Reaney, S.M., 2014. The role of tributary relative timing and sequencing in controlling large floods. Water Resources Research 50, 5444–5458. https://doi.org/10.1002/2013WR014067

Pearson, S.G., Prooijen, B.C. van, Elias, E.P.L., Vitousek, S., Wang, Z.B., 2020. Sediment Connectivity: A Framework for Analyzing Coastal Sediment Transport Pathways. Journal of Geophysical Research: Earth Surface 125, e2020JF005595. https://doi.org/10.1029/2020JF005595

Peterson, G., De Leo, G.A., Hellmann, J.J., Janssen, M.A., Kinzig, A., Malcolm, J.R., O'Brien, K.L., Pope, S.E., Rothman, D.S., Shevliakova, E., 1997. Uncertainty, climate change, and adaptive management. Conservation ecology 1.

Petts, G.E., 2009. Instream Flow Science For Sustainable River Management1. JAWRA Journal of the American Water Resources Association 45, 1071–1086. https://doi.org/10.1111/j.1752-1688.2009.00360.x

Petts, G.E., 1988. Regulated rivers in the United Kingdom. Regulated Rivers: Research & Management 2, 201–220. https://doi.org/10.1002/rrr.3450020303

Petts, G.E., 1984. Sedimentation within a regulated river. Earth Surf. Process. Landforms 9, 125–134. https://doi.org/10.1002/esp.3290090204

Petts, G.E., 1980. Long-term Consequences of Upstream Impoundment. Environmental Conservation 7, 325–332. https://doi.org/10.1017/S0376892900008183

Petts, G.E., 1979. Complex response of river channel morphology subsequent to reservoir construction. Progress in Physical Geography 3, 329–362.

Pfeiffer, A.M., Barnhart, K.R., Czuba, J.A., 2020. NetworkSedimentTransporter: A Landlab component for bed material transport through river networks. Journal of Open Source Software 5, 2341.

Pike, A.S., Scatena, F.N., Wohl, E.E., 2010. Lithological and fluvial controls on the geomorphology of tropical montane stream channels in Puerto Rico. Earth Surf. Process. Landforms 35, 1402–1417. https://doi.org/10.1002/esp.1978

Pipil, S., 2018. Extract data from NetCDF files to text files (For SWAT Model). - MATLAB Answers - MATLAB Central [WWW Document]. URL https://uk.mathworks.com/matlabcentral/answers/437025-extract-data-from-netcdf-files-to-text-files-for-swat-model (accessed 4.16.21).

Pires, A.P., Srivastava, D.S., Marino, N.A., MacDonald, A.A.M., Figueiredo-Barros, M.P., Farjalla, V.F., 2018. Interactive effects of climate change and biodiversity loss on ecosystem functioning. Ecology 99, 1203–1213.

Pitlick, J., Wilcock, P., 2001. Relations between streamflow, sediment transport, and aquatic habitat in regulated rivers, in: Dorava, J.M., Montgomery, D.R., Palcsak, B.B., Fitzpatrick, F.A. (Eds.), Water Science and Application. American Geophysical Union, Washington, D. C., pp. 185–198. https://doi.org/10.1029/WS004p0185

Pizzuto, J., 2002. Effects of Dam Removal on River Form and ProcessAlthough many well-established concepts of fluvial geomorphology are relevant for evaluating the effects of dam removal, geomorphologists remain unable to forecast stream channel changes caused by the removal of specific dams. BioScience 52, 683–691. https://doi.org/10.1641/0006-3568(2002)052[0683:EODROR]2.0.CO;2

Plesiński, K., Marek, A., Skalicz, F., Radecki-Pawlik, A., 2017. ON USING BASEGRAIN COMPUTER MODEL FOR GRAIN SIZE BED LOAD ANALYSIS ON PONIKIEWKA STREAM: A PHOTOGRAPHIC METHOD APPLICATION. Acta Scientiarum Polonorum. Formatio Circumiectus 16, 107.

Podolak, C.J.P., Wilcock, P.R., 2013. Experimental study of the response of a gravel streambed to increased sediment supply. Earth Surface Processes and Landforms 38, 1748–1764.

Poeppl, R.E., Keesstra, S.D., Hein, T., 2015. The geomorphic legacy of small dams—An Austrian study. Anthropocene 10, 43–55. https://doi.org/10.1016/j.ancene.2015.09.003

Poeppl, R.E., Keesstra, S.D., Maroulis, J., 2017. A conceptual connectivity framework for understanding geomorphic change in human-impacted fluvial systems. Geomorphology, Connectivity in Geomorphology from Binghamton 2016 277, 237–250. https://doi.org/10.1016/j.geomorph.2016.07.033

Poff, N.L., Allan, J.D., Palmer, M.A., Hart, D.D., Richter, B.D., Arthington, A.H., Rogers, K.H., Meyer, J.L., Stanford, J.A., 2003. River flows and water wars: emerging science for environmental decision making. Frontiers in Ecology and the Environment 1, 298–306. https://doi.org/10.1890/1540-9295(2003)001[0298:RFAWWE]2.0.CO;2

Poff, N.L., Hart, D.D., 2002. How Dams Vary and Why It Matters for the Emerging Science of Dam Removal: An ecological classification of dams is needed to characterize how the tremendous variation in the size, operational mode, age, and number of dams in a river basin influences the potential for restoring regulated rivers via dam removal. BioScience 52, 659–668.

Poff, N.L., Ward, J.V., 1990. Physical habitat template of lotic systems: Recovery in the context of historical pattern of spatiotemporal heterogeneity. Environmental Management 14, 629. https://doi.org/10.1007/BF02394714

Polvi, L.E., Lind, L., Persson, H., Miranda-Melo, A., Pilotto, F., Su, X., Nilsson, C., 2020. Facets and scales in river restoration: Nestedness and interdependence of hydrological, geomorphic, ecological, and biogeochemical processes. Journal of Environmental Management 265, 110288. https://doi.org/10.1016/j.jenvman.2020.110288

Post, J., Conradt, T., Suckow, F., Krysanova, V., Wechsung, F., Hattermann, F.F., 2008. Integrated assessment of cropland soil carbon sensitivity to recent and future climate in the Elbe River basin. Hydrological sciences journal 53, 1043–1058.

Poulos, H.M., Chernoff, B., 2021. Monitoring the Effects of Small Dam Removal on Fish Community Composition: Removal of the Zemko Dam Along the Eightmile River, Connecticut (US). Renewing Our Rivers: Stream Corridor Restoration in Dryland Regions 350.

Priestley, C.H.B., Taylor, R.J., 1972. On the Assessment of Surface Heat Flux and Evaporation Using Large-Scale Parameters. Monthly Weather Review 100, 81–92. https://doi.org/10.1175/1520-0493(1972)100<0081:OTAOSH>2.3.CO;2

Pringle, C.M., 1997. Exploring how disturbance is transmitted upstream: going against the flow. Journal of the north american Benthological society 16, 425–438.

Pringle, C.M., Freeman, M.C., Freeman, B.J., 2000. Regional Effects of Hydrologic Alterations on Riverine Macrobiota in the New World: Tropical–Temperate Comparisons. BioScience 50, 807. https://doi.org/10.1641/0006-3568(2000)050[0807:REOHAO]2.0.CO;2

Prudhomme, C., Dadson, S., Morris, D., Williamson, J., Goodsell, G., Crooks, S., Boelee, L., Davies, H., Buys, G., Lafon, T., Watts, G., 2012. Future Flows Climate: an ensemble of 1-km climate change projections for hydrological application in Great Britain 6.

Prudhomme, C., Jakob, D., Svensson, C., 2003. Uncertainty and climate change impact on the flood regime of small UK catchments. Journal of Hydrology 277, 1–23. https://doi.org/10.1016/S0022-1694(03)00065-9

Prudhomme, C., Reynard, N., Crooks, S., 2002. Downscaling of global climate models for flood frequency analysis: where are we now? Hydrological Processes 16, 1137–1150. https://doi.org/10.1002/hyp.1054

Quinlan, E., Gibbins, C.N., Batalla, R.J., Vericat, D., 2015. Impacts of Small Scale Flow Regulation on Sediment Dynamics in an Ecologically Important Upland River. Environmental Management 55, 671–686. https://doi.org/10.1007/s00267-014-0423-7

Radcliffe, D.E., Reid, D.K., Blombäck, K., Bolster, C.H., Collick, A.S., Easton, Z.M., Francesconi, W., Fuka, D.R., Johnsson, H., King, K., Larsbo, M., Youssef, M.A., Mulkey, A.S., Nelson, N.O., Persson, K., Ramirez-Avila, J.J., Schmieder, F., Smith, D.R., 2015. Applicability of Models to Predict Phosphorus Losses in Drained Fields: A Review. Journal of Environmental Quality 44, 614–628. https://doi.org/10.2134/jeq2014.05.0220

Ranganathan, J., Raudsepp-Hearne, C., Lucas, N., Irwin, F., Zurek, M., Bennett, K., Ash, N., West, P., 2008. A Guide for Decision Makers. World Resources Institute.

Raven, P.J., 1998. River Habitat Quality: the physical character of rivers and streams in the UK and Isle of Man. Environment Agency.

Recking, A., 2016. A generalized threshold model for computing bed load grain size distribution. Water Resources Research 52, 9274–9289. https://doi.org/10.1002/2016WR018735

Recking, A., Piton, G., Vazquez-Tarrio, D., Parker, G., 2016. Quantifying the Morphological Print of Bedload Transport. Earth Surface Processes and Landforms 41, 809–822. https://doi.org/10.1002/esp.3869

Remesan, R., Holman, I.P., 2015. Effect of baseline meteorological data selection on hydrological modelling of climate change scenarios. Journal of Hydrology 528, 631–642. https://doi.org/10.1016/j.jhydrol.2015.06.026

Rice, S., 1999. The nature and controls on downstream fining within sedimentary links. Journal of Sedimentary Research 69, 32–39.

Rice, S., Church, M., 1998. Grain size along two gravel-bed rivers: statistical variation, spatial pattern and sedimentary links. Earth Surface Processes and Landforms 23, 345–363. https://doi.org/10.1002/(SICI)1096-9837(199804)23:4<345::AID-ESP850>3.0.CO;2-B

Rice, S.P., 2017. Tributary connectivity, confluence aggradation and network biodiversity. Geomorphology, Connectivity in Geomorphology from Binghamton 2016 277, 6–16. https://doi.org/10.1016/j.geomorph.2016.03.027

Richardson, D., 2002. Flood risk—the impact of climate change, in: Proceedings of the Institution of Civil Engineers-Civil Engineering. Thomas Telford Ltd, pp. 22–24.

Richter, B.D., Baumgartner, J.V., Braun, D.P., Powell, J., 1998. A spatial assessment of hydrologic alteration within a river network. Regulated rivers: research & management 14, 329–340.

Richter, B.D., Postel, S., Revenga, C., Scudder, T., Lehner, B., Churchill, A., Chow, M., 2010. Lost in development's shadow: The downstream human consequences of dams. Water alternatives 3, 14.

Rigby, P.J., Thompson, A., Butcher, J., Jones, D.E., 2016. Haweswater Reservoir: an environmental asset or an environmental liability?, in: Dams–Benefits and Disbenefits; Assets or Liabilities? Proceedings of the 19th Biennial Conference of the British Dam Society Held at Lancaster University from 7–10 September 2016. ICE Publishing, pp. 175–184.

Rinaldi, M., Belletti, B., Van de Bund, W., 2015. REstoring rivers FOR effective catchment Management.

Rinaldi, M., Surian, N., Comiti, F., Bussettini, M., 2013. A method for the assessment and analysis of the hydromorphological condition of Italian streams: The Morphological Quality Index (MQI). Geomorphology 180–181, 96–108. https://doi.org/10.1016/j.geomorph.2012.09.009

Rinaldo, A., Gatto, M., Rodriguez-Iturbe, I., 2018. River networks as ecological corridors: A coherent ecohydrological perspective. Advances in Water Resources 112, 27–58. https://doi.org/10.1016/j.advwatres.2017.10.005

Ritter, J.R., Helley, E.J., 1968. An optical method for determining particle sizes of coarse sediment.

Robert, A., 2003. River processes: an introduction to fluvial dynamics. Arnold, London : New York : Distributed in the United States by Oxford University Press.

Roberts, S.J., Gottgens, J.F., Spongberg, A.L., Evans, J.E., Levine, N.S., 2007. Assessing potential removal of low-head dams in urban settings: An example from the Ottawa River, NW Ohio. Environmental management 39, 113–124.

Robinson, E., Blyth, E., Clark, D., Comyn-Platt, E., Finch, J., Rudd, A., 2017. Climate hydrology and ecology research support system meteorology dataset for Great Britain (1961-2015)[CHESS-met] v1. 2.

Robinson, E.L., Blyth, E., Clark, D.B., Comyn-Platt, E., Finch, J., Rudd, A.C., 2016. Climate hydrology and ecology research support system meteorology dataset for Great Britain (1961-2015) [CHESS-met].

Robinson, M., Moore, R.E., Nisbet, T.R., Blackie, J.R., 1998. From moorland to forest: the Coalburn catchment experiment. Institute of Hydrology.

Romanowicz, A.A., Vanclooster, M., Rounsevell, M., La Junesse, I., 2005. Sensitivity of the SWAT model to the soil and land use data parametrisation: a case study in the Thyle catchment, Belgium. Ecological modelling 187, 27–39.

Roni, P., Hanson, K., Beechie, T., 2008. Global Review of the Physical and Biological Effectiveness of Stream Habitat Rehabilitation Techniques. North American Journal of Fisheries Management 28, 856–890. https://doi.org/10.1577/M06-169.1

Rosenberg, D.M., McCully, P., Pringle, C.M., 2000. Global-Scale Environmental Effects of Hydrological Alterations: Introduction. BioScience 50, 746–751. https://doi.org/10.1641/0006-3568(2000)050[0746:GSEEOH]2.0.CO;2

Rossi, P., Mancini, F., Dubbini, M., Mazzone, F., Capra, A., 2017. Combining nadir and oblique UAV imagery to reconstruct quarry topography: methodology and feasibility analysis. European Journal of Remote Sensing 50, 211–221. https://doi.org/10.1080/22797254.2017.1313097

Rüther, N., Huber, S., Spiller, S., Aberle, J., 2013. Verifying a photogrammetric method to quantify grain size distribution of developed armor layers, in: Proceedings of the 35th IAHR Congress, Chengdu, China.

Ruz, C., 2011. The six natural resources most drained by our 7 billion people [WWW Document]. the Guardian. URL http://www.theguardian.com/environment/blog/2011/oct/31/six-natural-resources-population (accessed 4.8.21).

Sabater, S., Bregoli, F., Acuña, V., Barceló, D., Elosegi, A., Ginebreda, A., Marcé, R., Muñoz, I., Sabater-Liesa, L., Ferreira, V., 2018. Effects of human-driven water stress on river ecosystems: a meta-analysis. Sci Rep 8, 11462. https://doi.org/10.1038/s41598-018-29807-7

Santucci, V.J., Gephard, S.R., Pescitelli, S.M., 2005. Effects of Multiple Low-Head Dams on Fish, Macroinvertebrates, Habitat, and Water Quality in the Fox River, Illinois. North American Journal of Fisheries Management 25, 975–992. https://doi.org/10.1577/M03-216.1

Schick, R.S., Lindley, S.T., 2007. Directed connectivity among fish populations in a riverine network. Journal of applied ecology 44, 1116–1126.

Schiermeier, Q., 2018. Europe is demolishing its dams to restore ecosystems. Nature 557, 290–292.

Schmidt, J., Preston, N.J., 2003. Towards quantitative modelling of landform evolution through frequency and magnitude of processes: a model conception. Concepts and modelling in geomorphology: international perspectives. Tokyo: Terrapub 115–129.

Schmidt, J.C., Wilcock, P.R., 2008. Metrics for assessing the downstream effects of dams. Water Resources Research 44. https://doi.org/10.1029/2006WR005092

Schmitt, R.J.P., 2017. CASCADE-A framework for modeling fluvial sediment connectivity and its application for designing low impact hydropower portfolios.

Schmitt, R.J.P., Bizzi, S., Castelletti, A., 2016. Tracking multiple sediment cascades at the river network scale identifies controls and emerging patterns of sediment connectivity: TRACKING MULTIPLE SEDIMENT CASCADES AT RIVER NETWORK SCALE. Water Resources Research 52, 3941–3965. https://doi.org/10.1002/2015WR018097

Schmitt, R.J.P., Bizzi, S., Castelletti, A., Kondolf, G.M., 2018a. Improved trade-offs of hydropower and sand connectivity by strategic dam planning in the Mekong. Nature Sustainability 1, 96–104. https://doi.org/10.1038/s41893-018-0022-3

Schmitt, R.J.P., Bizzi, S., Castelletti, A.F., Kondolf, G.M., 2018b. Stochastic Modeling of Sediment Connectivity for Reconstructing Sand Fluxes and Origins in the Unmonitored Se Kong, Se San, and Sre Pok Tributaries of the Mekong River: Stochastic connectivity modelling. Journal of Geophysical Research: Earth Surface 123, 2–25. https://doi.org/10.1002/2016JF004105

Schmutz, S., Hein, T., Sendzimir, J., 2018. Landmarks, Advances, and Future Challenges in Riverine Ecosystem Management. Riverine Ecosystem Management 563.

Schumm, S.A., 1977. The fluvial system. John Wiley and Sons, New York.

Schuol, J., Abbaspour, K.C., 2006. Calibration and uncertainty issues of a hydrological model (SWAT) applied to West Africa. Advances in geosciences 9, 137–143.

Schwarz, U., 2021. The potential of barrier removal to reconnect Europe's Rivers. WWF, Austria.

Sear, D.A., Newson, M.D., 1991. Sediment and gravel transportation in rivers including the use of gravel traps. Foundation for Water Research.

Sear, D.A., Newson, M.D., Brookes, A., 1995. Sediment-related river maintenance: The role of fluvial geomorphology. Earth Surf. Process. Landforms 20, 629–647. https://doi.org/10.1002/esp.3290200706

Sedell, J.R., Reeves, G.H., Hauer, F.R., Stanford, J.A., Hawkins, C.P., 1990. Role of refugia in recovery from disturbances: modern fragmented and disconnected river systems. Environmental Management 14, 711–724.

Seifert, E., Seifert, S., Vogt, H., Drew, D., van Aardt, J., Kunneke, A., Seifert, T., 2019. Influence of Drone Altitude, Image Overlap, and Optical Sensor Resolution on Multi-View Reconstruction of Forest Images. Remote Sensing 11, 1252. https://doi.org/10.3390/rs11101252

Semrau, M., Hurck, R., 2012. Multi-Purpose, interlinked and without barriers: The Emscher River ecological concept. River conservation and management 243–247.

Servat, E., Dezetter, A., 1991. Selection of calibration objective fonctions in the context of rainfall-ronoff modelling in a Sudanese savannah area. Hydrological Sciences Journal 36, 307–330.

Setegn, S.G., Srinivasan, R., Dargahi, B., 2008. Hydrological modelling in the Lake Tana Basin, Ethiopia using SWAT model. The Open Hydrology Journal 2.

Sethi, S.A., Selle, A.R., Doyle, M.W., Stanley, E.H., Kitchel, H.E., 2004. Response of unionid mussels to dam removal in Koshkonong Creek, Wisconsin (USA). Hydrobiologia 525, 157–165.

Shafroth, P.B., Friedman, J.M., Auble, G.T., Scott, M.L., Braatne, J.H., 2002. Potential Responses of Riparian Vegetation to Dam Removal: Dam removal generally causes changes to aspects of the physical environment that influence the establishment and growth of riparian vegetation. BioScience 52, 703–712. https://doi.org/10.1641/0006-3568(2002)052[0703:PRORVT]2.0.CO;2

Sharpley, A.N., Williams, J.R., 1990. EPIC-Erosion/Productivity impact calculator. I: Model documentation. II: User manual. Technical Bulletin-United States Department of Agriculture.

Shen, Z.Y., Gong, Y.W., Li, Y.H., Hong, Q., Xu, L., Liu, R.M., 2009. A comparison of WEPP and SWAT for modeling soil erosion of the Zhangjiachong Watershed in the Three Gorges Reservoir Area. Agricultural Water Management 96, 1435–1442. https://doi.org/10.1016/j.agwat.2009.04.017

Shields, A., 1936a. Anwendung der Aehnlichkeitsmechanik und der Turbulenzforschung auf die Geschiebebewegung. PhD Thesis Technical University Berlin.

Shields, A., 1936b. Application of similarity principles and turbulence research to bed-load movement.

Shih, S.-M., Komar, P.D., 1990a. Hydraulic controls of grain-size distributions of bedload gravels in Oak Creek, Oregon, USA. Sedimentology 37, 367–376. https://doi.org/10.1111/j.1365-3091.1990.tb00965.x

Shih, S.-M., Komar, P.D., 1990b. Differential bedload transport rates in a gravel-bed stream: A grain-size distribution approach. Earth Surface Processes and Landforms 15, 539–552. https://doi.org/10.1002/esp.3290150606

Shimizu, Y., Nelson, J., 2021. iRIC Software: The International River Interface Cooperative. [WWW Document]. URL https://i-ric.org/en/solvers/ (accessed 7.5.21).

Shimizu, Y., Takebayashi, H., Inoue, T., Hamaki, M., Iwasaki, T., Nabi, M., 2014. Nays2DH solver manual. International River Interface.

Sindelar, C., Schobesberger, J., Habersack, H., 2017. Effects of weir height and reservoir widening on sediment continuity at run-of-river hydropower plants in gravel bed rivers. Geomorphology, SEDIMENT DYNAMICS IN ALPINE BASINS 291, 106–115. https://doi.org/10.1016/j.geomorph.2016.07.007

Singh, V.P., Frevert, D.K., 2010. Watershed models. CRC press.

Skalak, K., Pizzuto, J., Hart, D.D., 2009. Influence of Small Dams on Downstream Channel Characteristics in Pennsylvania and Maryland: Implications for the Long-Term Geomorphic Effects of Dam Removal1. JAWRA Journal of the American Water Resources Association 45, 97–109. https://doi.org/10.1111/j.1752-1688.2008.00263.x

Skalak, K.J., Benthem, A.J., Schenk, E.R., Hupp, C.R., Galloway, J.M., Nustad, R.A., Wiche, G.J., 2013. Large dams and alluvial rivers in the Anthropocene: The impacts of the Garrison and Oahe Dams on the Upper Missouri River. Anthropocene, Geomorphology of the Anthropocene: Understanding The Surficial Legacy of Past and Present Human Activities 2, 51–64. https://doi.org/10.1016/j.ancene.2013.10.002

Škarpich, V., Galia, T., Ruman, S., Máčka, Z., 2019. Variations in bar material grain-size and hydraulic conditions of managed and re-naturalized reaches of the gravel-bed Bečva River (Czech Republic). Science of The Total Environment 649, 672–685. https://doi.org/10.1016/j.scitotenv.2018.08.329

Skorulis, A.P., 2014. The geomorphic impacts of two weirs on their fluvial systems in the Illawarra Region of New South Wales, Australia.

Sloan, P.G., Moore, I.D., 1984. Modeling subsurface stormflow on steeply sloping forested watersheds. Water Resources Research 20, 1815–1822. https://doi.org/10.1029/WR020i012p01815

Smith, R.A., 2019. Lakeland rocks. The Crowood Press Ltd.

Smithers, H., Walker, S., 1997. England as a result of the 1995-1996 drought. Sustainability of water resources under increasing uncertainty 173.

Sood, A., Smakhtin, V., 2015. Global hydrological models: a review. Hydrological Sciences Journal 60, 549–565. https://doi.org/10.1080/02626667.2014.950580

Stahl, K., Hisdal, H., Hannaford, J., Tallaksen, L., 2010. Streamflow trends in Europe: evidence from a dataset of near-natural catchments. Hydrol. Earth Syst. Sci. 17.

Stahly, S., Friedrich, H., Detert, M., 2017. Size Ratio of Fluvial Grains' Intermediate Axes Assessed by Image Processing and Square-Hole Sieving. J. Hydraul. Eng. 143, 06017005. https://doi.org/10.1061/(ASCE)HY.1943-7900.0001286

Stanford, J.A., Ward, J.V., Liss, W.J., Frissell, C.A., Williams, R.N., Lichatowich, J.A., Coutant, C.C., 1996. A general protocol for restoration of regulated rivers. Regulated Rivers: Research & Management 12, 391–413.

Stanford, J.W.J., 1983. The serial discontinuity concept of lotic ecosystems. T. D Fontaine IIIand S. M Bartell (editors). Dynamics of lotic ecosystems. Ann Arbor Science Publishers, Ann Arbor, Michigan 29–42.

Stanley, E.H., Doyle, M.W., 2003. Trading off: the ecological effects of dam removal. Frontiers in Ecology and the Environment 1, 15–22. https://doi.org/10.1890/1540-9295(2003)001[0015:TOTEEO]2.0.CO;2

Statzner, B., Sagnes, P., Champagne, J.-Y., Viboud, S., 2003. Contribution of benthic fish to the patch dynamics of gravel and sand transport in streams: Benthic Stream Fish And Erosion. Water Resour. Res. 39. https://doi.org/10.1029/2003WR002270

Stewart, E.J., Morris, D.G., Jones, D.A., Gibson, H.S., 2012. Frequency analysis of extreme rainfall in Cumbria, 16–20 November 2009. Hydrology Research 43, 649–662. https://doi.org/10.2166/nh.2012.033

Stewart, G., Grant, G., 2005. What can we learn from the removal of little dinky dams?, in: Managing Watersheds for Human and Natural Impacts: Engineering, Ecological, and Economic Challenges. pp. 1–7.

Strauch, M., Bernhofer, C., Koide, S., Volk, M., Lorz, C., Makeschin, F., 2012. Using precipitation data ensemble for uncertainty analysis in SWAT streamflow simulation. Journal of Hydrology 414–415, 413–424. https://doi.org/10.1016/j.jhydrol.2011.11.014

Summers, M.F., Holman, I.P., Grabowski, R.C., 2015. Adaptive management of river flows in Europe: A transferable framework for implementation. Journal of Hydrology 531, 696–705. https://doi.org/10.1016/j.jhydrol.2015.10.057

Sun, J., Galib, S.M., Lucas, M.C., 2021. Rapid response of fish and aquatic habitat to removal of a tidal barrier. Aquatic Conservation: Marine and Freshwater Ecosystems n/a. https://doi.org/10.1002/aqc.3576

Sutherland, A.B., Meyer, J.L., Gardiner, E.P., 2002. Effects of land cover on sediment regime and fish assemblage structure in four southern Appalachian streams. Freshwater Biology 47, 1791–1805. https://doi.org/10.1046/j.1365-2427.2002.00927.x

Swallow, B.M., Sang, J.K., Nyabenge, M., Bundotich, D.K., Duraiappah, A.K., Yatich, T.B., 2009. Tradeoffs, synergies and traps among ecosystem services in the Lake Victoria basin of East Africa. Environmental Science & Policy, Special Issue: Food Security and Environmental Change 12, 504–519. https://doi.org/10.1016/j.envsci.2008.11.003

SWAT, 2021. Soil & Water Assessment Tool [WWW Document]. URL https://swat.tamu.edu/media/90112/swat-calibration-techniques_slides.pdf (accessed 5.16.21).

Syvitski, J.P.M., Kettner, A., 2011. Sediment flux and the Anthropocene. Proc. R. Soc. A 369, 957–975. https://doi.org/10.1098/rsta.2010.0329

Takagi, S., Maeda, S., Yoshida, K., Kuroda, H., 2019. Field observation and numerical simulation of bed evolution in agricultural drainage canal with eco-friendly physical structures. Presented at the 38th IAHR World Congress, pp. 4859–4862. https://doi.org/10.3850/38WC092019-0483

Tan, M.L., Ficklin, D.L., Dixon, B., Ibrahim, A.L., Yusop, Z., Chaplot, V., 2015. Impacts of DEM resolution, source, and resampling technique on SWAT-simulated streamflow. Applied Geography 63, 357–368. https://doi.org/10.1016/j.apgeog.2015.07.014

Tang, L., Mo, K., Zhang, J., Wang, J., Chen, Q., He, S., Zhu, C., Lin, Y., 2021. Removing tributary low-head dams can compensate for fish habitat losses in dammed rivers. Journal of Hydrology 598, 126204. https://doi.org/10.1016/j.jhydrol.2021.126204

Tangi, M., 2018. Balancing sediment stravation and hydropower production, The case study of Vjosa River. Politecnico di Milano, Italy.

Tangi, M., Schmitt, R., Bizzi, S., Castelletti, A., 2019a. The CASCADE toolbox for analyzing river sediment connectivity and management. Environmental Modelling & Software 119, 400–406. https://doi.org/10.1016/j.envsoft.2019.07.008

Tangi, M., Schmitt, R., Bizzi, S., Castelletti, A., 2019b. The CASCADE toolbox for analyzing river sediment connectivity and management. Environmental Modelling & Software 119, 400–406. https://doi.org/10.1016/j.envsoft.2019.07.008

Tanguy, M., Dixon, H., Prosdocimi, I., Morris, D.G., Keller, V.D.J., 2016. Gridded estimates of daily and monthly areal rainfall for the United Kingdom (1890-2015) [CEH-GEAR].

Tanner-McAllister, S.L., Rhodes, J., Hockings, M., 2017. Managing for climate change on protected areas: An adaptive management decision making framework. Journal of environmental management 204, 510–518.

Tarboton, D.G., Bras, R.L., Rodriguez-Iturbe, I., 1991. On the extraction of channel networks from digital elevation data. Hydrological Processes 5, 81–100. https://doi.org/10.1002/hyp.3360050107

Teshager, A.D., Gassman, P.W., Secchi, S., Schoof, J.T., Misgna, G., 2016. Modeling agricultural watersheds with the Soil and Water Assessment Tool (SWAT): Calibration and validation with a novel procedure for spatially explicit HRUs. Environmental management 57, 894–911.

Tharme, R.E., 2003. A global perspective on environmental flow assessment: emerging trends in the development and application of environmental flow methodologies for rivers. River Research and Applications 19, 397–441. https://doi.org/10.1002/rra.736

Thavhana, M.P., Savage, M.J., Moeletsi, M.E., 2018. SWAT model uncertainty analysis, calibration and validation for runoff simulation in the Luvuvhu River catchment, South Africa. Physics and Chemistry of the Earth, Parts A/B/C, The 17th WaterNet/WARFSA/GWPSA Symposium: Integrated Water Resources Management: Water Security, Sustainability and Development in Eastern and Africa Southern 105, 115–124. https://doi.org/10.1016/j.pce.2018.03.012

Thomson, J. r., Taylor, M. p., Fryirs, K. a., Brierley, G. j., 2001. A geomorphological framework for river characterization and habitat assessment. Aquatic Conserv: Mar. Freshw. Ecosyst. 11, 373–389. https://doi.org/10.1002/aqc.467

Thomson, J.R., Hart, D.D., Charles, D.F., Nightengale, T.L., Winter, D.M., 2005. Effects of removal of a small dam on downstream macroinvertebrate and algal assemblages in a Pennsylvania stream. Journal of the North American Benthological Society 24, 192–207. https://doi.org/10.1899/0887-3593(2005)024<0192:EOROAS>2.0.CO;2

Tockner, K., Pennetzdorfer, D., Reiner, N., Schiemer, F., Ward, J.V., 1999. Hydrological connectivity, and the exchange of organic matter and nutrients in a dynamic river–floodplain system (Danube, Austria). Freshwater Biology 41, 521–535. https://doi.org/10.1046/j.1365-2427.1999.00399.x

Tompkins, E.L., Adger, N.W., 2003. Building resilience to climate change through adaptive management of natural resources.

Tompkins, E.L., Adger, W.N., 2004. Does adaptive management of natural resources enhance resilience to climate change? Ecology and society 9.

Tonitto, C., Riha, S.J., 2016. Planning and implementing small dam removals: lessons learned from dam removals across the eastern United States. Sustain. Water Resour. Manag. 2, 489–507. https://doi.org/10.1007/s40899-016-0062-7

Tristram, D., Hughes, D., Bradshaw, K., 2014. Accelerating a hydrological uncertainty ensemble model using graphics processing units (GPUs). Computers & Geosciences 62, 178–186. https://doi.org/10.1016/j.cageo.2013.07.011

Tullos, D.D., Finn, D.S., Walter, C., 2014. Geomorphic and Ecological Disturbance and Recovery from Two Small Dams and Their Removal. PLoS ONE 9, e108091. https://doi.org/10.1371/journal.pone.0108091

Turnbull, L., Hütt, M.-T., Ioannides, A.A., Kininmonth, S., Poeppl, R., Tockner, K., Bracken, L.J., Keesstra, S., Liu, L., Masselink, R., Parsons, A.J., 2018. Connectivity and complex systems: learning from a multi-disciplinary perspective. Appl Netw Sci 3, 1–49. https://doi.org/10.1007/s41109-018-0067-2

Turner, D., Lucieer, A., Wallace, L., 2014. Direct Georeferencing of Ultrahigh-Resolution UAV Imagery. IEEE Transactions on Geoscience and Remote Sensing 52, 2738–2745. https://doi.org/10.1109/TGRS.2013.2265295

Uchida, T., Kawahara, Y., Hayashi, Y., Tateishi, A., 2020. Eulerian Deposition Model for Sediment Mixture in Gravel-Bed Rivers with Broad Particle Size Distributions. J. Hydraul. Eng. 146, 04020071. https://doi.org/10.1061/(ASCE)HY.1943-7900.0001783

UKCEH, 2021. Ullswater - UK Lakes Portal [WWW Document]. URL https://eip.ceh.ac.uk/apps/lakes/detail.html#wbid=28955 (accessed 4.16.21).

UKCEH, 2018. Wet Sleddale Reservoir - UK Lakes Portal [WWW Document]. URL https://eip.ceh.ac.uk/apps/lakes/detail.html#wbid=29133 (accessed 4.16.21).

Ullrich, A., Volk, M., 2009. Application of the Soil and Water Assessment Tool (SWAT) to predict the impact of alternative management practices on water quality and quantity. Agricultural Water Management 96, 1207–1217. https://doi.org/10.1016/j.agwat.2009.03.010

UNEP, U.N.E.P., 2017. Why does water matter? [WWW Document]. UNEP - UN Environment Programme. URL http://www.unep.org/explore-topics/water/why-does-water-matter (accessed 4.18.21).

Vale, M., Holman, I.P., 2009. Understanding the hydrological functioning of a shallow lake system within a coastal karstic aquifer in Wales, UK. Journal of Hydrology 376, 285–294. https://doi.org/10.1016/j.jhydrol.2009.07.041

Van De Wiel, M.J., Coulthard, T.J., Macklin, M.G., Lewin, J., 2007. Embedding reach-scale fluvial dynamics within the CAESAR cellular automaton landscape evolution model. Geomorphology 90, 283–301.

Van Griensven, A., Breuer, L., Di Luzio, M., Vandenberghe, V., Goethals, P., Meixner, T., Arnold, J., Srinivasan, R., 2006. Environmental and ecological hydroinformatics to support the implementation of the European Water

Framework Directive for river basin management. Journal of Hydroinformatics 8, 239–252. https://doi.org/10.2166/hydro.2006.010

Van Looy, K., Tormos, T., Souchon, Y., 2014. Disentangling dam impacts in river networks. Ecological Indicators 37, 10–20. https://doi.org/10.1016/j.ecolind.2013.10.006

van Oldenborgh, G.J., Otto, F.E., Haustein, K., Cullen, H., 2015. Climate change increases the probability of heavy rains like those of storm Desmond in the UK–an event attribution study in near-real time. Hydrology and Earth System Sciences Discussions 12, 13197–13216.

Vannote, R.L., Minshall, G.W., Cummins, K.W., Sedell, J.R., Cushing, C.E., 1980. The river continuum concept. Canadian journal of fisheries and aquatic sciences 37, 130–137.

Vaze, J., Teng, J., Spencer, G., 2010. Impact of DEM accuracy and resolution on topographic indices. Environmental Modelling & Software 25, 1086–1098. https://doi.org/10.1016/j.envsoft.2010.03.014

Velázquez, J.A., Schmid, J., Ricard, S., Muerth, M.J., Gauvin St-Denis, B., Minville, M., Chaumont, D., Caya, D., Ludwig, R., Turcotte, R., 2013. An ensemble approach to assess hydrological models' contribution to uncertainties in the analysis of climate change impact on water resources. Hydrol. Earth Syst. Sci. 17, 565–578. https://doi.org/10.5194/hess-17-565-2013

Vercruysse, K., Grabowski, R.C., 2021. Human impact on river planform within the context of multi-timescale river channel dynamics in a Himalayan river system. Geomorphology 381, 107659.

Verdú, J.M., Batalla, R.J., Martínez-Casasnovas, J.A., 2005. High-resolution grain-size characterisation of gravel bars using imagery analysis and geo-statistics. Geomorphology 72, 73–93.

Verstraeten, G., Poesen, J., 2000. Estimating trap efficiency of small reservoirs and ponds: methods and implications for the assessment of sediment yield. Progress in Physical Geography 24, 219–251.

Vigerstol, K.L., Aukema, J.E., 2011. A comparison of tools for modeling freshwater ecosystem services. Journal of Environmental Management 92, 2403–2409. https://doi.org/10.1016/j.jenvman.2011.06.040

Vigiak, O., Malagó, A., Bouraoui, F., Vanmaercke, M., Obreja, F., Poesen, J., Habersack, H., Fehér, J., Grošelj, S., 2017. Modelling sediment fluxes in the Danube River Basin with SWAT. Science of the Total Environment 599, 992–1012.

Viney, N.R., Bates, B.C., Charles, S.P., Webster, I.T., Bormans, M., 2007. Modelling adaptive management strategies for coping with the impacts of climate variability and change on riverine algal blooms. Global Change Biol 13, 2453–2465. https://doi.org/10.1111/j.1365-2486.2007.01443.x

Volk, M., Liersch, S., Schmidt, G., 2009. Towards the implementation of the European Water Framework Directive?: Lessons learned from water quality simulations in an agricultural watershed. Land use policy 26, 580–588.

Vorosmarty, C.J., McIntyre, P.B., Gessner, M.O., Dudgeon, D., Prusevich, A., Green, P., Glidden, S., Bunn, S.E., Sullivan, C.A., Liermann, C.R., Davies, P.M., 2010. Global threats to human water security and river biodiversity. Nature 467, 555–561. https://doi.org/10.1038/nature09440

Vu, M.T., Raghavan, S.V., Liong, S.Y., 2012. SWAT use of gridded observations for simulating runoff – a Vietnam river basin study. Hydrology and Earth System Sciences 16, 2801–2811. https://doi.org/10.5194/hess-16-2801-2012

Walker, J., 2001. The use of sediment modelling techniques to address the differing needs of management on the River Eden, Cumbria, UK. Water and Environment Journal 15, 252–257.

Walling, D.E., Collins, A.L., 2005. Suspended sediment sources in British rivers. Sediment budgets 1, 2005123–33.

Walling, D.E., Owens, P.N., Waterfall, B.D., Leeks, G.J.L., Wass, P.D., 2000. The particle size characteristics of fluvial suspended sediment in the Humber and Tweed catchments, UK. Science of The Total Environment 251–252, 205–222. https://doi.org/10.1016/S0048-9697(00)00384-3

Walter, C., Tullos, D.D., 2010. Downstream channel changes after a small dam removal: Using aerial photos and measurement error for context; Calapooia River, Oregon. River Res. Applic. 26, 1220–1245. https://doi.org/10.1002/rra.1323

Walters, C.J., 2007. Is adaptive management helping to solve fisheries problems? AMBIO: A Journal of the Human Environment 36, 304–307.

Wang, L., Melville, B.W., Guan, D., 2018. Effects of Upstream Weir Slope on Local Scour at Submerged Weirs. J. Hydraul. Eng. 144, 04018002. https://doi.org/10.1061/(ASCE)HY.1943-7900.0001431

Ward, A.J., Haan, C.T., Barfield, B.J., 1977. Simulation of the Sedimentology of Sediment Detention Basins. https://doi.org/10.13023/KWRRI.RR.103

Ward, J.V., 1989. The Four-Dimensional Nature of Lotic Ecosystems. Journal of the North American Benthological Society 8, 2–8. https://doi.org/10.2307/1467397

Ward, J.V., Stanford, J.A., 1995a. The serial discontinuity concept: extending the model to floodplain rivers. Regulated Rivers: Research & Management 10, 159–168.

Ward, J.V., Stanford, J.A., 1995b. Ecological connectivity in alluvial river ecosystems and its disruption by flow regulation. Regul. Rivers: Res. Mgmt. 11, 105–119. https://doi.org/10.1002/rrr.3450110109

Ward, J.V., Stanford, J.A., 1993. Research needs in regulated river ecology. Regul. Rivers: Res. Mgmt. 8, 205–209. https://doi.org/10.1002/rrr.3450080123

Warren, M., Dunbar, M.J., Smith, C., 2015. River flow as a determinant of salmonid distribution and abundance: A review. Environmental Biology of Fishes 98, 1695–1717.

Warrick, J.A., Bountry, J.A., East, A.E., Magirl, C.S., Randle, T.J., Gelfenbaum, G., Ritchie, A.C., Pess, G.R., Leung, V., Duda, J.J., 2015. Large-scale dam removal on the Elwha River, Washington, USA: Source-to-sink sediment budget and synthesis. Geomorphology 246, 729–750.

Waters, T.F., 1995. Sediment in streams: sources, biological effects, and control. American Fisheries Society.

Wathen, S.J., Ferguson, R.I., Hoey, T.B., Werritty, A., 1995. Unequal mobility of gravel and sand in weakly bimodal river sediments. Water Resources Research 31, 2087–2096.

Weichert, R., Wickenhäuser, M., Bezzola, G.R., Minor, H.E., 2004. Grain size analysis for coarse river beds using digital imagery processing. Proc. RF 753–760.

Wenger, R.B., Harris, H.J., Sivanpillai, R., DeVault, D.S., 1999. A graph-theoretic analysis of relationships among ecosystem stressors. Journal of Environmental Management 57, 109–122.

Westoby, M.J., Dunning, S.A., Woodward, J., Hein, A.S., Marrero, S.M., Winter, K., Sugden, D.E., 2015. Sedimentological characterization of Antarctic moraines

using UAVs and Structure-from-Motion photogrammetry. J. Glaciol. 61, 1088–1102. https://doi.org/10.3189/2015JoG15J086

Wheaton, J.M., Darby, S.E., Sear, D.A., 2008. The scope of uncertainties in river restoration. River restoration: Managing the uncertainty in restoring physical habitat 21–40.

Whiting, P.J., Bradley, J.B., 1993. A process-based classification system for headwater streams. Earth Surface Processes and Landforms 18, 603–612.

Whyte, I., 2009. Floods and their Impact on the Landscape: Flood Histories from Cumbria. Landscapes 10, 61–76. https://doi.org/10.1179/lan.2009.10.1.61

Wiens, J.A., 2002. Riverine landscapes: taking landscape ecology into the water. Freshwater Biology 47, 501–515. https://doi.org/10.1046/j.1365-2427.2002.00887.x

Wilby, R.L., Beven, K.J., Reynard, N.S., 2008. Climate change and fluvial flood risk in the UK: more of the same? Hydrological Processes 22, 2511–2523. https://doi.org/10.1002/hyp.6847

Wilby, R.L., Orr, H., Watts, G., Battarbee, R.W., Berry, P.M., Chadd, R., Dugdale, S.J., Dunbar, M.J., Elliott, J.A., Extence, C., 2010. Evidence needed to manage freshwater ecosystems in a changing climate: turning adaptation principles into practice. Science of the total environment 408, 4150–4164.

Wilcock, P., 1997. Friction between science and practice: The case of river restoration. Eos, Transactions American Geophysical Union 78, 454–454.

Wilcock, P., Pitlick, J., Cui, Y., 2009. Sediment transport primer: estimating bed-material transport in gravel-bed rivers. Gen. Tech. Rep. RMRS-GTR-226. Fort Collins, CO: US Department of Agriculture, Forest Service, Rocky Mountain Research Station. 78 p. 226.

Wilcock, P.R., 2001. Toward a practical method for estimating sediment-transport rates in gravel-bed rivers. Earth Surface Processes and Landforms 26, 1395–1408.

Wilcock, P.R., 1993. Critical shear stress of natural sediments. Journal of Hydraulic Engineering 119, 491–505.

Wilcock, P.R., Crowe, J.C., 2003. Surface-based transport model for mixed-size sediment. Journal of Hydraulic Engineering 129, 120–128. https://doi.org/10.1061/~ASCE!0733-9429~2003!129:2~120!

Wilcock, P.R., Kenworthy, S.T., 2002. A two-fraction model for the transport of sand/gravel mixtures. Water Resources Research 38, 12-1-12–12. https://doi.org/10.1029/2001WR000684

Wilcock, P.R., Kenworthy, S.T., Crowe, J.C., 2001. Experimental study of the transport of mixed sand and gravel. Water Resources Research 37, 3349–3358.

Wilcox, A.C., O'Connor, J.E., Major, J.J., 2014. Rapid reservoir erosion, hyperconcentrated flow, and downstream deposition triggered by breaching of 38 m tall Condit Dam, White Salmon River, Washington. Journal of Geophysical Research: Earth Surface 119, 1376–1394.

Wildman, L., 2013. Dam removal: A history of decision points. Rev Eng Geol 21, 1–10.

Willams, J.R., 1975. Sediment-yield prediction with universal equation using runoff energy factor. Present and prospective technology for predicting sediment yields and sources.

Williams, J.R., 1969. Flood routing with variable travel time or variable storage coefficients. Transactions of the ASAE 12, 100–0103.

Williams, J.R., Hann Jr, R.W., 1973. HYMO: Problem-oriented computer language for hydrologic modeling; users manual. ARS S US Agric Res Serv South Reg.

Williams, J.R., Jones, C.A., Dyke, P.T., 1984. The EPIC model and its application, in: Proc. Int. Symp. on Minimum Data Sets for Agrotechnology Transfer. Patancheru, pp. 111–121.

Wippelhauser, G., 2021. Recovery of diadromous fishes: A Kennebec River case study. Transactions of the American Fisheries Society 150, 277–290.

Wischmeier, W.H., Smith, D.D., 1978. Predicting soil erosion losses: a guide to conservation planning, vol 537, Agricultural handbook. US Department of Agriculture, Washington, DC 58.

Wishart, D., Warburton, J., Bracken, L., 2008. Gravel extraction and planform change in a wandering gravel-bed river: The River Wear, Northern England. Geomorphology 94, 131–152. https://doi.org/10.1016/j.geomorph.2007.05.003

Wohl, E., 2017. Connectivity in rivers. Progress in Physical Geography: Earth and Environment 41, 345–362. https://doi.org/10.1177/0309133317714972

Wohl, E., Bledsoe, B.P., Jacobson, R.B., Poff, N.L., Rathburn, S.L., Walters, D.M., Wilcox, A.C., 2015a. The Natural Sediment Regime in Rivers: Broadening the Foundation for Ecosystem Management. BioScience 65, 358–371. https://doi.org/10.1093/biosci/biv002

Wohl, E., Brierley, G., Cadol, D., Coulthard, T.J., Covino, T., Fryirs, K.A., Grant, G., Hilton, R.G., Lane, S.N., Magilligan, F.J., Meitzen, K.M., Passalacqua, P., Poeppl, R.E., Rathburn, S.L., Sklar, L.S., 2019. Connectivity as an emergent property of geomorphic systems. Earth Surface Processes and Landforms 44, 4–26. https://doi.org/10.1002/esp.4434

Wohl, E., Brierley, G., Cadol, D., Coulthard, T.J., Covino, T., Fryirs, K.A., Grant, G., Hilton, R.G., Lane, S.N., Magilligan, F.J., Meitzen, K.M., Passalacqua, P., Poeppl, R.E., Rathburn, S.L., Sklar, L.S., 2018. Connectivity as an emergent property of geomorphic systems: Geomorphic connectivity. Earth Surface Processes and Landforms. https://doi.org/10.1002/esp.4434

Wohl, E., Lane, S.N., Wilcox, A.C., 2015b. The science and practice of river restoration. Water Resour. Res. 51, 5974–5997. https://doi.org/10.1002/2014WR016874

Wohl, E., Merritts, D.J., 2007. What is a natural river? Geography Compass 1, 871–900.

Wohl, E., Rathburn, S., Chignell, S., Garrett, K., Laurel, D., Livers, B., Patton, A., Records, R., Richards, M., Schook, D.M., 2017. Mapping longitudinal stream connectivity in the North St. Vrain Creek watershed of Colorado. Geomorphology 277, 171–181.

Wong, M., Parker, G., 2006. Reanalysis and correction of bed-load relation of Meyer-Peter and Müller using their own database. Journal of Hydraulic Engineering 132, 1159–1168.

Wood, E.F., Sivapalan, M., Beven, K., Band, L., 1988. Effects of spatial variability and scale with implications to hydrologic modeling. Journal of hydrology 102, 29–47.

Woodget, A.S., Austrums, R., Maddock, I.P., Habit, E., 2017. Drones and digital photogrammetry: from classifications to continuums for monitoring river habitat and hydromorphology. WIREs Water 4, n/a-n/a. https://doi.org/10.1002/wat2.1222

Woodget, A.S., Carbonneau, P.E., Visser, F., Maddock, I.P., 2015. Quantifying submerged fluvial topography using hyperspatial resolution UAS imagery and

structure from motion photogrammetry. Earth Surface Processes and Landforms 40, 47–64. https://doi.org/10.1002/esp.3613

Wu, B., Molinas, A., Shu, A., 2003. Fractional Transport of Sediment Mixtures. International Journal of Sediment Research 18, 16.

WWF., 2016, 2016. Living Planet: Report 2016: Risk and Resilience in a New Era. World wide fund for nature.

WWF, E.P.O., 2021. 93% collapse in migratory freshwater fish populations in Europe - new report [WWW Document]. URL https://www.wwf.eu/?364693/93-collapse-in-migratory-freshwater-fish-populations-in-Europe---new-report (accessed 7.20.21).

Yan, Y., Wang, H., Zhu, R., Chu, L., Chen, Y., 2013. Influences of low-head dams on the fish assemblages in the headwater streams of the Qingyi watershed, China. Environ Biol Fish 96, 495–506. https://doi.org/10.1007/s10641-012-0035-0

Yang, C.T., 1984. Unit stream power equation for gravel. Journal of Hydraulic Engineering 110, 1783–1797.

Yang, D., Musiake, K., 2003. A continental scale hydrological model using the distributed approach and its application to Asia. Hydrological Processes 17, 2855–2869.

Yang, S.L., Milliman, J.D., Li, P., Xu, K., 2011. 50,000 dams later: Erosion of the Yangtze River and its delta. Global and Planetary Change 75, 14–20. https://doi.org/10.1016/j.gloplacha.2010.09.006

Yapo, P.O., Gupta, H.V., Sorooshian, S., 1998. Multi-objective global optimization for hydrologic models. Journal of hydrology 204, 83–97.

Yarnell, S.M., Petts, G.E., Schmidt, J.C., Whipple, A.A., Beller, E.E., Dahm, C.N., Goodwin, P., Viers, J.H., 2015. Functional Flows in Modified Riverscapes: Hydrographs, Habitats and Opportunities. BioScience 65, 963–972. https://doi.org/10.1093/biosci/biv102

Yasarer, L.M.W., Bingner, R.L., Momm, H.G., 2018. Characterizing ponds in a watershed simulation and evaluating their influence on streamflow in a Mississippi watershed. Hydrological Sciences Journal 63, 302–311. https://doi.org/10.1080/02626667.2018.1425954

Yu, D., Xie, P., Dong, X., Hu, X., Liu, J., Li, Y., Peng, T., Ma, H., Wang, K., Xu, S., 2018. Improvement of the SWAT model for event-based flood simulation on a sub-daily timescale. Hydrology and Earth System Sciences 22, 5001–5019. https://doi.org/10.5194/hess-22-5001-2018

Yuan, W., Liu, M., Wan, F., 2019. Calculation of Critical Rainfall for Small-Watershed Flash Floods Based on the HEC-HMS Hydrological Model. Water Resour Manage 33, 2555–2575. https://doi.org/10.1007/s11269-019-02257-0

Zaliapin, I., Foufoula-Georgiou, E., Ghil, M., 2010. Transport on river networks: A dynamic tree approach. Journal of Geophysical Research: Earth Surface 115. https://doi.org/10.1029/2009JF001281

Zanandrea, F., Michel, G.P., Kobiyama, M., Censi, G., Abatti, B.H., 2021. Spatial-temporal assessment of water and sediment connectivity through a modified connectivity index in a subtropical mountainous catchment. CATENA 204, 105380.

Zarfl, C., Berlekamp, J., He, F., Jähnig, S.C., Darwall, W., Tockner, K., 2019. Future large hydropower dams impact global freshwater megafauna. Scientific reports 9, 1–10.

Zarfl, C., Lehner, B., 2020. European rivers are fragmented by many more barriers than had been recorded. Nature 588, 395–396. https://doi.org/10.1038/d41586-020-03440-9

Zarfl, C., Lumsdon, A.E., Berlekamp, J., Tydecks, L., Tockner, K., 2015. A global boom in hydropower dam construction. Aquat Sci 77, 161–170. https://doi.org/10.1007/s00027-014-0377-0

Zavattero, E., Du, M., Ma, Q., Delestre, O., Gourbesville, P., 2016. 2D Sediment Transport Modelling in High Energy River – Application to Var River, France. Procedia Engineering, 12th International Conference on Hydroinformatics (HIC 2016) - Smart Water for the Future 154, 536–543. https://doi.org/10.1016/j.proeng.2016.07.549

Zhan, T.L., Zhang, W.J., Chen, Y.M., 2006. Influence of reservoir level change on slope stability of a silty soil bank, in: Unsaturated Soils 2006. pp. 463–472.

Zhang, J., Huang, Y.-F., Munasinghe, D., Fang, Z., Tsang, Y.-P., Cohen, S., 2018. Comparative analysis of inundation mapping approaches for the 2016 flood in the Brazos River, Texas. JAWRA Journal of the American Water Resources Association 54, 820–833.

Zhang, W., Montgomery, D.R., 1994. Digital elevation model grid size, landscape representation, and hydrologic simulations. Water Resources Research 30, 1019–1028. https://doi.org/10.1029/93WR03553

Photo credits: Front page image (Patrice Carbonnoeu, Eamont Weir, Penrith, U.K.) | Last page image (Lucio Marcello, Kingie River, Scottish Highland, U.K.).

***** Let It Flow *****